ALMA MATER STUDIORUM
UNIVERSITÀ DI BOLOGNA

DOTTORATO DI RICERCA IN
SCIENZE E TECNOLOGIE AGRARIE, AMBIENTALI E ALIMENTARI

Ciclo 36

Settore Concorsuale: 07/G1 SCIENZE E TECNOLOGIE ANIMALI
Settore Scientifico Disciplinare: AGR/18 - NUTRIZIONE E ALIMENTAZIONE ANIMALE

ADVANCED DIAGNOSTICS FOR PHYSIOLOGICAL CHARACTERISATION OF INTRAUTERINE GROWTH-RESTRICTED PIGS

Presentata da: Roberta Ruggeri

Coordinatore Dottorato

Prof. Massimiliano Petracci

Supervisore

Prof. Paolo Trevisi

Co-Supervisori

DVM Catherine Ollagnier

Dott. Giuseppe Bee

Esame finale anno 2024

Abstract

Intrauterine growth restriction (**IUGR**) affects up to 30% of piglets, leading to increased mortality and stunted growth. The lack of an accurate diagnostic method makes IUGR a challenge, limiting treatment development. This Ph.D. aimed to establish a model for the diagnosis of IUGR in newborn piglets and to characterise the IUGR subpopulation from a physiological perspective. The IUGR foetus increases blood flow towards the brain to survive when oxygen and nutrient supply through the placenta is limited. This mechanism results in a higher brain-to-liver weight ratio (**BrW/LW**) at birth. In this thesis, the BrW/LW was measured one day after birth with computed tomography or by weighing the organs, and compared with diagnosis based on head shape and birth weight (**BtW**). Moreover, pictures of the piglets were recorded to capture specific morphometric traits. Our findings revealed that identifying IUGR based on head morphology or BtW does not always align with an increased BrW/LW. Morphometric traits proved reliable indicators, allowing estimation of brain, liver weight, and BrW/LW with 6%, 17%, and 17% error, respectively. A higher BrW/LW correlated with extended time to reach market weight, negatively affecting growth from birth to slaughter, gain-to-feed ratio, and protein efficiency during the grower-finisher period, but without impacting fat and muscle mass at any stage. The BrW/LW affected the Beta diversity of faecal microbiota until the beginning of the finisher period. Plasma metabolome was unaffected by BrW/LW during lactation, and only asparagine was significantly lower in IUGR compared to normal pigs at the end of the starter period. Our research confirmed IUGR's lasting impact on several physiological traits. An accurate and standardized diagnostic method is needed to further characterise the affected pigs and enable consistent comparisons across studies. The use of predictive models based on image analysis represents a promising tool for early identification of IUGR.

Acknowledgements

Firstly, and above all, I would like to thank my supervisors. Catherine Ollagnier, Giuseppe Bee, and Paolo Trevisi: your dedication to research set a model for me to look up to. Through your guidance, I have discovered how research can be challenging yet deeply inspiring. Thank you for your steady support throughout this journey.

Thanks to Francesco and Inés: my colleagues, mental coaches, and dear friends. Without you, I would still be filing the documents to enroll in Switzerland. The chance to share my path at Agroscope with you has been an honor - and a great pleasure.

My sincere thank you goes to Agroscope Pig Group too: for their warm welcome since the very beginning and to the Animal Caretakers from the piggery, who have all been extremely patient with my (ongoing) struggle with speaking French. Merci!

Thanks to Omar, my dearest friend, for being an endless source of inspiration and always standing by my side. You're one of the people I love the most, perhaps one of the few who truly understands me. I miss the days when we lived close, studied together, and danced the night away. But even if we were apart for a decade, I know our connection would remain unchanged. Thanks for always being there.

Thanks to Luca and Coco, my companions throughout the entire lockdown. I love you guys, but let's agree to never touch Monopoly again. Luca, you have been more than just a cousin but a friend and an incredible Python teacher. Without your help, I would still be extracting frames from piglets' videos. Coco, it was an honour to share via Misa 2 with you (despite Angelucci and the cockroaches). I miss your pasta al parmigiano at 5 am. You've been an incredible flatmate, colleague, and friend.

Thanks to Fred, my partner in crime since '95. From Rieti to London, Bologna to Fribourg, and now Milano - who knows where else we'll end up causing trouble? I can't wait to find out!

Thanks to Seda and Sofia. Building such a close friendship was the last thing I expected to happen. Yet, you soon grew into my Swiss family: my life in Fribourg would have never been the same without you.

Thanks to Dave, my DJ teacher, cooking mate, camping buddy, and favourite pitocco. The last months we've spent together have been so nice. I can’t wait to share tons of different snacks with you!

Last but not least, thanks to my family. Thanks to my dad and my brother, with whom I share a passion for medical sciences, for always encouraging my curiosity and giving me great partners to discuss my findings with; thanks to my mom for her tireless support: you granted me the strength and determination I needed to navigate this journey.

This thesis is dedicated to the memory of the Palestinian students and scientists who lost their lives in Gaza.

Contents

List of original manuscripts included in the thesis

Manuscript I: Intrauterine growth restriction defined by increased brain-to-liver weight ratio affects postnatal growth and protein efficiency in pigs. *Published in Animal Journal.* https://doi.org/10.1016/j.animal.2023.101044

Manuscript II: Morphometric traits to estimate brain and liver weight and their ratio for the diagnosis of intrauterine growth restriction in newborn piglets. *Under revision by Animal Journal.*

Manuscript III: Intrauterine growth restriction, defined by an elevated brain-to-liver weight ratio, affects faecal microbiota composition and, to a lesser extent, plasma metabolome profile at different ages in pigs. *Unpublished.*

Abbreviations

^{1}H-NMR: proton nuclear magnetic resonance

AC: abdominal circumference

ADFI: average daily feed intake

ADG: average daily gain

BrW/LW: brain-to-liver weight ratio

BrW: brain weight

BrW_{CT}/LW_{CT}: brain-to-liver weight ratio obtained from CT scan volumes

BrW_{CT}: brain weight obtained from CT scan volume

BrW_{Eu}/LW_{Eu}: brain-to-liver weight ratio assessed with a scale after euthanasia

BrW_{Eu}: brain weight assessed with a scale after euthanasia

BtW: birth weight

BW: body weight

CANSCORE: clinical assessment of nutrition score

CP: crude protein

CT: computed tomography

DXA: dual-energy X-ray absorptiometry

EDTA: ethylenediaminetetraacetic acid

GIT: gastrointestinal tract

HC: head circumference

IUGR: intrauterine growth restriction

LBtW: low birth weight

LDA: linear discriminant analysis

LT: *longissimus thoracis* muscle

LW: liver weight

LW_{CT}: liver weight obtained from CT scan volume

LW_{Eu}: liver weight assessed with a scale after euthanasia

MAE: mean absolute error

MAPE: mean absolute percentage error

oLV: orthogonal latent variable

OPLS-DA: orthogonal projection to latent structures-discriminant analysis

PCA: principal component analysis

pLV: predictive latent variable

Q2Y: predictive ability of the OPLS-DA model

Q2Y-perm: predictive ability of the OPLS-DA model

R^2: R-squared value

R^2_{adj}: adjusted R-squared value

R2Y: goodness of fit of the OPLS-DA model

SD: standard deviation

SGA: small for gestational age

SM: *semitendinosus* muscle

VIP: variable importance in the projection

Background

The economy of modern pig breeding programs relies largely on sows' ability to produce a high number of piglets per year. For this reason, over the last decades, genetic selection in the sow breeding sector has focused on increasing the total number of piglets born per litter (Kemp et al., 2018). In European pig production, this approach has indeed resulted in a significant increase in litter size, with highly prolific sow lines now commonly giving birth to 18–20 live piglets per litter (Oliviero et al., 2019; Kemp et al., 2018). However, in parallel with this improved prolificacy, there has been an increase in the number of piglets experiencing intrauterine growth restriction (**IUGR**), a marked decline in the birth body weight (**BtW**), and an increase in perinatal piglet mortality rates (Farmer and Edwards, 2022). Insufficient space within the uterus represents a primary factor contributing to reduced foetal growth in highly prolific sow lines (Pere and Etienne in 2000; Town et al., 2004; Oliviero et al., 2019). Uterine overcrowding is indeed associated with reduced placental weight and decreased uterine blood flow per foetus (Pere and Etienne in 2000; Wu et al., 2006; Town et al., 2004). The impaired uteroplacental blood flow results in inadequate distribution of oxygen and nutrients to the foetus, which develops poorly (Cohen et al., 2015). In addition, in the hyperprolific sows, the number of piglets born often exceeds the total available teats (Oliviero, 2022; Farmer and Edwards, 2022). This results in increased competition among piglets to access a teat and suckle, leading to insufficient colostrum and milk intake. This situation is particularly challenging for low BtW (**LBtW**) and IUGR piglets, which possess inadequate energy reserves for thermoregulation and exhibit low vitality at birth (Farmer and Edwards, 2022). If IUGR piglets manage to survive the neonatal period, they typically experience higher morbidity and mortality rates, reduced efficiency of nutrient utilisation, long-term growth limitations, lower feed conversion efficiency, and poorer carcass quality (Krueger et al., 2014; Wu et al., 2006).

Given these reasons and the fact that they represent as much as 30% of a litter, IUGR piglets pose a significant problem within the pig production system, negatively affecting overall production efficiency.

Financial support statement

This research received funding from the European Union's Horizon 2020 research and innovation programme under a Marie Sklodowska-Curie grant (agreement no. 955374).

1. Intrauterine growth restriction

1.1 Definition

Intrauterine growth restriction (**IUGR**) is defined as the failure of the foetus to reach its genetically expected growth during gestation, resulting in a deviation from normal foetal growth patterns and impaired development of its organs (Gupta, 2008; Wu et al., 2006). It is important to differentiate the terms IUGR, low birth weight (**LBtW**), and small for gestational age (**SGA**). The diagnosis of LBtW is solely based on the birth weight (**BtW**) (Gupta, 2008). In contrast, SGA is diagnosed by comparing the newborn's weight with gestational age-specific normal birth weight values. Various normative curves are employed to classify newborn infants and piglets as SGA, appropriate for gestational age, or large for gestational age (De Vos et al., 2014; Gupta 2008). Typically, piglets whose BtW is below the 10^{th} percentile of the average BtW of the litter or below the 10^{th} percentile for their gestational age are classified as LBtW and SGA, respectively (De Vos et al., 2014). Although the terms SGA and IUGR are often used interchangeably, they do not describe the same concept. Neonates born SGA can be categorized into two major groups: constitutionally normal SGA and SGA who have not attained their full genetically determined size due to growth restriction in the uterus (Osuchukwu and Reed, 2022; De Vos et al., 2014). Indeed, depending on the threshold used to define SGA, a certain percentage of normally growing subjects may fall below the threshold and be classified as SGA without having IUGR. These subjects are just constitutionally small (Gupta, 2008). Likewise, some IUGR newborns may show a BtW above the 10^{th} percentile for their gestational age and do not fall into the SGA category (Osuchukwu and Reed, 2022).

1.2 Classification

In the field of human perinatology, the classification of IUGR involves two categories: symmetrical and asymmetrical, based on anthropometric measurements (Sharma et al., 2016).

1.2.1 Symmetrical IUGR

Symmetrical IUGR, which accounts for about 20–30% of total IUGR cases in humans, refers to a reduction in foetal growth that affects all developing organs and body parts in a balanced manner. As a result, the infant is born small but proportionally shaped (Rosenberg, 2008; Stephens et al., 2015). Symmetrical growth restriction is often indicative of an early intrinsic factor that hampers foetal growth, such as genetic disorders, infection of the foetus, or exposure to drugs or chemicals. The reason behind the symmetrical impairment lies in the timing of the insult, which occurs early in pregnancy when foetal growth primarily relies on cell division (Sharma et al., 2016; Resnik, 2002).

1.2.2 Asymmetrical IUGR

In contrast, asymmetrical IUGR represents a different scenario, where the rate of growth varies among different organs (Rosenberg, 2008; Stephens et al., 2015). Asymmetrical IUGR accounts for about 70–80% of IUGR cases in human perinatology and occurs due to external factors, often stemming from insufficient availability of substrates for foetal metabolism, such as oxygen and nutrients (Sharma et al., 2016; Resnik, 2002). In this pattern, oxygen and nutrients are prioritised for vital organs, resulting in spared head circumference (**HC**), while the abdominal circumference (**AC**) is reduced due to smaller liver size and a lack of subcutaneous fat (Resnik, 2002). The primary factors that commonly restrict the availability of metabolic substrates to the foetus are maternal vascular disorders and uteroplacental insufficiency. Typically, these conditions manifest later in the third trimester of pregnancy,

when the growth of most organs primarily relies on an increase in cell size rather than cell number (Sharma et al., 2016; Resnik, 2002).

1.2.3 IUGR in pigs

In several mammalian species, including pigs, IUGR occurs spontaneously. Bauer et al. (1998) demonstrated, using morphometric data, that naturally observed growth restriction in swine is asymmetrical. Indeed, it is characterised by relative brain sparing, while the organs primarily affected by foetal deprivation are the liver and kidney (Bauer et al., 1998). While asymmetrical IUGR is more commonly seen in pigs, symmetrical IUGR may also occur, although it is generally considered less frequent, and precise prevalence rates remain largely unknown.

Fig. 1. Picture of a normal piglets (back) and a piglet affected by intrauterine growth restriction (IUGR; front). Picture by Van Ginneken et al., 2022.

1.2.4 The brain-sparing effect

The compromised placental functionality in IUGR reduces the transfer of oxygen and glucose supply to the developing foetus (Cohen et al., 2015; Bauer et al., 1998). In addition, intrauterine overcrowding is associated with a decrease in placental size per foetus. This reduction in

placental size and, as a consequence, in the exchange surface renders normal compensatory mechanisms ineffective, leading to the occurrence of foetal hypoxemia (Bauer et al., 1998). To adapt to the chronic deprivation of oxygen and nutrients, the foetus initiates a response whereby the cardiac output is preferentially directed toward the brain (Cohen et al., 2015; Matheson et al., 2018). Within the foetal circulation, blood follows a parallel circuit, with the majority of right ventricular output passing through the *ductus arteriosus* to the descending aorta, while the left ventricle primarily supplies the upper body and brain (Cohen et al., 2015). In placenta insufficiency, structural and functional changes in the placental blood vessels occur, such as vasoconstriction, impaired vasodilation, and thickening of the vessel walls. These changes result in increased resistance to blood flow in the placenta, which significantly impacts foetal cardiac output (Spinillo et al., 2014). Specifically, the elevated resistance in the umbilical artery leads to an increase in right ventricular afterload and a redirection of cardiac output towards the left ventricle (Spinillo et al., 2014). The increase in right ventricular afterload is accompanied by the dilation of cerebral arteries and results in a decrease in left ventricular afterload. These adaptations facilitate a preferential shift of the cardiac output toward the left ventricle, optimizing blood flow to the brain (Cohen et al., 2015; Spinillo et al., 2014). While this redirection of blood flow preserves the vital functions of the brain and ensures the survival of the foetus, it compromises the development of other organs, including the liver, kidneys, intestine, and pancreas, due to reduced vascularization (Felicioni et al., 2019; Bauer et al., 1998).

1.3 Aetiology

During pregnancy, although genetics directly affects development, the quality of the uterine environment serves as a limiting factor for the growth of the embryo. Genetics safeguards the innate potential of the organism, while the quality of the uterine environment provides the

essential resources for the animal to effectively express its genetic growth potential (Felicioni et al., 2019). Insults experienced at various stages of prenatal life may negatively affect the quality of the uterine environment, resulting in growth restriction in the uterus (Felicioni et al., 2019).

In human perinatology, IUGR may be caused by foetal, placental, maternal, and genetic insults. Foetal factors include genetic conditions and chromosomal or congenital anomalies. Placental factors primarily involve abnormalities in placental implantation or formation. Maternal factors include infection, malnutrition, alteration of uterine blood flow to the placenta, and lifestyle factors, such as smoking or drug use. Genetic factors include polymorphisms in the genes of the mother, placenta, and foetus that influence intrauterine growth. It is important to note that these factors often overlap, contributing to the complex nature of foetal growth restriction (Sharma et al., 2016; Bernstein, 1997). In the majority of cases, the underlying cause of IUGR remains unknown. However, most of the IUGR cases exhibit a shared characteristic placental phenotype, referred to as "placental insufficiency", for an extended period of time (Cetin and Alvino, 2009; Miller et al., 2016).

For livestock animals, both environmentally and naturally occurring IUGR are well documented (Wu et al., 2006). Foetal growth, as in humans, can be affected by a variety of factors including genetics, uteroplacental insufficiency, maternal nutrition (low or high feed intake, and nutrient imbalance), toxins ingestions, infections of the foetus (Circovirus), environmental temperature and stress (Van Ginneken et al., 2022; Wu et al., 2006; Wu et al., 2004). However, uteroplacental insufficiency is recognized as the major factor that impairs foetal growth (Bauer et al., 2003; Town et al., 2004). Uteroplacental insufficiency can be both a consequence of the breeding systems or can occur naturally. Livestock animals are often bred at immature body weight (**BW**) to maximize production performance. As a result, the mother

and foetus grow simultaneously and have to compete for nutrients during pregnancy, leading to improper placental implantation and growth in the uterus (Wu et al., 2006; Wu et al., 2004). However, not just immature breeding but also increased age at breeding can lead to uteroplacental insufficiency. In highly prolific sows, the ovulation rate tends to increase with age and the number of conceptuses in the uterus exceeds uterine capacity, negatively affecting placental development (Foxcroft et al., 2006).

In polytocous species [species that give birth to multiple offspring in a single pregnancy], naturally occurring IUGR is a common phenomenon (Bauer et al., 1998; Wootton et al., 1983) and it is characterised by a reduction of the placental weight per foetus, resulting in relative placental insufficiency (Town et al., 2004). Pigs exhibit the most severe, naturally occurring IUGR among domestic animals (Wu et al., 2006), with up to 20-30% of the newborns affected in a single litter (Amdi et al., 2013; Wu et al., 2006). According to Bauer et al. (1998), the area of the placenta most likely affected by impaired development is situated at the intersection between the second and third parts of the uterine horns, where there is an overlap (compression) of vascular supply (Chand et al., 2022). In addition, an increased frequency of nidation [attachment to the uterine wall] of embryos may be higher in this region, leading to alterations in placental development in later gestation simply because of reduced space (Bauer et al., 1998).

1.4 Epidemiology

Foetal growth restriction impacts approximately 5 to 20% of human pregnancies, depending on the country (De Onis, 2001; Gatford et al., 2010; Chand et al., 2022). This condition predisposes individuals to a heightened risk of developing diabetes (Gatford et al., 2010), hypertension (Hennington and Alexander, 2013), and metabolic syndrome (Jahan-Mihan et al., 2015) later in life.

In the context of swine production, IUGR poses a significant challenge too. Within the modern pig industry, 20-30% of newborn piglets, born from highly prolific sows, are affected by IUGR, resulting in reduced birth weight, increased morbidity and mortality, impaired growth, and meat quality (Lynegaard et al., 2020a; Santos et al., 2022; Amdi et al., 2013; Wu et al., 2006). The incidence is elevated in primiparous sows due to their immature BW at the first breeding. It decreases in second and third-parity sows, as evidenced by the lower IUGR proportion in the litter, to rise again with increasing parity, as a result of higher ovulation rate and uterine overcrowding (Matheson et al., 2018; Foxcroft et al., 2006).

1.5 Diagnosis

1.5.1 Diagnosis of IUGR in human perinatology

The diagnosis of IUGR in human perinatology can be achieved through both antenatal and postnatal assessments.

1.5.1.1 Antenatal diagnosis

During the antenatal period, a variety of techniques are employed in the diagnosis of IUGR. These include evaluating maternal and familial history to identify potential risk factors, assessing maternal anthropometry and nutritional status (Sharma et al., 2016), utilising ultrasound to estimate foetal weight, and employing biometric measures such as AC and HC of the foetus. Furthermore, Doppler ultrasound is utilised to evaluate the circulation of the mother, placenta, and foetus simultaneously, providing valuable insights for diagnosis (Sharma et al., 2016; Gutaj and Wender-Ozegowska, 2016). The HC/AC ratio, assessed through pulsed ultrasound, is employed for the diagnosis of asymmetric foetal growth restriction (Campbell and Thoms, 1977). In cases of asymmetric IUGR, the liver size appears smaller in relation to the HC. An HC/AC ratio exceeding two standard deviations (**SD**) above the mean for

gestational age is considered abnormal and serves as a useful indicator to distinguish between symmetrical and asymmetrical IUGR (Sharma et al., 2016). Doppler ultrasound evaluations of the uterine artery, umbilical artery, middle cerebral artery, and cerebro-placental ratio (ratio between the foetal umbilical artery pulsatility index and the middle cerebral artery pulsatility index) provide valuable insights into the detection of placental insufficiency. Among these, umbilical artery Dopplers, combined with cerebro-placental ratio, are widely utilised for the identification of IUGR (Sharma et al., 2016; Bamberg and Kalache, 2004).

1.5.1.2 Postnatal diagnosis

The postnatal diagnosis of IUGR infants includes clinical examination (enlarged head when compared to rest of the body, reduced muscle mass and subcutaneous fat, peelable skin); the use of anthropometric charts to compare the characteristics of the newborn with reference values for ethnicity and gender (BtW and length, HC and mid-upper arm circumference); ponderal index measurement (BW to body length ratio), the clinical assessment of nutrition score, (**CANSCORE**, malnutrition effects on hair, cheeks, neck and chin, arms, legs, back, buttocks, chest, and abdomen); the cephalization index measurement (ratio of the HC to BW), and the mid-arm/HC ratio assessment (Pereira-da-Silva et al., 2019; Sharma et al., 2016). In the study of Adebami and Owa (2008), the CANSCORE method demonstrated greater accuracy in diagnosing cases of foetal malnutrition compared to using intrauterine growth charts and curves. The study showed that a considerable proportion of babies that experienced growth restriction did not meet the criteria based on BtW alone, indicating the limitations of using weight as the sole criterion. Likewise, several growth-restricted infants would have been misclassified using the ponderal index alone. Part of the reason for this may be due to the fact that IUGR not only affected BW but also the length of the body (Adebami and Owa, 2008).

1.5.2 Diagnosis of IUGR in newborn pigs

In pig production, the diagnosis of IUGR is only feasible after birth. Dullemen (2011) highlighted numerous constraints when employing Doppler velocimetry to assess IUGR in pig foetuses, making the technique particularly challenging. In addition, reference standards for biometric measurements like HC, AC, and crown-rump length—commonly employed in human medicine for estimating foetal weight and monitoring growth during pregnancy— are lacking in veterinary reproductive medicine, especially for pigs (Vernunft et al., 2022).

Even after birth, the identification of IUGR piglets remains notably challenging due to the absence of specific symptoms and reliable biomarkers. Diagnosis is commonly established by assessing various parameters based on the BW and the morphology of the piglet. Parameters related to BW include the absolute weight of the foetus or newborn, the BtW relative to a specific gestational age, and the BtW in comparison to the average weight of the litter (Van Ginneken et al., 2022). On the other hand, parameters associated with the morphology of the piglet include evaluation of the head shape (Hales et al., 2013; Amdi et al., 2013), the body mass index, and the crown-to-rump length (Feldpausch et al., 2019).

1.5.2.1 Birth body weight

Because it is easy to measure practically on farms and in a research context, foetal weight or BtW is often used as a criterion to detect IUGR (Wu et al., 2006). Most of the studies define IUGR as piglets weighing less than the 10^{th} percentile of the gestational age–specific normal BtW values at birth (Bauer et al., 2003). D'inca et al. (2010) classified piglets as IUGR when their BtW was at least 1.5 SD units lower than the average BtW of the litter. In the study of Wang et al. (2016) an IUGR piglet was defined as having a BtW between 0.75 and 0.90 kg and belonging to the lower quartile of the litter birth weight, whereas Ji et al. (2017) identified piglets with a BtW below 1.1 kg as IUGR.

1.5.2.2 Head shape

In the identification of IUGR piglets, it has been proposed that considering the head morphology as an additional criterion alongside BtW is relevant (Hales et al., 2013). Additionally, Huting et al. (2018) suggested that the morphology of newborn piglets could serve as a predictive factor for their future performance. Typically, piglets affected by growth restriction in the uterus exhibit distinct characteristics in head morphology, including a dolphin-like head shape, wrinkles perpendicular to the mouth, bulging eyes, and hair with no direction of growth (Hales et al., 2013; Amdi et al., 2020). In a study by Amdi et al. (2013), piglets were categorized as normal, mildly IUGR, or severely IUGR based on the criteria established by Hales et al. (2013). These criteria identified severe IUGR piglets as those displaying two or three of the above-mentioned characteristics (a steep, dolphin-like forehead, bulging eyes, and wrinkles perpendicular to the mouth). Piglets were classified as mildly IUGR if one of these characteristics was present. Finally, piglets without any of these characteristics were considered "normal" and served as control subjects.

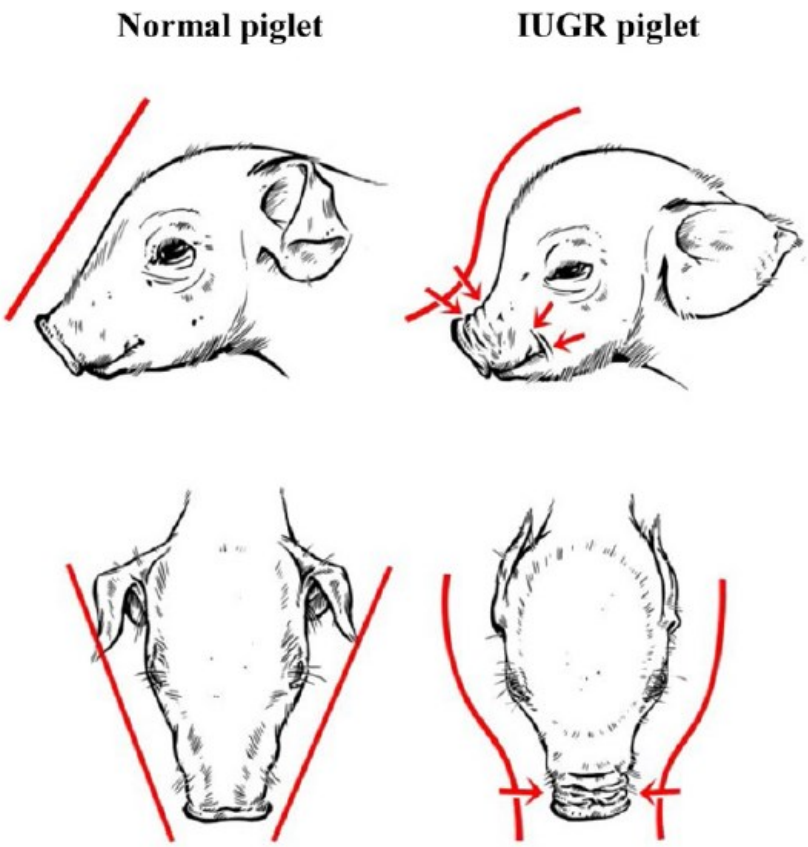

Fig. 2. Illustrations of a normal piglet (left) and a piglet affected by intrauterine growth restriction (IUGR; right). Criteria for IUGR identification: dolphin-like head shape, wrinkles perpendicular to the mouth, bulging eyes, and hair with no direction of growth. Picture by Hales et al., 2013.

1.5.2.3 Body shape

Morphological measurements, including the ponderal index (calculated as birth weight / (crown–rump length)^3) and the body mass index (calculated as birth weight / (crown–rump length)^2), have been considered to identify piglets that experienced growth restriction in the uterus and to predict their postnatal growth (Douglas et al., 2016). The study of Baxter et al. (2008) revealed that these morphological traits, which reflect body proportionality, can serve as valuable indicators of mortality risks. Hales et al. (2013), suggested that the body mass index of a piglet may be associated with its body fat percentage, and this might explain why body

mass index is important in relation to survivability. Typically, a combination of these measurements is utilised to differentiate between neonates who are constitutionally small and those who are small due to IUGR. This suggests a comparable situation in pigs, which are often used as models for this condition (Douglas et al., 2016). In the study by Douglas et al. (2016), the body mass index was the most effective predictor of postnatal growth for LBtW piglets. Piglets with a low body mass index consistently exhibited poorer performance. Similarly, Hales et al. (2013) observed that a higher body mass index was associated with increased survivability. Piglets that died within the first day after birth had a lower body mass index and displayed more pronounced signs of growth restriction, such as a steep, dolphin-like forehead, bulging eyes, and wrinkles perpendicular to the mouth. In both the studies of Amdi et al. (2013) and Hansen et al. (2018), piglets classified as IUGR due to their distinctive head shape, exhibited lower BtWs, shorter crown-rump lengths, and lower body mass index and ponderal index compared to their normal littermates.

1.5.2.4 Brain-to-organ weight ratio

Asymmetrical growth restriction in foetuses induces chronic hypoxia and nutrient deprivation, resulting in a significant alteration in blood flow distribution, primarily aimed at preserving cerebral functionality (Cohen et al., 2015; Matheson et al., 2018). This adaptive survival mechanism, known as the "brain-sparing effect," leads to a relative increase in brain size when compared to other organs such as the liver (Bauer et al., 1998). Hence, an appropriate metric for assessing the extent of IUGR should consider the ratio between the weight of the brain and the weight of other organs (Felicioni et al., 2019).

1.5.2.5 Limitations of diagnostic techniques

Growth restriction occurring in the uterus often leads to the SGA condition (Radlowski et al., 2014), and it may result in a characteristic head shape due to the brain-sparing effect (Hansen

et al., 2018). Therefore, the accuracy in identification of IUGR piglets can be improved by considering both the BtW and the head morphology at birth, enabling a more comprehensive evaluation of this condition. However, it is important to note that being SGA does not necessarily indicate an IUGR condition, despite SGA being a common feature among IUGR piglets (Gupta et al., 2008; De Vos et al., 2014).

Regarding the head shape, the subjective nature of classifying IUGR based on head shape relies on the observer and introduces a higher likelihood of variations in observations due to subjective judgement. Additionally, there are natural variations in head characteristics, unrelated to pathology, which result from domestication and subsequent selective pressures (Chakraborty et al., 2021; Wilkinson et al., 2013). These inherent limitations decrease the accuracy of diagnosis based solely on BtW, head shape, or a combination of both.

Employing the brain-to-organ weight ratio for the identification of IUGR piglets provides an objective approach as it directly reflects the brain-sparing effect. Nevertheless, the practical application of this ratio as a diagnostic technique is currently limited to research contexts using animal models. Indeed, to assess the ratio the utilisation of advanced imaging techniques such as CT scan or the euthanasia of newborn piglets is required (Felicioni et al., 2019).

1.6 Consequences of IUGR

1.6.1 Performance

1.6.1.1 Mortality

The preweaning mortality rates of live-born piglets in Europe range from 10% to 20% (Muns et al., 2016). Most piglet deaths occur within the first 72 hours after birth (Muns et al., 2016), primarily due to starvation and accidental crushing by the sow (Pedersen et al., 2011; Kielland et al., 2018). Newborn piglets are born with limited body fat and lack brown adipose tissue

(Trayhurn et al., 1989), which is essential for regulating non-shivering thermogenesis (Sjaastad et al., 2010). As a result, piglets need to generate heat by shivering, relying on energy derived from blood glucose (Staarvik et al., 2019).

Piglets are born with an underdeveloped ability for gluconeogenesis (Kaneko, 2008), and their glycogen reserves are quickly depleted as they try to maintain their body temperature (Herpin et al., 2002; Staarvik et al., 2019). During this critical period, the availability of energy through colostrum intake is crucial for the survival of neonatal piglets (Theil et al., 2011; Quesnel et al., 2012; Amdi et al., 2013). If piglets fail to consume enough colostrum, their blood glucose levels drop to hypoglycaemic levels within 24–36 hours (Kaneko, 2008; Staarvik et al., 2019). Hypoglycaemic piglets show signs of lethargy and weakness, and, in severe cases, may experience coma and death (Kaneko, 2008). Weak and lethargic piglets face a higher risk of being accidentally crushed by the sow, in addition to the direct risk of death caused by hypoglycaemia (Staarvik et al., 2019).

Piglets that experienced growth restriction in the uterus showed higher preweaning mortality rates due to their lower body reserves of glycogen and their inability to compete with littermates to achieve an early and adequate colostrum intake (Edwards and Baxter, 2015; Farmer and Edwards, 2022). In the study by Amdi et al. (2013), it was shown that IUGR piglets have less than half the total glycogen reserves in their liver compared to normal piglets 24 hours after birth, making it more difficult for them to maintain body temperature. Quesnel et al. (2012) suggest that each piglet requires at least 200 grams of colostrum during the neonatal phase to survive. However, severe IUGR piglets, as observed in Amdi et al.'s study (2013), receive only approximately half the required amount to ensure neonatal survival. Furthermore, the lower vitality observed in IUGR piglets may be linked to neural immaturity, as indicated by the reduced myelination and dendritic development in their brains compared to those of normal littermates (Dickerson et al., 1971; Farmer and Edwards, 2022). In the study of Matyba et al.

(2021), the majority of pigs that died before weaning exhibited signs of IUGR, such as a dolphin-like head shape, bulging eyes, and wrinkles perpendicular to the mouth. The mortality among IUGR-affected piglets was highest within the first two weeks of life, primarily occurring within the first 2-3 days after birth. However, there were no significant differences in the proportion of deaths between IUGR and normal pigs postweaning. Similarly, in the study of Hawe et al. (2020), LBtW pigs showed a higher preweaning mortality rate, with nearly half of the deaths due to starvation. Average-BtW piglets experienced fewer preweaning deaths, and these occurred later during lactation, suggesting that these heavier pigs were not affected to the same extent by impaired vitality and milk acquisition in the immediate postnatal period. However, also in this study, the difference in postweaning mortality rates between average and LBtW pigs was not statistically significant.

1.6.1.2 Growth

Growth restriction during foetal development has lasting effects on postnatal growth. Piglets experiencing IUGR typically exhibit slower growth rates and delayed development compared to their normal littermates (Wu et al., 2006). Several studies showed a reduced average daily gain (**ADG**) in IUGR pigs, identified based on their head shape or LBtW, whether it was from birth to weaning (Hansen et al., 2018), from birth to the growing phase (Lynegaard et al., 2020b; Alvarenga et al., 2012), or from birth to slaughter (Santos et al., 2022; Xiong et al., 2020). However, some of these studies (Lynegaard et al., 2020b; Hansen et al., 2018) also showed that IUGR piglets had a higher fractional growth rate (weight gain per day compared with starting weight) from birth to weaning when compared to their normal counterparts. In the study of Lynegaard et al. (2020b), IUGR piglets increased their BW sevenfold in the preweaning period, whereas normal piglets only increased their BW fivefold. These findings suggest that some growth potential in the IUGR-affected pigs exists. In addition, in the study

of Alvarenga et al. (2012), IUGR pigs, identified by their LBtW, initially displayed lower ADG from birth to the grower phase. However, by day 150, their ADG became similar to that of the normal pigs. Indeed, it was demonstrated that the influence of BtW on ADG diminishes with time and BtW is correlated to ADG only until approximately 70 days of age (Dwyer et al., 1993; Gondret et al., 2005). However, LBtW and IUGR piglets still require more days to reach the same slaughter weight of their heavier littermates (Quiniou et al., 2002 and Gondret et al., 2005) and this results in increased costs and reduced overall production efficiency.

1.6.1.3 Body composition

Results regarding the body composition in IUGR pigs are controversial and the question of whether BtW has a lasting effect on postnatal fat and muscle development remains unclear. Several studies reported that IUGR pigs, identified by their BtW, exhibit a lower proportion of muscle and a higher fat deposition compared to their heavier littermates at a constant slaughter weight (Liu et al., 2015; Krueger et al., 2014; Gondret et al., 2006). The reduced muscle mass in IUGR pigs may be partly responsible for the increased body fatness, as it results in reduced energy-consuming metabolically active tissue (Krueger et al., 2014). However, no effect of BtW on the deposition of lean and fat tissue was observed in other studies (Gondret et al., 2005; Nissen and Oksbjerg, 2011). In the study of Gondret et al. (2006), the low weight at birth unequivocally led to higher carcass fatness and lipid content in backfat and the *semitendinosus* muscle (**SM**) at the time of slaughter. Krueger et al. (2014) demonstrated that female IUGR pigs, defined by their BtW, have a reduced capacity for muscle development. The same study showed that IUGR pigs metabolize less fat than normal pigs, contributing to their higher body fat levels and resulting in accelerated fat deposition at an earlier age. Using BtW as a diagnostic method, Amdi et al. (2012) showed a higher percentage of fat tissue in LBtW (1.1 kg) piglets compared to medium-BtW (1.5 kg) and high-BtW (1.8 kg) piglets at 28 days of age. On the

contrary, in the study of Lynegaard (2020b), where IUGR piglets were identified based on their head shape rather than their BtW, no differences in fat or muscle percentage were found in relation to BtW at 24 days of age between the IUGR and the normal group.

1.6.1.4 Meat quality

As for body composition, results regarding the effect of IUGR on meat quality are controversial. Several studies have reported that growth restriction in the uterus can affect various meat quality traits, including pH (Li et al., 2015; Matyba et al., 2021), colour (Matyba et al., 2021; Cheng et al., 2020; Li et al., 2015), drip loss (Chen et al., 2023; Liu et He, 2014) and shear force (Liu et He, 2014). These effects may be linked to increased oxidative stress, reduced antioxidant capacity (Chen et al., 2023; He et al., 2023; Cheng et al., 2020), or to the presence of enlarged myofibres (Gondret et al., 2006) in the skeletal muscle of IUGR-affected pigs. Within the meat quality assessment, the pH of the *longissimus thoracis* muscle (**LT**) at 45 min and at 24 hours *postmortem* is one of the many parameters analysed. Depending on the study, the IUGR identification technique, and the slaughter weight or age, the pH in the LT of IUGR pigs can be equal to, higher, or lower than in their normal littermates. For instance, in the studies of Chen et al. (2023) and Zhang et al. (2018), where IUGR pigs were identified by their LBtW and slaughtered at day ~160, the pH did not differ from normal pigs. In contrast, Matyba et al. (2021) found higher pH levels 24 h *postmortem* in the LT of IUGR pigs, identified by both their head shape and BtW and slaughtered at day 188. Li et al. (2015) and Liu and He (2014), reported a significant decrease in the pH values of IUGR pigs, defined by LBtW and slaughtered at day 200 and at 110 kg of BW, respectively.

Similarly, conflicting results were reported about the colour of the muscle. Matyba et al. (2021) and Liu and He (2014), observed darker muscles in the IUGR group. However, in the studies conducted by Chen et al. (2023) and Li et al. (2015), the LT of the IUGR pigs showed a lighter

colour. Differences in slaughter age may influence the results. Several studies showed that older pigs tend to have lower pH, higher redness scores, and darker muscle colour (Latorre et al., 2003; Cisneros et al., 1996; Virgili et al., 2003). However, determining whether and to what extent consumers perceive the lighter or darker colour of the meat resulting from IUGR is difficult due to the subjective nature of colour perception, as well as variations in preferences influenced by culture and region.

Regarding the other parameters assessed in the meat quality analysis, in the study of Liu and He (2014), IUGR pigs exhibited a lower cooking loss, drip loss, and greater intramuscular fat content, parameters often associated with better meat quality, while the shear force was increased and consequently the meat less tender, compared to normal pigs. In contrast, Chen et al. (2023) reported significantly increased drip loss 48 h *postmortem* in the LT of IUGR pigs compared to their normal BtW littermates. However, there was no significant difference in the drip loss at 24 h *postmortem* or colour among the IUGR and normal pigs.

1.6.2 Physiology

1.6.2.1 Brain development, transcriptomic, and proteomic profile

The intrauterine environment may have an impact on the development of the foetal brain through gene expression and epigenetic modifications. These changes are thought to impair the normal development and maturation of the brain and may contribute to the foetal programming of metabolic and cardiovascular diseases (Rideau Batista Novais et al., 2016; Jahan-Mihan et al., 2015; Gatford et al., 2010).

The brain-sparing effect is a mechanism that redirects blood flow toward the brain to compensate for chronic oxygen and nutrient deprivation in the uterus (Cohen et al., 2015). While this process is crucial for safeguarding vital brain functions and ensuring the survival of the IUGR foetus, it does not guarantee normal brain development or function. Indeed, IUGR

is frequently linked to adverse motor, cognitive, and behavioural outcomes (Gilchrist et al., 2018; Mallard et al., 2000). Numerous studies, both in humans and animals, demonstrated a decrease in total brain volume following IUGR (Bie et al., 2010). Wixey et al. (2019), described neuronal and white matter impairment in the brain of newborn IUGR piglets, along with increases in activated microglia, astrocyte density, and levels of proinflammatory cytokines, suggesting a role of inflammation in the brain damage. Similarly, foetal growth restriction in rats is associated with impaired maturation of cerebral white matter, brain microstructure, and brain function/connectivity. In addition, transcriptomic analyses of the brain revealed not only a deficit in myelination in growth-restricted rats but also a significant dysregulation of genes controlling inflammation. These findings indicate a neuroinflammatory basis for the poor neurocognitive outcomes (Rideau Batista Novais et al., 2016).

1.6.2.1.1 Hippocampus

Among the brain regions, the hippocampus appears to be particularly susceptible to growth restriction in the uterus (Gilchrist et al., 2018). This area is extremely sensitive to hypoxemia, maternal corticosteroid hormones, and micronutrient deficiency, all likely to occur in IUGR pregnancies (Sizonenko et al., 2006). Lodygensky et al. (2008) detected a significant reduction in hippocampal volume in IUGR compared to normal infants, which could explain the increased occurrence of cognitive and memory dysfunction in these affected subjects (Sizonenko et al., 2006). Experiments using animal models, including, guinea pigs, sheep, rats, and rabbits indicated alterations in both the number and morphology of neurons in the hippocampus following IUGR (Gilchrist et al., 2018). The altered cellular composition and architecture of the hippocampus may result from an abnormal expression of neurotrophic factors. However, the exact cause of these structural alterations remains unclear (Gilchrist et al., 2018).

1.6.2.1.2 Hypothalamus

Another brain region of particular interest in the context of the IUGR condition is the hypothalamus. The hypothalamus is a key regulator of homeostasis; it receives and integrates a wide array of information and acts as a sensor for extracellular nutrients, humoral, and neuronal signals necessary to regulate a multitude of body functions. The hypothalamus is largely involved in energy homeostasis and feeding behaviour, as well as circadian rhythm, and stress response (Alexandre-Gouabau et al., 2012). The arcuate nucleus of the hypothalamus is the primary target for leptin, a peptide hormone released mainly from the adipocytes. Leptin regulates the balance between energy intake and utilisation by binding to hypothalamic receptors and producing a feeling of satiety (Münzberg and Gettys, 2013; Sarr et al., 2012). Attig et al. (2008) demonstrated that IUGR in female newborn piglets is associated with a lower expression of the leptin receptor gene in the arcuate nucleus. In addition, foetal growth restriction resulted in dramatic changes in the distribution of leptin receptors across different hypothalamic nuclei involved in metabolic regulation. These changes may lower sensitivity to the action of leptin and cause some of the adverse effects of IUGR such as metabolic syndrome and susceptibility to obesity (Attig et al., 2008). However, the association between IUGR and increased feed intake is not straightforward and may vary depending on complex interplay of genetic, metabolic, and environmental factors. Further research is needed to fully understand how IUGR affects feeding behaviours in pigs and its implications.

In rats, studies on the hypothalamus proteome of both newborn (Alexandre-Gouabau et al., 2012) and adult (Pedroso et al., 2017) individuals identified several differentially expressed proteins between IUGR-affected and control rats. These proteins are involved in energy and amino acid metabolism, redox status, as well as neurodevelopment.

1.6.2.2 Gastrointestinal tract development and microbial colonization

The physiology, metabolism, and growth of pigs are strongly associated with the integrity and function of the gastrointestinal tract (**GIT**) (Santos et al., 2022). The small intestine plays a vital role in the digestion, absorption, and transport of nutrients, water, and electrolytes. Moreover, it serves as a defensive barrier against both endogenous and dietary toxins, as well as antigens and pathogens (Moeser et al., 2017). The gut-associated lymphoid tissue represents the largest immune organ in the body, indicating the essential role of the GIT in host immunity (Pluske et al., 2018).

The GIT hosts a large, complex, and dynamic microbiota composed of bacteria, viruses, archaea, and fungi (Upadhaya and Kim, 2022). This microbial community is involved in the regulation of the overall health of the animal. Indeed, the GIT microbiota is essential in supporting the development and function of the immune system, it limits the nutrients available for the growth of potential pathogens and competitively excludes pathogens from binding to the gut epithelium (Maynard et al., 2012). In addition, the microbial population participates in the host's nutrient metabolism, including carbohydrate, amino acid, and lipid metabolism (Wang et al., 2020).

Growing evidence suggests that the uterine environment affects the development of the offspring's intestine. Therefore, insults during gestation can potentially compromise both its functionality and microbial colonization (Santos et al., 2022; Zhang et al., 2019). Previous research confirmed that IUGR can impair GIT development in piglets, leading to abnormal digestion and absorption. Reduced intestinal length and weight, decreased villus height, and increased crypt depth, as well as changes in the transcriptomic and proteomic profiles, were observed in IUGR-affected piglets at birth (D'inca et al., 2010; Wang et al., 2008; Wang et al., 2005) and at day 21 of age (He et al., 2011). Additionally, it appears that this impairment has long-lasting effects, resulting in a decline in villus height, decreased absorption area, and

reduced activity of key digestive enzymes in the duodenum at 70 days of age (Santos et al., 2022).

Growth restriction in the uterus also affects microbial colonization of the GIT. In the research conducted by Zhang et al. (2019), significant changes were observed in both the structure and function of the microbial community in IUGR-affected piglets, as compared to their normal counterparts. Newborn piglets with IUGR exhibited decreased microbial diversity and a distinct taxonomic profile. These changes included shifts in the relative abundances of *Firmicutes*, *Bacteroidetes, Proteobacteria, Bacteroides, Escherichia–Shigella*, and *Pasteurella*, which may have implications for nutrient digestion and absorption, inflammation, susceptibility to diseases, as well as growth and development of the piglets (Zhang et al., 2019). Specifically, piglets affected by IUGR showed a lower abundance of *Bacteroidetes* and *Bacteroides* in the jejunum at 7, 21, and 28 days of age, as well as decreased *Firmicutes* levels in the ileum at 21 days of age. Gut *Bacteroidetes* and *Bacteroides* can synthesize short-chain fatty acids (Besten et al., 2013), which contribute to intestinal health by strengthening barrier function and alleviating inflammation (Lan et al., 2023; Xiong et al., 2020). *Firmicutes* are highly abundant in the GIT of pigs and contribute to maintaining energy balance, suppressing the proliferation of opportunistic pathogens, and protecting the host from excessive intestinal inflammation (Yang et al., 2017). Conversely, IUGR-affected piglets had a higher abundance of *Proteobacteria* and *Pasteurella* in the ileum at 21 days of age and *Escherichia–Shigella* in the jejunum at 28 days of age compared to normal piglets. *Proteobacteria* include various pathogens such as *Escherichia–Shigella*, which are linked to inflammation and display negative correlations with body weight gain (Yang et al., 2021).

1.6.2.3 Blood metabolite profile

Metabolomics has the potential to identify novel biomarkers to differentiate constitutionally small from IUGR piglets and to provide insights into the underlying mechanism of the IUGR condition (Bahado-Singh; 2019). Despite the limited data on metabolomic profiling in IUGR, existing studies in both infants and piglets suggest excellent accuracy in discriminating IUGR from their healthy counterparts (Priante et al., 2019; He et al, 2011). However, interpretation of the collected data remains challenging. Primarily, there is not a standardized definition of IUGR and the diagnosis is based on different methodologies. In addition, studies are conducted at different ages (including preterm or term subjects, as well as assessments conducted within the first days after birth), using various analytical methods and sometimes small sample sizes. As a consequence, the reported findings are often inconsistent (Priante et al., 2019). Despite these constraints, the metabolic changes identified in IUGR neonates seem to indicate an early pattern of glucose intolerance, insulin resistance, altered amino acid metabolism, lipid oxidation, and abnormal liver function (Bahado-Singh et al., 2012; Priante et al., 2019). Likewise, findings in pigs suggest alterations in lipogenesis and lipid oxidation, energy, amino acid, and protein metabolism, and antioxidant capacity (He et al, 2011). These metabolic changes may contribute to the impaired development and growth of the IUGR-affected subjects. Bahado-Singh et al. (2019) identified creatinine, acetyl-carnitine, butyryl carnitine, and three lysophosphatidylcholines as the most accurate panel for diagnosing IUGR from cord blood serum. Favretto et al. (2012) identified phenylalanine, tryptophan, and glutamate that significantly contribute toward differentiating IUGR from average for gestational age foetuses. Liu et al. (2016), detected several metabolites, including alanine, methionine, ornithine, serine, tyrosine, isovaleryl carnitine, and eicosenoyl carnitine in lower concentrations in peripheral blood sampled within 3–7 days of birth in IUGR babies compared to average for gestational age newborn. In piglets, He et al. (2011), demonstrated lower concentrations in the serum of IUGR of lipids, particularly unsaturated lipids, citrate, glycerophosphorylcholine, choline,

myo-inositol, high-density lipoprotein, and inosine, while threonine and glycoproteins concentrations were elevated compared to the normal group.

1.6.2.4 Lean and adipose tissue development

Myocytes, adipocytes, and fibrocytes all originate from mesenchymal stem cells. Consequently, molecular processes that can affect the stem cell commitment to one lineage or another, directly influence the development of foetal muscle and adipose tissue during gestation (Yan et al., 2013).

1.6.2.4.1 Skeletal muscle

The shift towards myocyte production from mesenchymal stem cells is sensitive to the uterine environment and impacts the overall muscle fiber number (Yan et al., 2013). Intrauterine overcrowding has a strong effect on muscle hyperplasia in piglets, especially on the formation of secondary myofibers (Bérard et al., 2010; Foxcroft et al., 2006). In response to an imposed carbohydrate restriction, amino acids become a primary source of energy in the IUGR foetus, thus contributing to reduced muscle growth (Cortes-Araya et al., 2022). Newborn piglets that experience growth restriction during gestation typically have fewer muscle fibres, smaller muscle fiber diameters, and muscle cross-sectional area in the SM when compared to their normal littermates (Bérard et al., 2010; Alvarenga et al., 2013; Felicioni et al., 2020). Some authors suggest that the lower number of muscle fibres at birth cannot be fully compensated for by postnatal growth, resulting in lower muscle mass and greater susceptibility to fat deposition in the long term (Liu et al., 2015; Krueger et al., 2014; Gondret et al., 2006). However, despite having a lower number of fibres at birth, IUGR and LBtW pigs exhibit myofiber diameters equal to or even larger than those of their heavier littermates at a constant slaughter weight (Dwyer et al., 1993; Gondret et al., 2006; Alvarenga et al., 2013; Felicioni et al., 2020). This suggests that muscle hypertrophy, as opposed to hyperplasia, is not impaired

but rather enhanced by growth restriction in the uterus. Moreover, this finding is supported by the study conducted by Felicioni et al. (2020), which observed a similar gene expression pattern in the SM during the hypertrophy period (100-150 days of age) between IUGR and normal pigs. A higher rate of hypertrophy associated with fewer muscle fibres could compensate for the limited fiber count without affecting lean and fat deposition. This may explain why no differences in muscle and fat percentages were observed in other studies between IUGR and normal pigs (Gondret et al., 2005; Lynegaard et al., 2020b).

1.6.2.4.2 Adipose tissue

Adipose tissue development begins during the prenatal phase and is significantly influenced by the uterine environment. Several studies proposed that exposure to an adverse uterine environment during gestation can alter the development and proliferation of adipocytes (Sarr et al., 2012; Gondret et al., 2011; Attig et al., 2008). Conditions such as chronic oxygen deprivation and limited nutrient availability during gestation trigger metabolic and endocrine adaptations intended to improve the foetus's chances of survival. Within these adaptations, an increased adipocyte proliferation was observed. This foetal adaptative reaction can improve the long-term ability to store lipids and consequently the survival of the foetus under conditions of intermittent or poor nutrition (Sarr et al., 2012; Attig et al., 2008). However, when normal nutrition is restored in the postnatal environment, the changes adopted by the foetus before birth may lead to a nutritional mismatch between energy intake, storage, and expenditure, resulting in excess adiposity (Sarr et al, 2012; Attig et al., 2008). Gondret et al. (2011) suggested a delay in adipose tissue differentiation, with a prolonged preadipocyte state in small pig foetuses compared to their heavier littermates. This hypothesis is supported by reduced expression of genes associated with later stages of adipocytic differentiation in the subcutaneous backfat of smaller foetuses at day 75 of gestation. Attig et al. (2008) observed that an alteration in the adipose tissue structure is still evident two weeks after birth. In their

study, IUGR piglets showed a higher density of small white adipocytes compared to the controls, suggesting ongoing cell proliferation after birth in IUGR subjects. These adipocytes are probably less effective at ensuring lipid storage, as reflected by their smaller size and the presence of higher levels of circulating triglycerides in the blood of IUGR piglets (Attig et al., 2008). In growing pigs, several studies reported an overall increase in fat deposition and the presence of enlarged adipocyte diameters in the adipose tissues of IUGR pigs compared to the controls (Liu et al., 2015; Gondret et al., 2006). Moreover, Gondret et al. (2006) showed increased lipogenic enzyme activities in the backfat of LBtW pigs, indicating a greater potential for fatty acid synthesis.

2. Objectives and hypotheses

2.1 General objectives and hypotheses

The primary objective of this Ph.D. thesis was to develop a model for the accurate and non-invasive diagnosis of IUGR in newborn piglets. This research aimed to further characterise the IUGR subpopulation from a physiological perspective and provide insights into the underlying mechanisms of this condition. In the long term, the accurate diagnosis and characterisation of IUGR-affected pigs will facilitate the development of targeted postnatal interventions aimed at effectively treating these animals. Moreover, due to the similarities in terms of organ development, metabolism, and placental structure, the short gestation period, and the spontaneous occurrence of placenta insufficiency, pigs represent a highly relevant model of human IUGR.

The first hypothesis of this Ph.D. thesis was **that relying solely on current diagnostic techniques might not always provide an accurate diagnosis of IUGR in piglets**, potentially leading to misclassification of this condition. Given that an increased brain-to-liver weight ratio (**BrW/LW**) is the main feature of IUGR, we regarded it as the gold standard for diagnosis and further hypothesized that **it is possible to estimate this ratio and diagnose IUGR accurately from images of newborn piglets**, thus eliminating the need for animal sacrifice. Finally, based on an extensive review of the existing literature, we formulated our third hypothesis, suggesting that **the IUGR condition has a long-lasting and negative influence on a wide range of physiological functions in pigs, ultimately resulting in impaired growth, altered gut microbiota, and blood metabolome profile.**

To test our hypotheses, two animal experiments were conducted. In the first experiment, piglets underwent CT scan imaging at birth to assess the BrW/LW and accurately diagnose IUGR.

Photos of all of the piglets were also captured at birth. The pigs were then monitored throughout the whole production cycle and data regarding growth, feed intake, body composition, faecal microbiota, blood metabolome, and meat quality were collected. In the second experiment, piglets with a BtW below 1 kg, born within a 5-month timeframe, were selected for brain and liver sampling to assess the BrW/LW. In addition, photos of the same piglets were captured at birth. The data collected in the two experiments were used to address our research questions in three separate studies focused on the diagnosis (manuscript I and II) and the characterisation (manuscript I and III) of IUGR pigs. According to our knowledge, this is the first time that the effects of IUGR have been evaluated based on the piglets' BrW/LW at birth.

2.2 Specific objectives and hypotheses

2.2.1 Diagnosis

2.2.1.1 Evaluation of the current diagnostic techniques

In pigs, IUGR occurs spontaneously, mainly as a result of uteroplacental insufficiency. The altered placenta reduces the availability of oxygen and essential nutrients for the developing foetus. Consequently, adaptive responses are triggered to preserve brain functionality and enhance the survival chances of the foetus. A redirection of the blood flow named the "brain-sparing effect" takes place and prioritises brain development over the rest of the body, resulting in a relatively larger brain at birth. Among the other organs, the development of the liver, as well as its functioning, is one of the most affected by the altered blood circulation. Hence, an increased BrW/LW at birth represents a highly significant indicator of IUGR in piglets.

Head shape and BtW are commonly used criteria for diagnosing IUGR in newborn piglets due to their practical measurement on farms and in the research context. However, while growth restriction in the uterus often leads to LBtW, studies have demonstrated the existence of

neonates that are constitutionally small without experiencing any nutrient and oxygen deprivation during gestation. Similarly, characteristic morphological features of the head normally associated with IUGR may be simply linked to natural variations in the head shape unrelated to any pathology. For these reasons, **our first hypothesis was that relying solely on BtW or head shape is not enough to guarantee an accurate and reliable diagnosis of IUGR**. To test this hypothesis, the data collected during the first animal experiment through CT imaging were used to compare the diagnoses based on BrW/LW, BtW, and head shape. The results of this study are reported in manuscript I.

2.2.1.2 Development of a new diagnostic technique

Employing the brain-to-organ weight ratio for the identification of IUGR piglets provides an objective approach as it directly reflects the brain-sparing effect. However, the application of the ratio as a diagnostic method is currently limited as it requires the utilisation of advanced imaging techniques or the euthanasia of newborn piglets. **The second main hypothesis of this Ph.D. thesis was that using specific morphometric traits, the weight of the brain (BrW), that of the liver (LW), and their ratio could be estimated with sufficiently high accuracy from images of newborn piglets, enabling non-invasive and accurate diagnosis of IUGR**. To test this hypothesis, the images collected in both the first and second animal experiments were used to capture specific morphometric traits such as distance between the ears, abdominal area, and front head diameter and used to predict the BrW and LW, as well as their ratio. The results of this study are reported in manuscript II.

2.2.2 Characterisation

Our third hypothesis was that the IUGR condition has a long-lasting and negative influence on a wide range of physiological functions in pigs, ultimately resulting in impaired growth, altered gut microbiota, and blood metabolome profile.

2.2.2.1 Growth and body composition

In relation to our third hypothesis, we expected that **piglets exposed to IUGR would exhibit reduced growth rates compared to their normal littermates, leading to consistently lower BWs throughout the whole production cycle**. **Additionally, we hypothesized that altered nutrient partitioning during growth restriction would lead to reduced feed efficiency and nutrient utilisation in postnatal life.**

Newborn piglets experiencing IUGR typically exhibit fewer muscle fibres, smaller fiber diameters, and reduced muscle cross-sectional area compared to their normal littermates at birth. Most authors suggest that this reduction in fiber number cannot be compensated through postnatal growth. Furthermore, metabolic adaptations in response to IUGR, intended to improve foetal survival, include increased adipocyte proliferation that continues during postnatal life. As a consequence, in line with our third hypothesis, we expected **IUGR-affected pigs to have a lower percentage of lean tissue and an increased susceptibility to fat deposition compared to their normal littermates**.

Finally, we expected **IUGR to influence *postmortem* biochemical changes**, **negatively impacting meat quality traits, including pH levels, water-holding capacity, colour, and texture of the meat**.

To test these hypotheses, the data collected during the first animal experiment were used to accurately diagnose IUGR and to compare growth rates, feed intake, feed efficiency, body composition, energy, and protein efficiency, as well as meat quality traits between IUGR and normal pigs. The results of this study are described in manuscript I.

2.2.2.2 Faecal microbiota and blood metabolome

An adverse uterine environment can affect the development of the GIT and compromise both its functionality and microbial colonization. Growth restriction during foetal development results in changes in the structure and function of the intestinal mucosa, impairing nutrient absorption and barrier function. These changes are likely to affect the proliferation of specific bacterial populations within the gut, influencing the overall composition of the microbiota. In the context of our third hypothesis, we expected a **decreased microbial diversity and shifts in the abundances of bacterial taxa involved in nutrient digestion and absorption, inflammatory responses, and susceptibility to diseases, such as *Bacteroides*, *Ruminococcus*, *Prevotella*, *Escherichia–Shigella*, and *Pasteurella* in IUGR compared to normal pigs.**

Moreover, recent findings demonstrated that IUGR influences blood metabolomics. Considering the nutrient and oxygen deprivation during gestation and the metabolic mechanisms established in response to growth restriction, we also expected clear differences in the blood metabolome between IUGR and normal pigs. Specifically, **we hypothesized alterations in metabolite concentrations related to lipid oxidation, such as increased plasma glycerol, 3-hydroxybutyrate, and acetate, as well as changes in energy and amino acid metabolism, including reduced levels of plasma glucose and essential amino acids, and elevated levels of lactate**. To test these hypotheses, the data collected during the first animal experiment were used to accurately diagnose IUGR and to compare faecal microbiota and plasma metabolome at different time points between IUGR and normal pigs. The results of this study are detailed in manuscript III.

3. Manuscript I

Intrauterine growth restriction defined by increased brain-to-liver weight ratio affects postnatal growth and protein efficiency in pigs

R. Ruggeri[a, b], G. Bee[a], P. Trevisi [b], C. Ollagnier[a]

[a] *Swine Research Unit, Agroscope, Route de la Tioleyre 4, 1725 Posieux, Switzerland*

[b] *Department of Agricultural and Food Sciences (DISTAL), University of Bologna, viale G Fanin 44, 40127 Bologna, Italy*

Abstract

Intrauterine growth restriction (IUGR) refers to impaired foetal growth during gestation, resulting in permanent stunting effects on the offspring. This study aimed to investigate the effects of IUGR on growth performance, body composition, blood metabolites, and meat quality of pigs from birth (n = 268) to slaughter (n = 93). IUGR piglets have prioritised brain development as a foetal adaptive reaction to placental insufficiency. This survival mechanism results in a higher brain-to-liver weight ratio (BrW/LW). One day (± 1) after birth, computed tomography (CT) was performed on each piglet to assess their brain and liver weights. A threshold value of 0.78 (mean + SD) was chosen to divide the piglets into two categories – NORM (BrW/LW < 0.78) and IUGR (BrW/LW > 0.78). Moreover, each piglet was classified as either normal (score 1), mild IUGR (score 2), or severe IUGR (score 3) based on the head morphology. Body weight (BW) was recorded weekly, and average daily gain (ADG) was calculated for lactation, starter, grower, and finisher periods. Body composition was assessed after weaning (29.6 ± 0.7 d), at 20 kg (64 ± 7.2 d), 100 kg (165 ± 12.3 d), and on the carcasses using Dual-energy X-ray absorptiometry (DXA). Content and deposition rates of single

nutrients, as well as energy and crude protein (CP) efficiency, were measured at 20 and 100 kg. Feed intake was recorded from 20 kg to slaughter. Meat quality was assessed on the carcasses. A total of 70% of the piglets assigned a score of 3 were NORM according to their BrW/LW. The IUGR category showed a lower ADG in the lactation ($P < 0.01$), starter ($P = 0.07$), and grower phases ($P < 0.05$) and a reduced CP efficiency in the grower–finisher period ($P < 0.01$) compared to the NORM group. IUGR pigs had a lower gain-to-feed ratio in the finisher period ($P = 0.01$) despite similar average daily feed intake (ADFI), and they required more days ($P < 0.01$) to reach the slaughter weight. Additionally, their meat was darker ($P = 0.01$) than that of NORM pigs. The BrW/LW was inversely proportional to the ADG from birth to slaughter and negatively correlated with the CP deposition rate and efficiency in the grower–finisher period ($P < 0.01$). Furthermore, the higher the BrW/LW, the longer it took the pigs to reach the slaughter weight ($P < 0.01$). In conclusion, the identification of IUGR piglets based on head morphology does not always agree with an increased BrW/LW. IUGR affects growth performance from birth to slaughter, CP efficiency in the grower–finisher period, and meat quality.

Implications

Modern pig breeds show an increased percentage of piglets born undersized and exposed to IUGR. This condition is characterised by relative brain-sparing, while the liver is primarily affected by oxygen and nutrient deprivation. Employing the BrW/LW for the identification of the affected piglets provides an objective approach as it directly reflects the brain-sparing effect. Our study showed that the identification of growth-restricted piglets based on head shape or birth weight is not always consistent with a high ratio. Affected pigs exhibited reduced ADG, crude protein (**CP**) efficiency, and required more days to reach the target slaughter weight.

Introduction

The number of pigs produced per sow per year is a fundamental economic driver in the pig industry. One of the first objectives of the modern pig production system is to increase the number of weaned piglets per litter (Hansen et al., 2018). The increase in litter sizes has led to markedly lower BtW and an increased percentage of piglets born undersized and exposed to different degrees of growth restriction in the uterus (Amdi et al., 2013; Hansen et al., 2018). IUGR is defined as the impaired growth of the mammalian foetus during gestation (Wu et al., 2006). The principal cause behind this condition is an insufficiency of the placenta, which does not allow for an appropriate distribution of oxygen and nutrients to the foetus (Cohen et al., 2015). In the modern pig industry, 20-30% of newborn piglets are affected by IUGR (Lynegaard et al., 2020a; Amdi et al., 2013; Wu et al., 2006), and they usually show high morbidity and mortality, impaired metabolism, stunted growth and muscle development, reduced feed conversion efficiency (Krueger et al., 2014) and poor carcass quality (Wang et al., 2013; Wu et al., 2006). In order to develop effective management interventions to treat this condition, reliable tools are needed to identify IUGR-affected piglets (Amdi et al., 2013). Accurate diagnosis of piglets affected by IUGR holds the potential to provide physiological characterisation and valuable insights into the condition. This could facilitate the development of targeted and innovative strategies aimed at effectively treating them.

Different authors have characterised IUGR piglets based on their head morphology (Chevaux et al., 2010; Hales et al., 2013; Hansen et al., 2018). Compared to non-IUGR pigs, those suffering from growth restriction in the uterus show a dolphin-like head shape, bulging eyes, and wrinkles perpendicular to the mouth. Apart from these phenotypic traits, IUGR piglets prioritise brain development as part of a foetal adaptive reaction to placental insufficiency (Amdi et al., 2013). This survival mechanism is defined as “brain-sparing effect” and results in a relatively larger brain compared to other organs, such as the liver (Cohen et al., 2015; Matheson et al., 2018). For this reason, the optimal metric for identifying the degree of IUGR

considers the ratio between the weight of the brain and other organs (Felicioni et al., 2019). Nevertheless, to assess this ratio, newborn piglets must be euthanised. Consequently, this approach is feasible only in research contexts. The lack of more accurate and non-invasive methods to diagnose IUGR still makes this condition a major challenge in both human and animal health (Felicioni et al., 2019), as the development of management interventions is limited by poor diagnosis.

Our first hypothesis was that an increased BrW/LW does not always align with morphological alterations of the head shape or with a low BW at birth. The second hypothesis was that IUGR, defined by a high BrW/LW, has a long-lasting detrimental effect on the development of the progeny. To test the first hypothesis, this descriptive study used CT scan imaging as a non-invasive method to assess the BrW/LW in newborn piglets. As for the second hypothesis, a comprehensive investigation was conducted into how IUGR affects growth performance, body composition, blood metabolite traits, and meat quality in pigs from birth to slaughter.

Material and methods

Animal selection and classification

This experiment was performed at the Agroscope swine research facility in Posieux, Switzerland. In this study, 268 Swiss Large White piglets (females = 134 and males = 134) originating from 26 litters from two farrowing series (first farrowing series = 14 litters, second farrowing series = 12 litters) were included. On the day of farrowing (day 0), the BtW of each piglet was recorded. Piglets with a BtW < 1.1 kg were assigned to the low-BtW category (Low BtW), whereas those with a BtW > 1.1 kg were assigned to the normal-BtW category (Normal BtW). On day 1 (± 1) after birth, piglets were visually classified as either normal (score 1), mild IUGR (score 2), or severe IUGR (score 3) based on the morphological characteristics of the

head (Chevaux et al., 2010; Hales et al., 2013; Hansen et al., 2018). The morphological characteristics of the head of an IUGR piglet are described as follows – dolphin-like head shape, bulging eyes, hair with no direction of growth, and wrinkles perpendicular to the mouth. If none of the IUGR characteristics were identified, the piglet was defined as normal and assigned a score of 1. The piglet was classified with a score of 2 when one of the characteristics was present. Finally, a score of 3 was assigned when two, three or all the characteristics were present.

In addition to visual scoring, CT scan imaging (64-channel multislice scanner Siemens Emotion Duo CT, Siemens, Erlangen, Germany) was performed on all piglets on day 1 (± 1) after birth to non-invasively assess the volume of the brain and liver. For the CT measurements, all the animals were anaesthetised by isoflurane inhalation and positioned in sternal recumbency. Images of the head and thoracic regions were obtained. The raw image sequences were semi-automatically segmented to obtain the volume of the two organs (Turtleseg software 1.2.1). After the CT scan, 30 piglets were euthanised with an intra-cardiac injection of pentobarbital solution (Esconarkon, volume to effect). Three BtW categories (category 1 < 1.1 kg; category 2 ≥ 1.1 and < 1.8 kg; category 3 ≥ 1.8 kg), were defined to cover the full range of BtWs present in the actual population. From each BtW category 10 piglets were euthanised paying attention to keep a balanced female-to-male ratio (Supplementary Table S1). After euthanasia, the brain and the blood-filled liver were excised. The brain and liver weights were assessed with a scale, and the volume was determined using the water displacement method. The density of the organs was determined by calculating the ratio of their mass to volume using the equation: d = m (g) / V (mL), where d represents the organ density, m represents the mass in g, and V the volume of the organ in mL. The average brain and liver density, together with the brain and liver volumes obtained from the CT scan images, were used to determine the brain and liver weights and the BrW/LW. The average BrW/LW determined in 217 piglets was 0.63 ± 0.15 [mean ± SD].

Piglets with a BrW/LW ≥ 0.78, which correspond to the mean + one SD, were assigned to the IUGR category (IUGR; n = 32), whereas those with a BrW/LW < 0.78 were assigned to the "normal" category (NORM; n = 185). The threshold was calculated on the population surviving after weaning, considering the high preweaning mortality rate of severe IUGR until weaning (Farmer and Edwards, 2022). Indeed, piglets that were euthanised (n = 30) or died before weaning (n = 21), as well as stillborn piglets (n = 43) were excluded when determining the BrW/LW threshold. While we acknowledge the potential bias resulting from this exclusion, setting the threshold based on the surviving population includes moderately severe IUGR cases, allowing to investigate the long-term effects of the condition.

The pigs (n = 217) were weaned at 25.2 ± 1.2 days of age. Two piglets (IUGR = 1, NORM = 1) died in the postweaning phase and were not included in the statistical analysis of the starter period.

On day 73 ± 6.4 of age (24 ± 5.3 kg BW), a group of 96 piglets were selected for the grower–finisher phase. As at the time of selection, the CT scan results were not available, the selection relied on traditional traits, namely IUGR score and BtW. The group consisted of 48 castrated males and 48 females. For the selection, all the weaned piglets were first split into two groups according to their sex, castrated males and females. Within each sex, piglets were ranked by decreasing score and then by increasing BtW. The first 24 piglets with the highest IUGR score and lowest BtW were selected for finisher. Similarly, the last 24 pigs with the lowest IUGR score and highest BtW were also selected. The selection process was repeated for each sex (see Supplementary Table S2). Three pigs (NORM = 3) died before the end of the grower period and were not included in the statistical analysis of the grower–finisher period.

Rearing conditions during lactation, starter, grower, and finisher periods

During the whole experiment, *ad libitum* access to water was ensured through nipple drinkers or drinking troughs. Straws was always placed in pens to enrich the environment. The pigs were monitored daily for their health status by trained personnel.

The sows were housed in individual farrowing crates, starting 10 days before the expected farrowing time. During the entire lactation period, the sows were left free in the pen. Each farrowing crate was provided with a heated and covered nest for the piglets. Within the first 14 hours after birth, all the piglets were ear-tagged and treated with an iron injection (Ferridex® 10%, AMAG Pharmaceuticals, Inc., Waltham, USA). Male piglets were castrated under general anaesthesia 48 hours after birth and treated with ketofen (3mg/kg, Rifen®, Streuli Tiergesundheit AG, Uznach, Switzerland) for pain control. The temperature in the nest was 40°C immediately after birth and then gradually decreased daily by 0.5°C to reach a temperature of 32°C on day 16.

The temperature in the farrowing rooms was set to 24°C, and artificial lights were kept on from 8 am to 5 pm. Parturition was induced when gestation time exceeded 116 days by an intramuscular injection of 1 mL (0.25 g/mL) of cloprostenol (Estrumate®, MSD Animal Health GmbH, Luzern, Switzerland). The piglets were kept with their dam until day 25.2 ± 1.2 days of age.

All the pigs were housed by litter until 39.2 ± 1.3 days of age (approximately two weeks after weaning), then kept in groups of 12 piglets per pen until they reached an average BW of 24 ± 5.3 kg. The 96 pigs selected for the finisher period were housed in two large connected pens (17.35 m^2).

Growth performance and feeding

Piglets had *ad libitum* access to a standard pre-/early postweaning diet from day 16 after birth to 14 days postweaning (39.2 ± 1.3 days of age, 7.5 ± 1.5 kg BW [mean ± SD]). Subsequently,

they were offered *ad libitum* access to a starter diet until the start of the grower period (73 ± 6.4 days of age, 24 ± 5.3 kg BW [mean ± SD]). Piglets were switched to the grower diet when their BW was ≥ 20 kg at the day of the weekly weighing. The pre-/early postweaning feed, as well as the starter diet, was available through feeding troughs (Suisag, Sempach, Switzerland; Krieger AG, Ruswil, Switzerland). Fresh pre-/early postweaning feed was provided at least once a day, and leftovers were removed every day from day 16 to 39.2 ± 1.3 days of age. However, the feed intake during this period was not determined in this study.

In the grower and finisher periods, each pen was equipped with four automatic feeders and an individual pig recognition system (Schauer Maschinenfabrik GmbH & Co. KG, Prambachkirchen, Austria). The feeder allowed monitoring of the individual daily feed intake and the ADFI. The grower and finisher diets were offered from 24 ± 5.3 to 63.3 ± 2.1 kg and from 63.3 ± 2.1 to 108.3 ± 4.2 kg (mean ± SD), respectively. The ingredients used to formulate the pre-/early post-weaning, starter, grower, and finisher diets and the nutrient composition are presented in the supplementary materials (Supplementary Table S3). Starting from week 2 after birth, the pigs were weighed individually once a week until slaughter. The ADG was measured for each period (lactation, starter, grower, and finisher). Moreover, the feed intake was recorded from 20 kg until slaughter, and the gain-to-feed ratio was calculated for each pig.

Body composition

A GE lunar DXA (i-DXA, GE Healthcare Switzerland, Glattbrugg, Switzerland) with a narrow-angle fan beam (Collimator Model 42129) was used to scan live pigs right after weaning (n = 217; 29.6 ± 0.7 days, [mean ± SD]) at the start of the grower period (n = 90; BW ≥ 20 kg at the day of the weekly weighing; 64 ± 7.2 days [mean ± SD]) and before slaughter (n = 90; BW ≥ 100 kg at the day of the weekly weighing. 165 ± 12.3 days [mean ± SD]) as well as the carcasses (n = 88). The procedures to handle the pigs and the carcasses and to analyse the DXA scan

images have been described in detail by Kasper et al. (2021). Briefly, on the day of the scan, the pigs were anesthetized with isoflurane inhalation and then DXA scanned in sternal recumbency, with both the fore legs and the hind legs extended and pointed caudally. The window chosen for the analysis was the entire body scan in thick mode.

The half carcasses (left side) were scanned the day after slaughter. The pigs were slaughtered after 16 h of feed withdrawal at the Agroscope abattoir by exsanguination after CO_2 stunning. Immediately after exsanguination, the hair was removed and the animals were eviscerated. The carcass and head were sawed into two halves and chilled at 2°C. The scanned images from live animals and carcasses were processed to remove artefacts and position the regions of interest. The DXA output variables total mass, total lean mass, total fat mass, total bone mineral content and total bone mineral density were exported from the enCORE software and assessed at weaning, at the start of the grower period, before slaughter and in the carcass halves. Using the equations developed by Kasper et al. (2021), the total mass, total lean mass, total fat mass, and total bone mineral content were used to determine the water, ash, CP, lipid, and energy content of the empty body of the live animals at the start of the grower period, at the end of the finisher period, and of the carcasses. The energy, CP, and fat daily deposition rates, as well as the energy and crude protein efficiency, were assessed for the grower–finisher period. The equations published by Kasper et al. (2021) were validated within a range of 20–100 kg of BW and on the carcasses, thus limiting their applicability in estimating single nutrient content at weaning. Therefore, it was not possible to determine the water, ash, CP, lipid, and energy content of the empty body at weaning.

Blood metabolite traits and blood cell count

The pigs were slaughtered 16 h after feed withdrawal. Blood was sampled from the pigs (n = 91) at the slaughterhouse during bleeding. However, the time at which each pig consumed its

last meal before the feed withdrawal was not standardized. Blood was collected using Vacuette blood collection tubes with a serum clot activator for serum or ethylenediaminetetraacetic acid (**EDTA**) for native blood sampling (Greiner Bio-One GmbH, Kremsmünster, Austria). Serum tubes were stored upside down at room temperature for 1 h prior to centrifugation for 15 min at 3000 g and subsequently for 2 min at 4000 g. Two aliquots of serum were stored at -20° in Eppendorf tubes. The EDTA tubes were kept on ice until analysis and processed within 2 hours after collection with a Vetscan HM5 haematology analyser (Abaxis Inc., Union City, USA). The serum samples were assayed using commercially available kits according to the manufacturer's instructions on a BT1500 autoanalyzer (Biotecnica Instruments Ltd., Roma, Italy) to determine urea (Greiner Diagnostic GmbH, Langenthal, Switzerland) and non-esterified fatty acid (Randox Laboratories Ltd., Crumlin, UK) concentrations. Moreover, from the EDTA samples, the concentrations of glucose, haemoglobin, haematocrit, mean corpuscular haemoglobin, mean corpuscular haemoglobin concentration, mean corpuscular volume, and the count of granulocytes, lymphocytes, monocytes, platelets, red blood cells, and white blood cells were assessed. Serum insulin concentration was measured using a Porcine Insulin Kit (Mercodia, Uppsala, Sweden) following the manufacturer's instructions adapted to the use of a Crocodile 4-in-one assay mini workstation (Berthold GmbH, Bad Wildbad, Germany). Absorbance was read with an Asys UVM340 microplate reader in combination with the MikroWin 2000 software (Biochrom Ltd., Cambridge, UK).

Meat quality

After slaughter, temperature and pH were monitored at 45 min and 24 h *postmortem* in the LT (at the 10th rib level; n = 91) using a Testo 205 pH meter (Testo Inc., Lenzkirch, Germany). One day after slaughter, the LT was excised from the left carcass side at the 8th to 10th rib level, and 5 × 1.5 cm thick chops were cut for further analysis. The first chop was immediately

vacuum-packaged and stored at -20°C for chemical analysis. Two chops were used to assess the quantity of purge generated during storage at 4°C for 48 h, expressed as a percentage of the initial sample weight (Honikel 1998). The colour was assessed after a 20 min bloom period on the two other chops using a CM-700d Chroma Meter (Konica, Minolta, Tokyo, Japan) in the CIE lightness, redness, and yellowness colour space. Three replicated measurements were performed on each sample. Afterward, the chops were blotted-dry weighed, vacuum-packaged, and then stored for 24 h at 2°C. At the end of this aging period, the meat slices were frozen and stored at -20°C. Within one month after slaughter, these chops were thawed for 24 h at 2–4°C in vacuum plastic bags, blotted dry, and weighed to assess the thaw loss. The chops were then cooked for 5 min on a preheated (170°C) Indu-Griddle grill (SH/GR 3500, Schöhbühl, Switzerland) to a core temperature of 69 ± 2°C and reweighed to determine cooking loss. After being kept at room temperature for 2 h, the Warner-Bratzler shear force was measured in cooked chops using a Texture Analyzer TA HD plus (Stable Micro Systems, Goldaming, UK) equipped with a 2.5-mm-thick Warner-Bratzler shear blade.

Statistical analysis

All calculations and statistical analyses were performed using R (version 4.0.2). The data were analysed with linear mixed-effect models using the "lmer" function of the lme4 package. For the BW analysis during lactation, starter, grower, and finisher phases, the IUGR category (IUGR, NORM) or BrW/LW, sex (female, castrate), and age and their two- and three-way interactions were considered fixed effects. The interactions were tested and removed if not significant. Age and piglet ID nested into the litter of origin were considered random effects using piglet ID nested into the litter of origin as the grouping factor. The lmer models were routinely checked for the normality of the residuals and the homoscedasticity. If the fixed factors were significant, multiple comparisons were performed using the modified Tukey test

from the emmeans package. For the rest of the data, the IUGR category (IUGR, NORM) or the BrW/LW and sex (female, castrate) were considered fixed effects and the litter of origin as a random effect. The two-way interaction between the two fixed effects was always tested and removed if not significant. The pig was considered the experimental unit.

Data for ADG were analysed separately for the lactation, starter, grower, and finisher periods, and those for daily feed intake, and gain-to-feed ratio were analysed for the grower and finisher periods. The DXA results at weaning, at the start of the grower period, before slaughter, and of the carcasses were analysed separately. For the pigs whose DXA results were available at the start of the grower period and at slaughter, nutrient and energy content, deposition rates as well as energy and CP efficiency were calculated. The content of nutrient and energy in the empty body was calculated from the DXA output variables total mass, total lean mass, total fat mass, and total bone mineral content. The rates of nutrient and energy deposition were determined by dividing the difference in nutrient and energy content in the empty body at 100 and 20 kg of BW by the total nutrient and energy intake between the two DXA scans. The daily nutrient deposition rates were calculated by dividing the deposition by the number of days on feed between the two DXA scans. Energy and CP efficiency were calculated by dividing the energy and CP deposition between 20 and 100 kg of BW by the total energy and CP intake between the two DXA scans. For the haematological data, the value of the lower limit of quantification was considered for measurements that were quantifiable but below the value itself. Values below the lower limit of detection were assigned a value of 0. In addition, for the statistical analysis of meat quality, the day of slaughter was set as a random effect together with the litter of origin. The results are presented as least square means and pooled SEM. The IUGR category, BrW/LW and sex effects were considered different at $P \leq 0.05$.

Results

Intrauterine growth restriction classification

On average, IUGR piglets had 55% greater BrW/LW ($P < 0.01$) and 29% lower BtW ($P < 0.01$) compared to NORM pigs (Table 1). In total, 114, 83, and 20 piglets were assigned scores 1, 2, and 3, respectively. Of the NORM pigs, 91% and 81% had scores of 1 and 2, respectively. The remaining pigs were IUGR pigs. Interestingly, 70% of the piglets with a score of 3 were NORM pigs, as they had a BrW/LW < 0.78 (Fig. 1). Out of the 217 pigs, 12 piglets had a BtW < 1.1 kg; however, three were NORM pigs, which led to a misclassification of 25% of the IUGR piglets using the BtW classification.

Table 1. Effect of classifying the pigs based on the brain-to-liver weight ratio (BrW/LW), head shape, birth weight (BtW), and sex on the BrW/LW and the BtW.

	BrW/LW[1]		Sex			P-value[2]	
Item	IUGR	NORM	Female	Castrate	SEM[3]	BrW/LW	Sex
Number of pigs	32	185	115	102			
BrW/LW	0.90	0.58	0.74	0.73	0.018	< 0.001	0.45
BtW	1.23	1.59	1.39	1.42	0.043	< 0.001	0.37
	Head shape[4]			Sex		P-value[5]	
	Score 1	Score 2	Score 3	Female	Castrate	SEM	Head shape	Sex
Number of pigs	114	83	20	115	102			
BrW/LW	0.58	0.66	0.76	0.67	0.66	0.032	< 0.001	0.82
BtW	1.63	1.47	1.28	1.45	1.47	0.057	< 0.001	0.50
	Birth weight[6]		Sex			P-value[7]	
	Low BtW	Normal BtW	Female	Castrate	SEM	BtW	Sex
Number of pigs	12	205	115	102			
BrW/LW	0.87	0.61	0.74	0.74	0.041	< 0.001	0.93
BtW	1.01	1.57	1.28	1.30	0.071	< 0.001	0.62

[1] BrW/LW: IUGR: piglets with a BrW/LW ≥ 0.78; NORM: piglets with BrW/LW < 0.78.

[2] P-value for the main effect of the BrW/LW and sex.

[3] Pooled SEM.

[4] Head shape based on the morphological characteristics of the head (Chevaux et al., 2010; Hales et al., 2013; Hansen et al., 2018): score 1: “normal” piglet, score 2: mild intrauterine growth restriction (IUGR); score 3: severe IUGR.

[5] P-value for the main effect of head shape classification and sex.

[6] Birth weight: low BtW: piglets with BtW < 1.1kg; normal BtW: piglets with a BtW ≥ 1.1kg.

[7] P-value for the main effect of BtW and sex.

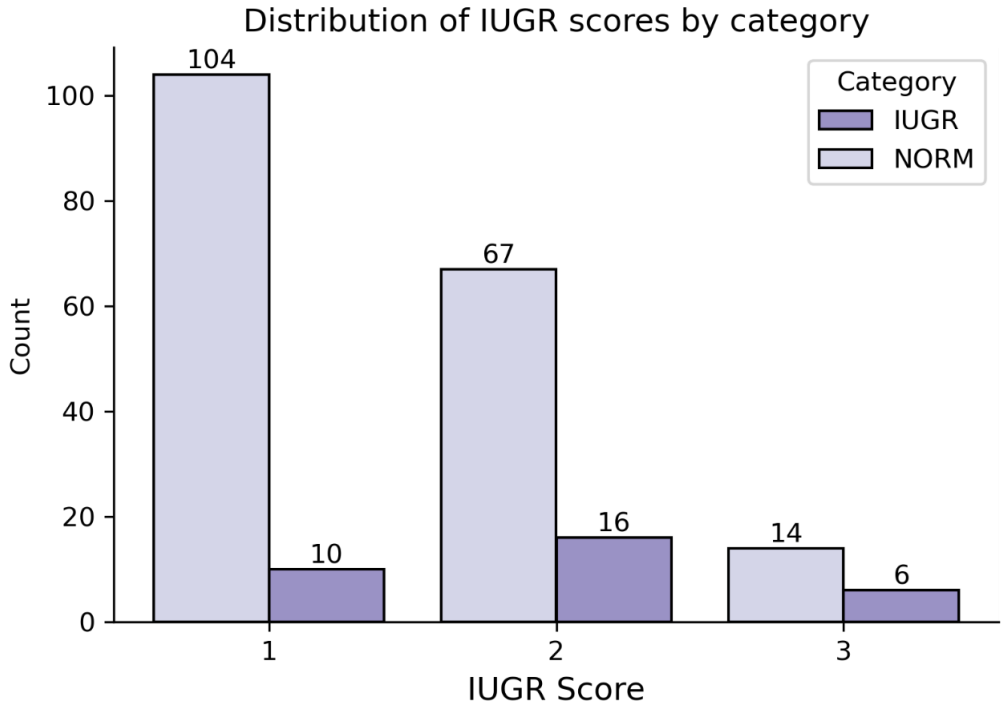

Fig. 1. Comparison between the classification of intrauterine growth restriction (IUGR) based on the head shape of the piglets (score 1,2 and 3) and the classification based on the brain-to-liver weight ratio (BrW/LW; IUGR and NORM). X-axis: IUGR: piglets with a BrW/LW ≥ 0.78; NORM: piglets with BrW/LW < 0.78; head shape based on the morphological characteristics of the head (Chevaux et al., 2010; Hales et al., 2013; Hansen et al., 2018): score 1: “normal” piglet, score 2: mild IUGR; score 3: severe IUGR. Y-axis: number of pigs (count).

Growth performance traits from birth to slaughter

Compared to the NORM pigs, the IUGR pigs weighed, on average, 1.1 kg less at weaning ($P < 0.01$), as their ADG during lactation was 37 g/d lower ($P < 0.01$, Table 2). Likewise, from weaning to the start of the grower period, the IUGR pigs grew slower than the NORM pigs, as they tended to display a 27 g/d lower ADG ($P = 0.07$, Table 2). At the end of the starter period, IUGR females weighed 3.4 kg less ($P < 0.01$) than their NORM counterparts. By contrast, IUGR castrates were 2.7 kg lighter ($P = 0.01$) than the NORM castrates, which explains the significant interaction ($P = 0.03$) between category (IUGR and NORM) and sex. Similarly, the BrW/LW was inversely proportional ($P < 0.01$) to the ADG in both the lactation and starter periods (Fig. 2). At the start of the grower period (23.5 ± 1.41 kg BW [least square mean ± SEM]), the IUGR pigs were 4.1 days older ($P = 0.03$) than the NORM pigs. As the study progressed, the age difference between the groups continued to increase, reaching an additional 4 days by the start of the finisher period (63.5 ± 2.53 kg BW [least square mean ± SEM]). However, the age difference did not further increase during finisher period, where the IUGR pigs at slaughter were 8 days older ($P < 0.01$) than the NORM pigs. Accordingly, from the start of the grower period to slaughter, the IUGR pigs grew 4.7% slower ($P = 0.04$) than the NORM pigs (Table 2), which was mainly due to slower ($P = 0.04$) growth in the grower but not in the finisher period. Apart from being less efficient ($P = 0.01$) in the finisher period, ADFI and total feed intake did not differ between the two groups. When considering the BrW/LW instead of the category, pigs with a higher ratio grew slower ($P < 0.01$, Fig. 2) and displayed a lower ADFI ($P = 0.05$, Supplementary Fig. S1) from the start of the grower period to slaughter. This was mainly due to slower growth ($P < 0.01$) and lower daily feed intake ($P = 0.04$) in the grower but not in the finisher period ($P = 0.10$, Supplementary Fig. S1). Accordingly, as the BrW/LW increased, the gain-to-feed ratio decreased ($P = 0.01$) in the grower–finisher period (Fig. 2).

The higher the BrW/LW, the longer ($P < 0.01$) it took for the pigs to reach slaughter weight. At the start of the grower and finisher periods, and at slaughter, the age of the pigs was positively correlated ($P < 0.01$) with the BrW/LW (Fig. 3).

Table 2. Effect of classifying the pigs based on the brain-to-liver weight ratio (BrW/LW) and sex on growth performance traits from birth to slaughter.

	BrW/LW[1]		Sex			P-value[2]	
Item[3]	IUGR	NORM	Female	Castrate	SEM[4]	BrW/LW	Sex
From birth to the start of the grower period[5]							
Number of pigs	32	185	115	102			
BW, kg							
At weaning	6.2	7.3	6.7	6.7	0.31	< 0.001	0.35
At the end of the starter period[6]	20.3	23.4	21.6	22.1	0.84	-	-
ADG, kg/d							
Lactation	0.19	0.23	0.21	0.21	0.012	< 0.001	0.14
Starter	0.33	0.36	0.35	0.34	0.016	0.07	0.16
Age, d							
At weaning	25.2	25.2	25.2	25.1	0.25	0.98	0.11
At the end of the starter period	74.2	72.3	72.8	73.7	0.90	< 0.01	0.06
From the grower period to slaughter							
Number of pigs[7]	22	71	47	46			
BW, kg							
At the start of the grower period	21.4	25.5	26.4	20.5	1.41	0.73	< 0.01
At the start of the finisher period	59.7	67.2	66.1	60.8	2.53	< 0.01	< 0.01
At slaughter	106	114	112	107	3.5	< 0.01	< 0.01

ADG, g/d							
Grower period	0.81	0.85	0.79	0.87	0.028	0.04	< 0.001
Finisher period	0.91	0.95	0.89	0.97	0.025	0.19	< 0.001
Overall	0.86	0.90	0.84	0.92	0.024	0.04	< 0.001
Total feed intake, kg							
Grower period	85.8	84.7	84.4	86.0	1.25	0.41	0.15
Finisher period	129.3	129.8	126.9	132.2	3.09	0.88	0.05
Total	215.1	214.4	211.4	218.2	3.11	0.84	0.01
ADFI, kg/d							
Grower period	1.7	1.7	1.6	1.8	0.04	0.22	< 0.001
Finisher period	2.7	2.7	2.5	2.8	0.06	0.51	< 0.001
Overall	2.1	2.2	2.1	2.3	0.05	0.21	< 0.001
Gain-to-feed							
Grower period	0.47	0.48	0.48	0.48	0.005	0.31	0.34
Finisher period	0.34	0.35	0.35	0.34	0.004	0.01	0.08
Overall	0.40	0.41	0.41	0.40	0.006	0.08	0.28
Day on feed, d							
Grower period	52.2	47.9	52.9	49.0	1.53	0.07	< 0.001
Finisher period	48.5	48.7	50.4	46.8	1.46	0.87	< 0.001
Overall	100.4	98.1	102.9	95.6	2.33	0.24	< 0.001
Age, d							

At the start of the grower period	75	71	74	75	1.5	0.03	0.21
At the start of the finisher period	127	119	124	122	2.4	< 0.001	0.19
At slaughter	175	167	174	168	2.9	< 0.001	< 0.001

[1] BrW/LW: IUGR: piglets with a BrW/LW ≥ 0.78; NORM: piglets with BrW/LW < 0.78.

[2] P-value for the main effect of the BrW/LW and sex.

[3] ADG = average daily gain, ADFI = average daily feed intake.

[4] Pooled SEM.

[5] From birth to weaning the growth performance traits were determined in 217 piglets. From weaning to the start of the grower period, growth performance traits were determined in 215 out of 217 pigs.

[6] Significant interaction between the category (IUGR, NORM) and the sex ($P = 0.03$). IUGR females and castrates were lighter than their NORM counterparts ($P < 0.01$). Average BW of the IUGR females: 19.9 kg; average BW of the NORM females: 23.3 kg; average BW of the IUGR castrates: 20.8 kg; average BW of the NORM castrates: 23.5 kg.

[7] In the grower and finisher period, the growth performance traits were determined in 93 of the 217 pigs.

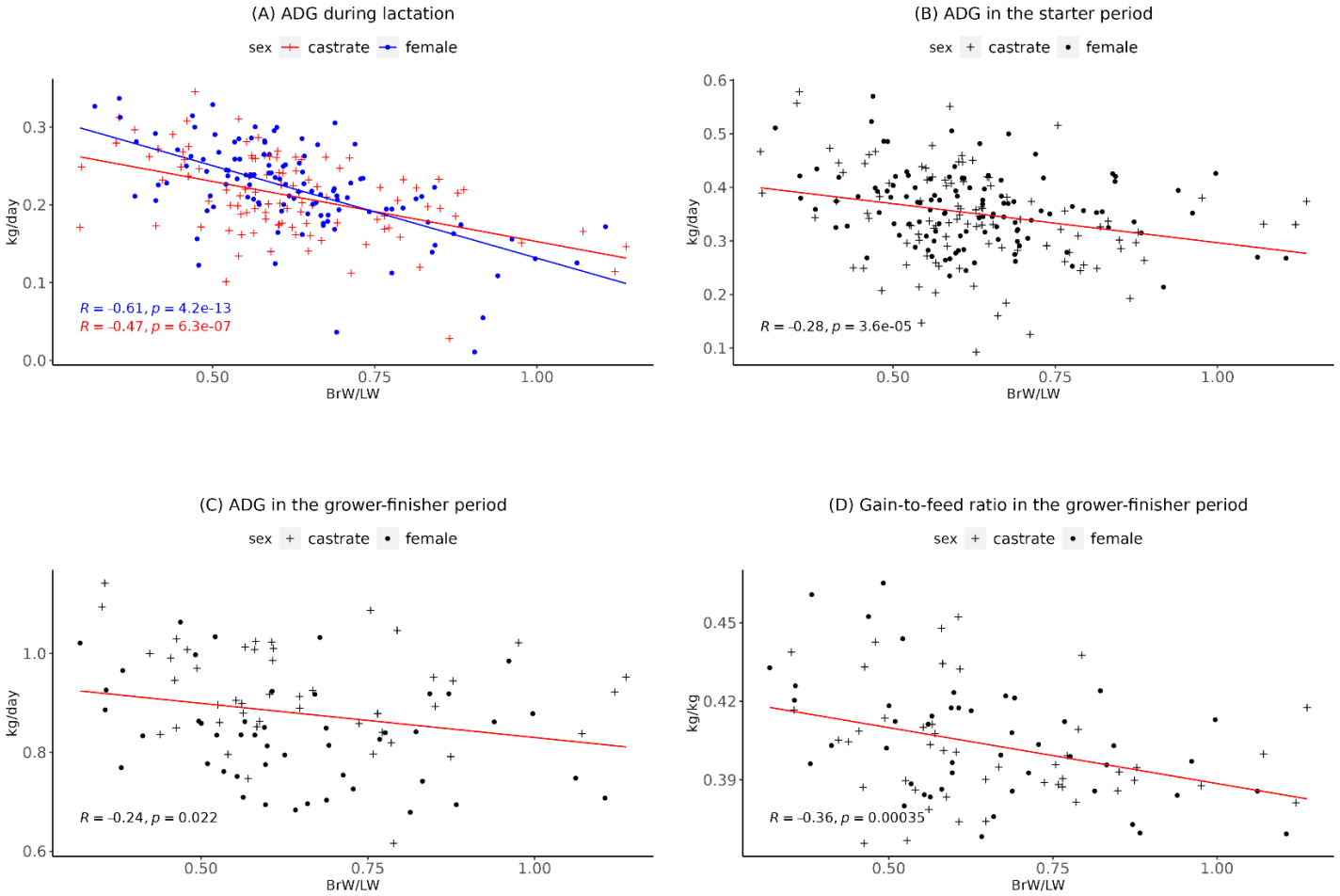

Fig. 2. Effect of the brain-to-liver weight ratio (BrW/LW) and sex on the average daily gain (ADG, g/day) of the pigs from birth to slaughter and the gain-to-feed (kg/kg) ratio in the grower–finisher period. X-axis: BrW/LW; y-axis: ADG of the lactation (A), starter (B), and grower–finisher

period (C) and gain-to-feed ratio of the grower–finisher period (D). R: Pearson correlation coefficient; p: P-value of the linear correlation. Regression equations: ADG lactation = (BrW/LW × (-0.20)) + 0.34; ADG starter = (BrW/LW × (-0.15)) + 0.44; ADG grower–finisher = (BrW/LW × (-0.14)) + 0.97; gain-to-feed ratio grower–finisher = (BrW/LW × (-0.04)) + 0.43.

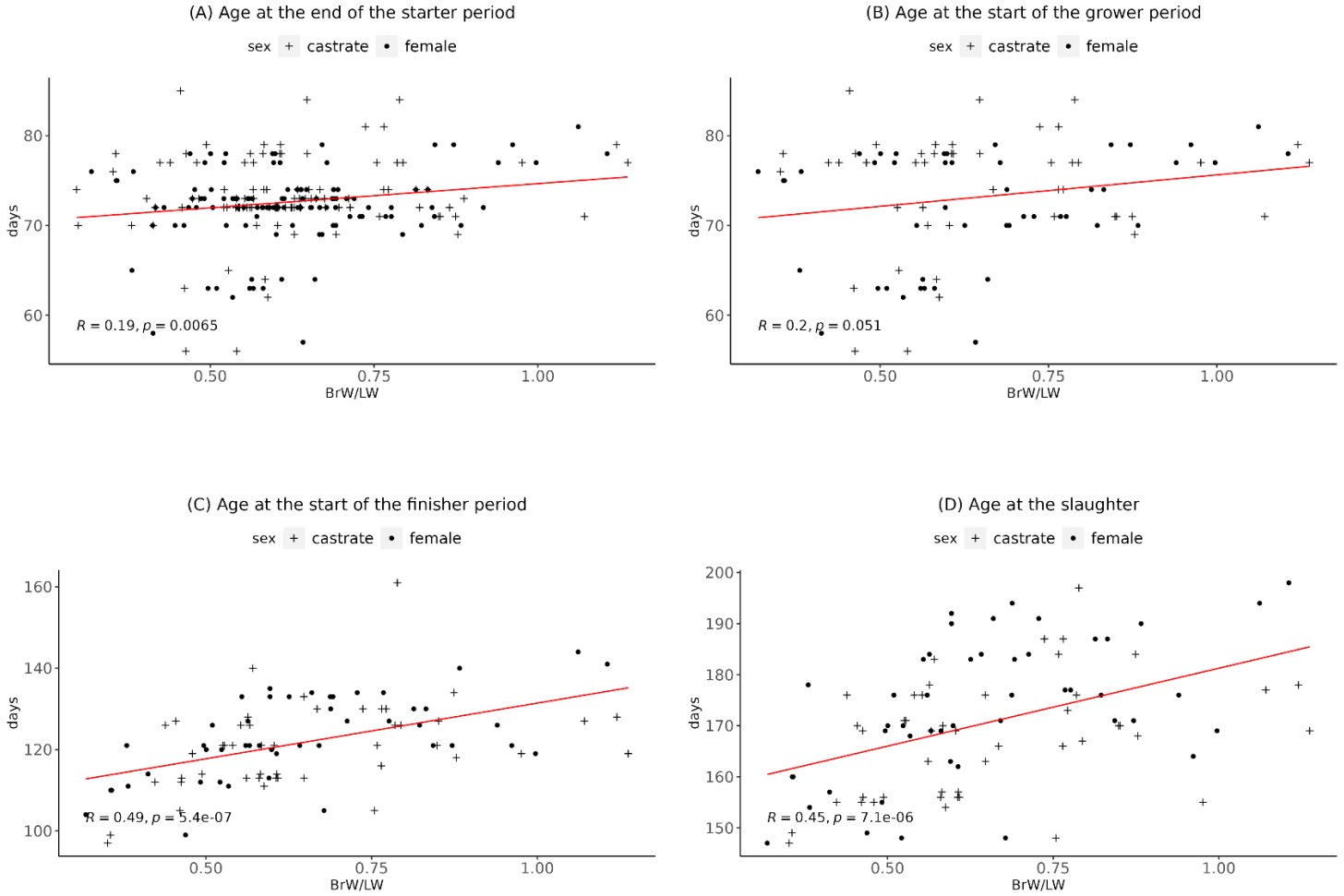

Fig. 3. Effect of the brain-to-liver weight ratio (BrW/LW) and sex on the age (days) of the pigs from the starter period to slaughter. X-axis: BrW/LW; y-axis: age at the end of the starter period (A), at the start of the grower period (B), at the start of the finisher period (C), at slaughter

(D). R: Pearson correlation coefficient; p: P-value of the linear correlation. Regression equations: age at the end of the starter period = (BrW/LW × 5.39) + 69.3; age at the start of the grower period = (BrW/LW × 7) + 68.6; age at the start of the finisher period = (BrW/LW × 27.4) + 104.1; age at slaughter = (BrW/LW × 30.5) + 150.7.

Empty body composition

Regardless of sex, the total bone mineral density, the total bone mineral content, the total lean and fat mass in the empty body were lower at weaning ($P < 0.01$) in the IUGR pigs compared to the NORM pigs (Table 3). However, when these variables were expressed as percentages of the BW, only the total bone mineral density differed between the two groups, showing a higher ($P < 0.01$) value in the IUGR pigs. Similarly, the total bone mineral density, the total bone mineral content, the total lean and fat mass in the empty body decreased ($P < 0.01$) as the BrW/LW increased. However, when these variables were expressed as a percentage of the BW, only the total bone mineral density was affected by the BrW/LW, showing a positive correlation ($P < 0.01$) with the ratio (Fig. 4). The ash content ($P = 0.06$, Table 4) in the empty body tended to be lower in the IUGR pigs than in the NORM pigs at 20 kg but not at 100 kg. In contrast, neither at 20 kg nor at 100 kg BW did empty BW, energy, water, CP, and lipid content differ between IUGR and NORM pigs (Table 4). Except for the daily CP deposition rate that tended ($P = 0.08$) to be lower in the IUGR pigs than in the NORM pigs, the daily energy and fat deposition rates were similar between the two groups. Due to the numerically greater CP intake ($P = 0.15$) and the numerically lower CP content ($P = 0.10$) in the empty body at 100 kg BW, the CP efficiency of IUGR pigs was lower ($P < 0.01$) than that of the NORM pigs. Regarding the BrW/LW, the ash content in the empty body decreased ($P < 0.01$) with an increase in the ratio at 20 kg but not at 100 kg of BW (Fig. 4). In the grower–finisher period, except for the daily CP deposition rate, which was inversely proportional ($P < 0.01$) to the BrW/LW (Fig. 5), the daily energy and fat deposition rate were not affected by the ratio. The CP intake tended to increase ($P = 0.07$) and the CP content in the empty body decreased ($P < 0.01$) with a higher BrW/LW (Fig. 5). As a consequence, the CP efficiency was negatively correlated ($P < 0.01$) with the BrW/LW (Fig. 5).

Table 3. Effect of classifying the pigs based on the brain-to-liver weight ratio (BrW/LW) and sex on total and relative bone mineral density, bone mineral content, lean, and fat mass at weaning.

	BrW/LW[1]		Sex			P-value[2]	
Item	IUGR	NORM	Female	Castrate	SEM[3]	BrW/LW	Sex
Number of pigs	32	185	115	102			
BW, g	6 233	7 345	6 877	6 701	285.0	< 0.001	0.20
Bone mineral density, g/cm^3	0.35	0.37	0.36	0.36	0.007	< 0.001	0.70
Bone mineral content, g	137	161	150	147	6.0	< 0.001	0.19
Lean mass, g	5 385	6 350	5 947	5 788	244.0	< 0.001	0.17
Fat mass, g	710	835	780	766	45.9	< 0.001	0.53
Expressed as % of total body mass							
Total bone mineral density, %	0.006	0.005	0.006	0.006	0.0002	< 0.001	0.53
Bone mineral content, %	2.22	2.22	2.21	2.21	0.036	0.34	0.90
Lean mass, %	86.5	86.5	86.6	86.5	0.39	0.90	0.57
Fat mass, %	11.2	11.3	11.2	11.3	0.40	0.82	0.56

[1] BrW/LW: IUGR: piglets with a BrW/LW ≥ 0.78; NORM: piglets with BrW/LW < 0.78.

[2] P-value for the main effect of the BrW/LW and sex.

[3] Pooled SEM.

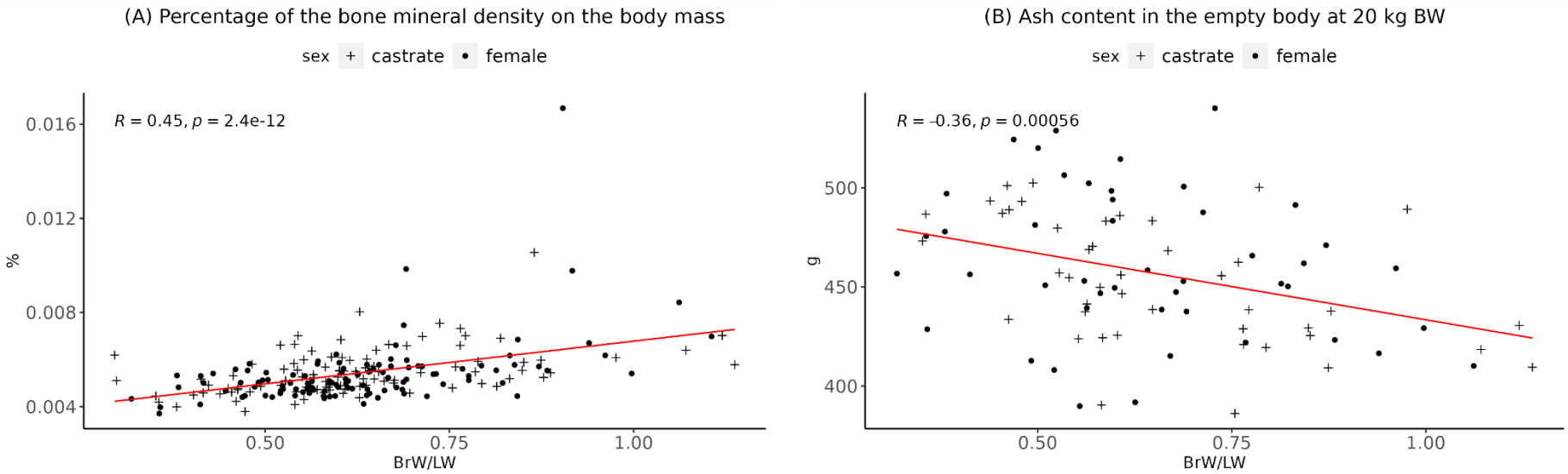

Fig. 4. Effect of the brain-to-liver weight ratio (BrW/LW) and sex on the body composition of the pigs at weaning and at 20 kg of BW. X-axis: BrW/LW; y-axis: percentage (%) of the total bone mineral density (g/cm^2) on the BW at weaning (A); ash content (kg) in the empty body at 20 kg BW (B). R: Pearson correlation coefficient; p: P-value of the linear correlation. Regression equations: percentage of the total bone mineral density = (BrW/LW × 3.630e-05) + 3.152e-05; ash = (BrW/LW × (-67)) + 500.5.fi

Table 4. Effect of classifying the pigs based on the brain-to-liver weight ratio (BrW/LW) and sex on the content of single nutrients in the empty body at 20 kg and 100 kg.

	BrW/LW[1]		Sex			P-value[2]	
Item[3]	IUGR	NORM	Female	Castrate	SEM[4]	BrW/LW	Sex
Number of pigs[5]	20	70	46	44			
Total intake							
Feed, kg	205.0	200.9	199.2	206.8	2.71	0.16	< 0.01
CP, kg	30.3	29.7	29.4	30.5	0.39	0.15	< 0.01
DE, MJ	2 809	2 752	2 728	2 833	37.1	0.16	< 0.01
NE, MJ	2 052	2 010	1 993	2 069	27.2	0.16	< 0.01
Empty body, kg							
At 20 kg	18.6	18.4	18.6	18.5	0.36	0.72	0.75
At 100 kg	107.9	108.7	107.3	109.3	0.10	0.51	0.03
Gross energy, MJ/pig							
At 20 kg	140	139	140	139	3.9	0.65	0.64
At 100 kg	1 324	1 303	1 370	1 434	22.1	0.34	< 0.001
Water, kg/pig							
At 20 kg	12.7	12.6	12.7	12.6	0.21	0.73	0.79
At 100 kg	59.6	60.7	60.5	59.8	0.64	0.10	0.19
Ash, kg/pig							
At 20 kg	0.46	0.46	0.46	0.45	0.008	0.06	0.13

At 100 kg	2.96	3.03	3.06	2.93	0.073	0.31	< 0.01
CP, kg/pig							
At 20 kg	2.6	2.5	2.6	2.5	0.06	0.73	0.79
At 100 kg	16.3	16.7	16.6	16.4	0.19	0.10	0.19
Lipids, kg/pig							
At 20 kg	1.9	1.9	1.9	1.9	0.06	0.61	0.58
At 100 kg	23.0	22.3	21.1	24.2	0.57	0.21	< 0.001
Daily nutrient and energy deposition							
Fat g/d	210	208	186	231	8.6	0.79	< 0.001
CP, g/d	136	141	134	144	3.3	0.08	< 0.001
Gross energy, MJ/d	12	12	11	13	0.4	0.84	< 0.001
Nutrient and energy efficiency[6]							
CP_{eff}	0.46	0.48	0.48	0.46	0.007	< 0.01	< 0.001
DE_{eff}	0.42	0.43	0.41	0.44	0.007	0.63	< 0.001
NE_{eff}	0.58	0.58	0.56	0.60	0.010	0.63	< 0.001

[1] BrW/LW: IUGR: piglets with a BrW/LW ≥ 0.78; NORM: piglets with BrW/LW < 0.78.

[2] P-value for the main effect of the BrW/LW and sex.

[3] CP = crude protein; DE = digestible energy; NE = net energy.

[4] Pooled SEM.

[5] At 100 kg of BW, the Dual-energy X-ray absorptiometry (DXA) scan was not available for three of the 93 pigs. The content of single nutrients, nutrients deposition rate and efficiency were determined for the 90 pigs scanned with DXA at both 20 kg and 100 kg of BW.

[6] CP_{eff} = expressed as deposited CP between the two DXA scans divided by total CP intake in the same period; DE_{eff} = expressed as deposited gross energy between the two DXA scans divided by total DE intake in the same period; NE_{eff} = expressed as deposited gross energy between the two DXA scans divided by total NE intake in the same period.

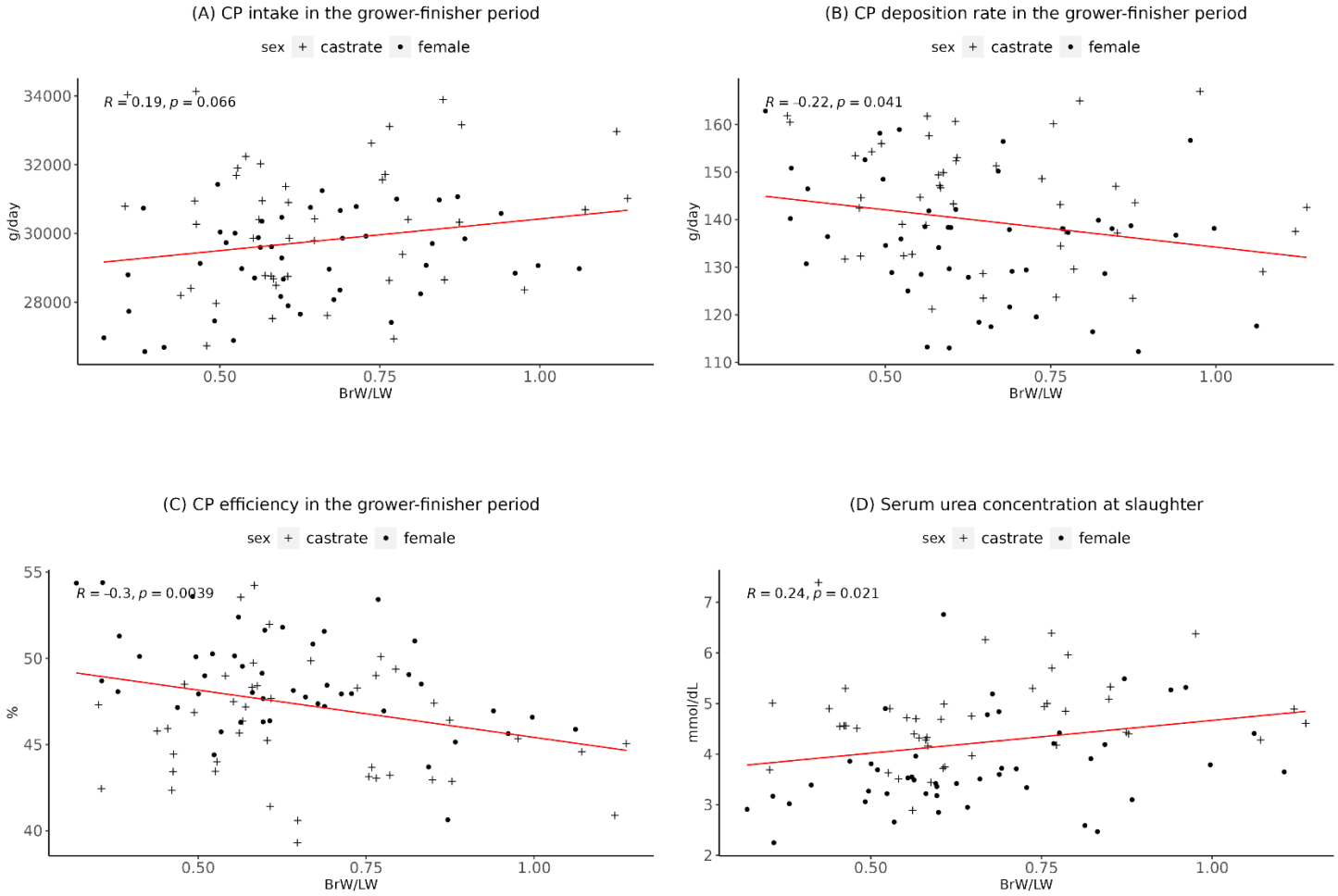
(A) CP intake in the grower-finisher period
sex castrate female
R = 0.19, p = 0.066
g/day
BrW/LW
(B) CP deposition rate in the grower-finisher period
sex castrate female
R = -0.22, p = 0.041
g/day
BrW/LW
(C) CP efficiency in the grower-finisher period
sex castrate female
R = -0.3, p = 0.0039
%
BrW/LW
(D) Serum urea concentration at slaughter
sex castrate female
R = 0.24, p = 0.021
mmol/dL
BrW/LW

Fig. 5. Effect of the brain-to-liver weight ratio (BrW/LW) and sex on the CP intake (kg/day), deposition rate (g/day), and efficiency (%) in the grower–finisher period and serum urea concentration (mmol/dL) of the pigs at slaughter. X-axis: BrW/LW; y-axis: CP intake (A), deposition rate (B), and efficiency (C) in the grower–finisher period and serum urea concentration at slaughter (D). R: Pearson correlation coefficient; p: P-value of the linear correlation. Regression equations: CP intake = (BrW/LW × 1843) + 28 578; CP deposition rate = (BrW/LW × (-15.7)) + 149.9; CP efficiency = (BrW/LW × (-0.05)) + 0.51; serum urea concentration = (BrW/LW × 1.29) + 3.37.

Blood metabolite traits and blood cell count

At slaughter, the lymphocyte count tended to be higher ($P = 0.09$) and the monocyte counts were higher ($P < 0.01$) for the IUGR category compared to the NORM group (Table 5). For the glucose and haemoglobin concentration in the serum and the red blood cell count, despite the significant interaction ($P \leq 0.02$) between the category and the sex, the multiple mean comparisons between IUGR and NORM females and castrates were not significant (Table 6). The other parameters, including urea concentration, non-esterified fatty acids, haematocrit, mean corpuscular haemoglobin, mean corpuscular haemoglobin concentration, mean corpuscular volume, granulocytes count, and platelets count, showed similar values between the IUGR and NORM categories (Table 5).

When considering the BrW/LW, the serum urea tended to increase ($P = 0.09$) as the BrW/LW increased at slaughter (Fig. 5). The monocyte count was positively correlated ($P < 0.01$) with the ratio (Fig. 6). For the castrated pigs, as the BrW/LW increased, the haemoglobin concentration in the blood ($P = 0.05$) and the red blood cell count ($P < 0.01$) increased (Fig. 6). For high values of the BrW/LW, females displayed a lower haematocrit ($P = 0.02$) compared to the castrates (Fig. 6). Serum insulin was detectable in just 67 out of 90 pigs (in 76% of the IUGR and 73% of the NORM category). For these animals, the insulin concentration did not differ between IUGR and NORM pigs (Table 5). However, the insulin concentration in the serum tended to be positively correlated ($P = 0.08$) with the BrW/LW (Fig. 7).

Regardless of the IUGR status, the blood metabolite traits and blood cell counts were within normal ranges (Ježek et al., 2018; Etim et al., 2014; Chmielowiec-Korzeniowska et al., 2012) with the exception of slightly elevated levels of red blood cells, lymphocytes, and glucose concentration.

Table 5. Effect of classifying the pigs based on the brain-to-liver weight ratio (BrW/LW) and sex on the blood metabolite traits, blood cell count, and insulin concentration at slaughter[1].

	BrW/LW[2]		Sex			P-value[3]	
Item	IUGR	NORM	Female	Castrate	SEM[4]	BrW/LW	Sex
Number of pigs[5]	21	70	47	44			
Urea, mmol/L	4.33	4.19	3.77	4.75	0.221	0.50	<0.001
Non-Esterified Fatty Acids, mmol/L	0.184	0.167	0.177	0.175	0.0364	0.62	0.95
Haematocrit, %	49.1	48.9	48.5	49.4	0.91	0.81	0.15
Mean corpuscular haemoglobin, p/g	16.8	16.7	16.6	16.8	0.21	0.62	0.22
Mean corpuscular haemoglobin concentration, g/dL	30.9	30.9	31.1	30.7	0.17	0.60	0.01
Mean corpuscular volume, fL	54.4	54.2	53.6	54.9	0.72	0.72	0.01
Granulocytes, 10^9 cells/L	5.69	5.09	5.15	5.63	0.449	0.16	0.16
Lymphocytes, 10^9 cells/L	16.0	14.5	15.4	15.0	0.81	0.09	0.59
Monocytes, 10^9 cells/L	0.205	0.139	0.173	0.170	0.0164	< 0.001	0.86
Platelets, 10^9 cells/L	388	398	397	389	30.1	0.72	0.72
White blood cells, 10^9 cells/L	18.9	18.4	18.5	18.7	0.57	0.40	0.75
Number of pigs[6]	22	68	45	45			
Insulin, mU/L	7.98	5.36	6.57	6.77	1.63	0.13	0.89

[1] The pigs were slaughtered at 110 kg BW.

[2] BrW/LW: IUGR: piglets with a BrW/LW ≥ 0.78; NORM: piglets with BrW/LW < 0.78.

[3] P-value for the main effect of the BrW/LW and sex.

[4] Pooled SEM.

[5] For two of the 93 pigs, it was not possible to collect the blood at slaughter and to perform the blood metabolite traits and blood cell count analysis.

[6] For one of the 91 pigs from which the blood was collected at slaughter it was not possible to perform the insulin concentration analysis. For 23 of the 90 samples analysed, the insulin concentration was not detectable in the serum and was assigned a value of 0.

Table 6. Effect of classifying the pigs based on the brain-to-liver weight ratio (BrW/LW) and sex on the blood glucose, haemoglobin, and red blood cell count at slaughter[1].

	BrW/LW[2]					P-value[3]		
	Females		Castrates					
	IUGR	NORM	IUGR	NORM	SEM	BrW/LW	Sex	BrW/LW x Sex[4]
Number of pigs	11	36	10	34				
Glucose, mmol/L	7.59	8.39	9.43	7.65	0.794	0.32	0.06	0.02
Haemoglobin, g/dL	14.7	15.1	15.6	14.9	0.33	0.19	0.02	0.02
Red blood cells, 10^{12} cells/L	8.85	9.14	9.31	8.92	0.175	0.11	0.04	< 0.01

[1] The pigs were slaughtered at 110 kg BW.

[2] BrW/LW: IUGR: piglets with a BrW/LW ≥ 0.78; NORM: piglets with BrW/LW < 0.78.

[3] P-value for the main effect of the BrW/LW, sex, and the two-way interaction (BrW/LW × Sex).

[4] Significant interaction between the category (IUGR, NORM) and the sex ($P < 0.05$) but not significant multiple mean comparisons between IUGR and NORM females and castrates for glucose, haemoglobin, and red blood cell count.

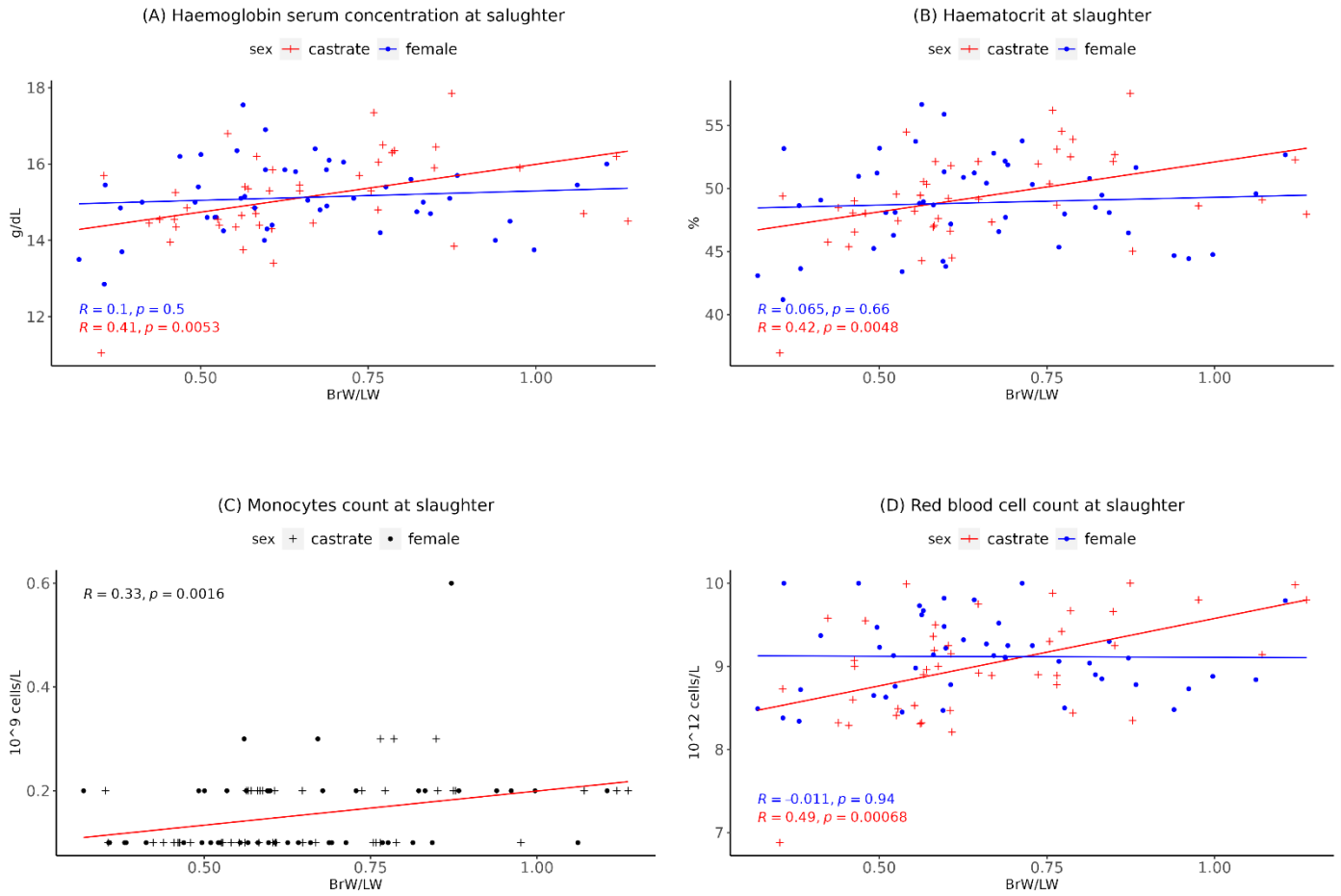

Fig. 6. Effect of the brain-to-liver weight ratio (BrW/LW) and sex on the haemoglobin serum concentration (g/dL), haematocrit value (%), monocytes (10^9 cells/L) and red blood cell (10^{12} cells/L) counts of the pigs at slaughter. X-axis: BrW/LW; y-axis: haemoglobin serum concentration

(A), haematocrit value (B), monocytes (C), and red blood cell counts in the serum (D). R: Pearson correlation coefficient; p: P-value of the linear correlation. Regression equations: serum haemoglobin concentration = (BrW/LW × 1.48) + 14.2; haematocrit = (BrW/LW × 4.51) + 46.2; monocytes count = (BrW/LW × 0.13) + 0.07; red blood cell count = (BrW/LW × 0.77) + 8.57.

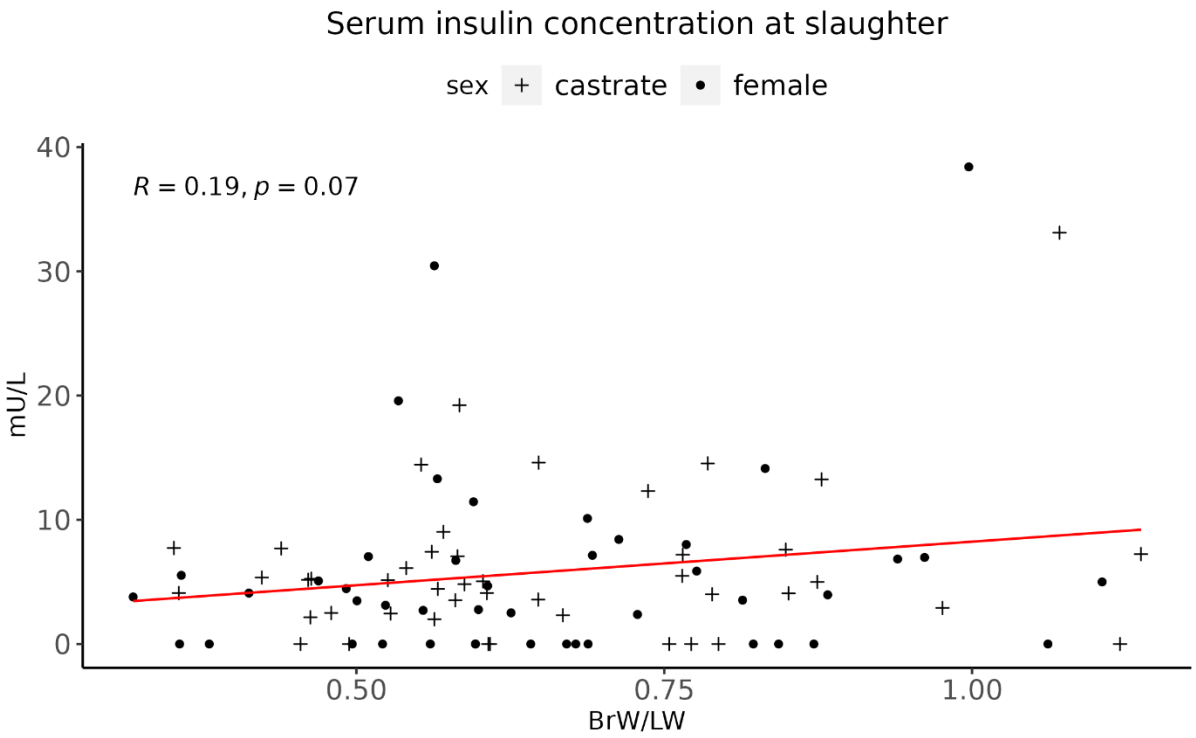

Fig. 7. Effect of the brain-to-liver weight ratio (BrW/LW) and sex on serum insulin (mu/L) of the pigs at slaughter. X-axis: BrW/LW; y-axis: serum insulin concentration: Pearson correlation coefficient; p: P-value of the linear correlation. Regression equations: serum insulin = (BrW/LW × 7.02)) + 1.23.

Carcass composition and meat quality

Carcass weight, energy, water, ash, CP, and lipid content did not differ between the IUGR and NORM pigs (Supplementary Table S4). Likewise, no significant differences were detected when testing the effect of the BrW/LW on the composition of the carcasses.

In the IUGR category, the lightness of the LT muscle was lower ($P = 0.01$) while the shear force was increased ($P < 0.01$) compared to the NORM group (Supplementary Table S4). The other traits did not show significant differences between the two groups. Likewise, the BrW/LW was inversely proportional ($P < 0.01$) to the lightness of the LT muscle (Supplementary Fig. S2). In addition, the cooking loss tended to be negatively correlated ($P = 0.09$) with the BrW/LW (Supplementary Fig. S2).

Discussion

Intrauterine growth restriction identification

In this study, the BrW/LW, BtW, and head morphology at birth were considered as traits to identify IUGR piglets. Our results showed a discrepancy between the three methods. Based on our assumption that a piglet with a BrW/LW > 0.78 is IUGR, some piglets were classified differently using the phenotypic scoring systems. If BrW/LW is thought to be the optimal measure to identify IUGR, these findings support the hypothesis that the identification of IUGR piglets only based on the head morphology and/or BtW does not always agree with an increased BrW/LW. Indeed, a low BtW does not necessarily imply an IUGR condition, even if the IUGR condition is generally associated with a low BtW (Gupta et al., 2008; De Vos et al., 2014). The classification of IUGR based on head shape can be subjective and may depend on the observer. There is a greater probability of variance in observations when the judgement is subjective. In addition, the head morphology of piglets can be correlated to their parents' features or specific

breed traits. There are natural variations in facial characteristics, unrelated to pathology, that arise as a result of domestication and subsequent selective pressures (Chakraborty et al., 2021; Wilkinson et al., 2013). In contrast, the identification of IUGR piglets based on increased BrW/LW may be considered as objective, as it is the direct consequence of the brain-sparing effect.

To our knowledge, this is the first study to identify IUGR piglets based on BrW/LW. Therefore, it is challenging to compare the present results with those obtained with other IUGR classifications, either head shape or low BtW. As mentioned before, constituting groups based on head shape or BtW may result in groups containing a mix of IUGR and normal piglets. In the following discussion, the method of determining the IUGR condition will be reported when comparing the characteristics and effects of IUGR between studies. In addition, the two categories used in the present study (IUGR and NORM) were defined based on a threshold set according to the distribution of the population studied. Nevertheless, this binary classification is a simpler model of a condition that has varying degrees of severity. One could argue for a lower or higher threshold for BrW/LW, and changing the threshold may have an impact on the final results. The present discussion will, therefore, not only cover the effects of the IUGR category on the different parameters but will also present the general trend reflected by the correlation between the parameters and the BrW/LW.

Effect of intrauterine growth restriction on growth and average daily gain

In this study, the IUGR pigs showed reduced ADG in the lactation and grower phases, even though the feed intake was similar between the two groups in the grower phase. During the starter period, the IUGR pigs tended to have a lower ADG compared to the normal group. In addition, the BrW/LW was negatively correlated with the ADG from birth to slaughter, with a decreasing effect with time. Similarly, in the study of Alvarenga et al. (2012), the IUGR pigs,

defined by their low BtW, displayed a lower ADG from birth to the grower phase compared to their normal littermates. In the finisher period, despite a lower gain-to-feed ratio in the IUGR category, the ADG was similar between the IUGR pigs and the NORM pigs. Our results complied with those of Alvarenga et al. (2012), who described a similar ADG on day 150 between IUGR and normal pigs. Moreover, the study of Gondret et al. (2005) showed a decreasing effect of BtW on ADG over time. Santos et al. (2022), on the contrary, observed a reduction in both the BW and the ADG from birth to slaughter in the IUGR group, defined by a LBtW. However, the differences observed in the studies may be attributed to the different techniques used to define IUGR piglets (BtW, head shape, and brain-to-organ weight ratio). In this study, the IUGR pigs were 8 days older than the NORM pigs at slaughter. Moreover, as the BrW/LW increased, the age at which the pigs reached the target slaughter weight increased. Our findings comply with the results of previous studies (Gondret et al., 2005) showing that IUGR pigs require more days to reach slaughter weight compared to their normal littermates. This prolonged time results in an increase in management costs and a reduction in the production efficiency (Díaz et al., 2017).

Effect of intrauterine growth restriction on body composition

In the current experiment, there was no difference between IUGR and NORM pigs in the bone, lean, and fat tissue when expressed as a percentage of the BW. Similarly, the BrW/LW did not affect the body composition at weaning. This complies with the study of Lynegaard (2020), in which no differences in fat or muscle percentage were found in relation to BW at 24 days of age between the IUGR group (defined by their head shape) and the NORM group. On the contrary, using BtW as a classification criterion, Amdi et al. (2012) showed an increased percentage of fat tissue in low-BtW (1.1 kg) piglets compared to medium-BtW (1.5 kg) and high-BtW (1.8 kg) piglets at 28 days of age. Neither the absolute nor the relative (expressed per

empty BW) CP and lipid mass and energy content of the empty body differed at 20 kg and 100 kg BW and in the carcasses between the IUGR and NORM groups. However, the ash content in the empty body tended to be lower in the IUGR group at 20 kg BW. Despite a similar energy, fat, and CP deposition rate in the grower–finisher period, the IUGR category showed a lower CP efficiency. When considering the effect of the BrW/LW, the latter was negatively correlated to both the CP deposition rate and CP efficiency in the grower–finisher period. The results regarding body composition in IUGR pigs are not consistent. Several studies have reported that pigs with a LBtW had a decreased percentage of muscle and an increased percentage of body fat than their heavier littermates at slaughter (Zhang et al., 2022; Krueger et al., 2014; Gondret et al., 2006). On the contrary, no effect of BtW on fat deposition was observed in other studies of low- and high-birth BW pigs (Nissen and Oksbjerg, 2011; Gondret et al., 2005).

Effect of intrauterine growth restriction on blood biochemistry and blood cell count

The urea concentration in the serum is negatively correlated with the efficiency of nutrient utilisation and the deposition of lean tissue (Whang and Easter 2000). For this reason, it can be used as a marker of CP efficiency in pig production. In the present study, the IUGR pigs were less CP-efficient in the grower–finisher period. In addition, the BrW/LW was negatively correlated to the CP deposition rate in the grower–finisher period, and the urea concentration at slaughter tended to increase as the BrW/LW increased. Using the BtW as a classification criterion, Zhang et al. (2018) showed significantly increased levels of urea nitrogen in IUGR pigs at 160 days of age. Similarly, Li et al. (2021) detected a high plasma urea concentration in the portal vein of IUGR pigs, defined by a LBtW, compared to normal pigs at 85 days of age.
In this study, the serum insulin concentration tended to be positively correlated with the BrW/LW. This complies with the study of Yan et al. (2015) in which the IUGR pigs, identified

by a LBtW, showed increased fasting plasma insulin levels at 178 days of age, independent of postnatal nutrition. Nevertheless, the pigs were slaughtered after 16 h of feed withdrawal in this study, and the insulin concentration was not detectable and consequently assigned a value of 0 in the serum of 23 animals, perhaps as a consequence of their fasted status. For these reasons, our results regarding serum insulin concentration at slaughter must be interpreted with caution.

Effect of intrauterine growth restriction on meat quality

The results regarding the colour of the LT muscle are not consistent. Our findings agree with those of Matyba et al. (2021), in which the LT was darker in the IUGR group. Pigs affected by IUGR, identified according to their LBtW, show a higher number of type I compared to type II fibres in the skeletal muscle (Felicioni et al., 2020). Type I fibres contain more myoglobin (Yu at al. 2017) and this could explain the darker colour of the meat in the IUGR group. Indeed, the BrW/LW was negatively correlated with the lightness of the LT muscle in this study. The reduced lightness resulting from IUGR may have a negative effect on consumer perception, although it remains unclear whether the different colour is indeed perceived by the consumer. In contrast, in the study by Li et al. (2015), the muscle of the IUGR pigs was lighter. The differences observed among studies may be attributed not just to the different techniques used to define IUGR piglets but also to the different ages at which the animals were slaughtered (day 170 in our study and 200 and 188 in the studies of Li et al., and Matyba et al., respectively). Latorre et al. (2003) showed that pigs slaughtered at 160 days had a lower redness score and intensity of the colour of the LT muscle compared to pigs slaughtered at 175 days. This result is in line with the study of Virgili et al. (2003), who found that older pigs produced a redder and darker *semimembranosus* muscle.

In conclusion, our study used the BrW/LW to characterise the physiological traits of IUGR piglets. Our results showed that IUGR identification based on head shape or BtW may lead to

inaccurate classification, as these characteristics are not always consistent with an increased BrW/LW. Moreover, this study demonstrated that the BrW/LW is inversely proportional to ADG from birth to slaughter and the gain-to-feed ratio in the grower–finisher period. From the start of the grower period to slaughter, the BrW/LW was negatively correlated with the CP deposition rate and CP efficiency and positively correlated with the urea and insulin ($P = 0.08$) concentration in the serum at slaughter. In general, the higher the BrW/LW, the longer it took for the pigs to reach the target slaughter weight of 110 kg. The BrW/LW did not affect the proportion of lean, fat, and bone mineral content, but the meat was darker as the BrW/LW increased. For these reasons, the IUGR pigs represent a great economic loss for swine producers, and the development of breeding and management strategies to reduce the frequency of IUGR will be of great importance in pig production.

Ethics approval

The experimental procedures complied with the Swiss animal welfare guidelines and were approved (experimental approval number 32751) by the Cantonal Veterinary Office of Fribourg (Switzerland).

Supplementary material

Supplementary Table S1. Piglets selected for euthanasia.

Item	Number of pigs		
	Total	Females	Males
Category[1]			
Category 1	10	4	6
Category 2	10	7	3
Category 3	10	5	6
BtW[2]			
Low BtW	12	5	7
Norm BtW	18	10	8
Head shape[3]			
Score 1	20	10	10
Score 2	2	1	1
Score 3	8	4	4

[1] Category: category 1: piglets with a birth weight (BtW) < 1.1 kg; category 2: piglets with a BtW ≥ 1.1 and < 1.8 kg; category 3: piglets with a BtW ≥ 1.8.

[2] BtW: low BtW: piglets with a BtW < 1.1kg; normal BtW: piglets with a BtW ≥ 1.1kg.

[3] Head shape based on the morphological characteristics of the head (Chevaux et al., 2010; Hales et al., 2013; Hansen et al., 2018): score 1: "normal" piglet, score 2: mild intrauterine growth restriction (IUGR); score 3: severe IUGR.

Supplementary Table S2. Piglets selected for fattening.

	Females	Males	BtW-range1
Number of pigs2	48	48	0.83 kg – 2.16 kg
Score 1	23	20	0.99 kg – 2.16 kg
Score 2	17	22	0.96 kg – 2.16 kg
Score 3	8	6	0.83 kg – 1.3 kg

[1] Range of birth weight (BtW).

[2] Selection of the piglets (n = 96) for the grower-finisher period.

Supplementary Table S3. Ingredients and gross chemical composition of the pre/early post-weaning, starter, grower, and finisher diet administered to the pigs.

	Pre/early postweaning diet[1]	Starter diet[2]	Grower diet[3]	Finisher diet[4]
Ingredients (%)				
Wheat, ground	40.413	44.550	50.000	50.000
Corn, ground	14.185	1.570	-	-
Potato proteins	7.243	8.026	-	-
Oats, ground	6.162	10.000	-	-
Beet pulp	5.842	5.202	5.923	5.961
Soybean meal	5.361	3.746	11.555	6.104
Whey permeate	5.000	5.000	-	-
Barley, ground	3.636	3.470	26.584	32.418
Rapeseed oil	2.500	3.864	-	-
Rapeseed meal			0.711	1.371
Oats flakes	2.000	2.000	-	-
Apple pomace, dried	2.000	8.560	-	-
Animal fat RS 6	-	-	1.530	1.353
Chestnut extract[5]	2.000	-	-	-
Calcium formate	0.800	1.000	-	-
Monocalcium phosphate	0.487	0.486	-	-
Dicalcium phosphate	-	-	1.417	0.913

Wheat barn	-	0.560	-	-
Wheat meal	0.400	-	-	-
Vitamin-mineral premix starter[6]	0.400	0.400	-	-
Vitamin-mineral premix fattening[7]	-		0.400	0.400
Lysine pure	0.392	0.394	-	-
L-Lysine HCL	-	-	0.397	0.275
Salt	0.391	0.544	0.307	0.254
Pellan[8]	0.300	0.300	0.300	0.300
Greencab-70-C[9]	0.200	0.200	-	-
Calcium carbonate	0.165	-	0.725	0.588
Threonine pure	0.087	0.088	-	-
L-Threonine	-	-	0.103	0.057
Methionine 98%	0.016	0.020	-	-
DL-Methionine	-	-	0.047	0.005
Luctarom[10]	0.010	0.010	-	-
Natuphos 5000 G[11]	0.010	0.010	-	-
Gross chemical composition analysed (g/kg as fed)				
DM	45	46	54	45

CP	170	170	158	140
Fat	46	58	31	30
Crude fibre	50	50	40	40
Digestible energy (MJ/kg)	14	14.0	13.7	13.7
Lysine	11	11.5	9.7	7.6
Methionine	3.1	3.1	2.8	2.2
Threonine	7.5	7.5	6.2	5.1
Tryptophan	1.9	2.0	1.8	1.6
Calcium	5.8	5.8	8	6.1
Phosphorus	4.5	4.4	6.4	5.4
Sodium	1.9	2.5	1.3	1.1
Vitamin A (IE/kg)	8000	8000	4000	4000
Vitamin D3 (IE/kg)	1000	1000	400	400
Vitamin E	25	25	65	65
Iodine (mg/kg)	0.15	0.15	0.15	0.15
Manganese (mg/kg)	10	10	10	10
Copper (mg/kg)	6	6	4	4
Zinc (mg/kg)	75	75	55	55
Selenium (mg/kg)	0.20	0.20	0.15	0.15

[1] Diet for the piglets from 15 days after birth to 14 days post-weaning, formulated and produced by Agroscope according to the Swiss feeding recommendations for pigs.

[2] Diet for the piglets from 14 days postweaning to 20 kg BW, formulated and produced by Agroscope according to the Swiss feeding recommendations for pigs.

[3] Diet for pigs from 20kg to 60 kg of BW, formulated and produced by Agroscope according to the Swiss feeding recommendations for pigs.

[4] Diet for pigs from 60kg of BW to slaughter, formulated and produced by Agroscope according to the Swiss feeding recommendations for pigs.

[5] Chestnut extract (containing 54% of hydrolysable tannins) provided by Silvateam (Silvafeed Nutri P/ENC for Swine; Italy).

[6] Supplied per kg of diet: vitamin A, 8000 IU; vitamin D3, 1000 IU; vitamin E, 25 mg; menadione, 3 mg; thiamine, 2 mg; riboflavin, 5 mg; biotin, 0.1 mg; niacin, 20 mg; pantothenic acid, 15 mg; iron, 80 mg as iron sulphate monohydrate; iodine, 0.15 mg as calcium iodate; copper, 6 mg as copper sulphate; manganese, 10 mg as manganese oxide; zinc, 75 mg as zinc oxide; selenium, 0.2 mg as sodium selenite.

[7] Supplied per kg of diet: Vitamin A, 4000 IU; vitamin D3, 400 IU; vitamin E, 65 IU; choline, 200 mg; vitamin B6, 3 mg; folic acid 0.5 mg; menadione, 1 mg; thiamine, 2 mg; riboflavin, 3 mg; biotin, 50.4 µg; niacin, 15 mg; pantothenic acid, 15.1 mg; iron, 20.1 mg; iodine, 0.15 mg; copper, 4 mg; manganese, 10 mg; zinc, 55.1 mg; selenium, 0.15 mg.

[8] Pellet binding aid: Pellan, Mikro-Technik, Bürgstadt, Germany.

[9] Coated calcium butyrate: Greencab 70-c, Brenntag; Denmark.

[10] Luctarom, Lucta; Montornès del Vallès, Spain.

[11] Phytase; 500 units of aspergillus niger phytase/kg diet; 1 phytase unit corresponds to the amount of enzyme that releases 1 µmol P from 5 mM phytate/min at pH 5.5 and 37˚C.

Supplementary Table S4. Effect of classifying the pigs based on the brain-to-liver weight ratio (BrW/LW) and sex on the energy and nutrient content of the carcass and meat quality traits of the *longissimus thoracis* (LT) muscles.

	BrW/LW[1]		Sex			P-value[2]	
Item[3]	IUGR	NORM	Female	Castrate	SEM[4]	BrW/LW	Sex
Number of carcasses[5]	19	69	47	41			
Carcass weight, kg	87.5	88.1	86.9	88.8	0.74	0.45	< 0.01
Gross energy, MJ	1113	1107	1053	1167	22.3	0.77	< 0.001
Water, kg	49.4	49.9	50.1	49.1	0.59	0.37	0.03
Ash, kg	3.06	3.10	3.13	3.02	0.050	0.38	< 0.001
CP, kg	14.9	15.1	15.2	14.9	0.19	0.39	0.03
Lipids, kg	20.3	20.1	18.7	21.8	0.61	0.74	< 0.001
Number of *longissimus thoracis* samples[6]	21	70	47	44			
pH 1	6.75	6.78	6.73	6.81	0.080	0.72	0.30
pH 24	5.57	5.56	5.57	5.56	0.034	0.69	0.55
Temperature 1	33.9	33.9	33.6	34.2	0.309	0.97	0.02
Temperature 24	3.45	3.36	3.33	3.48	0.116	0.32	0.04
Meat colour							
Lightness	56.8	57.8	56.6	57.9	0.644	0.01	< 0.001
Redness	2.56	2.60	2.29	2.87	0.244	0.84	< 0.01
Yellowness	12.4	12.6	12.1	12.9	0.301	0.27	< 0.001

Water holding capacity							
Drip loss, %	2.26	2.51	0.03	0.04	0.189	0.17	0.25
Purge loss, %	3.43	3.48	3.40	3.51	0.213	0.75	0.41
Cooking loss, %	20.90	21.70	21.90	20.80	0.894	0.18	0.03
Shear force, N	54.8	48.2	53.0	50.0	2.32	< 0.01	0.08

[1] BrW/LW: IUGR: piglets with a BrW/LW ≥ 0.78; NORM: piglets with BrW/LW < 0.78.

[2] P-value for the main effect of the BrW/LW and sex.

[3] pH 1: muscle pH at 45 min *postmortem*; pH 24: muscle pH at 24 h *postmortem*; temperature 1: muscle temperature at 45 min *postmortem*; temperature 24: muscle temperature at 24 h *postmortem*; drip loss: drip loss 24 h *postmortem*; purge loss: purge loss during maturation.

[4] Pooled SEM.

[5] After slaughter, the Dual-energy X-ray absorptiometry (DXA) scan was not available for five of the 93 carcass halves. The content of single nutrients was determined for the 88 carcasses scanned with DXA after slaughter.

[6] For two of the 93 pigs, it was not possible to perform the meat quality analysis.

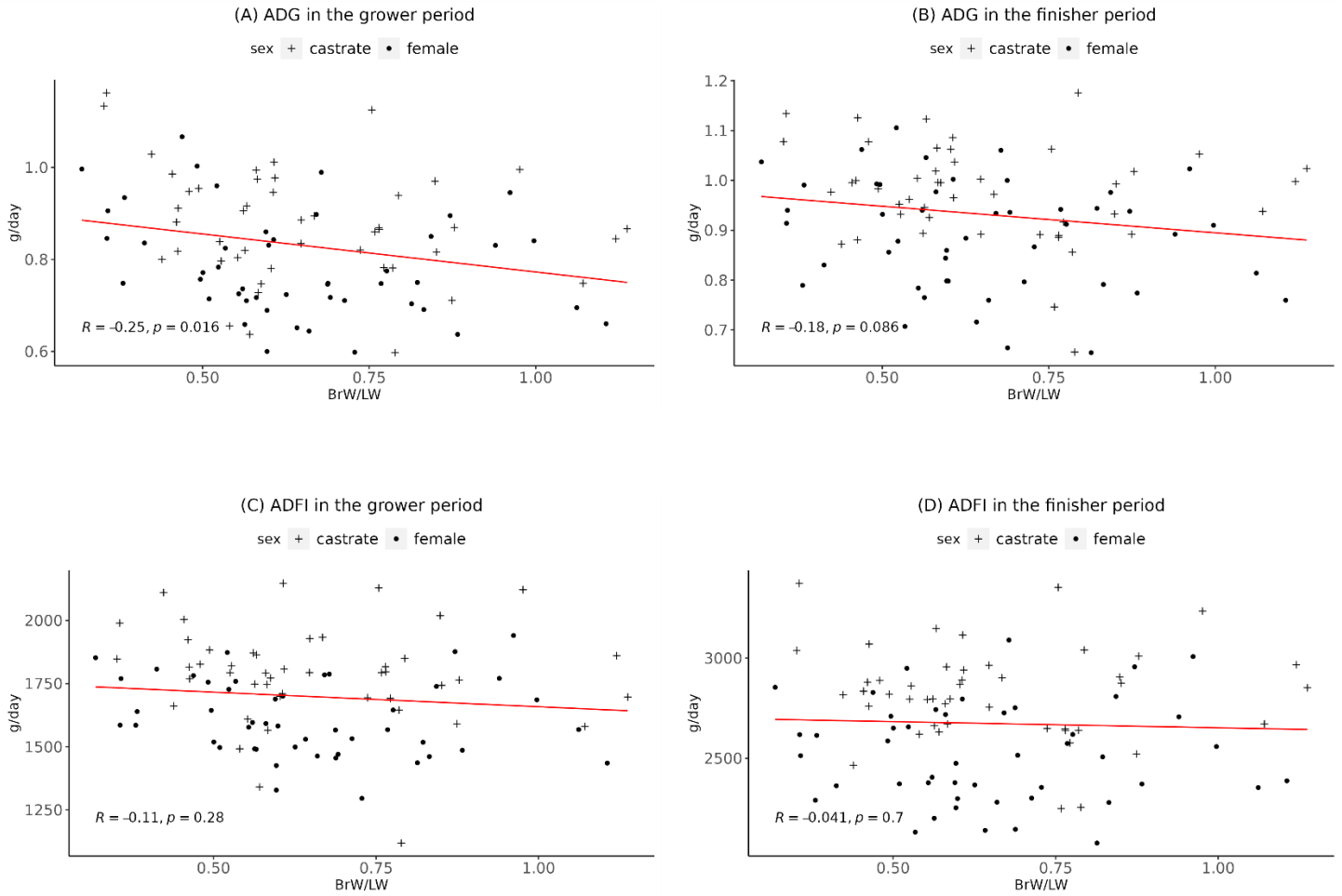

Supplementary Fig. S1. Effect of the brain-to-liver weight ratio (BrW/LW) and sex on the average daily gain (ADG, g/day) and average daily feed intake (ADFI, kg/day) of the pigs in the grower-finisher period. X-axis: BrW/LW; y-axis: ADFI in the grower (A) and finisher period (B);

average daily gain (ADG) in the grower (C) and finisher period (D). R: Pearson correlation coefficient of the linear correlation; p: P-value of the linear correlation. Regression equations: ADG grower = (BrW/LW * (-0.17)) + 0.94; ADG finisher = (BrW/LW * (-0.11) + 1; ADFI grower = (BrW/LW * (-115.5) + 1773.9; ADFI finisher = (BrW/LW * (-61.1)) + 2713.

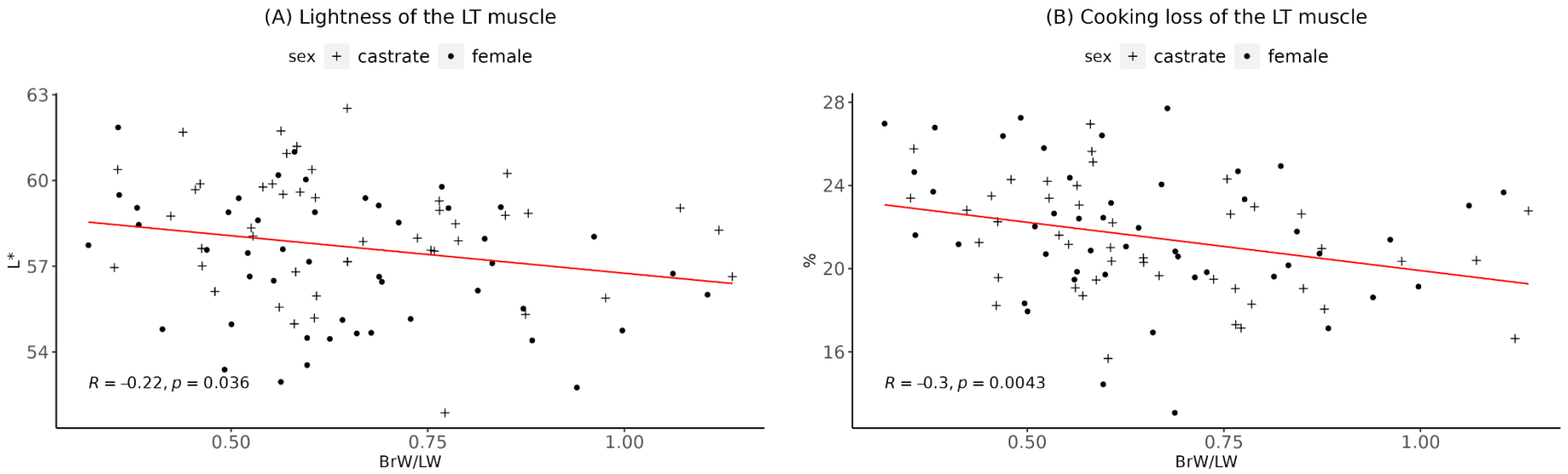

Supplementary Fig. S2. Effect of the brain-to-liver weight ratio (BrW/LW) and sex on meat quality of the pigs. X-axis: BrW/LW; y-axis: lightness (L*) value of the longissimus thoracis (LT) muscle (A); cooking loss (%) determined in the LT muscle (B); R: Pearson correlation coefficient; p: P-value of the linear correlation. Regression equations: L* = (BrW/LW × (-2.62)) + 59.4; cooking loss = (BrW/LW × (-0.05)) + 0.25.

4. Manuscript II

Morphometric traits to estimate brain and liver weight and their ratio for the diagnosis of intrauterine growth restriction in newborn piglets

R. Ruggeri[a, b], G. Bee[a], P. Trevisi [b], C. Ollagnier[a]

[a] *Swine Research Unit, Agroscope, Route de la Tioleyre 4, 1725 Posieux, Switzerland*

[b] *Department of Agricultural and Food Sciences (DISTAL), University of Bologna, viale G Fanin 44, 40127 Bologna, Italy*

Abstract

Intrauterine growth restriction (IUGR) is defined as inadequate foetal growth during gestation. In response to placenta insufficiency, IUGR piglets prioritise brain development as a survival mechanism. This adaptation leads to a higher brain-to-liver weight ratio (BrW/LW) at birth. This study assessed the potential of using morphometric traits to estimate brain (BrW) and liver (LW) weights, thus enabling non-invasive diagnosis of IUGR in newborn piglets. At birth, the birth body weight (BtW) of individual piglets (n = 144) was recorded. One day (±1) after birth, BrW and LW were measured with CT (n = 94) or by weighing the organs after natural death or euthanasia (n = 50). Additionally, 20 morphometric traits were captured from images of each piglet and correlated with the BrW and LW. The morphometric traits that showed a Pearson coefficient ≥0.70 in linear correlation with the BrW or LW were selected. Each selected trait was then combined as an independent variable with BtW to develop multiple linear regression models to predict the BrW and LW. The six models (three to estimate the BrW and three the

LW) with the highest adjusted R-squared value were selected. The dataset was then randomly divided into a training (75% of the data) and a testing (remaining 25%) subset. Within the training subset, three equations to predict the BrW and three to predict the LW were extrapolated from the six best-performing models (highest adjusted R-squared value). The equations were then applied to the testing subset. The accuracy of the equations in predicting organ weight was assessed by calculating mean absolute and mean absolute percentage error (MAE and MAPE) between predicted and actual BrW and LW. To predict the BrW/LW, an equation including BtW and the two morphometric traits which better predicted BrW and LW was used. In the testing dataset, the equation combining the ear distance and BtW better estimated the BrW. The equation performed with a MAE of 1.95 and a MAPE of 0.06 between the true and estimated weight of the brain. For the liver, the equation combining the abdominal area delimited by a square and the BtW displayed the best performance, with a MAE of 9.29 and a MAPE of 0.17 between the true and estimated weight. Finally, the MAE and MAPE between the actual and estimated BrW/LW were 0.14 and 0.17, respectively. These findings suggest that specific morphometric traits can be used to estimate brain and liver weights, facilitating accurate and non-invasive identification of IUGR in newborn piglets.

Implications

Selection to improve sows' prolificacy has led to an increased percentage of piglets exposed to IUGR. This condition is characterised by a relative increase in brain size compared with other organs, such as the liver. Therefore, the diagnosis should consider the ratio between the weight of the brain and that of other organs. Our study shows that there are morphometric traits which can be used to estimate BrW and LW in newborn piglets. Predictive models based on these traits represent a promising tool for the early detection of affected piglets, enabling the development of targeted postnatal interventions.

Introduction

Efforts to improve sows' prolificacy have led to a significant increase in the number of piglets born and weaned per year (Quiniou et al., 2002; Campos et al., 2012). Although litter sizes have increased, not all piglets born in these larger litters attain their full genetic growth potential. This can be attributed to increased exposure to IUGR experienced during gestation (Quiniou et al., 2002; Amdi et al., 2013). Growth restriction in the uterus is a pathological condition characterised by impaired development of the foetus or its organs during gestation (Wu et al., 2006). The primary cause behind IUGR is placental insufficiency, which results in inadequate supply of oxygen and nutrients to the foetus (Cohen et al., 2015). This condition is associated with increased morbidity and mortality, long-term growth limitation, and low efficiency in nutrient utilisation (Wu et al., 2006). At present, this condition represents the main cause of LBtW in the pig industry and can affect up to 20-30% of piglets within a litter (Santos et al., 2022; Amdi et al., 2013; Wu et al., 2006). The identification of IUGR piglets is challenging due to the lack of specific symptoms and reliable biomarkers. Diagnosis is frequently established by considering either the absolute BW of the foetus or newborn or the BW in relation to a specific gestational age (Van Ginneken et al., 2022). D'inca et al. (2010) classified piglets as IUGR when their BtW was at least 1.5 SD units lower than the average BtW of the litter. Other studies have defined IUGR as weighing at birth less than the tenth percentile of gestational age–specific normal BtW values (Bauer et al., 2003). In a study by Wang et al. (2016), an IUGR piglet was defined as having a BtW between 0.75 and 0.90 kg and belonging to the lower quartile of the litter BtWs. However, it is important to differentiate between the definitions of IUGR, LBtW, and SGA. These terms are often used interchangeably but have important differences, as they each represent a distinct aspect of foetal growth and development (Gupta et al., 2008). Indeed, within the LBtW and SGA categories, there are subjects that do not achieve their full genetically determined size because of growth restriction

in the uterus (De Vos et al., 2014). It has been suggested that in order to identify IUGR piglets, it is important to consider their head morphology as an additional criterion (to BtW) (Hales et al., 2013). Moreover, Huting et al. (2018) demonstrated that the morphology of a newborn piglet may also be useful in predicting its later performance. Piglets that suffer from growth restriction in the uterus often show a dolphin-like head shape, wrinkles perpendicular to the mouth, bulging eyes, and hair with no direction of growth (Hales et al., 2013; Amdi et al., 2020). Besides these phenotypic traits, IUGR has been associated with a relatively larger brain compared to other organs at birth, such as the liver. Due to the oxygen and nutrient deprivation during foetal growth, the development of the brain is prioritised. This survival mechanism is called the "brain-sparing effect" and results in a higher brain-to-organ weight ratio (Cohen et al., 2015). In manuscript I (Ruggeri et al., 2024) it was demonstrated that the diagnosis of IUGR in piglets solely based on head morphology or BtW does not always align with an increased BrW/LW. For this reason, to accurately assess IUGR in newborn piglets, measurements like BtW and head shape should be complemented by evaluating the proportional relationship between brain weight and the weight of other organs (Chand et al., 2022; Felicioni et al., 2019). The absence of a non-invasive method to assess this ratio and diagnose IUGR remains a significant challenge in pig production, limiting treatment development due to poor diagnosis (Felicioni et al., 2019). Considering the adverse effects of IUGR on pig production and the inconsistencies in studies on growth-restricted pigs, there is a clear need for an accurate and standardized diagnostic approach. Models based on image analysis offer a promising tool for the early and non-invasive identification of IUGR in piglets, facilitating interventions to mitigate its negative effects.

Our hypothesis was that using specific morphometric traits, the weight of the brain, that of the liver, and their ratio could be estimated with sufficiently high accuracy, enabling non-invasive diagnosis of IUGR in newborn piglets. To test this hypothesis, we conducted a study in which

the weight of the brain and liver of newborn piglets was measured through either scale measurement after natural death or euthanasia (**BrW_{Eu}**, **LW_{Eu}**) or with CT scan imaging (**BrW_{CT}, LW_{CT}**). In addition, pictures of the same piglets were taken to capture specific body measurements such as distance between the ears, body length, and front head diameter, which were used to predict the BrW, LW, and BrW/LW.

Material and methods

Animal selection and classification

The experiment was performed at the Agroscope swine research facility situated in Posieux (Switzerland). Two studies were carried out. In the first study, 310 Swiss Large White piglets (alive = 268, stillborn/dead = 42) were included. The BtW of each piglet was registered on the day of farrowing (day 0). The BtW of the piglets born during the evening or night was measured the following morning. One day (± 1) after birth, CT scan imaging (64-channel multislice scanner Siemens Emotion Duo CT, Siemens, Erlangen, Germany) was conducted to non-invasively measure brain and liver volumes for each piglet. The procedures for handling the pigs and analysing the CT scan images were described in detail in manuscript I (Ruggeri et al., 2024). Briefly, all the animals were anaesthetized with isoflurane and positioned in sternal recumbency for CT scans of the head and the thoracic region. The resulting images were then semi-automatically processed (Turtleseg software 1.2.1) to calculate the volumes of the brain and liver. After the CT scan, 30 piglets were selected and euthanised with an intra-cardiac injection of pentobarbital solution (Esconarkon, Streuli Tiergesundheit AG, Uznach, Switzerland), as described in manuscript I (Ruggeri et al., 2024). The selection was based on the BtW. Three BtW categories were defined to include the full range of BtWs present in the study population. From each category 10 piglets were euthanised. The brain and the blood-

filled liver were excised. Brain ($BrW_{Eu)}$ and liver (LW_{Eu}) weights were assessed with a scale, and the volumes were determined with the water displacement method (Lemke et al., 2006). Volume and weight were used to calculate the density of the organs according to the following equation, where *d* represents the density of the organ, *m* represents the mass in g, and *V* the volume in mL:

$$d = m\,(g) \,/\, V\,(mL)$$

The average brain and liver densities together with the brain and liver volumes measured with the CT scan were used to assess brain weight (BrW_{CT}), liver weight (LW_{CT}), and the brain-to-liver weight ratio (**BrW_{CT}/LW_{CT}**) for each piglet.

To extend the dataset, which was unbalanced due to the limited number of piglets exhibiting a high BrW_{CT}/LW_{CT} compared to the population mean, a second experiment was performed at the same facility. All Swiss Large White piglets born from 35 litters with a BtW lower than 1 kg were included (n = 67, alive = 35, stillborn/dead = 32). On the day of farrowing (day 0), the BtW of each piglet was recorded. The BtW of the piglets born during the evening or night was measured the following morning. On day one (± 1) after birth, the piglets (n = 35) were euthanised with an overdose of pentobarbital (Esconarkon). The brain and blood-filled liver were then excised from each piglet (alive = 35, stillborn/dead = 32), as described before. The BrW_{Eu} and LW_{Eu} were assessed with a scale and used to determine the BrW_{Eu}/LW_{Eu}. Three regression equations were then developed and used to calculate the BrW_{CT}, LW_{CT}, and BrW_{CT}/LW_{CT} from the weights obtained after death/euthanasia. The objective was to standardize the data, as the CT scan was not available for the second study.

Image collection

To capture specific morphometric traits, videos of all the piglets (first study = 310, second study = 67) were recorded on day one (± 1) using a 3D camera (RealSense depth camera D435i, Intel, USA) placed at 40 cm from the animal. Each piglet was positioned in a hammock and a short (~2 s) video was recorded, with the camera moving from the right lateral side to the top of the piglet. A fixed distance between the camera and the piglet was maintained by using a pivoting arm. Videos were then saved in BAG format. From each video, a series of individual RGB images were extracted one by one to create a collection of frames. The frame extraction procedure was performed using Python programming language (version 3.8.8). The frames were then converted into PNG format through the rs-convert.exe tool, available within the Intel RealSense program (SDK 2.0, Intel Corporation, USA).

Body measurements

Body measurements were collected from frames of 144 piglets, 94 from the first study and 50 from the second study. The piglets were selected randomly, with a target total of 150, including 100 piglets from the first study and 50 from the second study, due to the latter's smaller dataset. However, six piglets from the first study were subsequently excluded because of the poor quality of their images. The first frame (frame 1) shows the piglet from the right lateral side and the second (frame 2) from the top (Fig. 1). Specific measurements were taken on the frames by using ImageJ software (version 1.53, U.S. National Institutes of Health, Bethesda, Maryland, USA). For each piglet, 20 body measurements were recorded in total: 13 (frame 1 = 8, frame 2 = 5) to correlate to the weight of the brain (Fig. 2), 6 (frame 1 = 3, frame 2 = 3) to the weight of the liver (Fig. 3), and 1 (frame 2) to both the organs' weights (Fig. 2 and Fig. 3). To test the repeatability of the method, a subset of the morphometric traits (n = 12) was measured by a second observer (see Supplementary Table S1).

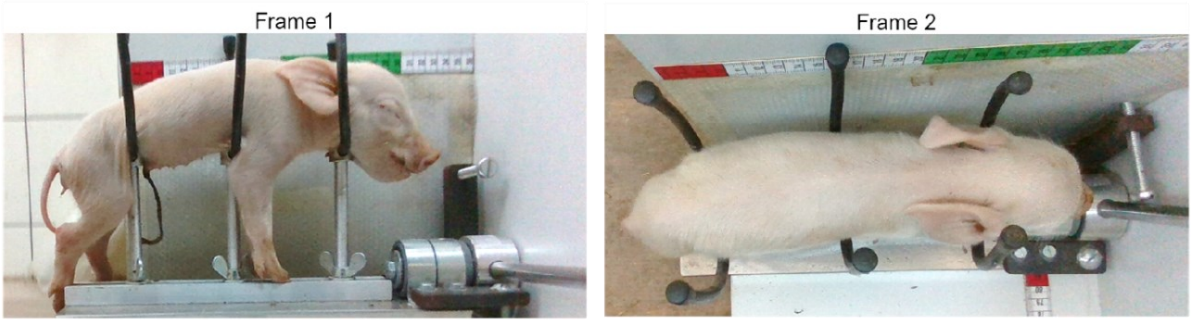

Fig 1. Two frames were selected for each piglet to perform body measurements. Frame 1 (left) shows the piglet from the right lateral side and frame 2 (right) from the top.

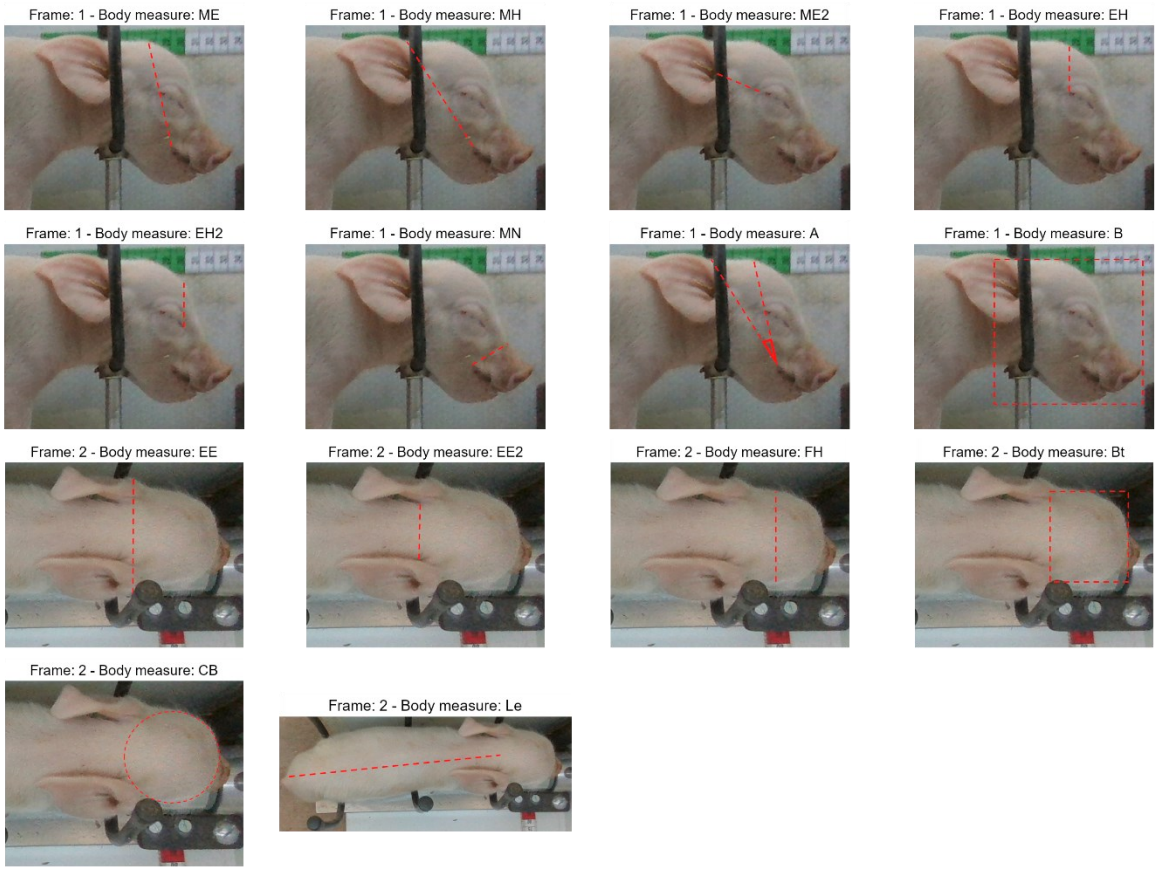

Fig. 2. Body measurements recorded to correlate with the weight of the brain of the piglets. ME: distance between the mouth and the front head passing by the lateral edge of the eye, seen from the side; MH: distance between the mouth and the front head passing by the medial edge of the ear, seen from the side; ME2: distance between the caudal edge of the eye and the ear, seen from the side; EH: distance between the lateral edge of the eye and the front head, following a straight line, seen from the side; EH2: distance between the medial edge of the eye and the front head, following a straight line, seen from the side; MN: distance between the caudal edge of the mouth and the nose, following a line perpendicular to the nose, seen from the side; A: angle between ME and MH; B: area of the head delimited by a square, seen from the side; EE: distance between the lateral edge of the ears, seen from above; EE2: distance between the medial edge of the ears, seen from above; FH: larger diameter of the front head, seen from above; Bt: area of the front head delimited by a square, seen from above; CB: area

of the front head delimited by a circle, seen from above; Le: length of the body, from the caudal edge of the head to the end of the body following the spine, seen from above.

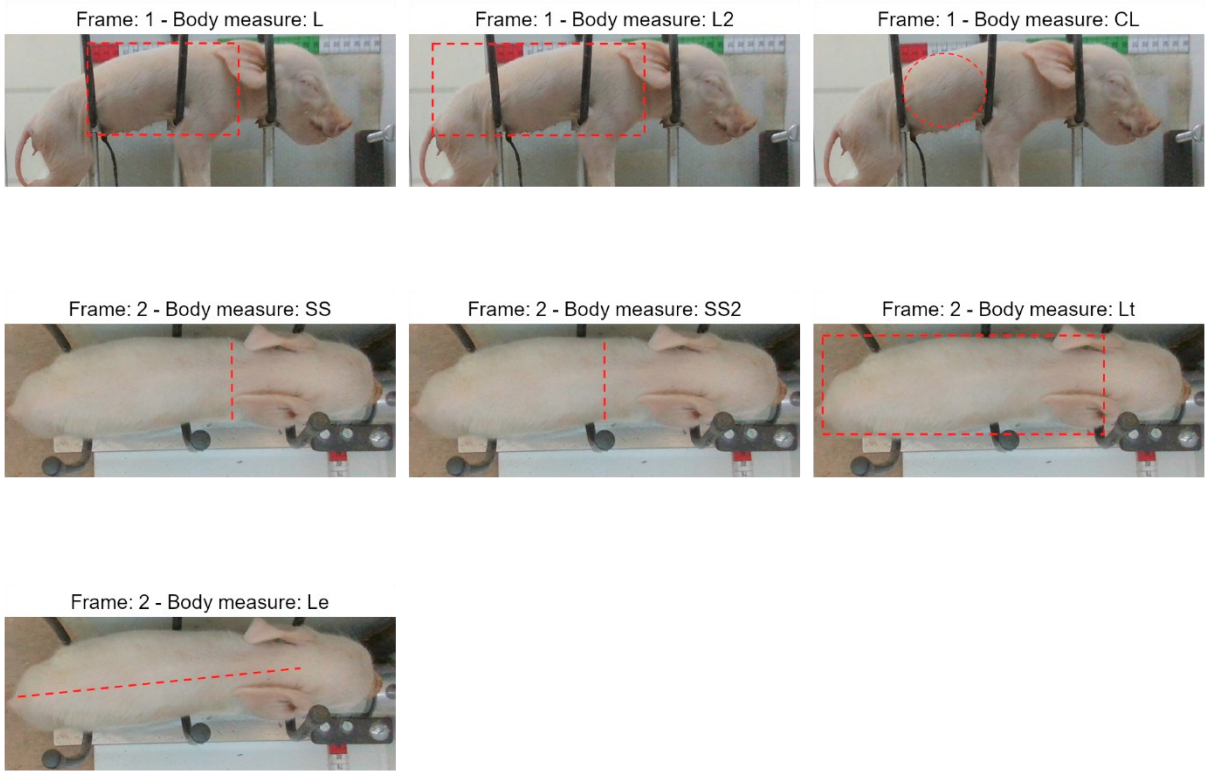

Fig. 3. Body measurements recorded to correlate with the weight of the liver of the piglets. L: area of the body delimited by a square from the caudal edge of the head to the caudal edge of the abdomen, seen from the side; L2: area of the body delimited by a square from the caudal edge of the head to the caudal edge of the body, seen from the side; CL: area of the abdomen delimited by a circle, seen from the side; SS: distance between the shoulders, seen from above; SS2: diameter of the abdomen measured caudally to the shoulders, seen from above; Lt: area of the body delimited by a square from the caudal edge of the head to the caudal edge of the body, seen from above; Le: length of the body, from the caudal edge of the head to the end of the body following the spine, seen from above.

Data analysis

All calculations and statistical analyses were performed using Python (version 3.8.8). The packages employed were numpy, pandas, seaborn, matplotlib, scipy, scipy.stats, statsmodels.api, statsmodels.formula.api, sklearn.model_selection, and sklearn.metrics.

Brain weight, liver weight, and correlation between calculated CT weight and actual weights of organs

For the 30 piglets euthanised, the weights of the brain and liver were measured both directly with a scale after euthanasia (BrW_{Eu}, LW_{Eu}) and by multiplying the densities of the two organs by the volumes obtained from the CT scan images (BrW_{CT}, LW_{CT}). The correlation between the weights obtained by the two methodologies was tested, and three regression equations were then developed to calculate the BrW_{CT}, LW_{CT}, and BrW_{CT}/LW_{CT} from the weights obtained after euthanasia (BrW_{Eu}, LW_{Eu}, and BrW_{Eu}/LW_{Eu}). The equations were applied to the data collected during the second study to standardize the datasets from the two studies.

Body measurements to predict brain weight, liver weight, and their ratio (brain weight/liver weight)

The BtW and body measurements of each selected piglet (n = 144, 94 from study one and 50 from study two) were used to correlate with the BrW_{CT} and the LW_{CT}. The linear relation of the BtW and each morphometric trait (shown in Fig. 2 and Fig. 3) with the BrW_{CT} and LW_{CT} was tested, and the degree of correlation was expressed as the Pearson correlation coefficient. The morphometric traits which correlated with a Pearson correlation coefficient ≥0.70 with either brain or liver weight were selected for further analysis. In addition, each morphometric trait was used, in combination with the BtW, as an independent variable to develop multiple linear regression models to predict the BrW_{CT} and LW_{CT}. Among the resulting models, the six morphometric traits — three to correlate with the brain and three to correlate with the liver—

which, in combination with BtW, displayed the highest adjusted R^2 value ($\boldsymbol{R^2_{adj}}$) were selected. This selection process allowed identification of the most influential variables for predicting BrW_{CT} and LW_{CT}.

Having determined these key morphometric traits, the dataset was randomly divided into two distinct subsets: a training dataset containing 75% of the data (108 piglets, 69 from study one and 39 from study two) and a testing dataset including the remaining 25% (36 piglets, 25 from study one and 11 from study two). Using the training dataset, three equations to predict BrW_{CT} and three additional equations to predict LW_{CT} were developed based on the six most predictive variables (as indicated by the highest R^2_{adj} derived from the multiple regression models). These equations were applied on the training dataset first and subsequently on the testing datasets, to assess the predictive performances of the models on unseen data. When applying these prediction equations to both the training and testing datasets, six distinct predicted values of BrW_{CT} were obtained for each piglet, three for the training datasets and three for the testing dataset. The same results were obtained for the liver.

In order to predict the BrW_{CT}/LW_{CT}, two approaches were tested. In the first, the two variables which, along with the BtW, better predicted the BrW_{CT} and LW_{CT} (lower percentage error in the testing dataset) were used in combination to develop a multiple linear regression model to predict the BrW_{CT}/LW_{CT}. Prior to this analysis, a log transformation was applied to the BrW_{CT}/LW_{CT} values, as the residuals exhibited a characteristic of non-linearity. The regression equation extrapolated from the model in the training dataset was then applied to the testing dataset. In the second approach, the predicted BrW_{CT} and LW_{CT}, calculated using the previous models, were directly employed to determine the BrW_{CT}/LW_{CT}, both in the training and testing subsets. Throughout this process, the linear relation between the true and the predicted BrW_{CT}, $LW_{CT,}$ and BrW_{CT}/LW_{CT} was always tested, and the Pearson correlation coefficient was reported for both the training and the testing dataset.

Finally, the models' predictive performances were evaluated using mean absolute error (**MAE**) and mean absolute percentage error (**MAPE**) between the true and predicted BrW_{CT}, $LW_{CT,}$ and BrW_{CT}/LW_{CT}. The MAE and MAPE were reported for both the training and the testing dataset. Additionally, the MAE and MAPE between the true and predicted BrW_{CT}/LW_{CT} were measured excluding from the calculation the piglets born with a BtW below 800 g, as euthanasia of these piglets is a common practice in modern swine production systems. When the BrW_{CT}/LW_{CT} was predicted according to the first approach, the correlation coefficient, MAE, and MAPE between true and predicted BrW_{CT}/LW_{CT} were assessed after reversing the logarithmic transformation of the data. The *P* value of the correlation coefficient was always tested and considered significant at <0.05.

The predictive ability of the BtW alone to estimate the BrW_{CT} and LW_{CT} was consistently tested throughout the various steps of the analysis. The inclusion of BtW as the only predictor at each step provided a baseline for comparison, enabling the evaluation of how the addition of morphometric traits improved the models' performance. Simple linear regression models, incorporating only BtW, were developed to predict BrW_{CT}, LW_{CT}, and BrW_{CT}/LW_{CT} (Supplementary Table S2), and their performances were evaluated on both training and testing datasets. In addition, the models including BtW as sole predictor (e.g., $BrW_{CT} \sim$ BtW) and the models including BtW in combination with morphometric traits (e.g., $BrW_{CT} \sim$ BtW + EE) were compared with an analysis of variance (ANOVA). This statistical test was used to evaluate whether the inclusion of morphometric traits in addition to BtW results in a significant improvement in the models' ability to explain the variance in the dependent variables (BrW_{CT}, LW_{CT}, BrW_{CT}/LW_{CT}).

Results

The average BrW_{CT}/LW_{CT} determined in the first (n = 310) and second (n = 67) studies was 0.62 ± 0.31 and 1.01 ± 0.43 [harmonic mean ± SD], respectively (Table 1).

Brain weight, liver weight, and correlation between calculated CT weight and actual weight of each organ

The euthanized piglets (n = 30) exhibited an average BrW_{Eu} of 32.3 ± 2.5 and BrW_{CT} of 34.4 ± 3.7 [mean ± SD]. In terms of LW_{Eu} and LW_{CT}, the mean values were 58.1 ± 27.1 and 67.0 ± 33.5, respectively. The average BrW_{Eu}/LW_{Eu} and BrW_{CT}/LW_{CT} were 0.57 ± 0.4 and 0.53 ± 0.4 [harmonic mean ± SD], respectively (Table 1).

The correlation coefficients between the BrW, LW, and BrW/LW determined after death/euthanasia or by CT are presented in Table 2. Generally, all traits were highly correlated ($P < 0.001$), with values ranging from 0.83 to 0.97. The correlation coefficients between LW_{Eu} and LW_{CT} and BrW_{Eu}/LW_{Eu} and BrW_{CT}/LW_{CT} were higher ($P < 0.001$) than those between BrW_{Eu} and BrW_{CT}. Nevertheless, the obtained correlation coefficients were highly significant (Table 2) and let us conclude that determinations of BrW_{CT}, LW_{CT}, and BrW_{CT}/LW_{CT} from the weights obtained after euthanasia were likely accurate enough for further analysis, despite the limited dataset.

Table 1. Mean values of brain and liver weights and brain-to-liver weight ratio assessed after death/euthanasia (BrW_{Eu}, LW_{Eu}, BrW_{Eu}/LW_{Eu}), brain and liver weights and brain-to-liver weight ratio obtained from CT scan volumes (BrW_{CT}, LW_{CT}, BrW_{CT}/LW_{CT}), and brain and liver weights and brain-to-liver weight ratio estimated from BrW_{Eu}, LW_{Eu}, BrW_{Eu}/LW_{Eu} through regression equations (estimated BrW_{CT}, estimated LW_{CT}, estimated BrW_{CT}/LW_{CT}).

	BrW Mean ± SD			LW Mean ± SD			BrW/LW Harmonic mean ± SD		
	BrW_{Eu}[1]	BrW_{CT}[2]	Estimated BrW_{CT}[3]	LW_{Eu}[4]	LW_{CT}[5]	Estimated LW_{CT}[6]	BrW_{Eu}/LW_{Eu}[7]	BrW_{CT}/LW_{CT}[8]	Estimated BrW_{CT}/LW_{CT}[9]
Study 1									
All piglets (n=310)	-	34.8 ± 3.1	-	-	57.0 ± 21.3	-	-	0.62 ± 0.3	-
Selected piglets (n=94)	-	34.8 ± 2.8	-	-	57.3 ± 18.5	-	-	0.62 ± 0.3	-
Euthanised piglets (n=30)	32.3 ± 2.5	34.4 ± 3.7	-	58.1 ± 27.1	67.0 ± 33.5	-	0.57 ± 0.4	0.53 ± 0.4	0.50 ± 0.4
Study 2									
All piglets (n=67)	26.5 ± 3.2	-	27.4 ± 4.0	24.7 ± 9.7	-	27.1 ± 11.6	1.05 ± 0.4	-	1.00 ± 0.4
Selected piglets (n=50)	27.0 ± 2.9	-	28.0 ± 3.6	25.1 ± 9.2	-	27.5 ± 11.0	1.19 ± 0.4	-	1.15 ± 0.4

[1] BrW_{Eu} = brain weight assessed with a scale after euthanasia.

[2] BW_{CT} = brain weight obtained from CT scan volume.

[3] Estimated BrW_{CT} = estimated BrW_{CT} from the weight assessed after euthanasia (BrW_{Eu}) through the equation: $BrW_{CT} = (1.23 \times BrW_{Eu}) - 5.19$.

[4] LW_{Eu} = liver weight assessed with a scale after euthanasia.

[5] LW_{CT} = liver weight obtained from CT scan volume.

[6] Estimated LW_{CT} = estimated LW_{CT} from the weight assessed after euthanasia (LW_{Eu}) through the equation: $LW_{CT} = (1.2 \times LW_{Eu}) - 2.57$.

[7] BrW_{Eu}/LW_{Eu} = brain-to-liver weight ratio assessed with a scale after euthanasia.

[8] BrW_{CT}/LW_{CT} = brain-to-liver weight ratio obtained from CT scan volumes.

[9] Estimated BrW_{CT}/LW_{CT} = estimated BrW_{CT}/LW_{CT} from the brain-to-liver weight ratio assessed after euthanasia (BrW_{Eu}/LW_{Eu}) through the equation: $BrW_{CT}/LW_{CT} = (0.97 \times BrW_{Eu}/LW_{Eu}) - 0.014$.

Table 2. Simple linear regression models to correlate brain weight (BrW_{Eu}), liver weight (LW_{Eu}), and brain-to-liver weight ratio (BrW_{Eu}/LW_{Eu}) assessed after death/euthanasia of the piglets to brain weight (BrW_{CT}), liver weight (LW_{CT}), and brain-to-liver weight ratio (BrW_{CT}/LW_{CT}) obtained from computed tomography (CT) scan volumes.

	r[1]	P value[2]	R^2_{adj}[3]	a[4]	Intercept
Item[5]					
$BrW_{CT} \sim BrW_{Eu}$	0.83	< 0.001	0.68	1.23	−5.19
$LW_{CT} \sim LW_{Eu}$	0.97	< 0.001	0.94	1.20	−2.57
$BrW_{CT}/LW_{CT} \sim BrW_{Eu}/LW_{Eu}$	0.97	< 0.001	0.95	0.97	−0.01

[1] r = Pearson correlation coefficient.

[2] P value of the Pearson correlation coefficient.

[3] R^2_{adj} = adjusted R-squared.

[4] a = slope of the regression line.

[5] BrW_{Eu} = brain weight assessed with a scale on 30 piglets after euthanasia; LW_{Eu} = liver weight assessed with a scale on 30 piglets after euthanasia.

Body measurements to predict brain weight, liver weight, and brain weight/liver weight ratio

Twenty morphometric measurements were taken from each pig. The correlation coefficients between the BtW and each morphometric measurement with the BrW_{CT} or LW_{CT} are reported in Table 3 and Table 4, respectively. The correlation coefficients ranged from −0.42 to 0.83 for the BrW_{CT} and from 0.80 to 0.88 for the LW_{CT}. Except for morphometric measurements A and EH, for which the correlation with the BrW_{CT} was not statistically significant, the other traits had r-values with *P* values <0.05. The morphometric traits that were correlated with the BrW_{CT} (n = 6) and LW_{CT} (n = 7) with a Pearson correlation coefficient ≥0.70 are depicted in Fig. 4 and Fig. 5**.**

Table 3. Correlation coefficients between birth body weight (BtW)/morphometric measurements and brain weight (BrW_{CT}) determined after computed tomography (CT) scan or death/euthanasia of the piglets.

	r[1]	P value[2]
Item[3]		
BtW, kg	0.83	< 0.001
EE, pixel	0.82	< 0.001
Bt, pixel^2	0.78	< 0.001
EE2, pixel	0.77	< 0.001
Le, pixel	0.75	< 0.001
FH, pixel	0.75	< 0.001
CB, pixel^2	0.74	< 0.001
MH, pixel	0.69	< 0.001
ME, pixel	0.63	< 0.001
B, pixel^2	0.61	< 0.001
ME2, pixel	0.29	< 0.001
MN, pixel	0.19	0.02
A, °	−0.16	0.05
EH, pixel	−0.13	0.12
EH2, pixel	−0.42	< 0.001

[1] r = Pearson correlation coefficient.

[2] *P* value of the Pearson correlation coefficient.

[3] BtW = birth body weight; EE = distance between the lateral edge of the ears, seen from above; Bt = area of the front head delimited by a square, seen from above; EE2 = distance between the medial edge of the ears, seen from above; Le = length of the body, from the caudal edge of the head to the end of the body following the spine, seen from above; FH = larger diameter of the front head, seen from above; CB = area of the front head delimited by a circle, seen from above; MH = distance between the mouth and the front head passing by the medial edge of the ear, seen from the side; ME = distance between the mouth and the front head passing by the lateral edge of the eye, seen from the side; B: area of the head delimited by a square, seen from the side; ME2 = distance between the caudal edge of the eye and the ear, seen from the side; MN = distance between the caudal edge of the mouth and the nose, following a line perpendicular to the nose, seen from the side; A = angle between ME and MH; EH = distance between the lateral edge of the eye and the front head, following a straight line, seen from the side; EH2 = distance between the medial edge of the eye and the front head, following a straight line, seen from the side.

Table 4. Correlation coefficients between birth body weight (BtW)/morphometric measurements and liver weight (LW_{CT}) determined after computed tomography (CT) scan or death/euthanasia of the piglets.

	r[1]	P value[2]
Item[3]		
BtW, kg	0.88	< 0.001
Lt, pixel^2	0.87	< 0.001
L2, pixel^2	0.86	< 0.001
L, pixel^2	0.86	< 0.001
SS2, pixel	0.84	< 0.001
SS, pixel	0.83	< 0.001
CL, pixel^2	0.83	< 0.001
Le, pixel	0.80	< 0.001

[1] r = Pearson correlation coefficient.

[2] *P* value of the Pearson correlation coefficient.

[3] BtW = birth body weight; Lt = area of the body delimited by a square from the caudal edge of the head to the caudal edge of the body, seen from above; L2 = area of the body delimited by a square from the caudal edge of the head to the caudal edge of the body, seen from the side; L= area of the body delimited by a square, from the caudal edge of the head to the caudal edge of the abdomen, seen from the side; SS2 = diameter of the abdomen measured caudally of the shoulders, seen from above; SS = distance between the shoulders, seen from above; CL = area of the abdomen delimited by a circle, seen from the side; Le = length of the body, from the caudal edge of the head to the end of the body following the spine, seen from above.

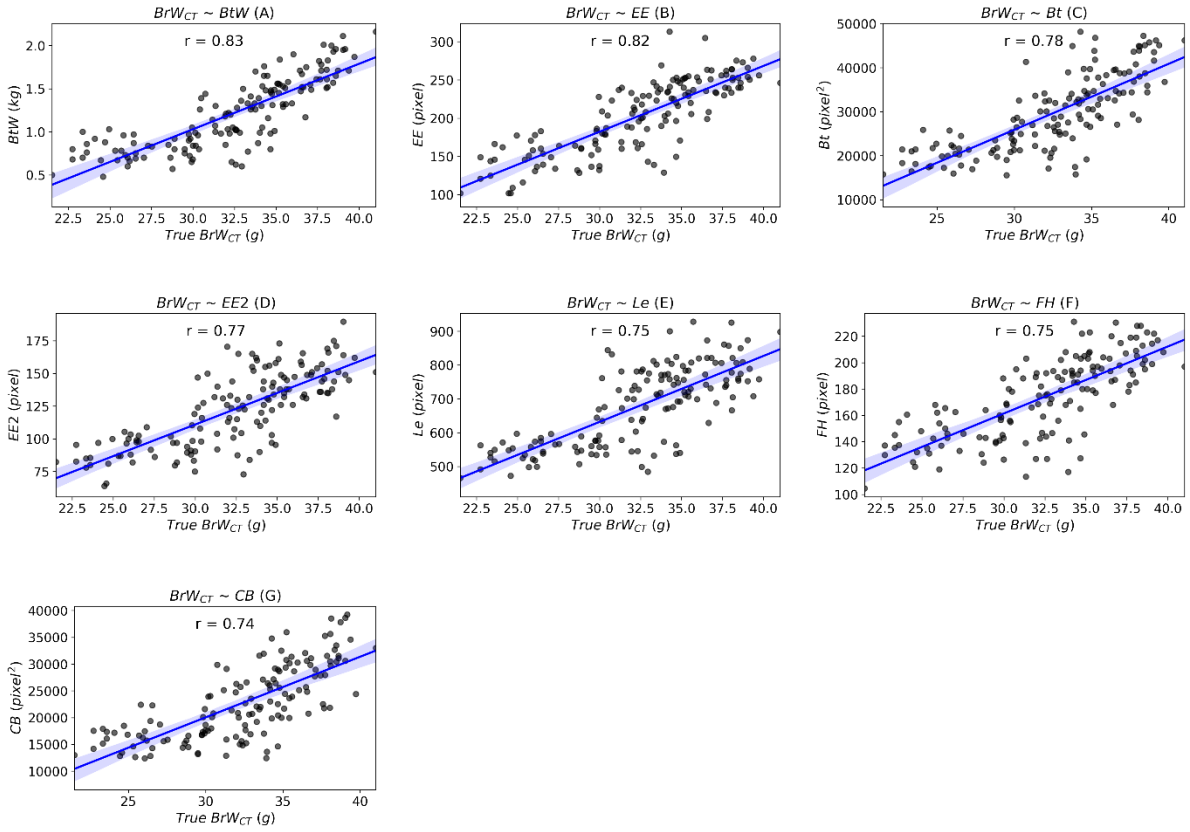

Fig. 4. Variables which showed a Pearson coefficient (r) ≥0.70 in the linear correlation with brain weight (BrW_{CT}) of the piglets. x-Axis: BrW_{CT} (g); y-axis: (A) birth body weight (BtW); (B) EE: distance between the lateral edge of the ears, seen from above; (C) Bt: area of the front head delimited by a square, seen from above; (D) EE2: distance between the medial edge of the ears, seen from above; (E) Le: length of the body, from the caudal edge of the head to the end of the body following the spine, seen from above; (F) FH: larger diameter of the front head, seen from above; (G) CB: area of the front head delimited by a circle, seen from above.

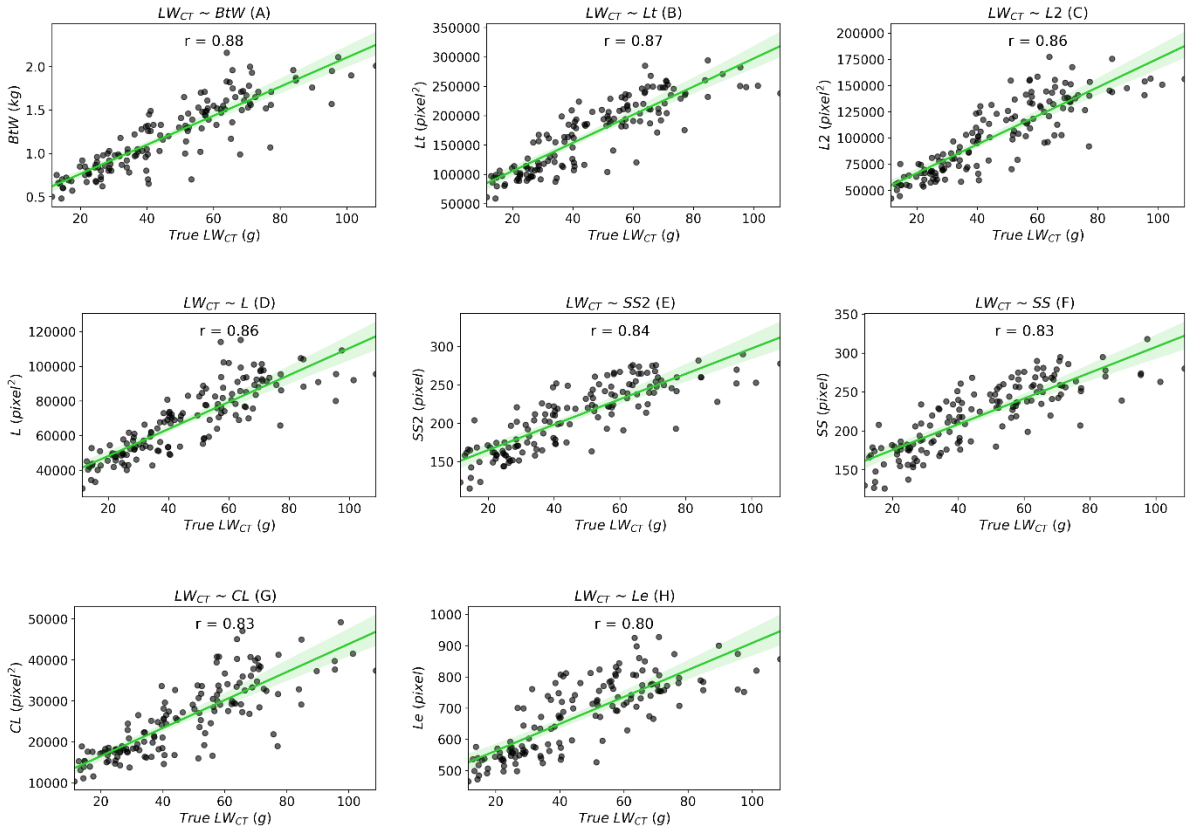

Fig. 5. Variables which showed a Pearson coefficient (r) ≥0.70 in the linear correlation with the LW_{CT} of the piglets. x-Axis: LW_{CT} (g); y-axis: (A) birth body weight (BtW); (B) Lt: area of the body delimited by a square from the caudal edge of the head to the caudal edge of the body, seen from above; (C) L2: area of the body delimited by a square from the caudal edge of the head to the caudal edge of the body, seen from the side; (D) L: area of the body delimited by a square from the caudal edge of the head to the caudal edge of the abdomen, seen from the side; (E) SS2: diameter of the abdomen measured caudally of the shoulders, seen from above; (F) SS: distance between the shoulders, seen from above; (G) CL: area of the abdomen delimited by a circle, seen from the side; (H) Le: length of the body, from the caudal edge of the head to the end of the body following the spine, seen from above.

Using the morphometric measurements reported in Fig. 4 and Fig. 5, a variety of multiple linear regression models were computed to predict the BrW_{CT} (Table 5) and LW_{CT} (Table 6). The linear combination of the BtW and the distance between the lateral edge of the ears (EE, Fig. 2) showed the highest R^2_{adj} (0.72) in predicting the BrW_{CT}, followed by the distance between the medial edge of the ears (EE2, Fig. 2; 0.71) and the area of the front head delimited by a square (Bt, Fig. 2; 0.71) (Table 5). Regarding the LW_{CT}, the highest R^2_{adj} was achieved by the linear combination of BtW and the area of the body delimited by a square from the caudal edge of the head to the caudal edge of the body (Lt, Fig. 3; $R^2_{adj} = 0.80$), followed by the area of the body delimited by a square from the caudal edge of the head to the caudal edge of the abdomen (L, Fig. 3; $R^2_{adj} = 0.79$) and the length of the body, from the caudal edge of the head to the end of the body following the spine (Le, Fig. 3; $R^2_{adj} = 0.79$) (Table 6).

These six morphometric measurements (EE, EE2, and Bt to estimate the BrW_{CT} and Lt, L, and Le to estimate the LW_{CT}) which, in combination with the BtW, showed the highest R^2_{adj} in the multiple linear regressions were selected and used to develop equations in the training dataset to calculate the BrW_{CT} and LW_{CT}. The degree of correlation between the true and the predicted BrW_{CT} and LW_{CT} was tested for all the equations in the training and testing datasets and is reported in Fig. 6 and Fig. 7, respectively.

Table 5. Adjusted R^2 values (R^2_{adj}) of multiple linear regression models to predicted brain weight (BrW_{CT}) determined after computed tomography (CT) scan or death/euthanasia of the piglets from birth weight (BtW) and morphometric measurements.

	R^2_{adj}[1]	a1[2]	a2[3]	Intercept
Item[4]				
BrW_{CT} ~ BtW + EE	0.72	5.39	0.04	18.4
BrW_{CT} ~ BtW + EE2	0.71	6.76	0.04	19.1
BrW_{CT} ~ BtW + Bt	0.71	6.75	0.0001	20.3
BrW_{CT} ~ BtW + CB	0.70	7.31	0.0001	20.5
BrW_{CT} ~ BtW + Le	0.70	7.37	0.007	18.5
BrW_{CT} ~ BtW + FH	0.70	7.43	0.03	18.7
BrW_{CT} ~ BtW	0.69	9.12	-	21.4

[1] R^2_{adj} = adjusted R-squared.

[2] a1 = regression coefficient associated with the first predictor variable (BtW).

[3] a2 = regression coefficient associated with the second predictor variable (EE; EE2; Bt; CB; Le; FH)

[4] BtW = birth body weight; EE = distance between the lateral edge of the ears, seen from above; EE2 = distance between the medial edge of the ears, seen from above; Bt = area of the front head delimited by a square, seen from above; CB = area of the front head delimited by a circle, seen from above; Le = length of the body, from the caudal edge of the head to the end of the body following the spine, seen from above; FH= larger diameter of the front head, seen from above.

Table 6. Adjusted R^2 values (R^2_{adj}) of multiple linear regression models to predicted the liver weight (LW_{CT}) determined after computed tomography (CT) scan or death/euthanasia of the piglets from birth weight (BtW) and morphometric measurements.

	R^2_{adj}[1]	a1[2]	a2[3]	Intercept
Item[4]				
LW_{CT} ~ BtW + Lt	0.80	27.3	0.0001	−10.8
LW_{CT} ~ BtW + L	0.79	33.0	0.0003	−14.2
LW_{CT} ~ BtW + Le	0.79	37.5	0.04	−24.2
LW_{CT} ~ BtW + L2	0.78	33.9	0.0002	−10.7
LW_{CT} ~ BtW + SS2	0.78	36.3	0.11	−19.8
LW_{CT} ~ BtW + SS	0.78	37.5	0.1	−19.5
LW_{CT} ~ BtW + CL	0.78	40.9	0.0003	−9.95
LW_{CT} ~ BtW	0.78	46.5	-	−9.53

[1] R^2_{adj} = adjusted R-squared.

[2] a1 = regression coefficient associated with the first predictor variable (BtW).

[3] a2 = regression coefficient associated with the second predictor variable (Lt; L; Le; L2; SS2; SS; CL)

[4] BtW = birth body weight; Lt = area of the body delimited by a square from the caudal edge of the head to the caudal edge of the body, seen from above; L = area of the body delimited by a square from the caudal edge of the head to the caudal edge of the abdomen, seen from the side; Le = length of the body, from the caudal edge of the head to the end of the body following the spine, seen from above; L2 = area of the body delimited by a square from the caudal edge of the head to the caudal edge of the body, seen from the side; SS2 = diameter of the abdomen measured caudally to the shoulders, seen from above; SS = distance between the shoulders, seen from above; CL = area of the abdomen delimited by a circle, seen from the side.

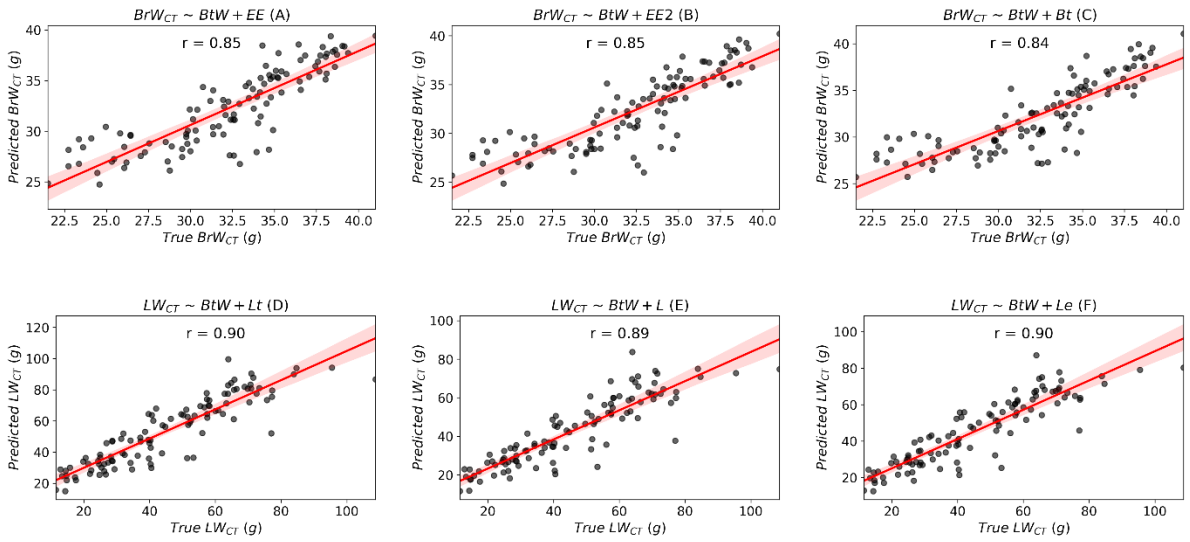

Fig. 6. Linear regressions between true and predicted BrW_{CT} and LW_{CT} of the piglets of the training dataset. x-Axis: true brain weight (true BrW_{CT}) (panel A, B, C) and true liver weight (true LW_{CT}) (panel E, F, G); y-axis: (A) brain weight (predicted BrW_{CT}) predicted from birth body weight (BtW) and the distance between the lateral edge of the ears, seen from above (EE); (B) brain weight (predicted BrW_{CT}) predicted from BtW and the distance between the medial edge of the ears, seen from above (EE2); (C) brain weight (predicted BrW_{CT}) predicted from BtW and the area of the front head delimited by a square, seen from above (Bt); (D) liver weight (predicted LW_{CT}) predicted from BtW and the area of the body delimited by a square from the caudal edge of the head to the caudal edge of the body, seen from above (Lt); (E) liver weight (predicted LW_{CT}) predicted from BtW and the area of the body delimited by a square from the caudal edge of the head to the caudal edge of the abdomen, seen from the side (L); (F) liver weight (predicted LW_{CT}) predicted from BtW and the length of the body, from the caudal edge of the head to the end of the body following the spine; seen from above (Le). r: Pearson correlation coefficient.

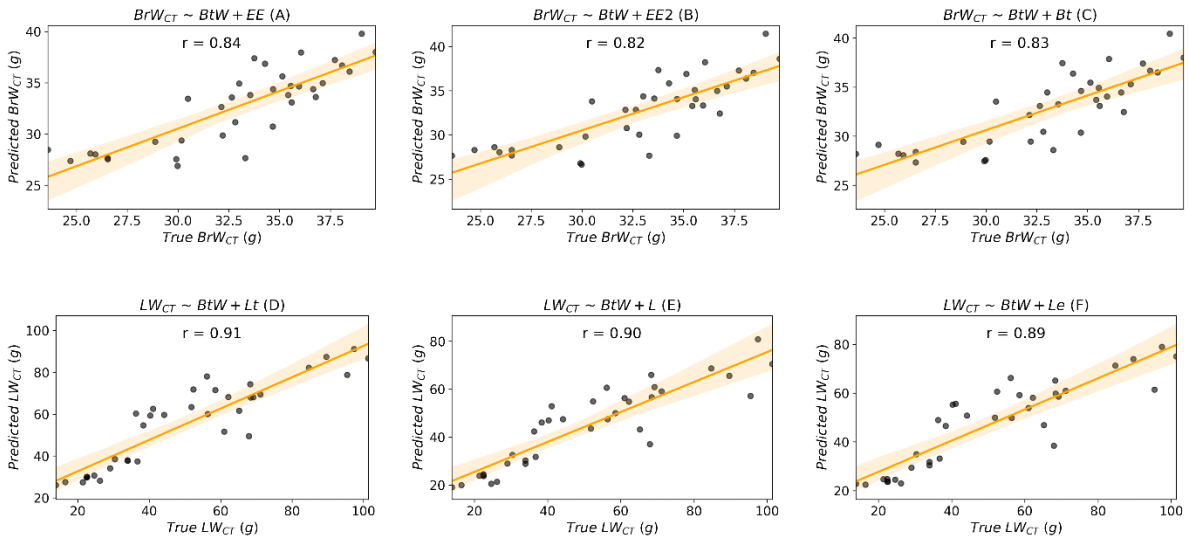

Fig. 7. Linear regressions between true and predicted BrW_{CT} and LW_{CT} of the piglets of the training dataset. x-Axis: true brain weight (true BrW_{CT}) (panel A, B, C) and true liver weight (true LW_{CT}) (panel E, F, G); y-axis: (A) brain weight (predicted BrW_{CT}) predicted from birth body weight (BtW) and the distance between the lateral edge of the ears, seen from above (EE); (B) brain weight (predicted BrW_{CT}) predicted from BtW and the distance between the medial edge of the ears, seen from above (EE2); (C) brain weight (predicted BrW_{CT}) predicted from BtW and the area of the front head delimited by a square, seen from above (Bt); (D) liver weight (predicted LW_{CT}) predicted from BtW and the area of the body delimited by a square from the caudal edge of the head to the caudal edge of the body, seen from above (Lt); (E) liver weight (predicted LW_{CT}) predicted from BtW and the area of the body delimited by a square from the caudal edge of the head to the caudal edge of the abdomen, seen from the side (L); (F) liver weight (predicted LW_{CT}) predicted from BtW and the length of the body, from the caudal edge of the head to the end of the body following the spine; seen from above (Le). r: Pearson correlation coefficient.

The three regression equations (Table 7) developed to predict the BrW_{CT} showed similar performance. When EE was used alongside BtW (BrW_{CT} ~ BtW + EE), the resulting MAE and MAPE between true and predicted BrW_{CT} values were 1.78 and 0.06 in the training dataset (Table 8) and 1.95 and 0.06 in the testing dataset, respectively (Table 9). When EE2 was included in combination with the BtW (BrW_{CT} ~ BtW + EE2), the MAE and MAPE between the true and the predicted BrW_{CT} values were 1.74 and 0.06 in the training dataset (Table 8) and 2.07 and 0.07 in the testing dataset (Table 9). Similarly, when Bt was included in combination with the BtW (BrW_{CT} ~ BtW + Bt), the MAE and MAPE between the true and the predicted BrW_{CT} values were 1.79 and 0.06 in the training dataset (Table 8) and 1.99 and 0.06 in the testing dataset (Table 9), respectively.

Of the three regression equations (Table 7) predicting the LW_{CT}, the one which showed better performance included the combination of BtW and L (LW_{CT} ~ BtW + L). In this case, the MAE and MAPE were equal to 7.03 and 0.16 in the training dataset (Table 8) and 9.29 and 0.17 in the testing dataset (Table 9), respectively.

As previously described, two approaches were tested to predict the BrW_{CT}/LW_{CT}. In the first case, an equation was constructed on the training dataset to estimate the BrW_{CT}/LW_{CT} by incorporating the distance between the lateral edges of the ears (EE, Fig. 2) and the area of the body delimited by a square from the caudal edge of the head to the caudal edge of the abdomen (L, Fig. 3), along with the BtW (BrW_{CT}/LW_{CT} ~ BtW + EE+ L). Indeed, these were the measures that better predicted the BrW_{CT} and LW_{CT}. In the second approach, the values of BrW_{CT} and LW_{CT} estimated with the equations developed in the training dataset, derived from EE in combination with BtW (BrW_{CT} ~ BtW + EE) and L in combination with BtW (LW_{CT} ~ BtW + L), respectively, were directly employed to determine the BrW_{CT}/LW_{CT}. The degree of correlation between the true and the predicted BrW_{CT}/LW_{CT} was tested in the training and testing datasets for the first (Fig. 8 and Fig. 9, panel A) and the second approach (Fig. 10 and

Fig. 11, panel A). Using the first approach, the MAE and MAPE between the true and predicted BrW_{CT}/LW_{CT} were equal to 0.16 and 0.19 in the training dataset (Table 8) and 0.14 and 0.17 in the testing dataset, respectively (Table 9). For the second approach, the MAE and MAPE between the true and predicted BrW_{CT}/LW_{CT} were equal to 0.16 and 0.19 in the training (Table 8) and to 0.14 and 0.20 in the testing dataset, respectively (Table 9).

When BtW was used alone to predict BrW_{CT} ($BrW_{CT} \sim BtW$), the resulting MAE and MAPE between the true and the predicted BrW_{CT} values were similar to those of the models including the various morphometric traits ($BrW_{CT} \sim BtW + EE$; $BrW_{CT} \sim BtW + EE2$; $BrW_{CT} \sim BtW$ +Bt), showing values of 1.80 and 0.06 in the training dataset (Supplementary Table S3) and 2.17 and 0.07 in the testing dataset (Supplementary Table S4), respectively. In line with the trend observed for BrW_{CT}, when BtW was used as the only independent variable to predict the LW_{CT} ($LW_{CT} \sim BtW$), the resulting MAE and MAPE values were similar to those obtained with the models including the various morphometric traits ($LW_{CT} \sim BtW + L$; $LW_{CT} \sim BtW + Lt$; $BrW_{CT} \sim BtW + Le$), showing values of 6.95 and 0.18 in the training dataset (Supplementary Table S3) and 8.73 and 0.18 in the testing dataset (Supplementary Table S4), respectively. The BrW_{CT}/LW_{CT} was also estimated using the BtW alone, according to the first (Supplementary Fig. S1 and S2, panel A) and second approach (Supplementary Fig. S3 and S4, panel A). In the first case, the MAE and MAPE between the true and predicted BrW_{CT}/LW_{CT} were equal to 0.17 and 0.19 in the training dataset (Supplementary Table S3) and 0.15 and 0.18 in the testing dataset (Supplementary Table S4), respectively. For the second approach, the MAE and MAPE between the true and predicted BrW_{CT}/LW_{CT} were equal to 0.16 and 0.18 in the training (Supplementary Table S3) and to 0.14 and 0.18 in the testing dataset (Supplementary Table S4), respectively.

The error rates in predicting BrW_{CT}, LW_{CT}, and BrW_{CT}/LW_{CT} were similar, or in some cases even lower when using BtW as sole predictor or in conjunction with morphometric traits.

However, the correlation coefficients between the true and predicted BrW_{CT}, LW_{CT}, and BrW_{CT}/LW_{CT} in the testing dataset were always higher when using the BtW in combination with the morphometric traits compared to BtW alone, with the only exception of Le. Using the BtW alone ($LW_{CT} \sim BtW$) or in combination with Le ($LW_{CT} \sim BtW + Le$) resulted in the same correction coefficient between true and estimated LW_{CT} in the testing dataset. Moreover, comparisons between models involving only BtW (e.g., $BrW_{CT} \sim BtW$) and models combining BtW with morphometric traits (e.g., $BrW_{CT} \sim BtW + EE$) using ANOVA demonstrate that the inclusion of each morphometric trait to the models significantly improved the model fit ($P < 0.05$). These results imply that incorporating morphometric traits along with BtW in the models increase their ability to predict the variable of interest (BrW_{CT}, LW_{CT}, BrW_{CT}/ LW_{CT}). The sole exception was observed with the variable Bt. The non-significant coefficient for Bt in the model ($BrW_{CT} \sim BtW + Bt$) and the non-significant ANOVA suggest that this specific variable may not be relevant or contributing significantly to explaining the variability in BrW_{CT} when BtW is already included in the model.

Body measurements to predict the brain-to-liver weight ratio in piglets with a birth weight above 800 g

When the equation to predict the BrW_{CT}/LW_{CT} developed in the first approach ($BrW_{CT}/LW_{CT} \sim BtW + EE + L$) was tested on piglets with a BtW >800 g, the performance did not change considerably. MAE and MAPE between the true and predicted BrW_{CT}/LW_{CT} were equal to 0.12 and 0.16 in the training (Table 8) and to 0.11 and 0.18 in the testing dataset, respectively (Table 9). When the estimated BrW_{CT} ($BrW_{CT} \sim BtW + EE$) and LW_{CT} ($LW_{CT} \sim BtW + L$) were used to predict the BrW_{CT}/LW_{CT} in piglets with a BtW >800 g, according to the second approach, the MAE and MAPE between the true and predicted BrW_{CT}/LW_{CT} were equal to 0.12 and 0.16 in the training dataset (Table 8) and 0.12 and 0.21 in the testing dataset (Table 9). The degree of correlation between the true and the predicted BrW_{CT}/LW_{CT} was tested in the

training and testing datasets for the first (Fig. 8 and Fig. 9, panel B) and the second approach (Fig. 10 and Fig. 11, panel B).

The performance of the models including BtW as the sole predictor was also tested on piglets with a BtW >800 g according to the first (Supplementary Fig. S1 and S2, panel B) and the second approach (Supplementary Fig. S3 and S4, panel B). When the equation to predict the BrW_{CT}/LW_{CT} developed in the first approach ($BrW_{CT}/LW_{CT} \sim BtW$) was tested on piglets with a BtW >800 g MAE and MAPE between the true and predicted BrW_{CT}/LW_{CT} were equal to 0.12 and 0.17 in the training (Supplementary Table S3) and to 0.11 and 0.19 in the testing dataset (Supplementary Table S4), respectively. When the estimated BrW_{CT} ($BrW_{CT} \sim BtW$) and LW_{CT} ($LW_{CT} \sim BtW$) were used to predict the BrW_{CT}/LW_{CT} in piglets with a BtW >800 g, according to the second approach, the MAE and MAPE between the true and predicted BrW_{CT}/LW_{CT} were equal to 0.12 and 0.15 in the training dataset (Supplementary Table S3) and 0.11 and 0.18 in the testing dataset (Supplementary Table S4), respectively.

Table 7. Regression equations developed with the training dataset to predict brain weight (BrW_{CT}), liver weight (LW_{CT}), and brain-to-liver weight ratio (BrW_{CT}/LW_{CT}) determined by computed tomography (CT) or death/euthanasia of the piglets.

	Equation
Item[1]	
BrW_{CT}	
BrW_{CT} ~ BtW + EE	$BrW_{CT} = 18.6 + 6.06 \times BtW + 0.03 \times EE$
BrW_{CT} ~ BtW + Bt	$BrW_{CT} = 20.5 + 7.56 \times BtW + 9.183e^{-05} \times Bt$
BrW_{CT} ~ BtW + EE2	$BrW_{CT} = 18.8 + 7.02 \times BtW + 0.04 \times EE2$
LW_{CT}	
LW_{CT} ~ BtW + Lt	$LW_{CT} = -8.13 + 23.5 \times BtW + 0.0002 \times Lt$
LW_{CT} ~BtW + L	$LW_{CT} = -10.9 + 33.2 \times BtW + 0.0002 \times L$
LW_{CT} ~BtW + Le	$LW_{CT} = -24.4 + 33.1 \times BtW + 0.04 \times Le$
BrW_{CT}/LW_{CT}	
BrW_{CT}/LW_{CT} ~ BtW + EE + L^2	$\log(BrW_{CT}/LW_{CT}) = 0.839 + -0.377 \times BtW + -0.0007 \times EE + -7.165e^{-06} \times L$
BrW_{CT} ~ BtW + EE / LW_{CT} ~ BtW + L[3]	$BrW_{CT}/LW_{CT} = \frac{BrW_{CT} = 18.4 + 5.39 \times BtW + 0.04 \times EE}{LW_{CT} = -14.2 + 33 \times BtW + 0.0003 \times L}$

[1] BtW = birth body weight; EE = distance between the lateral edge of the ears, seen from above; Bt = area of the front head delimited by a square, seen from above; EE2 = distance between the medial edge of the ears, seen from above; Lt = area of the body delimited by a square from the caudal edge of the head to the caudal edge of the body, seen from above; L = area of the body delimited by a square from the caudal edge of the head to the caudal edge of the abdomen, seen from the side; Le = length of the body, from the caudal edge of the head to the end of the body following the spine, seen from above.

[2] BrW_{CT}/LW_{CT} ~ BtW + EE + L = brain-to-liver weight ratio predicted according to the first approach. An equation was constructed on the training dataset to estimate the BrW_{CT}/LW_{CT} by incorporating the distance between the lateral edges of the ears (EE) and the area of the body delimited by a square from the caudal edge of the head to the caudal edge of the abdomen (L), along with the BtW. These were the measures that better predicted the BrW_{CT} and LW_{CT}.

[3] BrW_{CT} ~ BtW + EE / LW_{CT} ~ BtW + L = brain-to-liver weight ratio predicted according to the second approach. The values of BrW_{CT} and LW_{CT} estimated with the equations developed in the training dataset, derived from EE in combination with BtW and L in combination with BtW, respectively, were directly employed to determine the BrW_{CT}/LW_{CT}.

Table 8. Pearson correlation coefficient, *P* value of the Pearson coefficient, mean absolute error (MAE), and mean absolute percentage error (MAPE) between true and predicted brain weight (BrW_{CT}), liver weight (LW_{CT}), and brain-to-liver weight ratio (BrW_{CT}/LW_{CT}) of the piglets in the training dataset.

	r[1]	P value[2]	MAE	MAPE
Item[3]				
BrW_{CT}				
$BrW_{CT} \sim BtW + EE$	0.85	< 0.001	1.78	0.06
$BrW_{CT} \sim BtW + Bt$	0.84	< 0.001	1.79	0.06
$BrW_{CT} \sim BtW + EE2$	0.85	< 0.001	1.74	0.06
LW_{CT}				
$LW_{CT} \sim BtW + Lt$	0.90	< 0.001	10.7	0.28
$LW_{CT} \sim BtW + L$	0.89	< 0.001	7.03	0.16
$LW_{CT} \sim BtW + Le$	0.90	< 0.001	6.75	0.17
BrW_{CT}/LW_{CT}				
$BrW_{CT}/LW_{CT} \sim BtW + EE + L$[4]	0.80	< 0.001	0.16	0.19
$BrW_{CT}/LW_{CT} \sim BtW + EE + L$ (BtW >800 g)[5]	0.78	< 0.001	0.12	0.16
$BrW_{CT} \sim BtW + EE$ / $LW_{CT} \sim BtW + L$[6]	0.81	< 0.001	0.16	0.19
$BrW_{CT} \sim BtW + EE$ / $LW_{CT} \sim BtW + L$ (BtW >800 g)[7]	0.81	< 0.001	0.12	0.16

[1] r = Pearson correlation coefficient between true and predicted BrW_{CT}, LW_{CT}, BrW_{CT}/LW_{CT}.

[2] *P* value of the Pearson correlation coefficient.

[3] BtW = birth body weight; EE = distance between the lateral edge of the ears, seen from above; Bt = area of the front head delimited by a square, seen from above; EE2 = distance between the medial edge of the ears, seen from above; Lt = area of the body delimited by a square from the caudal edge of the head to the caudal edge of the body, seen from above; L = area of the body delimited by a square from the caudal edge of the head to the caudal edge of the abdomen, seen from the side; Le = length of the body, from the caudal edge of the head to the end of the body following the spine, seen from above.

[4] BrW_{CT}/LW_{CT} ~ BtW + EE + L = brain-to-liver weight ratio predicted according to the first approach. An equation was constructed on the training dataset to estimate the BrW_{CT}/LW_{CT} by incorporating the distance between the lateral edges of the ears (EE) and the area of the body delimited by a square from the caudal edge of the head to the caudal edge of the abdomen (L), along with the BtW. These were the measures that better predicted the BrW_{CT} and LW_{CT}.

[5] BrW_{CT}/LW_{CT} ~ BtW + EE + L (BtW > 800 g) = brain-to-liver weight ratio predicted according to the first approach. An equation was constructed on the training dataset to estimate the BrW_{CT}/LW_{CT} by incorporating the distance between the lateral edges of the ears (EE) and the area of the body delimited by a square from the caudal edge of the head to the caudal edge of the abdomen (L), along with the BtW. These were the measures that better predicted the BrW_{CT} and LW_{CT}. Piglets with a BtW < 800 g were excluded from the calculation of r, MAE, MAPE.

[6] BrW_{CT} ~ BtW + EE / LW_{CT} ~ BtW + L = brain-to-liver weight ratio predicted according to the second approach. The values of BrW_{CT} and LW_{CT} estimated with the equations developed in the training dataset, derived from EE in combination with BtW and L in combination with BtW, respectively, were directly employed to determine the BrW_{CT}/LW_{CT}.

[7] BrW_{CT} ~ BtW + EE / LW_{CT} ~ BtW + L (BtW > 800 g) = brain-to-liver weight ratio predicted according to the second approach. The values of BrW_{CT} and LW_{CT} estimated with the equations developed in the training dataset, derived from EE in combination with BtW and L in combination with BtW, respectively, were directly employed to determine the BrW_{CT}/LW_{CT}. Piglets with a BtW < 800 g were excluded from the calculation of *r*, MAE, MAPE.

Table 9. Pearson correlation coefficient, *P* value of the Pearson coefficient, mean absolute error (MAE), and mean absolute percentage error (MAPE) between true and predicted brain weight (BrW_{CT}), liver weight (LW_{CT}), and brain-to-liver weight ratio (BrW_{CT}/LW_{CT}) of the piglets in the testing dataset.

	r^1	*P* value[2]	MAE	MAPE
Item[3]				
BrW_{CT}				
BrW_{CT} ~ BtW + EE	0.84	< 0.001	1.95	0.06
BrW_{CT} ~ BtW + Bt	0.83	< 0.001	1.99	0.06
BrW_{CT} ~ BtW + EE2	0.82	< 0.001	2.07	0.07
LW_{CT}				
LW_{CT} ~BtW + Lt	0.91	< 0.001	9.35	0.24
LW_{CT} ~BtW + L	0.90	< 0.001	9.29	0.17
LW_{CT} ~BtW + Le	0.89	< 0.001	9.00	0.18
BrW_{CT}/LW_{CT}				
BrW_{CT}/LW_{CT} ~ BtW + EE + L[4]	0.85	< 0.001	0.14	0.17
BrW_{CT}/LW_{CT} ~ BtW + EE + L (BtW >800 g)[5]	0.79	< 0.001	0.11	0.18
BrW_{CT} ~ BtW + EE / LW_{CT} ~ BtW + L[6]	0.88	< 0.001	0.14	0.20
BrW_{CT} ~ BtW + EE / LW_{CT} ~ BtW + L (BtW >800 g)[7]	0.75	< 0.001	0.12	0.21

[1] r = Pearson correlation coefficient

[2] *P* value of the Pearson correlation coefficient.

[3] BtW = birth body weight; EE = distance between the lateral edge of the ears, seen from above; Bt = area of the front head delimited by a square, seen from above; EE2 = distance between the medial edge of the ears, seen from above; Lt = area of the body delimited by a square from the caudal edge of the head to the caudal edge of the body, seen from above; L = area of the body delimited by a square from the caudal edge of the head to the caudal edge of the abdomen, seen from the side; Le = length of the body, from the caudal edge of the head to the end of the body following the spine, seen from above.

[4] BrW_{CT}/LW_{CT} ~ BtW + EE + L = brain-to-liver weight ratio predicted according to the first approach. An equation was constructed on the training dataset to estimate the BrW_{CT}/LW_{CT} by incorporating the distance between the lateral edges of the ears (EE) and the area of the body delimited by a square from the caudal edge of the head to the caudal edge of the abdomen (L), along with the BtW. These were the measures that better predicted the BrW_{CT} and LW_{CT}.

[5] BrW_{CT}/LW_{CT} ~ BtW + EE + L (BtW > 800 g) = brain-to-liver weight ratio predicted according to the first approach. An equation was constructed on the training dataset to estimate the BrW_{CT}/LW_{CT} by incorporating the distance between the lateral edges of the ears (EE) and the area of the body delimited by a square from the caudal edge of the head to the caudal edge of the abdomen (L), along with the BtW. These were the measures that better predicted the BrW_{CT} and LW_{CT}. Piglets with a BtW < 800 g were excluded from the calculation of r, MAE, MAPE.

[6] BrW_{CT} ~ BtW + EE / LW_{CT} ~ BtW + L = brain-to-liver weight ratio predicted according to the second approach. The values of BrW_{CT} and LW_{CT} estimated with the equations developed in the training dataset, derived from EE in combination with BtW and L in combination with BtW, respectively, were directly employed to determine the BrW_{CT}/LW_{CT}.

[7] BrW_{CT} ~ BtW + EE / LW_{CT} ~ BtW + L (BtW > 800 g) = brain-to-liver weight ratio predicted according to the second approach. The values of BrW_{CT} and LW_{CT} estimated with the equations developed in the training dataset, derived from EE in combination with BtW and L in combination with BtW, respectively, were directly employed to determine the BrW_{CT}/LW_{CT}. Piglets with a BtW < 800 g were excluded from the calculation of r, MAE, MAPE.

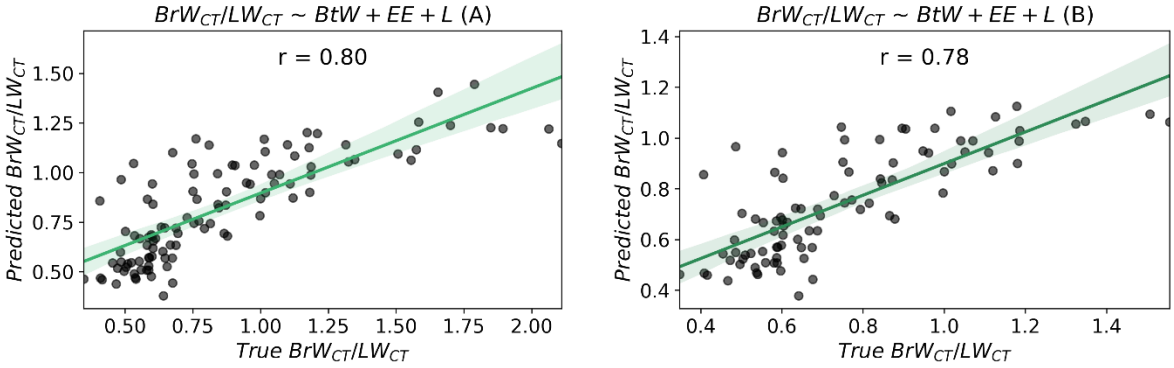

Fig. 8. Linear regressions between true and predicted BrW_{CT}/LW_{CT} of the piglets of the training dataset according to the first approach. Panel A: all population; panel B: piglets with a birth weight (BtW) above 800 g. x-Axis: true brain-to-liver weight ratio (true BrW_{CT}/LW_{CT}); y-axis: predicted brain-to-liver weight ratio (predicted BrW_{CT}/LW_{CT}). To predict the BrW_{CT}/LW_{CT}, a multiple linear regression model including BtW, distance between the lateral edge of the ears, seen from above (EE), and area of the body delimited by a square from the caudal edge of the head to the caudal edge of the abdomen, seen from the side (L) was used. r: Pearson correlation coefficient.

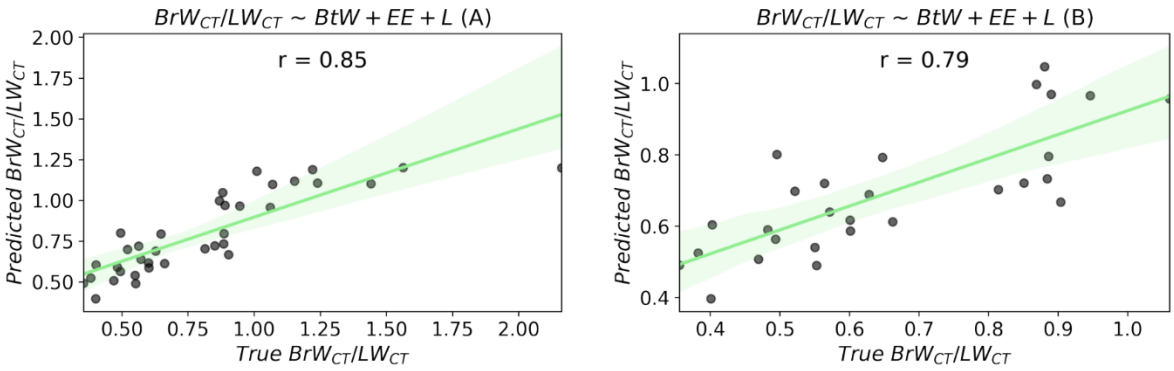

Fig. 9. Linear regressions between true and predicted BrW_{CT}/LW_{CT} of the piglets of the testing dataset according to the first approach. Panel A: all population; panel B: piglets with a birth weight (BtW) above 800 g. x-Axis: true brain-to-liver weight ratio (true BrW_{CT}/LW_{CT}); y-axis: predicted brain-to-liver weight ratio (predicted BrW_{CT}/LW_{CT}). To predict the BrW_{CT}/LW_{CT}, a multiple linear regression model including BtW, distance between the lateral edge of the ears, seen from above (EE), and area of the body delimited by a square from the caudal edge of the head to the caudal edge of the abdomen, seen from the side (L) was used. r: Pearson correlation coefficient.

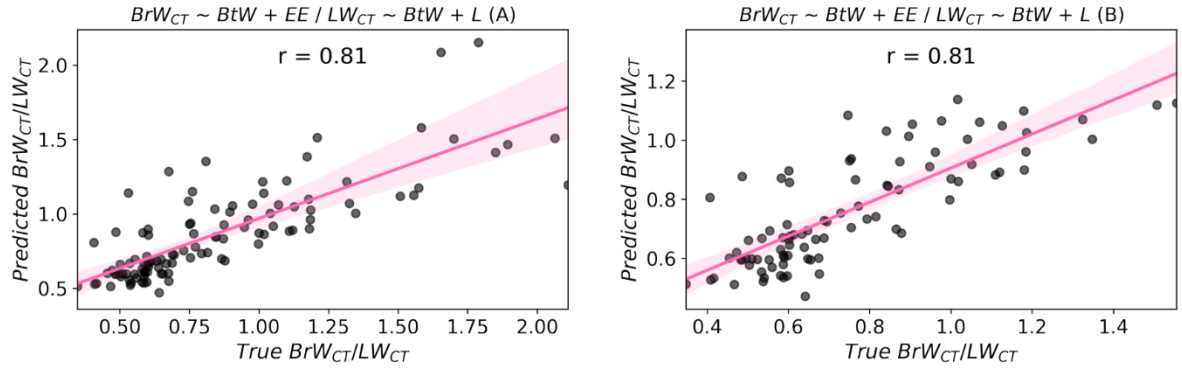

Fig. 10. Linear regressions between true and predicted BrW_{CT}/LW_{CT} of the piglets of the training dataset according to the second approach. Panel A: all population; panel B: piglets with a birth weight (BtW) above 800g. x-Axis: true brain-to-liver weight ratio (true BrW_{CT}/LW_{CT}); y-axis: predicted brain-to-liver weight ratio (predicted BrW_{CT}/predicted LW_{CT}). To assess the BrW_{CT}/LW_{CT}, predicted BrW_{CT} and LW_{CT}, calculated using the previous models (BrW_{CT} ~ BtW + EE; LW_{CT} ~ BtW + L), were directly employed to determine the BrW_{CT}/LW_{CT}. r: Pearson correlation coefficient.

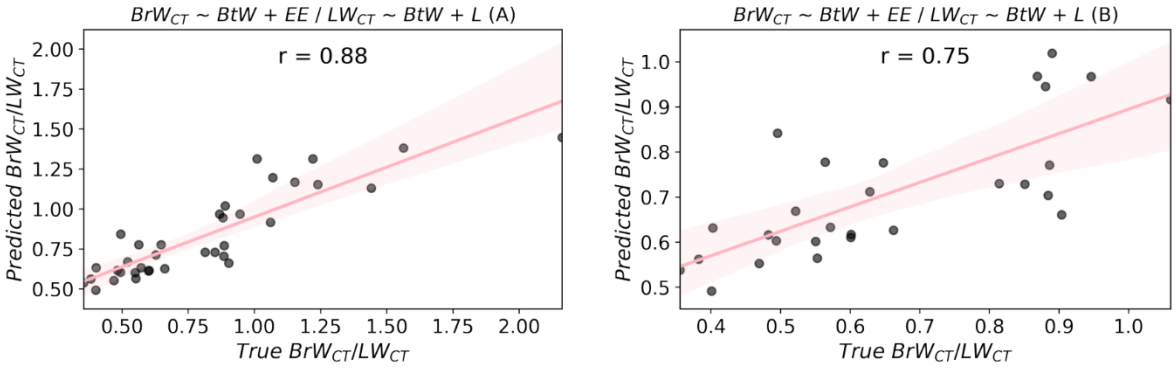

Fig. 11. Linear regressions between true and predicted BrW_{CT}/LW_{CT} of the piglets of the testing dataset according to the second approach. Panel A: all population; panel B: piglets with a birth weight (BtW) above 800 g. x-Axis: true brain-to-liver weight ratio (true BrW_{CT}/LW_{CT}); y-axis: predicted brain-to-liver weight ratio (predicted BrW_{CT}/predicted LW_{CT}). To assess the BrW_{CT}/LW_{CT}, predicted BrW_{CT} and LW_{CT}, calculated using the previous models (BrW_{CT} ~ BtW + EE; LW_{CT} ~ BtW + L), were directly employed to determine the BrW_{CT}/LW_{CT}. r: Pearson correlation coefficient.

Discussion

Foetal growth restriction often occurs as a result of chronic placental insufficiency, which hampers the delivery of sufficient oxygen and nutrients to the foetus in the uterus, leading to abnormal foetal development (Chand et al., 2022; Cohen et al., 2015). As a consequence, IUGR piglets can be identified by their distinctive head shape and LBtW. However, in manuscript I (Ruggeri et al., 2024), it was demonstrated that identification of IUGR piglets solely based on head morphology or BtW does not always agree with an increased BrW/LW and can lead to inaccurate classification of this condition. For these reasons, to accurately assess growth restriction in piglets, measurements such as BtW and head shape should be complemented by evaluating the relative brain-to-body weight or BrW/LW, as these directly reflect the brain-sparing effect (Chand et al., 2022; Felicioni et al., 2019).

In this study, the BtW of newborn piglets was recorded and the weights of their brain and liver were measured through either scale measurement or with CT scan imaging. Additionally, pictures of the same piglets were taken to capture specific body measurements. Our findings support the hypothesis that certain morphometric traits can serve as indicators of brain and liver weights, as well as their ratio. Using the distance between the ears (EE), in combination with the BtW, the BrW could be predicted with an error of 6%. Notably, the studies conducted by Amdi et al. (2013) and Hansen et al. (2018) postulated that if the relative BrW of a newborn piglet is below 3% of its BtW, the piglet can be diagnosed as normal. If this statement is true, the BrW estimated with the present equation could be simply compared with the piglet's BtW, enabling an accurate and non-invasive identification of normal piglets with a narrow margin of error. It would also offer insights into piglets with a relative BrW above 3% of their BtW which might have suffered growth restriction in the uterus.

The LW was highly correlated with most of the collected morphometric traits. However, when using these measurements along with the BtW in the prediction models, the error rate could not be reduced below 17%. As the actual LW_{CT} increased, the accuracy of the predictions worsened. This suggests that beyond a certain weight of the liver, the body's structure may no longer be associated with the organ's weight, unlike what was observed with the brain.

When a combination of measures (BtW, EE, and L) that better predicted the BrW and the LW was employed for estimating the BrW/LW, an error rate of 17% was observed. Using the second approach, in which the BrW and LW predicted with the previous models were directly employed to determine the BrW/LW, we observed a slight increase in the error rate to 20%. This outcome is likely attributable to the cumulative impact of errors encountered when predicting the weights of both organs. However, the BrW/LW allows for consideration of the different levels of growth restrictions that piglets may be exposed to during gestation. With a Pearson correlation up to 0.88 (according to the different methods), the estimated BrW/LW is highly correlated with the true BrW/LW. Accordingly, the estimated BrW/LW can be used to assess the general tendency of an increase in BrW/LW for different traits, as analysed in manuscript I (Ruggeri et al., 2024).

The euthanasia of piglets born with a BtW below 800 g is a common practice in modern swine production systems, primarily due to the high mortality rate observed among these piglets during the first days after birth (Muns et al., 2016). We hypothesized that in cases of extremely LBtWs, the association between organ weight and body morphology may weaken. When these piglets were excluded from the analysis, there was a reduction in the percentage error between actual and predicted BrW_{CT}/LW_{CT} in the training set. However, this reduction did not translate to the testing set, where excluding these piglets slightly increased the percentage error. A possible explanation for the increased MAPE in the testing set after excluding piglets with a BtW below 800 g may be that the number of samples in the testing set dropped below 30. This

reduction in sample size could have resulted in unreliable predictions due to statistical instability or insufficient representation of the population (Jenkins and Quintana-Ascencio, 2020; Austin and Steyerberg, 2015).

In this study, to ensure the repeatability of the method, a subset of the morphometric traits was taken by a second observer. The measurements taken by the authors and the second observer were highly correlated, reinforcing the consistency and accuracy of the identified morphometric traits to estimate BrW and LW. This correlation validates the method and shows that the results are not solely a consequence of subjective measurement but rather are indicative of a link between these morphometric traits and the BrW and LW.

In addition, the division of the dataset into training and testing subsets was helpful in evaluating the ability of the predictive models to generalize on new data. By creating a clear division between training and testing data, the study replicates the real-world scenario where predictive models are applied to new, unseen observations. This evaluation mechanism protects against overfitting, a situation where the models become overly specialized to the training data and may perform poorly when exposed to new inputs (Hawkins, 2004).

In conclusion, this study demonstrates the potential of using body measurements as non-invasive indicators of the brain-to-organ weight ratio for diagnosing IUGR in newborn piglets. The developed predictive models provide a promising tool for the early identification of IUGR piglets, facilitating timely interventions and improved management strategies. Future studies should focus on validating these models in larger populations and different breeds. Additionally, developing techniques for automating the extraction of morphometric traits from images will enhance the applicability of these models under field conditions. The successful implementation of such non-invasive diagnostic approaches will contribute to the welfare and productivity of pig production systems by facilitating early intervention to mitigate the negative

effect of IUGR, and by optimizing breeding programs to select for healthier and more efficient pigs.

Ethics approval

All the experimental procedures complied with Swiss animal welfare guidelines and were approved (experimental approval numbers 32751 and 35131) by the Cantonal Veterinary Office of Fribourg (Switzerland).

Supplementary material

Supplementary Table S1. Correlations between the measures taken on the images of the piglets by the first and second observer to test the repeatability of the method.

	r[1]	P-value[2]
Item[3]		
EE, pixel	0.94	< 0.001
Bt, pixel^2	0.93	< 0.001
EE2, pixel	0.88	< 0.001
Le, pixel	0.97	< 0.001
FH, pixel	0.94	< 0.001
CB, pixel^2	0.91	< 0.001
Lt, pixel^2	0.95	< 0.001
SS, pixel	0.97	< 0.001
SS2, pixel	0.97	< 0.001
L, pixel^2	0.90	< 0.001
L2, pixel^2	0.95	< 0.001
CL, pixel^2	0.91	< 0.001

[1] r = Pearson correlation coefficient.

[2] *P* value of the Pearson correlation coefficient.

[3] EE: distance between the lateral edge of the ears, seen from above; Bt: area of the front head delimited by a square, seen from above; EE2: distance between the medial edge of the ears, seen from above; Le: length of the body, from the caudal edge of the head to the end of the body following the spine, seen from above; FH: larger diameter of the front head, seen from above; CB: area of the front head delimited by a circle, seen from above; Lt: : area of the body delimited by a square from the caudal edge of the head to the caudal edge of the body, seen from above; SS: distance between the shoulders, seen from above; SS2: diameter of the abdomen measured caudally to the shoulders, seen from above; L: area of the body delimited by a square from the caudal edge of the head to the caudal edge of the abdomen, seen from the side; L2: area of the body delimited by a square from the caudal edge of the head to the caudal edge of the body, seen from the side; CL: area of the abdomen delimited by a circle, seen from the side.

Supplementary Table S2. Regression equations developed with the training dataset to predict brain weight (BrW_{CT}), liver weight (LW_{CT}), and brain-to-liver weight ratio (BrW_{CT}/LW_{CT}) determined by computed tomography (CT) or death/euthanasia of the piglets using only the BtW as independent variable.

	Equation
Item[1]	
BrW_{CT} ~ BtW	$BrW_{CT} = 21.1 + 9.28 \times BtW$
LW_{CT} ~ BtW	$LW_{CT} = -7.19 + 44.0 \times BtW$
BrW_{CT}/LW_{CT} ~ BtW[2]	$\log (BrW_{CT}/ LW_{CT}) = 0.677 + -0.765 \times BtW$
BrW_{CT} ~ BtW / LW_{CT} ~ BtW [3]	$BrW_{CT}/ LW_{CT} = \frac{BrW_{CT} = 21.1 + 9.28 \times BtW}{LW_{CT} = -7.19 + 44.0 \times BtW}$

[1] BtW = birth body weight; EE = distance between the lateral edge of the ears, seen from above; Bt = area of the front head delimited by a square, seen from above; EE2 = distance between the medial edge of the ears, seen from above; Lt = area of the body delimited by a square from the caudal edge of the head to the caudal edge of the body, seen from above; L = area of the body delimited by a square from the caudal edge of the head to the caudal edge of the abdomen, seen from the side; Le = length of the body, from the caudal edge of the head to the end of the body following the spine, seen from above.

[2] BrW_{CT}/LW_{CT} ~ BtW = brain-to-liver weight ratio predicted according to the first approach but using the BtW as sole predictor. An equation was constructed on the training dataset to estimate the BrW_{CT}/LW_{CT} by incorporating only the BtW as independent variable.

[3] BrW_{CT} ~ BtW / LW_{CT} ~ BtW = brain-to-liver weight ratio predicted according to the second approach but using the BtW as sole predictor. The values of BrW_{CT} and LW_{CT} estimated with the equations developed in the training dataset incorporating only the BtW as independent variable, were directly employed to determine the BrW_{CT}/LW_{CT}.

Supplementary Table S3. Pearson correlation coefficient, *P* value of the Pearson coefficient, mean absolute error (MAE), and mean absolute percentage error (MAPE) between true and predicted brain weight (BrW_{CT}), liver weight (LW_{CT}), and brain-to-liver weight ratio (BrW_{CT}/LW_{CT}) of the piglets in the training dataset.

	r[1]	*P* value[2]	MAE	MAPE
Item[3]				
BrW_{CT} ~ BtW	0.84	< 0.001	1.80	0.06
LW_{CT} ~ BtW	0.89	< 0.001	6.95	0.18
BrW_{CT}/LW_{CT} ~ BtW[4]	0.77	< 0.001	0.17	0.19
BrW_{CT}/LW_{CT} ~ BtW (BtW >800 g)[5]	0.77	< 0.001	0.12	0.17
BrW_{CT} ~ BtW / LW_{CT} ~ BtW[6]	0.79	< 0.001	0.16	0.18
BrW_{CT} ~ BtW / LW_{CT} ~ BtW (BtW >800 g)[7]	0.79	< 0.001	0.12	0.15

[1] r = Pearson correlation coefficient between true and predicted BrW_{CT}, LW_{CT}, BrW_{CT}/LW_{CT}.

[2] *P* value of the Pearson correlation coefficient.

[3] BtW = birth body weight; EE = distance between the lateral edge of the ears, seen from above; Bt = area of the front head delimited by a square, seen from above; EE2 = distance between the medial edge of the ears, seen from above; Lt = area of the body delimited by a square from the caudal edge of the head to the caudal edge of the body, seen from above; L = area of the body delimited by a square from the caudal edge of the head to the caudal edge of the abdomen, seen from the side; Le = length of the body, from the caudal edge of the head to the end of the body following the spine, seen from above.

[4] BrW_{CT}/LW_{CT} ~ BtW = brain-to-liver weight ratio predicted according to the first approach but using the BtW as sole predictor. An equation was constructed on the training dataset to estimate the BrW_{CT}/LW_{CT} by incorporating only the BtW as independent variable.

[5] BrW_{CT}/LW_{CT} ~ BtW (BtW > 800 g) = brain-to-liver weight ratio predicted according to the first approach but using the BtW as sole predictor. An equation was constructed on the training dataset to estimate the BrW_{CT}/LW_{CT} by incorporating only the BtW as independent variable. Piglets with a BtW < 800 g were excluded from the calculation of r, MAE, MAPE.

[6] BrW_{CT} ~ BtW / LW_{CT} ~ BtW = brain-to-liver weight ratio predicted according to the second approach but using the BtW as sole predictor. The values of BrW_{CT} and LW_{CT} estimated with the equations developed in the training dataset incorporating only the BtW as independent variable, were directly employed to determine the BrW_{CT}/LW_{CT}.

[7] BrW_{CT} ~ BtW / LW_{CT} ~ BtW (BtW >800 g) = brain-to-liver weight ratio predicted according to the second approach but using the BtW as sole predictor. The values of BrW_{CT} and LW_{CT} estimated with the equations developed in the training dataset incorporating only the BtW as independent variable, were directly employed to determine the BrW_{CT}/LW_{CT}. Piglets with a BtW < 800 g were excluded from the calculation of r, MAE, MAPE.

Supplementary Table S4. Pearson correlation coefficient, *P* value of the Pearson coefficient, mean absolute error (MAE), and mean absolute percentage error (MAPE) between true and predicted brain weight (BrW_{CT}), liver weight (LW_{CT}), and brain-to-liver weight ratio (BrW_{CT}/LW_{CT}) of the piglets in the testing dataset.

	r[1]	P value[2]	MAE	MAPE
Item[3]				
BrW_{CT} ~ BtW	0.80	< 0.001	2.17	0.07
LW_{CT} ~ BtW	0.89	< 0.001	8.73	0.18
BrW_{CT}/LW_{CT} ~ BtW[4]	0.83	< 0.001	0.15	0.18
BrW_{CT}/LW_{CT} ~ BtW (BtW >800 g)[5]	0.72	< 0.001	0.11	0.19
BrW_{CT} ~ BtW / LW_{CT} ~ BtW[6]	0.87	< 0.001	0.14	0.18
BrW_{CT} ~ BtW / LW_{CT} ~ BtW (BtW >800 g)[7]	0.69	< 0.001	0.11	0.18

[1] r = Pearson correlation coefficient

[2] *P* value of the Pearson correlation coefficient.

[3] BtW = birth body weight; EE = distance between the lateral edge of the ears, seen from above; Bt = area of the front head delimited by a square, seen from above; EE2 = distance between the medial edge of the ears, seen from above; Lt = area of the body delimited by a square from the caudal edge of the head to the caudal edge of the body, seen from above; L = area of the body delimited by a square from the caudal edge of the head to the caudal edge of the abdomen, seen from the side; Le = length of the body, from the caudal edge of the head to the end of the body following the spine, seen from above.

[4] BrW_{CT}/LW_{CT} ~ BtW = brain-to-liver weight ratio predicted according to the first approach but using the BtW as sole predictor. An equation was constructed on the training dataset to estimate the BrW_{CT}/LW_{CT} by incorporating only the BtW as independent variable.

[5] BrW_{CT}/LW_{CT} ~ BtW (BtW >800 g) = brain-to-liver weight ratio predicted according to the first approach but using the BtW as sole predictor. An equation was constructed on the training dataset to estimate the BrW_{CT}/LW_{CT} by incorporating only the BtW as independent variable. Piglets with a BtW < 800 g were excluded from the calculation of r, MAE, MAPE.

[6] BrW_{CT} ~ BtW / LW_{CT} ~ BtW = brain-to-liver weight ratio predicted according to the second approach but using the BtW as sole predictor. The values of BrW_{CT} and LW_{CT} estimated with the equations developed in the training dataset incorporating only the BtW as independent variable, were directly employed to determine the BrW_{CT}/LW_{CT}.

[7] BrW_{CT} ~ BtW / LW_{CT} ~ BtW (BtW >800 g) = brain-to-liver weight ratio predicted according to the second approach but using the BtW as sole predictor. The values of BrW_{CT} and LW_{CT} estimated with the equations developed in the training dataset incorporating only the BtW as independent variable, were directly employed to determine the BrW_{CT}/LW_{CT}. Piglets with a BtW < 800 g were excluded from the calculation of r, MAE, MAPE.

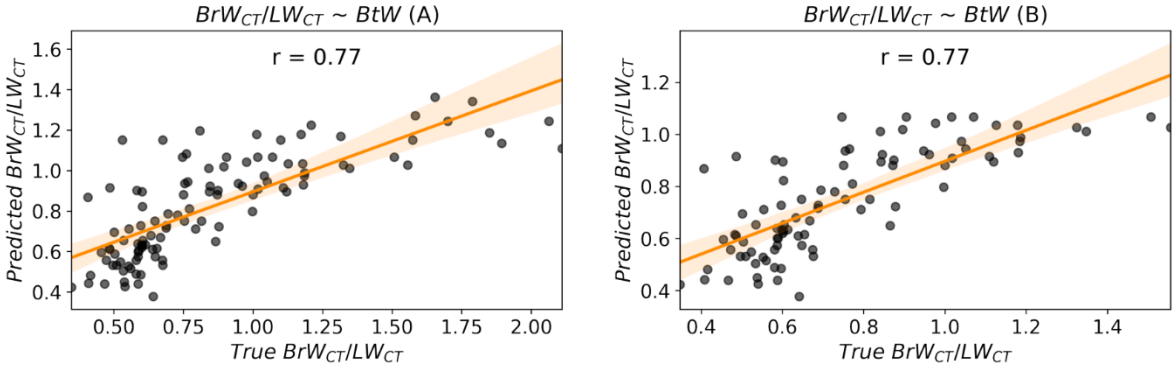

Supplementary Fig. S1. Linear regressions between true and predicted BrW_{CT}/LW_{CT} of the piglets of the training dataset according to the first approach but using the BtW as sole predictor. Panel A: all population; panel B: piglets with a birth weight (BtW) above 800 g. x-Axis: true brain-to-liver weight ratio (true BrW_{CT}/LW_{CT}); y-axis: predicted brain-to-liver weight ratio (predicted BrW_{CT}/LW_{CT}). To predict the BrW_{CT}/LW_{CT}, a simple linear regression model including only the BtW was used. r: Pearson correlation coefficient.

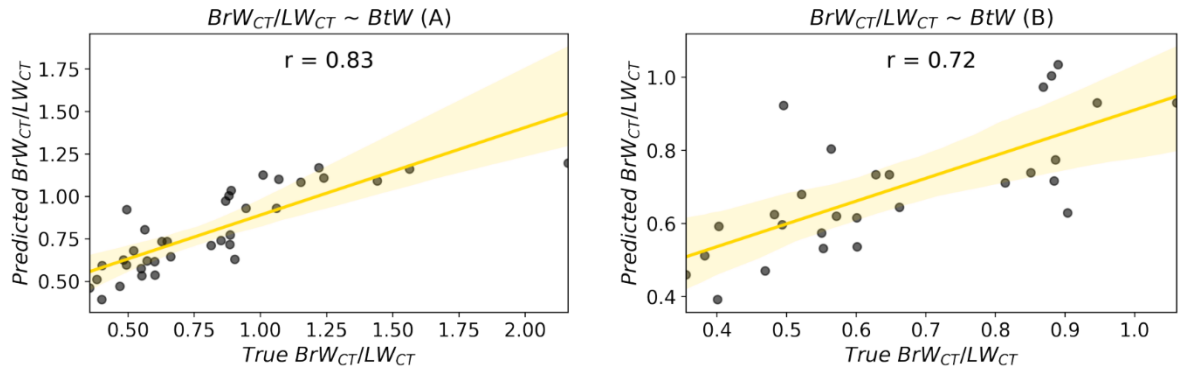

Supplementary Fig. S2. Linear regressions between true and predicted BrW_{CT}/LW_{CT} of the piglets of the testing dataset according to the first approach but using the BtW as sole predictor. Panel A: all population; panel B: piglets with a birth weight (BtW) above 800 g. x-Axis: true brain-to-liver weight ratio (true BrW_{CT}/LW_{CT}); y-axis: predicted brain-to-liver weight ratio (predicted BrW_{CT}/LW_{CT}). To predict the BrW_{CT}/LW_{CT}, a simple linear regression model including only the BtW was used. r: Pearson correlation coefficient.

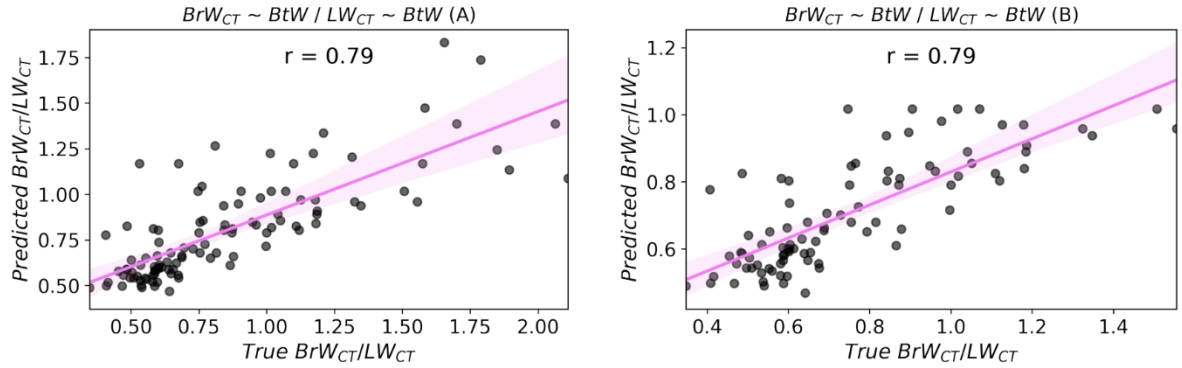

Supplementary Fig. S3. Linear regressions between true and predicted BrW_{CT}/LW_{CT} of the piglets of the training dataset according to the second approach but using the BtW as sole predictor. Panel A: all population; panel B: piglets with a birth weight (BtW) above 800g. x-Axis: true brain-to-liver weight ratio (true BrW_{CT}/LW_{CT}); y-axis: predicted brain-to-liver weight ratio (predicted BrW_{CT}/predicted LW_{CT}). To assess the BrW_{CT}/LW_{CT}, predicted BrW_{CT} and LW_{CT}, calculated using the previous models (BrW_{CT} ~ BtW; LW_{CT} ~ BtW), were directly employed to determine the BrW_{CT}/LW_{CT}. r: Pearson correlation coefficient.

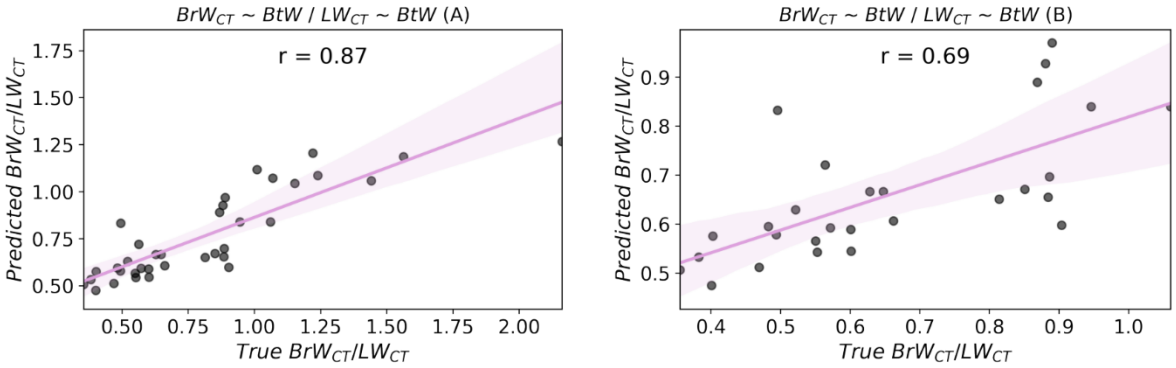

Supplementary Fig. S4. Linear regressions between true and predicted BrW_{CT}/LW_{CT} of the piglets of the testing dataset according to the second approach but using the BtW as sole predictor. Panel A: all population; panel B: piglets with a birth weight (BtW) above 800 g. x-Axis: true brain-to-liver weight ratio (true BrW_{CT}/LW_{CT}); y-axis: predicted brain-to-liver weight ratio (predicted BrW_{CT}/predicted LW_{CT}). To assess the BrW_{CT}/LW_{CT}, predicted BrW_{CT} and LW_{CT}, calculated using the previous models (BrW_{CT} ~ BtW; LW_{CT} ~ BtW), were directly employed to determine the BrW_{CT}/LW_{CT}. r: Pearson correlation coefficient.

5. Manuscript III

Intrauterine growth restriction, defined by an elevated brain-to-liver weight ratio, affects faecal microbiota composition and, to a lesser extent, plasma metabolome profile at different ages in pigs.

R. Ruggeri[a, b], G. Bee[a], F. Correa [b], P. Trevisi [b], C. Ollagnier[a]

[a] *Swine Research Unit, Agroscope, Route de la Tioleyre 4, 1725 Posieux, Switzerland*

[b] *Department of Agricultural and Food Sciences (DISTAL), University of Bologna, viale G Fanin 44, 40127 Bologna, Italy*

Abstract

Intrauterine growth restriction (IUGR) affects up to 30% of newborn piglets, leading to increased mortality and altered metabolism, as well as compromised intestinal development and microbial colonization. The IUGR foetus increases blood flow towards the brain to survive in situations of limited oxygen and nutrient supply through the placenta. This adaptive mechanism results in a higher brain-to-liver weight ratio (BrW/LW) at birth. This study aimed to investigate the effects of IUGR on the faecal microbiota and blood metabolome profiles of pigs, from birth to slaughter, to better understand the underlying mechanisms of this condition. One day (±1) after birth, CT was performed on each piglet to assess their brain and liver weights. The pigs with the highest (IUGR = 12; BrW/LW: 1.00 ± 0.09) and the lowest (NORM = 12; BrW/LW: 0.36 ± 0.04) BrW/LW were selected to collect faeces and blood during lactation (day 16 ± 0.6, T1) and at the end of the starter period (day 63 ± 8.6, T2), and faeces at the beginning (day 119 ± 11.4, T3) and end of the finisher period (day 162 ± 14.3, T4). The

pigs were fed the same standard pre-/early postweaning, starter, grower, and finisher diets. The IUGR status did not impact faecal microbial Alpha diversity at any time point but it changed the Beta diversity at T1 ($P = 0.002$), T2 ($P = 0.079$), and at T3 ($P = 0.027$), while no effect was observed at T4. Specifically, IUGR pigs displayed a higher abundance of *Clostridium sensu stricto 1* ($P_{adj} = 0.029$) and *Romboutsia* ($P_{adj} = 0.047$) at T1, *Prevotellaceae* NK3B31 group ($P_{adj} = 0.021$), *Rikenellaceae* RC9 gut group ($P_{adj} = 0.030$), and *Alloprevotella* ($P_{adj} = 0.030$) at T2, and p-2534-18B5 gut group ($P_{adj} = 0.03$) at T3. Conversely, the NORM group exhibited a higher abundance of *Ruminococcus* ($P_{adj} = 0.010$) at T1, HT002 ($P_{adj} = 0.048$) at T2, and *Prevotella*_9 ($P_{adj} < 0.001$) at T3. None of the plasma metabolites showed significant differences at T1 between IUGR and NORM pigs. However, at T2, asparagine was lower in the IUGR compared to the NORM group ($P < 0.05$). In conclusion, our study demonstrated that growth restriction in the uterus has a significant and long-lasting impact on the faecal microbiota composition in pigs, from birth to the beginning of the finisher period. The identified microbial taxa that exhibit differences between IUGR-affected and NORM pigs could potentially serve as biomarkers for IUGR, facilitating the early identification of affected piglets and the development of targeted interventions. By contrast, the blood metabolome profile at different stages of growth was minimally affected.

Implications

Genetic selection for sows' prolificacy has resulted in an increase in piglets suffering from IUGR. This condition is characterised by increased mortality and permanently stunted growth. Physiological characterisation of the affected piglets, by investigating their blood metabolome and faecal microbiota profiles, may enable biomarkers to be identified, facilitating the development of early and targeted postnatal interventions. The effective treatment of these piglets could improve the overall efficiency of pig production.

Introduction

Growth restriction in the uterus is characterised by the failure of the foetus to achieve its genetic growth potential during gestation (Sharma et al., 2016). As a consequence of the genetic selection to improve litter size, this condition affects up to 30% of newborn piglets in the modern pig industry (Santos et al., 2022; Oliviero et al., 2019; Amdi et al., 2013). Foetal growth restriction is associated with an increased risk of neonatal morbidity and mortality, as well as with long-term effects resulting from foetal programming, such as impaired metabolism (Shen et al., 2018), stunted post-natal growth, and reduced feed conversion efficiency (Krueger et al., 2014; Wu et al., 2006). The study detailed in manuscript I (Ruggeri et al., 2024) demonstrated that IUGR detrimentally affected several traits in pigs, including ADG, gain-to-feed ratio, CP efficiency and time to reach the target slaughter weight. These factors are crucial for optimizing production efficiency within the swine industry.

Numerous studies have demonstrated the strong relationship between the health and growth of pigs and the optimal functioning of their GIT (Santos et al., 2022). The GIT, particularly the small intestine, is essential for the digestion, absorption, and transportation of nutrients, water, and electrolytes. It also acts as a defensive barrier against pathogens, dietary toxins, and antigens (Moeser et al., 2017). The GIT hosts a dynamic microbiota including bacteria, viruses, archaea, and fungi. This microbial population regulates the development and function of the immune system, limits the nutrients available for the growth of potential pathogens, competitively excludes pathogens from binding to the gut epithelium (Maynard et al., 2012), and is involved in the host's carbohydrate, amino acid, and lipid metabolism (Wang et al., 2020).

Growing evidence suggests that the uterine environment can influence intestinal development, potentially compromising both its function and microbial colonization (Santos et al., 2022; Zhang et al., 2019). Several studies have shown reduced intestinal length and weight, decreased

villus height, and increased crypt depth, as well as changes in proteomic profile in IUGR-affected piglets compared to their normal littermates from the lactation period (He et al., 2011; D'inca et al., 2010; Wang et al., 2008; Wang et al., 2005) up to 70 days of age (Santos et al., 2022). IUGR not only affects the structure but also the microbial colonization of the GIT. In the study of Zhang et al. (2019), newborn piglets with IUGR exhibited reduced microbial diversity and a distinct taxonomic profile compared to their normal littermates.

Clear differences between IUGR and normal neonates were also demonstrated at a blood metabolome level in both human and pig studies (Priante et al., 2019; He et al., 2011). Although data on blood metabolomic profiling in IUGR is limited, the metabolic changes identified in IUGR neonates seem to indicate an early pattern of glucose intolerance, insulin resistance, alterations in lipogenesis and lipid oxidation, energy, and amino acid metabolism (Priante et al., 2019; Bahado-Singh et al., 2012; He et al, 2011).

Growth restriction in the uterus leads to a reduced glucose supply during foetal development. In response, the foetus initiates metabolic and endocrine adaptations to optimize the utilisation of alternative energy sources, such as fatty acids. Indeed, within these adaptive responses, an increase in adipocyte proliferation was reported in IUGR foetuses (Sarr et al., 2012; Gondret et al., 2011; Attig et al., 2008). The increased adipogenesis facilitates the long-term storage of fatty acids, which, in turn, can undergo oxidation to provide energy for the organism. This adaptation is crucial for enhancing the foetus's survival under conditions of intermittent or poor nutrition (Sarr et al., 2012; Attig et al., 2008). Moreover, different studies suggest that this increased adipogenesis continues in the postnatal life in IUGR-affected pigs (Attig et al., 2008; Gondret et al. 2006).

Considering the modifications that IUGR imposes on the structure and function of the intestinal mucosa, along with the endocrine and metabolic mechanisms established during gestation in response to nutrient restriction, we expected distinct differences in the faecal microbiota and

blood metabolome profiles between IUGR and normal piglets. Specifically, we hypothesized a reduction in microbial diversity and shifts in the abundances of genera involved in nutrient digestion, inflammatory responses, and susceptibility to diseases, such as *Bacteroides, Ruminococcus, Prevotella, Escherichia–Shigella*, and *Pasteurella* in IUGR compared to normal pigs. Moreover, we hypothesized changes in the concentration of metabolites involved in lipid metabolism, such as increased plasma glycerol and ketone bodies, reflecting an increased reliance on fat metabolism for energy supply in the IUGR group, particularly during the early stages of life, as well as alterations in energy and amino acid metabolism, including lower levels of plasma glucose and essential amino acids in IUGR compared to normal pigs. The identification of specific bacterial genera and blood metabolites implicated in IUGR could facilitate the development of targeted interventions to mitigate its adverse effects. This might involve manipulating gut microbiota through prebiotic and probiotic administration, adjusting diets, and providing metabolic intermediates to optimize the impaired metabolic pathways.

To test our hypotheses, CT scan imaging was used in this study to non-invasively assess the BrW/LW in newborn piglets, enabling accurate diagnosis of IUGR (see manuscript I). In addition, blood and faeces samples were obtained from both IUGR and normal pigs at different ages to determine the effects of IUGR on faecal microbiota and plasma metabolome.

Material and methods

Animal selection and classification

This research was carried out at the Agroscope swine research facility in Posieux, Switzerland. Detailed information on all the procedures concerning the CT scan and the determination of the brain and liver weight is described in detail in manuscript I (Ruggeri et al., 2024). Briefly, the study included 268 piglets of the Swiss Large White breed (134 females and 134 males)

born from 26 litters that were obtained from two farrowing batches (14 litters in the first batch and 12 litters in the second batch). On day one (± 1) after birth, CT scan imaging was performed on all piglets to measure the brain and liver volume and weight.

On day 16 ± 0.6 [mean + SD] (T1), 24 piglets were chosen to sample faeces and blood for conducting analyses on faecal microbiota and blood metabolomics. The selection was based on the BrW/LW. Specifically, the 12 piglets with the highest BrW/LW (IUGR; BrW/LW: 1.00 ± 0.09) and the 12 with the lowest BrW/LW (NORM; BrW/LW: 0.36 ± 0.04) were selected for sampling (Supplementary Table S1). Due to pre-weaning mortality, out of the 24 pigs that were chosen for faecal and blood sampling on day 16 ± 0.6, 15 were still present. To maintain a group of 24 pigs (IUGR = 12 and NORM = 12) and repeat the analyses on faecal microbiota and blood metabolomics at different time points, the 9 pigs that were lost (IUGR = 3 and NORM = 6) were replaced with the subsequent 9 pigs that had the highest (IUGR = 3; BrW/LW: 0.90 ± 0.05) and the lowest (NORM = 6; BrW/LW: 0.43 ± 0.04) ratio in the new group, respectively. The selected pigs (IUGR = 12; BrW/LW: 1.00 ± 0.09; NORM = 12; BrW/LW: 0.40 ± 0.05) were sampled to collect blood and faeces at the end of the starter period (day 63 ± 8.6, T2) and faeces at the beginning (day 119 ± 11.4, T3) and at the end of the finisher period (day 162 ± 14.3, T4) (Supplementary Table S1).

Rearing conditions and feeding

The conditions in which the pigs were reared and the feeding techniques employed were described in manuscript I (Ruggeri et al., 2024). Briefly, the pigs were raised under a conventional Swiss rearing system, with unrestricted access to water and straw provided in the pens throughout the whole experimental period.

The piglets had *ad libitum* access to the same standard pre-/early postweaning diet from day 16 after birth until approximately 14 days post-weaning. Later, they were provided unrestricted

access to the same starter, grower, and finisher diet. The transition from the starter to the grower diet and from the grower to the finisher diet occurred when the pigs' BW was ≥ 20 kg and ≥ 60 kg on the day of the weekly weighing, respectively.

Faeces sampling

Faeces (~ 2 g) were collected from the piglets (IUGR = 12, NORM = 12) directly from the rectum just before the administration of the pre-/early postweaning diet (day 16 ± 0.6, T1). Likewise, faeces were collected from the pigs (IUGR = 12, NORM = 12) at the end of the starter period (day 63 ± 8.6, T2), at the beginning of the finisher period (day 119 ± 11.4, T3) and the end of the finisher period (day 162 ± 14.3, T4). After collection, each sample was divided into two aliquots and snap frozen in liquid nitrogen at −80°C.

Microbial DNA extraction

Total bacterial DNA for microbiota analysis was extracted from the faecal samples using FastDNA Spin Kit for Soil (MP Biomedicals, Europe, LLC) according to the manufacturer's instructions. DNA quantity and quality were assessed using a Nanodrop ND 1000 spectrophotometer (Nanodrop Technologies Inc., Wilmington, DE, USA). The DNA underwent amplification targeting the V3-V4 hypervariable regions of the 16S rRNA gene. Amplicons were produced using the primersPro341F: 50-TCGTCGGCAGCGTCAGATGTGTATAAGAGACAGCCTACGGGNBGCASCAG-30 and Pro805R: 50GTCTCGTGGGCTCGGAGATGTGTATAAGAGACAGGACTACNVGGGTATCTAATCC-30 (Takahashi et al., 2014), using Platinum TM Taq DNA Polymerase High Fidelity (Thermo Fisher Scientific, Italy). The libraries were prepared according to the standard

protocol for MiSeq Reagent Kit v3 and underwent sequencing on the MiSeq platform (Illumina Inc., San Diego, CA, USA).

Blood sampling

Blood (~ 3 mL) was collected from the piglets (IUGR = 12, NORM = 12) via the jugular vein using heparin-treated tubes just before the administration of the pre-/early postweaning diet (day 16 ± 0.6, T1). Following the same procedure, blood (~ 5 mL) was sampled from the pigs (IUGR = 12, NORM = 12) at the end of the starter period (day 63 ± 8.6, T2). Samples were refrigerated on ice after collection for 30 minutes. Plasma was then separated from the whole blood through centrifugation at 3000 rpm for 10 minutes. Following centrifugation, each plasma sample was split into two aliquots and stored at −80°C until metabolome analysis via proton nuclear magnetic resonance (**^{1}H-NMR**).

Plasma ^{1}H-NMR analysis

An ^{1}H-NMR analysis solution with D_2O, 10 mmol/L of 3-(trimethylsilyl)-propionic-2,2,3,3-d4 acid sodium salt and 2 mmol/L of NaN_3 was prepared. The pH of the solution was set at 7.00 ± 0.02 using phosphate buffer 1 M. The acid sodium salt was employed as a reference for the NMR chemical shift. To avoid microorganism proliferation, NaN_3 was used. Before the ^{1}H-NMR analysis, 1 mL of each plasma sample was centrifuged (18,630 g; 900 s; 4 °C). Then, 0.7 mL of supernatant was then added to 0.1 mL of the ^{1}H-NMR solution. Finally, centrifugation was performed on each sample once again as previously described. ^{1}H-NMR spectra were registered (600.13 MHz; 298 K) with an AVANCE™ III spectrometer (Bruker, Milan, Italy), provided with Topspin v3.5 software. Signals from broad resonances due to large molecules were suppressed with a CPMG-filter. The CPMG-filter was composed of 400 echoes with a τ of 400 μs and a 180° pulse of 24 μs, for a total filter of 330 ms. The water residual

signal was suppressed using presaturation employing the cpmgpr1d sequence, included in the standard pulse sequence library. Each spectrum was generated by combining 256 transients, each consisting of 32,000 data points covering a frequency window of 7184 Hz, with intervals separated by a relaxation delay of 5 seconds. ^{1}H-NMR spectra were then phase-adjusted in Topspin v3.5 and exported to ASCII format employing the built-in script convbin2asc. Spectra were processed with R software (R Core Team, 2020) using in-house developed scripts. Baseline adjustment on spectra was performed by differentiating baseline imperfection from NMR signals according to the "rolling ball" principle (Kneen and Annegarn, 1996), as implemented in the R package baseline (Liland et al., 2010). Signal assignment was performed by comparing their chemical shift and multiplicity with the Human Metabolome Database (Wishart et al., 2007) and Chenomx software library (Chenomx Inc., Edmonton, Canada, v10). Plasma molecule concentrations were assessed by quantifying the molecules of the first sample analysed using an external standard. Differences in water content between samples were then taken into account by probabilistic quotient normalization (Dieterle et al., 2006). The quantification of each metabolite was assessed using rectangular integration, considering one of its signals free from interferences (Brugaletta et al., 2022).

Statistical analysis and bioinformatic analysis of microbiome data

Microbiota analysis was carried out using the DADA2 pipeline (Callahan et al., 2016), and taxonomic categories were assigned using the Silva Database (release 138.1) as a reference for the assignment (Quast et al., 2012). Alpha (Shannon, Chao1, and Simpson indices) and Beta diversity (calculated as Bray Curtis distance matrix), as well as the abundance of taxonomic categories, were calculated and analysed with the R software 3.6, using the PhyloSeq (McMurdie and Holmes, 2013), Vegan (Dixon, 2003) and microbiomeMarker (Cao et al., 2022) packages. Differences between groups regarding Alpha diversity indices were tested

using a first a linear mixed model including category (IUGR, NORM), time (T1, T2, T3, T4), and their interaction as a fixed factor, and the litter of origin as a random factor. Then a separate model within each time point was performed including only the category as a fixed factor and the litter of origin as a random factor. For Beta diversity, a dissimilarity matrix was constructed using the Bray-Curtis distance matrix as metrics, and the results were plotted using a Non-metric multidimensional scaling (NMDS) plot. Furthermore, the betadisper test was conducted to test differences in the samples' dispersion among the groups. Differences were tested using first a PERMANOVA (Adonis) model with 9,999 permutations, including category, time, and their interaction and litter of origin as factors. Secondly, a PERMANOVA model within each time point was performed including the category as a factor. For the differential analysis of taxa, the LEfSe algorithm was used at the genus level. Specifically, taxa were considered significant if they possessed a Linear Discriminant Analysis (LDA) score > 4 and an $P_{adj} < 0.05$ within each time point, including the category as a factor.

For the metabolome data, all calculations and statistical analyses were performed using Python (version 3.8.8). The Shapiro-Wilk test was performed to identify the metabolites whose concentration in the blood showed a normal distribution. For these latter, the Student's t-test was used to compare the metabolite concentrations in blood samples for the IUGR and NORM groups. Metabolites whose concentrations did not show a normal distribution were compared using the non-parametric Mann–Whitney between the two groups. The Benjamini–Hochberg correction was applied in both cases to account for the risk I inflation associated with multiple comparisons. Before being subjected to unsupervised and supervised algorithms, the concentration of each metabolite was normalized and centered. In the multivariate analysis, Principal Component Analysis (**PCA**) and Orthogonal Projection to Latent Structures-Discriminant Analysis (**OPLS-DA**) were employed as the unsupervised and supervised methods, respectively. PCA was used for the identification of outliers (Mahalanobis distance

metric), as well as the spontaneous clustering of similar samples in the scatter plot of the two principal components. In the OPLS-DA analysis, the X matrix consisted of metabolite concentrations, while the Y vector contained information regarding the group (IUGR or NORM). The goodness of fit of the OPLS-DA model (**R2Y**) was reported, and predictive performance was assessed through cross-validation. Metrics such as the predictive ability of the model (**Q2Y**) and the predictive ability of permuted models (**Q2Y-perm**) were calculated for evaluation. OPLS-DA loadings plots were used to show the metabolites that contributed the most to the separation between the IUGR and NORM groups. The identification of metabolites of interest was made through the combination of the variable importance in the projection (**VIP**) and the loading between the metabolite in the X matrix and the predictive latent variable (**pLV**) of the model. Metabolites with VIP >1.0 and absolute high loading values were considered important in the metabolomics signature (Chao de la Barca et al., 2022).

Results

Faecal microbiota

A total of 3,436,549 sequence reads were attributed to a total of 9,256 Amplicon Sequence Variants distributed among all samples as shown in Supplementary Table S2. The relative rarefaction curves illustrated the tendency to plateau for all the samples, suggesting that the sequencing depth was sufficient to describe the variability within the microbial communities analysed among the samples (Supplementary Fig. S1). One sample from the NORM group was removed from the analysis due to the low number of reads. The taxonomic assignment resulted in the identification of 22 phyla, 117 families, and 338 genera. The most abundant phyla were Firmicutes (70.89 ± 14%) and Bacteroidota (21.11 ± 11%). The most abundant families were *Lactobacillaceae* (20.93 ± 17%), *Lachnospiraceae* (12.34 ± 6%), and *Prevotellaceae* (11.67 ±

9%). The most represented genera were *Lactobacillus* (16.63 ± 15%), *Streptococcus* (4.76 ± 6%), and HT002 (3.69 ± 6%).

Line plots showing the Alpha diversity values within the IUGR and NORM groups across different time points are shown in Fig. 1. The time (i.e., age of the pigs) significantly affected the Chao1 and Shannon indices ($P < 0.001$ and $P < 0.001$, respectively), while the InvSimpson was not affected. No effects were observed for the category and for the interaction between category and time. Separate models within each time point were then fitted. No significant differences between IUGR and NORM categories were observed at T1, T2, and T3 except for a tendency for higher Chao1 ($P = 0.066$) and Shannon indices ($P = 0.053$) in the IUGR group compared to the NORM group at T2.

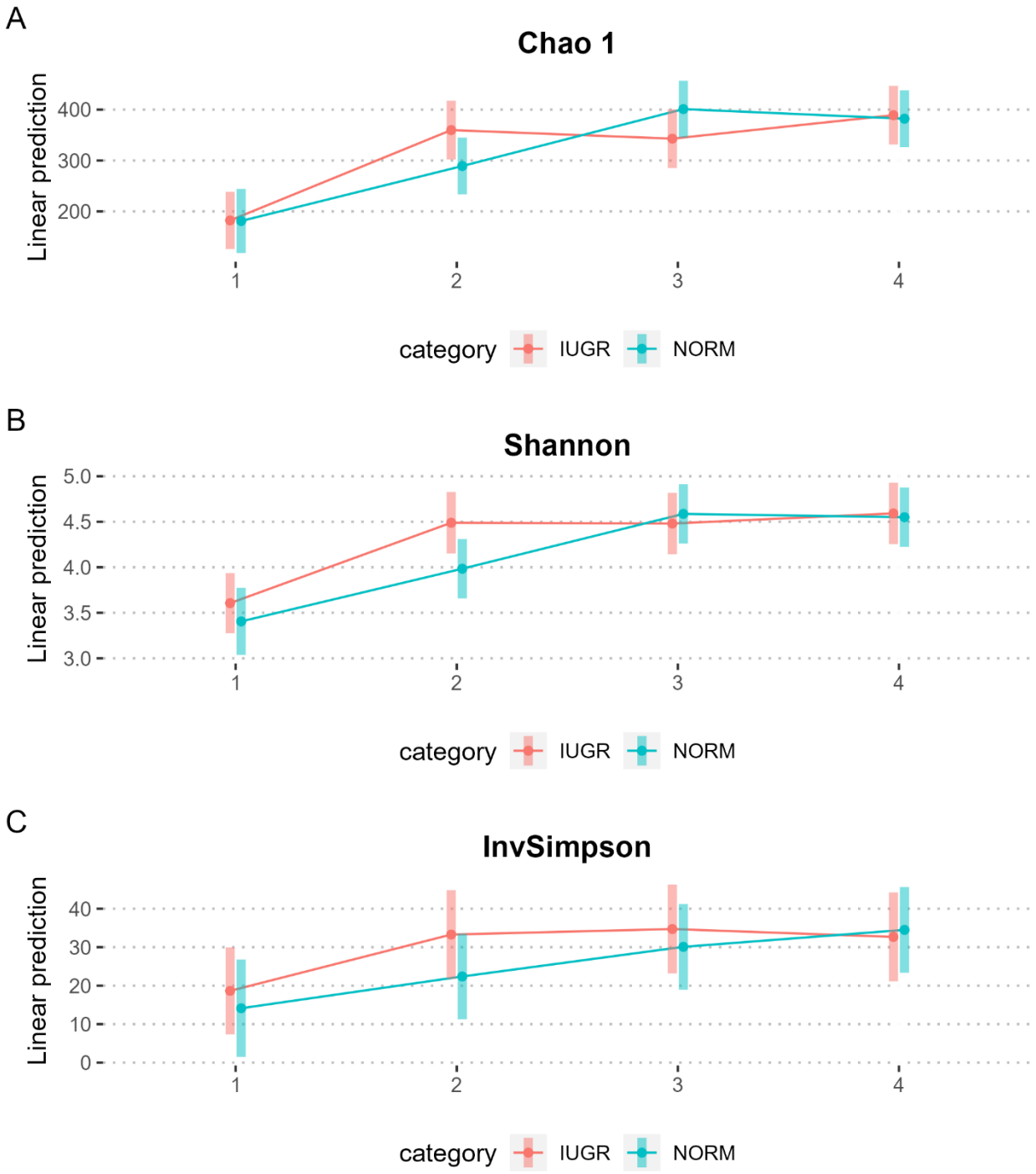

Fig. 1. Line plots showing the Alpha diversity values within each category (IUGR = pigs affected by intrauterine growth restriction; NORM = normal pigs) over time measured with Chao1 (panel A), Shannon (panel B), and InvSimpson (panel C) indexes. T1 = day 16 ± 0.6; T2 = day 63 ± 8.6; T3 =

day 119 ± 11.4; T4 = day 162 ± 14.3. The time significantly affected the Chao1 ($P < 0.001$) and Shannon ($P < 0.001$) indices.

The Adonis test carried out on the Beta diversity showed a significant effect of the category (P = 0.011, R^2 = 0.017), time (P = 0.001, R^2 = 0.185), their interaction (P = 0.016, R^2 = 0.039) and by the litter of origin (P = 0.016, R^2 = 0.039, data not shown). Samples tended to cluster according to the IUGR/NORM status within each time point as evidenced by the NMDS plot in Fig. 2. Separate Adonis models on Beta diversity matrix within each time point were then carried out. At T1, the Beta diversity was affected by the category (P = 0.002, R^2 = 0.083) and litter of origin (P = 0.001, R^2 = 0.616). At T2, a tendency was recorded (P = 0.079, R^2 = 0.068) for the category, and no differences were observed for the litter of origin. At T3, the Beta diversity was affected by the category (P = 0.027, R^2 = 0.066), and a trend was observed for the litter of origin (P = 0.082, R^2 = 0.301). At T4, no effect was observed on the Beta diversity.

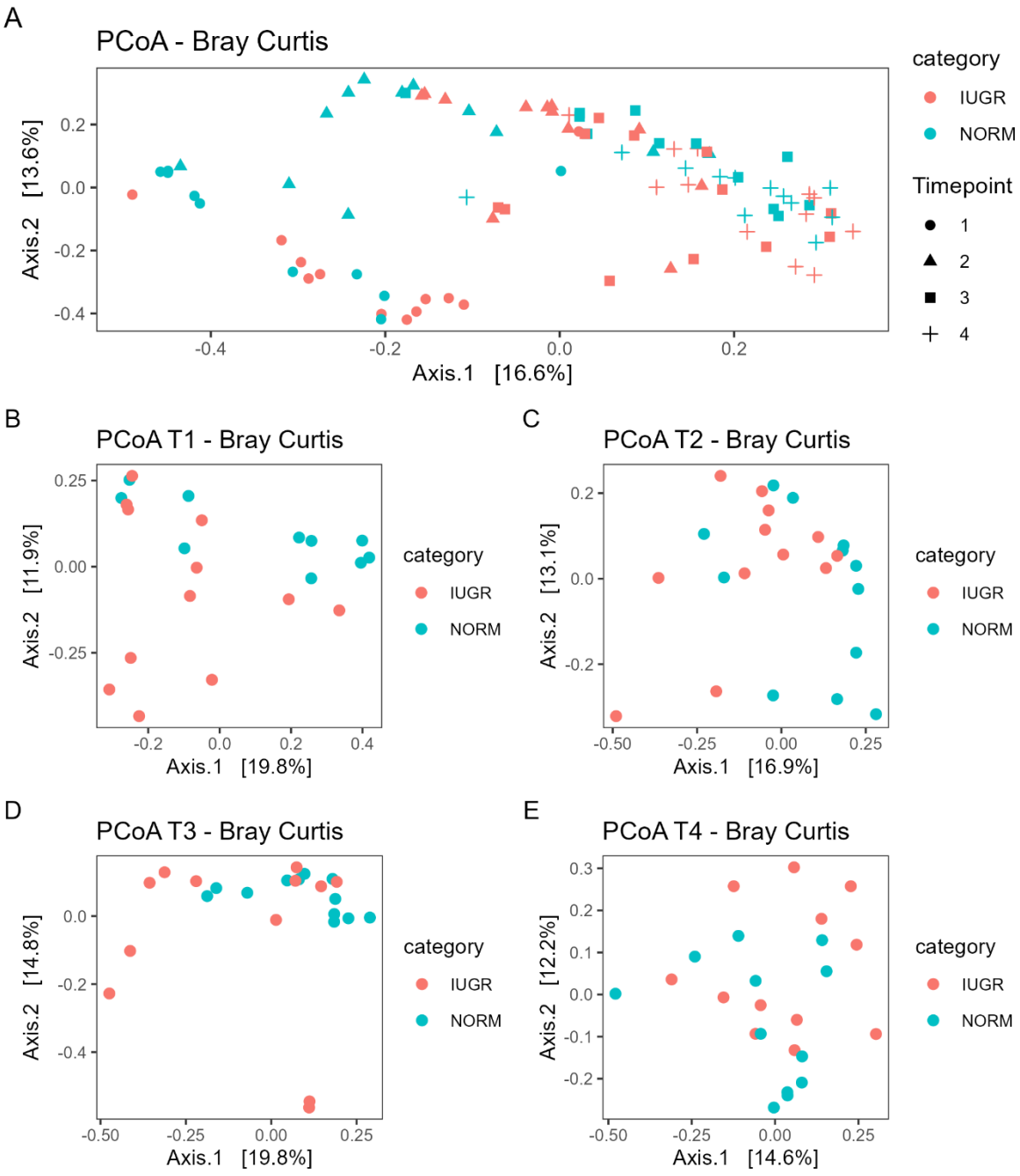

Fig. 2. NMDS plot using Bray-Curtis dissimilarity matrix showing the differences in bacterial composition between pigs affected by intrauterine growth restriction (IUGR) and normal pigs (NORM) over time (panel A) and at T1 (panel B), T2 (panel C), T3 (panel D) and T4 (panel E). T1 = day 16 ± 0.6; T2 = day 63 ± 8.6; T3 = day 119 ± 11.4; T4 = day 162 ± 14.3.

To identify which taxa contributed to the differences among the categories, the LEfSe algorithm on the data aggregated at genus levels was applied within each time point. No differences were observed at T4. The microbiological markers observed at T1, T2, and T3 are shown in Fig. 3A, 3B, and 3C, respectively. At T1, the IUGR group showed a higher abundance of *Clostridium sensu stricto 1* (LDA score = 4.55; $P_{adj} = 0.029$) and *Romboutsia* (LDA score = 4.04; $P_{adj} = 0.047$), while the NORM group was characterised by a higher abundance of *Ruminococcus* (LDA score = 4.39; $P_{adj} = 0.010$). At T2, IUGR pigs had higher abundances of *Prevotellaceae* NK3B31 group (LDA score = 4.5; $P_{adj} = 0.021$), *Rikenellaceae* RC9 gut group (LDA score = 4.49; $P_{adj} = 0.030$) and *Alloprevotella* (LDA score = 4.26; $P_{adj} = 0.030$), while the NORM group showed a higher abundance of HT002 (LDA score = 4.27; $P_{adj} = 0.048$) an uncultured genus of *Lactobacillaceae* family. At T3, the IUGR group was characterised by a higher abundance of p-2534-18B5 gut group (LDA score = 4.3, $P_{adj} = 0.03$) from the Bacteroidales order, while the NORM group was characterised by a higher abundance of *Prevotella_9* (LDA score = 4.6; $P_{adj} < 0.001$).

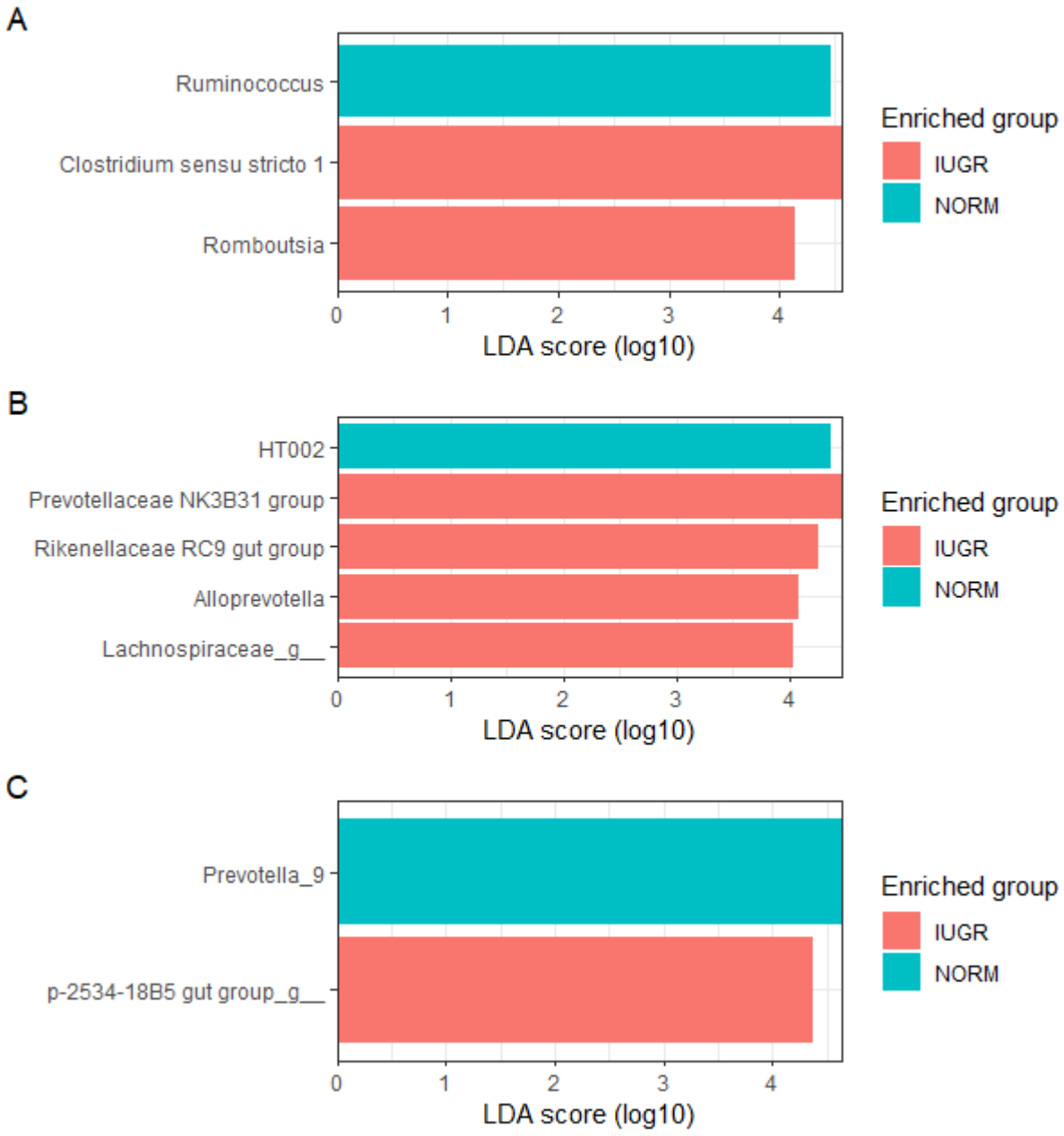

Fig. 3. LDA plot showing the bacterial markers characterising pigs affected by intrauterine growth restriction (IUGR) and normal pigs (NORM) at T1 (panel A), T2 (panel B), and T3 (panel C). No differences were observed at T4. T1 = day 16 ± 0.6; T2 = day 63 ± 8.6; T3 = day 119 ± 11.4; T4 = day 162 ± 14.3.

Plasma metabolome

From the plasma samples of 24 pigs (IUGR = 12, NORM = 12) collected at T1, 65 metabolites were analysed. Out of the 65 metabolites measured at T1, 44 were in the quantitation range for each sample and were analysed statistically. The others were not detectable in any or most of the plasma samples after centrifugation and were excluded from the statistical analysis (Supplementary Table S3). Only leucine and 2-aminobutyrate exhibited significant differences between IUGR and NORM pigs at T1, with IUGR pigs showing lower plasma concentrations of both metabolites compared to the NORM group ($P < 0.01$). Nevertheless, after applying the Benjamini-Hochberg correction, none of the metabolites demonstrated significant differences between the IUGR and NORM pigs. The PCA analysis identified two outliers (both from the IUGR group), and no spontaneous sample grouping was observed (Fig. 4). Even after the removal of outliers, no significant variations were observed in the metabolite concentrations between IUGR and NORM pigs, and the PCA analysis continued to show a lack of spontaneous grouping of the samples (Fig. 5).

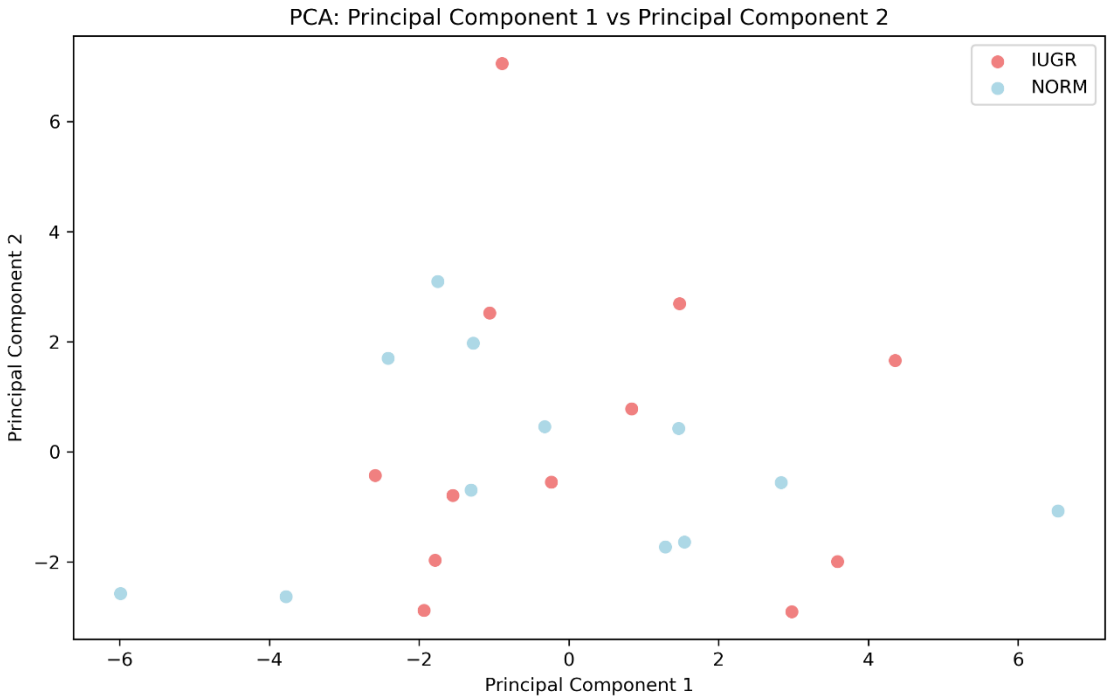

Fig. 4. Scatter plot to visualize the principal components of the unsupervised principal component analysis (PCA) of the metabolomic data from the samples collected at day 16 ± 0.6 (T1). Each data point is represented by its coordinates in the first and second principal components. The data points belonging to the normal pigs (NORM) are plotted in blue, the ones belonging to pigs affected by intrauterine growth restriction (IUGR) are plotted in red. Samples do not group together according to the IUGR/NORM status in the scatter plot of the PCA first principal plan.

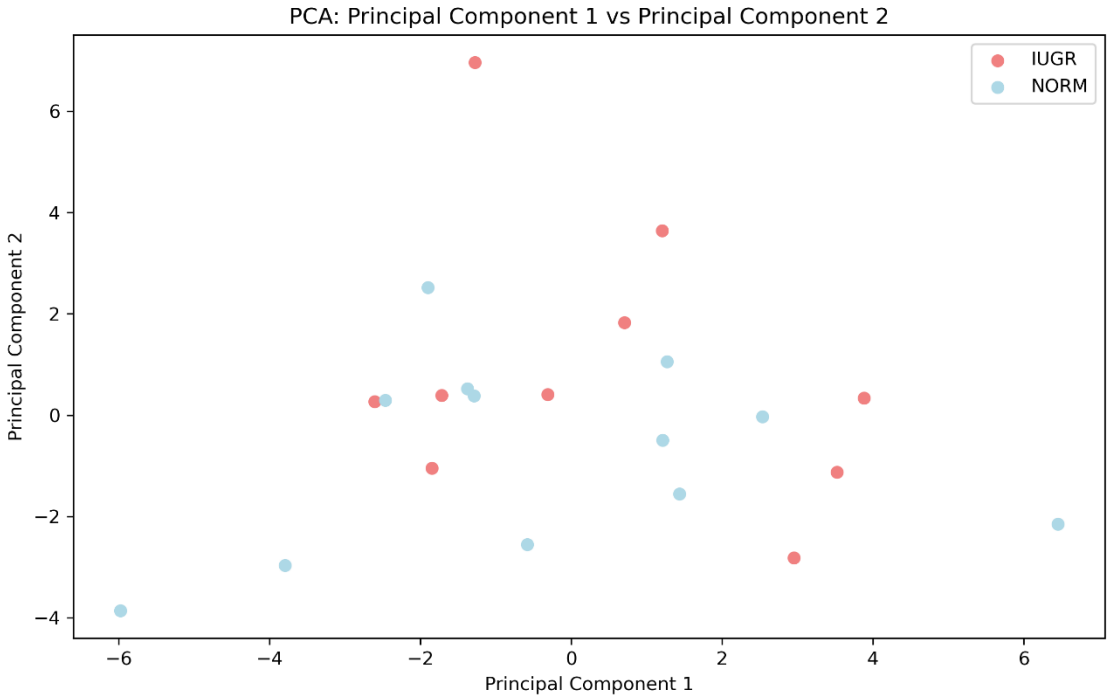

Fig. 5. Scatter plot to visualize the principal components of the unsupervised principal component analysis (PCA) of the metabolomic data from the samples collected at day 16 ± 0.6 (T1) after the removal of outliers. Each data point is represented by its coordinates in the first and second principal components. The data points belonging to the normal pigs (NORM) are plotted in blue, and the ones belonging to pigs affected by intrauterine growth restriction (IUGR) are plotted in red. Samples do not group together according to the IUGR/NORM status in the scatter plot of the PCA first principal plan.

The OPLS-DA model enabled good group discrimination (R2Y = 0.85, Fig. 6) but weak predictive ability and high risk of overfitting (Q2Y = -0.47, Q2Y perm test = 0.04). Plasma metabolites that contribute the most to the separation between the IUGR and NORM group are shown in the OPLS-DA loading plot in Fig. 7. None of the plasma metabolites showed a VIP >1.0 in the OPLS-DA analysis (Table 1).

Table 1. Identification of metabolites of interest at day 16 ± 0.6 (T1) through the combination of the variable importance in the projection (VIP) and the loading between the metabolite in the X matrix and the predictive latent variable (pLV) of the OPLS-DA model. Metabolites are sorted by decreasing VIP.

Metabolite	VIP	Loading
Tyrosine	0.20	-0.04
Leucine	0.20	0.04
Aspartate	0.19	0.04
Sarcosine	0.19	0.17
Alanine	0.18	0.27
Myo-inositol	0.16	0.26
Serine	0.16	0.17
Citramalate	0.15	0.32
2-Oxoglutarate	0.15	0.18
Glycerol	0.15	0.25
Acetate	0.14	0.19
2-Aminobutyrate	0.14	0.25
Threonine	0.13	-0.24
Beta-alanine	0.13	-0.04
Arginine	0.13	-0.18
Phenylalanine	0.13	0.14
Lysine	0.13	0.14
Glucose	0.12	0.25
Glyoxylate	0.12	0.06
Glutamine	0.12	0.25
Isoleucine	0.11	0.19
3-Hydroxyisobutyrate	0.11	0.01
TMAO	0.11	-0.12
Citrate	0.10	0.10
Dimethyl-sulfone	0.09	0.18
Glycine	0.09	-0.02
Ascorbate	0.09	0.18

Mannose	0.08	0.16
Betaine	0.08	0.17
Asparagine	0.08	0.01
Succinate	0.08	-0.12
Formate	0.07	-0.13
Creatine	0.07	-0.09
Valine	0.07	0.14
3-Aminoisobutyrate	0.06	-0.08
Acetone	0.06	-0.11
Methionine	0.06	-0.04
N,N-Dimethylglycine	0.05	0.01
Arabinose	0.04	0.05
Fumarate	0.03	-0.06
Trans-4-Hydroxy-L-proline	0.02	0.02
Proline	0.02	-0.03
Lactate	0.02	-0.03
Choline	0.01	-0.02

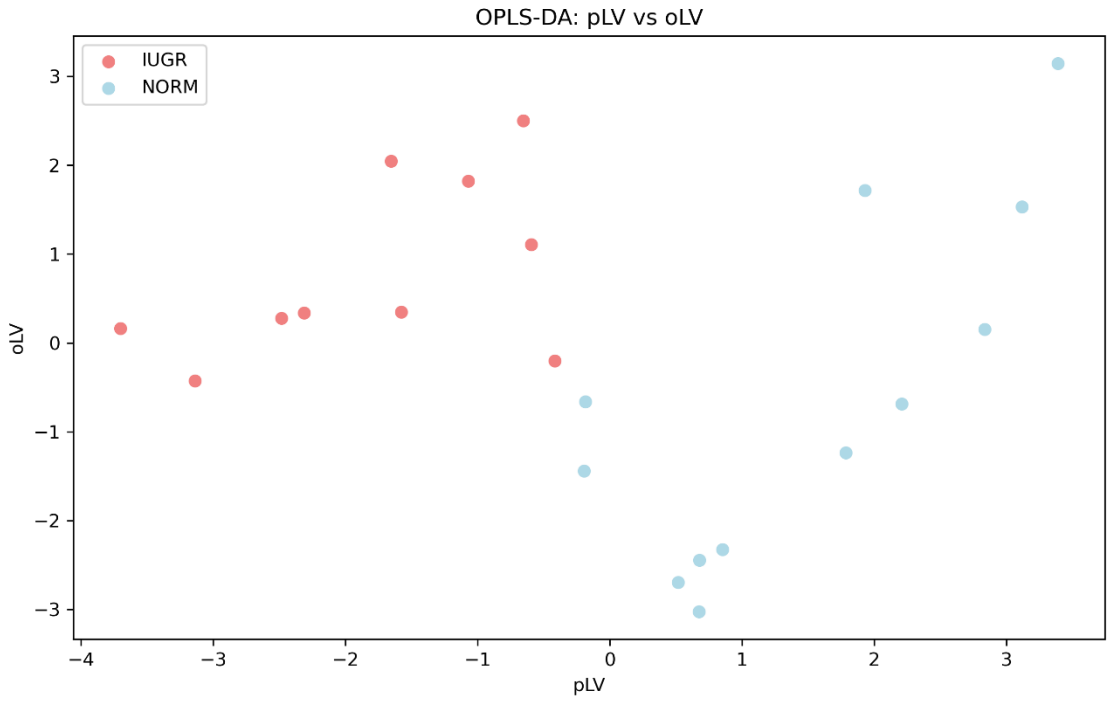

Fig. 6 Scatter plot to visualize the principal components of the supervised orthogonal partial least squares discriminant analysis (OPLS-DA) of the metabolomic data from the plasma samples collected at day 16 ± 0.6 (T1) after the removal of outliers. Each data point is represented by its coordinates in two components, predictive latent variable (pLV) and orthogonal latent variable (oLV). The data points belonging to the normal pigs (NORM) are plotted in blue, and the ones belonging to pigs affected by intrauterine growth restriction (IUGR) are plotted in red. Samples group together according to the IUGR/NORM status in the scatter plot of the OPLS-DA first principal plan.

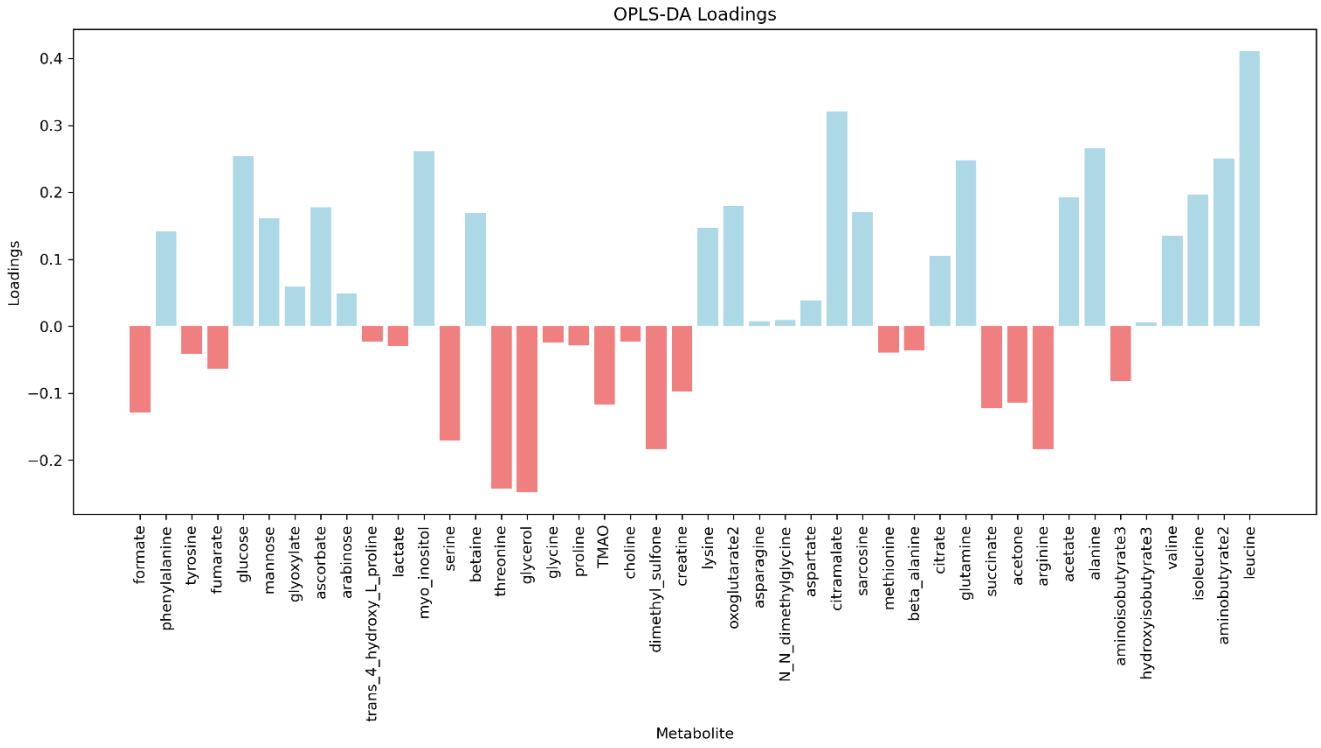

Fig. 7. Orthogonal partial least squares discriminant analysis (OPLS-DA) loadings plot of the metabolomic data from the plasma samples collected at day 16 ± 0.6 (T1) after the removal of outliers. X-axis: metabolites present in the plasma; y-axis: loadings for each metabolite. Loadings indicate the contribution of each metabolite to the separation between the two groups: pigs affected by intrauterine growth restriction (IUGR) and normal pigs (NORM). Positive loadings indicate that higher levels of the metabolite are associated with the NORM groups, while negative loadings indicate higher levels in the IUGR group. The metabolites with the highest positive and negative loadings. contribute the most to the separation between the two groups.

From the plasma samples of 24 pigs (IUGR = 12, NORM = 12) collected at T2, 65 metabolites were analysed (Supplementary Table S4). Out of the 65 metabolites measured at T2, 44 were in the quantitation range and were analysed statistically. The others were not detectable in any or most of the plasma samples and were excluded from the statistical analysis (Supplementary Table S4). Arabinose, arginine, ascorbate, asparagine, creatine, dimethyl-sulfone, glyoxylate, proline, and sarcosine exhibited significant differences between IUGR and NORM pigs at T2. Nevertheless, after applying the Benjamini-Hochberg correction, only asparagine was significantly different between the IUGR and NORM groups. The PCA analysis showed one outlier (from the NORM group) and a tendency of the samples to group spontaneously (Fig. 8). After the removal of the outlier, asparagine was still the only metabolite showing significant variations between IUGR and NORM pigs. Compared with the NORM group, IUGR pigs had significantly lower ($P < 0.05$ and t-statistic $\neq 0$) concentrations of asparagine at T2 (Fig. 9). The PCA analysis continued to show a tendency for spontaneous sample grouping after the removal of the outlier (Fig. 10). The OPLS-DA model enabled good group discrimination (R2Y = 0.77, Fig. 11) but weak predictive ability and high risk of overfitting (Q2Y = -1.48, Q2Y perm test = 0.05). Plasma metabolites that contribute the most to the separation between the IUGR and NORM group are shown in the OPLS-DA loading plot in Fig. 12. None of the plasma metabolites showed a VIP >1.0 in the OPLS-DA analysis (Table 2).

Table 2. Identification of metabolites of interest at day 63 ± 8.6 (T2) through the combination of the variable importance in the projection (VIP) and the loading between the metabolite in the X matrix and the predictive latent variable (pLV) of the OPLS-DA model. Metabolites are sorted by decreasing VIP.

Metabolite	VIP	Loading
Asparagine	0.19	-0.24
Mannose	0.19	0.28
3-Aminoisobutyrate	0.18	0.15
Beta-alanine	0.18	0.24
Sarcosine	0.17	-0.13
Proline	0.16	-0.15
Fumarate	0.15	0.24
Arabinose	0.15	0.29
Ascorbate	0.14	0.27
2-Aminobutyrate	0.14	0.12
Aspartate	0.13	0.22
Succinate	0.13	-0.14
Glycine	0.13	0.11
Myo-inositol	0.13	0.10
Dimethyl-sulfone	0.12	0.27
Isoleucine	0.12	-0.09
Acetate	0.12	0.23
Creatine	0.11	0.23
Acetone	0.11	0.17
Methionine	0.11	0.20
Glyoxylate	0.11	0.23
Citrate	0.11	-0.03
Arginine	0.10	0.16
Tyrosine	0.09	-0.15
Glucose	0.09	0.20
TMAO	0.09	-0.02
Serine	0.08	-0.18

Phenylalanine	0.08	-0.03
Alanine	0.08	-0.17
Trans-4-Hydroxy-L-proline	0.08	0.09
Lactate	0.07	-0.09
Formate	0.07	-0.14
Glycerol	0.07	0.08
Lysine	0.07	0.14
2-Oxoglutarate	0.06	0.04
Citramalate	0.06	-0.04
Glutamine	0.06	-0.10
Threonine	0.06	-0.00
N,N-Dimethylglycine	0.05	0.06
3-Hydroxyisobutyrate	0.04	0.09
Leucine	0.04	0.05
Choline	0.04	0.01
Betaine	0.03	-0.06
Valine	0.01	-0.02

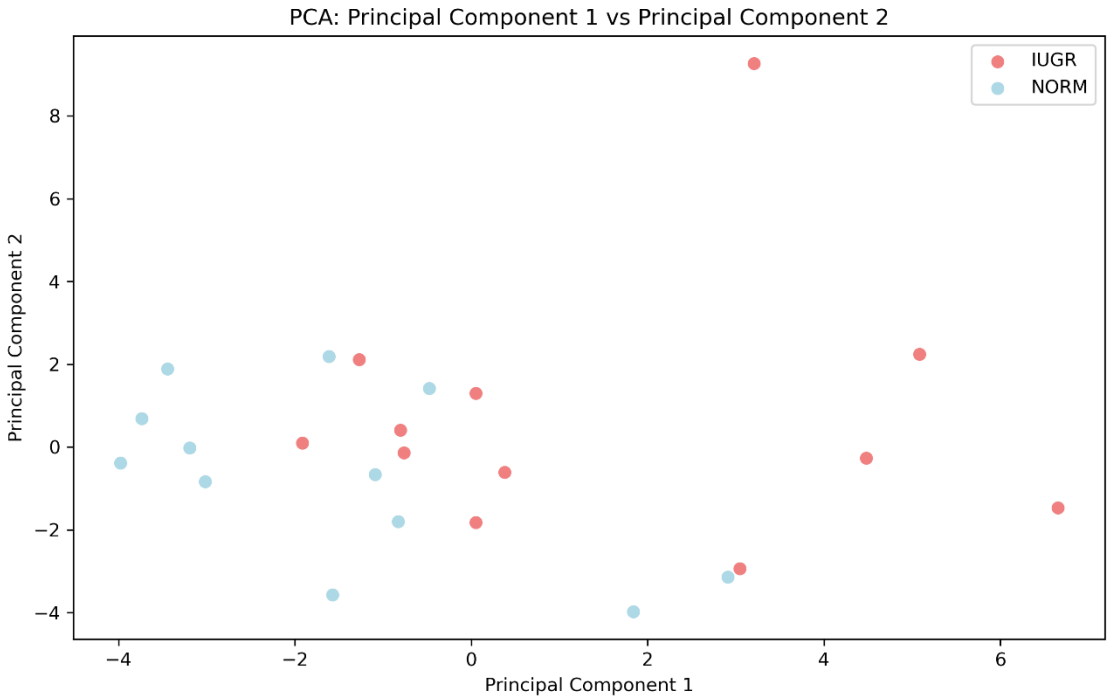

Fig. 8. Scatter plot to visualize the principal components of the unsupervised principal component analysis (PCA) of the metabolomic data from the samples collected at day 63 ± 8.6 (T2). Each data point is represented by its coordinates in the first and second principal components. The data points belonging to the normal pigs (NORM) are plotted in blue, and the ones belonging to pigs affected by intrauterine growth restriction (IUGR) are plotted in red. Samples tend to group together according to the IUGR/NORM status in the scatter plot of the PCA first principal plan.

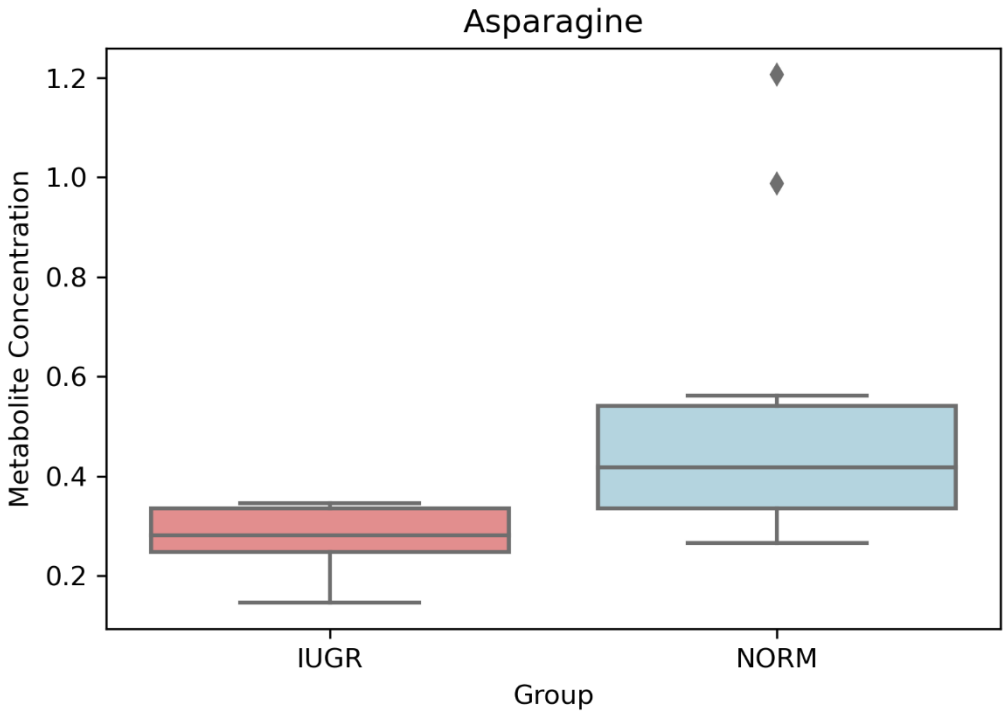

Fig. 9. Box plot to show the different plasma asparagine concentration observed between pigs affected by intrauterine growth restriction (IUGR) and normal pigs (NORM) at day 63 ± 8.6 (T2). X-axis: IUGR: 12 piglets with the highest brain-to-liver weight ratio (BrW/LW); NORM: 12 piglets with the lower BrW/LW. Y-axis: plasma metabolite concentration (mmol/L).

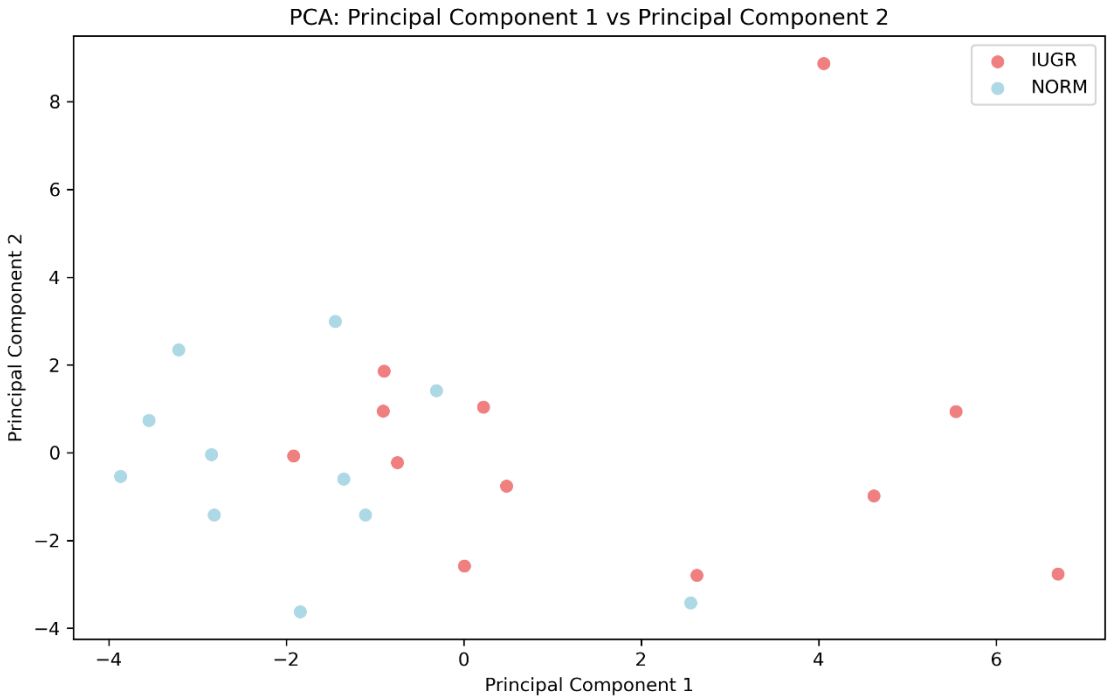

Fig. 10. Scatter plot to visualize the principal components of the unsupervised principal component analysis (PCA) of the metabolomic data from the samples collected at day 63 ± 8.6 (T2) after the removal of the outlier. Each data point is represented by its coordinates in the first and second principal components. The data points belonging to the normal pigs (NORM) are plotted in blue, and the ones belonging to pigs affected by intrauterine growth restriction (IUGR) are plotted in red. Samples tend to group together according to the IUGR/NORM status in the scatter plot of the PCA first principal plan.

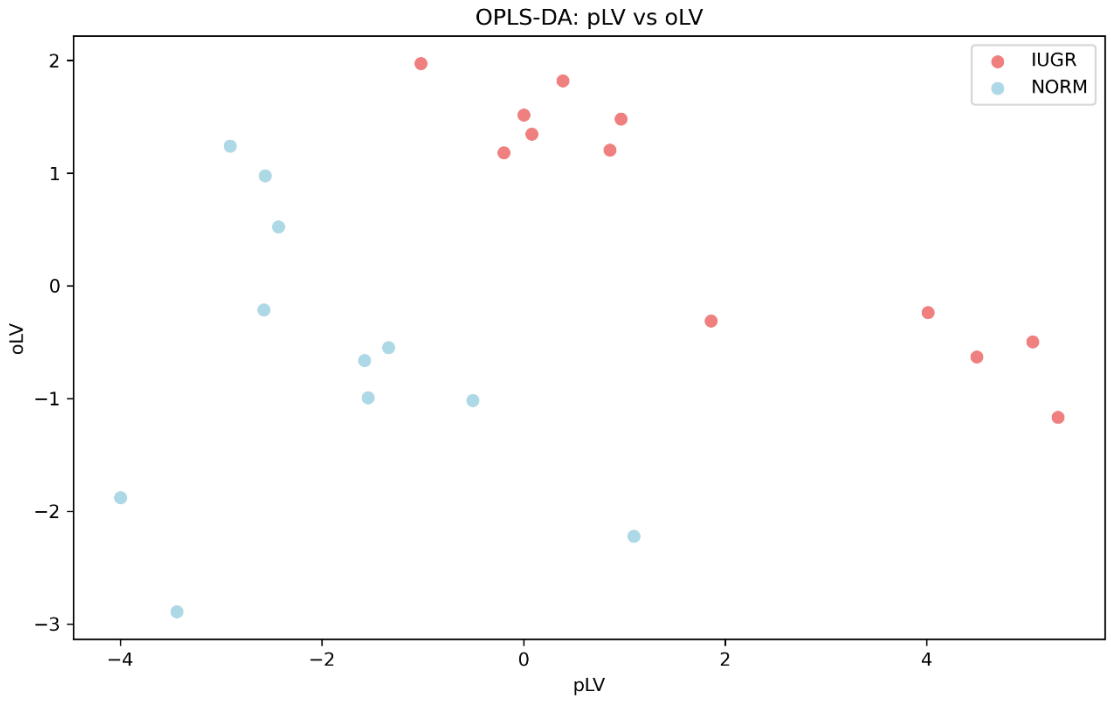

Fig. 11. Scatter plot to visualize the principal components of the supervised orthogonal partial least squares discriminant analysis (OPLS-DA) of the metabolomic data from the plasma samples collected at day 63 ± 8.6 (T2) after the removal of outliers. Each data point is represented by its coordinates in two components, predictive latent variable (pLV) and orthogonal latent variable (oLV). The data points belonging to the normal pigs (NORM) are plotted in blue, and the ones belonging to pigs affected by intrauterine growth restriction (IUGR) are plotted in red. Samples group together according to the IUGR/NORM status in the scatter plot of the OPLS-DA first principal plan.

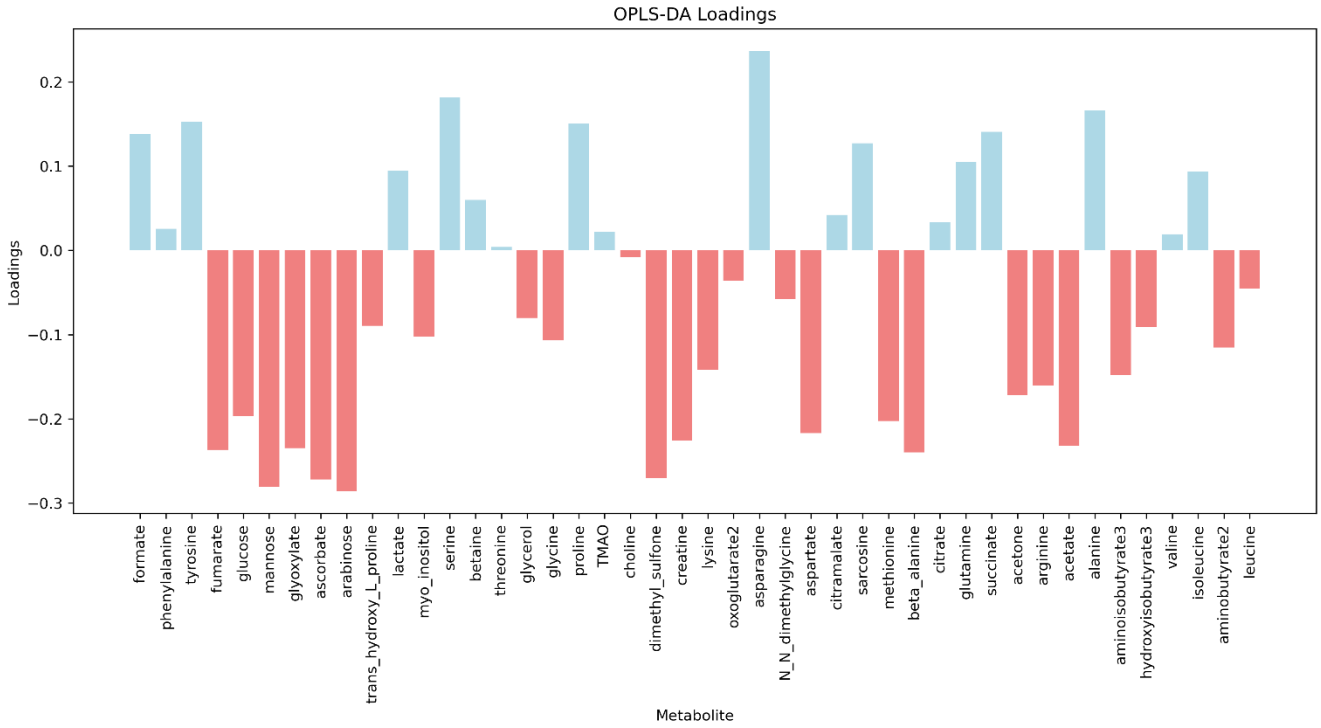

Fig. 12. Orthogonal partial least squares discriminant analysis (OPLS-DA) loadings plot of the metabolomic data from the plasma samples collected at day 63 ± 8.6 (T2) after the removal of the outlier. X-axis: metabolites present in the plasma; y-axis: loadings for each metabolite. Loadings indicate the contribution of each metabolite to the separation between the two groups: pigs affected by intrauterine growth restriction (IUGR) and normal pigs (NORM). Positive loadings indicate that higher levels of the metabolite are associated with the NORM groups, while negative loadings indicate higher levels in the IUGR group. The metabolites with the highest positive and negative loadings. contribute the most to the separation between the two groups.

Discussion

Microbiota and metabolome analyses hold the potential to identify biomarkers of IUGR and offer insights into the underlying mechanisms of this condition. To our knowledge, this is the first time that the effects of IUGR on faecal microbiota and blood metabolome have been evaluated based on the piglets' BrW/LW at birth.

Faecal microbiota

In this study, faecal samples were collected from IUGR and normal pigs at different time points and analysed for microbiota composition. The objective was to provide insights into the dynamic profile of faecal microbiota in pigs affected by IUGR compared to normal pigs across different developmental stages. At the phylum level, the faecal microbiota of both IUGR and normal pigs was dominated by Firmicutes and Bacteroidetes at all time points, which is consistent with previous literature (Yang et al., 2021; Gaukroger et al., 2020; Kim et al., 2011). Unlike other studies, the Alpha diversity of the faecal microbiota in the lactation, starter, grower, and finisher period was not affected by the IUGR status in our experiment, except for a tendency for a higher Alpha diversity in the IUGR group at the end of the starter period. Zhang et al. (2019) reported the Alpha diversity of the jejunal microbiota in IUGR piglets, defined by their BtW, to be significantly lower than that of control piglets at 7 and 21 days of age, suggesting a dysbiosis in the gut of IUGR piglets during the lactation period. In contrast, Xiong et al. (2020) observed that Alpha diversity of the jejunum and ileum microbiota in IUGR pigs, identified based on their BtW, was significantly higher than in normal pigs at 25 kg (beginning of the grower period), 50 kg (end of the grower period), and 100 kg (end of the finisher period) of BW, indicating a more diversified intestinal microbiota in the IUGR pigs during the grower-finisher phase.

In our study, the Beta diversity of the faecal microbiota across the lactation, starter, and grower periods was significantly affected by the IUGR status, with the samples clustering according to the category within each time point. Accordingly, in the study of Xiong et al. (2020), the Beta diversity analysis showed that IUGR pigs had a different microbial community in the small intestine at 25, 50, and 100 kg BW compared to normal pigs. Regarding the differential abundance analysis at the genus level, our findings revealed a higher abundance of the genera *Clostridium sensu stricto 1* and *Romboutsia* in the IUGR group during the lactation period, while the NORM group was characterized by a higher abundance of *Ruminococcus*.

The function of *Clostridium sensu stricto 1* and *Romboutsia* in suckling piglets is still unclear. Nonetheless, there have been reports suggesting that protein-derived metabolites produced by proteolytic bacteria like *Clostridia* could disrupt barrier function by changing mucus composition and tight junctions (Huang et al., 2019; Shi et al., 2019; Pieper et al., 2016).

Ruminococcus belongs to the *Lachnospiraceae* family. These bacteria ferment dietary fibre and produce short-chain fatty acids, which play a beneficial role in the maintenance of intestinal health by improving barrier function and reducing inflammation (Lan et al., 2023; Nowland et al., 2022; Xiong et al. 2020). The lower abundance of these bacteria in the IUGR pigs may contribute to the higher morbidity and mortality (Farmer and Edwards, 2022), as well as the reduced growth observed in IUGR piglets compared to their normal littermates during lactation, as documented in manuscript I and other studies (Ruggeri et al., 2024; Santos et al., 2022; Farmer and Edwards, 2022; Wu et al., 2006).

At the end of the starter period, our results showed a higher abundance of *Prevotellaceae* NK3B31 group, *Rikenellaceae* RC9 gut group, and *Alloprevotella* in the IUGR pigs, while the NORM group exhibited a higher abundance of HT002 an uncultured genus of *Lactobacillaceae* family. Le Sciellour et al. (2018), reported a positive link between the abundance of OTUs belonging to *Lactobacillaceae* and the digestibility of nitrogen and energy in grower-finisher

pigs. In addition, *Lactobacillaceae* are also known to improve the health of the small intestine by modulating the gut microbiota, promoting beneficial fermentation, and exerting antagonistic activity against pathogens in pigs (Dowarah et al., 2017). Considering the positive effect of *Lactobacillaceae* on the ability to digest feed, the lower abundances of bacteria belonging to this family may partly explain the reduced feed efficiency of IUGR compared to normal pigs described in manuscript I and in the existing literature on IUGR pigs (Ruggeri et al., 2024; Santos et al., 2022; Farmer and Edwards, 2022; Wu et al., 2006). However, at the same time point, the IUGR group showed higher abundances of bacteria belonging to the *Prevotellaceae* family. These bacteria are able to degrade complex carbohydrates and can be helpful in promoting intestinal health and growth of the pigs (Le Sciellour et al., 2018; Zhang et al., 2018). While numerous studies suggest a positive association between *Prevotella*, feed efficiency, and growth performance, contradictory results indicate an inverse relationship between certain *Prevotella* species and feed efficiency in pigs (Amat et al., 2020). This highlights the importance of additional research into *Prevotella* species or strains associated with diverse growth outcomes.

At the beginning of the finisher period, the IUGR group was characterised by a higher abundance of p-2534-18B5 gut group from the Bacteroidales order, while the NORM group was characterised by a higher abundance of *Prevotella*_9. Bacteria belonging to the *Prevotellaceae* family, as mentioned above, are generally considered beneficial for gut health, as they are involved in the fermentation of dietary fiber in the hindgut and the resultant production of short-chain fatty acids (Zhang et al., 2018). A reduction of this beneficial bacteria from the start of the grower to the finisher period may worsen the performance of the IUGR-affected pigs.

The findings of our study suggest dynamic changes in faecal microbiota composition in pigs with IUGR compared to normal pigs across different developmental stages, independent of

their diets. The observed differences in microbial composition, particularly in families associated with short-chain fatty acid production and gut health, may contribute to the impaired health and growth of IUGR pigs. Moreover, differences in the taxa identified could potentially serve as microbial biomarkers for this condition.

Plasma metabolome

In this study, blood samples were collected from IUGR and normal pigs during the lactation period and at the end of the starter phase to perform metabolome analysis. Considering the restricted glucose availability and the increased adipocyte proliferation observed in IUGR foetuses (Sarr et al., 2012; Gondret et al., 2011; Attig et al., 2008), along with the ongoing enhanced adipogenesis reported in the postnatal life (Attig et al., 2008), we hypothesized differences in plasma metabolites associated with lipid and energy metabolism between IUGR and NORM piglets at both time points. Since no significant differences in metabolites were observed between IUGR and NORM pigs during the lactation period, we had to partially reject our hypothesis. Nevertheless, tyrosine and leucine emerged as main contributors to the separation between IUGR and NORM groups in the OPLS-DA analysis, showing lower concentrations in the plasma of IUGR piglets in the lactation period. This is in agreement with the findings of Lin et al. (2012) who reported reduced leucine and tyrosine concentrations in the plasma of IUGR foetuses (defined by their foetal weight) in late gestation, and He et al. (2011) who observed decreased serum tyrosine in IUGR piglets, identified based on their BtW, at 21 days of age. Leucine, a branched-chain essential amino acid, acts as a nutrient signal, stimulating muscle protein synthesis in both newborn (Suryawan et al., 200; Escobar et al., 2005) and weaned pigs (Yin et al., 2010). Tyrosine, a non-essential aromatic amino acid, serves as a precursor for catecholamines (dopamine, norepinephrine, and epinephrine), crucial neurotransmitters in the central and peripheral nervous systems, and thyroid hormones,

essential in the control of growth, development, and metabolism. The lower concentrations of leucine and tyrosine observed in IUGR-affected pigs may contribute to the reduced growth, altered metabolism, and impaired maturation of the nervous system reported in the literature in IUGR-affected piglets (Santos et al., 2022; Wixey et al., 2019; Shen et al., 2018).

At the end of the starter period, only asparagine was significantly lower in the plasma of IUGR compared to NORM pigs and it was the metabolite that contributed the most to the separation between the IUGR and NORM groups in the OPLS-DA analysis. Asparagine is a non-essential amino acid involved in energy and amino acid metabolism, as well as in protein synthesis (Wang et al., 2015). Asparagine can act as a precursor for other amino acids of the arginine family, such as aspartate, glutamine, and glutamate, which are the major sources of ATP in mammalian enterocytes (Wu, 2013). Additionally, asparagine contributes to immune function, as demonstrated by studies in weaned piglets indicating its positive impact on the intestine and liver during inflammation (Chen et al., 2016; Wu et al., 2015). Considering the physiological functions of asparagine, the lower concentration of this amino acid could be associated with the reduced growth of IUGR pigs compared to their normal littermates and their higher susceptibility to diseases reported in several studies (Ruggeri et al., 2024; Santos et al., 2022; Farmer and Edwards, 2022; Wu et al., 2006). However, other metabolites associated with lipid oxidation, energy, and protein metabolism, which showed changes between IUGR and normal pigs in other studies (Lin et al., 2012; He et al., 2011), were not affected in the present study. The literature on metabolomic profiling in IUGR pigs across different growth stages is limited and the interpretation of the results is challenging. There is not a standardized definition of IUGR and the diagnosis is often based just on the BW of the foetus or the BtW of the piglet. This may be a reason why the reported findings were inconsistent (Priante et al., 2019).

In conclusion, our study demonstrated that growth restriction in the uterus has a significant and long-lasting impact on the faecal microbiota composition in pigs, from birth to the beginning

of the finisher period. In contrast, growth restriction minimally affected the blood metabolome profile of pigs at different growing stages. Identifying biomarkers associated with IUGR could provide novel insights into this condition, facilitating early interventions and effective management strategies. These may include proving dietary supplements, administering specific probiotics and prebiotics to shape the gut microbiota, ensuring colostrum intake after birth, maintaining optimal environmental conditions, and conducting regular health checks. The successful treatment of the IUGR-affected pigs holds the potential to improve the overall efficiency of pig production systems.

Ethics approval

All the experimental procedures complied with Swiss animal welfare guidelines and were approved (experimental approval numbers 32751) by the Cantonal Veterinary Office of Fribourg (Switzerland).

Supplementary material

Supplementary Table S1. Selection based on their brain-to-liver weight ratio (BrW/LW) to compare the blood metabolome and faecal microbiota between pigs affected by intrauterine growth restriction (IUGR) and normal pigs (NORM) at different time points.

	Category[1]		Sex	
Item[2]	IUGR	NORM	Female	Castrate
T1	12	12	15	9
BrW/LW	1.00	0.36	0.69	0.66
T2, T3, T4	12	12	12	12
BrW/LW	1.00	0.40	0.72	0.68

[1] Category: IUGR: 12 pigs with the highest BrW/LW; NORM: pigs with the lowest BrW/LW.

[2] T1 = blood and faeces collected before the administration of the pre-/early postweaning diet (day 16 ± 0.6); T2 = blood and faeces collected at the end of the starter period (day 63 ± 8.6); T3 = faeces collected at the beginning of the finisher period (day 119 ± 11.4); T4 = faeces collected at the end of the finisher period (day 162 ± 14.3). BrW/LW = mean BrW/LW in the IUGR and NORM groups.

Supplementary Table S2. Per sample information regarding sequencing depth.

ID[1]	Sow ID[2]	Parity	Sex	BtW[3]	BrW/LW[4]	Category[5]	Time point[6]	Selected	Depth
9205	5262-FE4	3	female	1.11	1.10	IUGR	4	1	28819
9069	7162-FE4	1	castrate	1.95	0.42	NORM	2	1	26669
9124	5906-FE4	2	female	1.61	0.41	NORM	1	1	49488
9092	1773-FE4	7	female	1.18	0.99	IUGR	1	1	32163
9108	5953-FE4	2	castrate	2.03	0.35	NORM	2	1	25222
9110	5953-FE4	2	female	1.89	0.32	NORM	2	1	35540
9166	338-FE4	9	female	2.16	0.38	NORM	2	1	54012
9266	709-FE4	8	castrate	1.87	0.46	NORM	2	1	30261
9110	5953-FE4	2	female	1.89	0.32	NORM	4	1	47032
9143	6076-FE4	1	female	0.83	1.06	IUGR	4	1	29679
9166	338-FE4	9	female	2.16	0.38	NORM	4	1	38775
9165	338-FE4	9	female	2.15	0.41	NORM	4	1	41079
9093	1773-FE4	7	female	1.08	0.94	IUGR	1	1	32841
9193	5262-FE4	3	castrate	1.51	0.89	IUGR	1	1	31073
9236	7201-FE4	1	castrate	1.94	0.46	NORM	2	1	31613
9239	7201-FE4	1	castrate	1.95	0.44	NORM	2	1	29614
9059	3188-FE4	5	castrate	1.76	0.46	NORM	3	1	28108
9006	7151-FE4	1	castrate	1.03	1.12	IUGR	1	1	22955
9007	7151-FE4	1	castrate	1.07	0.41	NORM	1	1	29748
9108	5953-FE4	2	castrate	2.03	0.35	NORM	1	1	38794
9165	338-FE4	9	female	2.15	0.41	NORM	1	1	8851
9236	7201-FE4	1	castrate	1.94	0.46	NORM	4	1	1272
9239	7201-FE4	1	castrate	1.95	0.44	NORM	3	1	56528
9059	3188-FE4	5	castrate	1.76	0.46	NORM	2	1	44147
9048	4062-FE4	4	castrate	1.57	0.40	NORM	1	1	28884
9282	709-FE4	8	female	0.97	0.88	IUGR	2	1	56314
9016	7151-FE4	1	female	0.99	0.96	IUGR	1	1	36803
9110	5953-FE4	2	female	1.89	0.32	NORM	1	1	28746
9006	7151-FE4	1	castrate	1.03	1.12	IUGR	2	1	45261
9284	3459-FE4	5	castrate	1.31	0.88	IUGR	4	1	33257

9085	1773-FE4	7	castrate	1.15	0.98	IUGR	2	1	1238
9205	5262-FE4	3	female	1.11	1.10	IUGR	1	1	32393
9236	7201-FE4	1	castrate	1.94	0.46	NORM	3	1	30554
9112	1684-FE4	7	female	1.76	0.38	NORM	2	1	40088
9104	757-FE4	8	female	1.49	0.90	IUGR	1	1	34718
9085	1773-FE4	7	castrate	1.15	0.98	IUGR	4	1	31491
9205	5262-FE4	3	female	1.11	1.11	IUGR	2	1	45294
9033	7146-FE4	1	castrate	1.9	0.36	NORM	2	1	19047
9086	1773-FE4	7	castrate	1.11	1.14	IUGR	2	1	41018
9006	7151-FE4	1	castrate	1.03	1.12	IUGR	3	1	62877
9183	7202-FE4	1	castrate	1.17	1.07	IUGR	2	1	40677
9166	338-FE4	9	female	2.16	0.38	NORM	1	1	27838
9092	1773-FE4	7	female	1.18	1.00	IUGR	2	1	41374
9093	1773-FE4	7	female	1.08	0.94	IUGR	4	1	29702
9108	5953-FE4	2	castrate	2.03	0.35	NORM	4	1	25700
9122	5906-FE4	2	female	1.84	0.36	NORM	3	1	38052
9093	1773-FE4	7	female	1.08	0.94	IUGR	2	1	41000
9013	7151-FE4	1	female	1.05	0.87	IUGR	3	1	40499
9122	5906-FE4	2	female	1.84	0.36	NORM	1	1	22663
9108	5953-FE4	2	castrate	2.03	0.35	NORM	3	1	44204
9121	5906-FE4	2	female	1.96	0.36	NORM	1	1	30670
9205	5262-FE4	3	female	1.11	1.11	IUGR	3	1	32822
9122	5906-FE4	2	female	1.84	0.36	NORM	2	1	32933
9143	6076-FE4	1	female	0.83	1.06	IUGR	3	1	31782
9092	1773-FE4	7	female	1.18	1.00	IUGR	3	1	41411
9016	7151-FE4	1	female	0.99	0.96	IUGR	4	1	55016
9016	7151-FE4	1	female	0.99	0.96	IUGR	3	1	6492
9016	7151-FE4	1	female	0.99	0.96	IUGR	2	1	60599
9110	5953-FE4	2	female	1.89	0.32	NORM	3	1	38896
9013	7151-FE4	1	female	1.05	0.87	IUGR	2	1	57628
9165	338-FE4	9	female	2.15	0.41	NORM	3	1	50687
9143	6076-FE4	1	female	0.83	1.06	IUGR	2	1	43745
9086	1773-FE4	7	castrate	1.11	1.13	IUGR	1	1	53553
9166	338-FE4	9	female	2.16	0.38	NORM	3	1	69256

9069	7162-FE4	1	castrate	1.95	0.42	NORM	3	1	23014
9033	7146-FE4	1	castrate	1.9	0.36	NORM	4	1	44073
9266	709-FE4	8	castrate	1.87	0.46	NORM	3	1	54524
9284	3459-FE4	5	castrate	1.31	0.88	IUGR	2	1	47954
9112	1684-FE4	7	female	1.76	0.38	NORM	3	1	37984
9282	709-FE4	8	female	0.97	0.88	IUGR	1	1	30306
9282	709-FE4	8	female	0.97	0.88	IUGR	4	1	42453
9165	338-FE4	9	female	2.15	0.41	NORM	2	1	63679
9106	757-FE4	8	female	1.08	0.92	IUGR	1	1	52217
9069	7162-FE4	1	castrate	1.95	0.42	NORM	4	1	34925
9059	3188-FE4	5	castrate	1.76	0.46	NORM	4	1	40414
9006	7151-FE4	1	castrate	1.03	1.12	IUGR	4	1	39642
9143	6076-FE4	1	female	0.83	1.06	IUGR	1	1	29546
9183	7202-FE4	1	castrate	1.17	1.07	IUGR	3	1	50258
9093	1773-FE4	7	female	1.08	0.90	IUGR	3	1	32798
9239	7201-FE4	1	castrate	1.95	0.43	NORM	4	1	45838
9112	1684-FE4	7	female	1.76	0.38	NORM	1	1	31543
9183	7202-FE4	1	castrate	1.17	1.07	IUGR	4	1	39263
9033	7146-FE4	1	castrate	1.9	0.35	NORM	3	1	43388
9119	5906-FE4	2	castrate	1.68	0.29	NORM	1	1	27982
9086	1773-FE4	7	castrate	1.11	1.13	IUGR	4	1	40526
9013	7151-FE4	1	female	1.05	0.87	IUGR	4	1	22027
9160	338-FE4	3	castrate	1.96	0.29	NORM	1	1	0
9183	7202-FE4	1	castrate	1.17	1.07	IUGR	1	1	27679
9266	709-FE4	8	castrate	1.87	0.46	NORM	4	1	28537
9085	1773-FE4	7	castrate	1.15	0.97	IUGR	3	1	21369
9122	5906-FE4	2	female	1.84	0.35	NORM	4	1	26619
9284	3459-FE4	5	castrate	1.31	0.87	IUGR	3	1	27701
9086	1773-FE4	7	castrate	1.11	1.13	IUGR	3	1	43488
9092	1773-FE4	7	female	1.18	0.99	IUGR	4	1	41610
9112	1684-FE4	7	female	1.76	0.38	NORM	4	1	31182
9282	709-FE4	8	female	0.97	0.88	IUGR	3	1	2545

[1] ID = identification number of the pig.

[2] Sow ID = identification number of the sow.

[3] BtW = birth body weight.

[4] BrW/LW = brain-to-liver weight ratio.

[5] IUGR = 12 pigs with the highest BrW/LW; NORM = 12 pigs with the lowest BrW/LW.

[6] T1 = blood and faeces collected before the administration of the pre-/early postweaning diet (day 16 ± 0.6); T2 = blood and faeces collected at the end of the starter period (day 63 ± 8.6); T3 = faeces collected at the beginning of the finisher period (day 119 ± 11.4); T4 = faeces collected at the end of the finisher period (day 162 ± 14.3). BrW/LW = mean BrW/LW in the IUGR and NORM groups.

Supplementary Table S3. Metabolites analysed at day 16 ± 0.6 (T1) from plasma samples of 24 piglets to compare the blood metabolome profile between piglets affected by intrauterine growth restriction (IUGR = 12) and normal piglets (NORM = 12).

Item[1]	Statistical analysis[2]
2,3-Butanediol	Not included
2-Aminobutyrate	Included
2-Hydroxybutyrate	Not included
3-Aminoisobutyrate	Included
3-Hydroxybutyrate	Not included
3-Hydroxyisobutyrate	Included
3-Methyl-2-oxovalerate	Not included
3-Methylhistidine	Not included
Acetate	Included
Acetone	Included
Alanine	Included
Alpha-ketoisovalerate	Not included
Anserine	Not included
Arabinose	Included
Arginine	Included
Ascorbate	Included
Asparagine	Included
Aspartate	Included
Beta-alanine	Included
Betaine	Included
Carnosine	Not included
Choline	Included
Citramalate	Included
Citrate, glutamine	Included
Creatine	Included
Dimethylamine	Not included
Dimethyl-sulfone	Included
Ethanol	Not included

Formate	Included
Fumarate	Included
Glucose	Included
Glycerol	Included
Glycine	Included
Glyoxylate	Included
Histidine	Not included
Hypoxanthine	Not included
Isoleucine	Included
Isopropanol	Not included
Lactate	Included
Leucine	Included
Levulinate	Not included
Lysine, 2-oxoglutarate	Included
Mannose	Included
Methanol	Not included
Methionine	Included
Methylmalonate	Not included
Myo-inositol	Included
N,N-Dimethylglycine	Included
Phenylalanine	Included
Proline	Included
Pyroglutamate	Not included
Pyruvate	Not included
Sarcosine	Included
Serine	Included
Succinate, pyruvate	Included
Theophylline	Not included
Threonine	Included
TMAO (trimethylamine N-oxide)	Included
Trans-4-Hydroxy-L-proline	Included
Tyrosine	Included
UDP-glucose	Not included

Uridine	Not included
Valine	Included

[1] Plasma metabolites analysed at day 16 ± 0.6 (T1) from 24 pigs (IUGR = 12, NORM = 12).

[2] Included = metabolites with plasma concentration in the quantitation range for each sample, included in the statistical analyses; not included = metabolites with plasma concentration not detectable in any (2-hydroxybutyrate, 3-methyl-2-oxovalerate, 3-methylhistidine, alpha-ketoisovalerate, anserine, carnosine, dimethylamine, hypoxanthine, pyroglutamate, and UDP-glucose) or most (2,3 butanediol, 3-hydroxybutyrate, ethanol, histidine, isopropanol, levulinate, methanol, methylmalonate, pyruvate, theophylline, and uridine) of the samples after centrifugation, not included in the statistical analysis.

Supplementary Table S4. Metabolites analysed at day 63 ± 8.6 (T2) from plasma samples of 24 piglets to compare the blood metabolome profile between piglets affected by intrauterine growth restriction (IUGR = 12) and normal piglets (NORM = 12).

Item[1]	Statistical analysis[2]
2,3-Butanediol	Not included
2-Aminobutyrate	Included
2-Hydroxybutyrate	Not included
3-Aminoisobutyrate	Included
3-Hydroxybutyrate	Not included
3-Hydroxyisobutyrate	Included
3-Methyl-2-oxovalerate	Not included
3-Methylhistidine	Not included
Acetate	Included
Acetone	Included
Alanine	Included
Alpha-ketoisovalerate	Not included
Anserine	Not included
Arabinose	Included
Arginine	Included
Ascorbate	Included
Asparagine	Included
Aspartate	Included
Beta-alanine	Included
Betaine	Included
Carnosine	Not included
Choline	Included
Citramalate	Included
Citrate, glutamine	Included
Creatine	Included
Dimethylamine	Not included
Dimethyl-sulfone	Included
Ethanol	Not included

Formate	Included
Fumarate	Included
Glucose	Included
Glycerol	Included
Glycine	Included
Glyoxylate	Included
Histidine	Not included
Hypoxanthine	Not included
Isoleucine	Included
Isopropanol	Not included
Lactate	Included
Leucine	Included
Levulinate	Not included
Lysine, 2-oxoglutarate	Included
Mannose	Included
Methanol	Not included
Methionine	Included
Methylmalonate	Not included
Myo-inositol	Included
N,N-Dimethylglycine	Included
Phenylalanine	Included
Proline	Included
Pyroglutamate	Not included
Pyruvate	Not included
Sarcosine	Included
Serine	Included
Succinate, pyruvate	Included
Theophylline	Not included
Threonine	Included
TMAO (trimethylamine N-oxide)	Included
Trans-4-Hydroxy-L-proline	Included
Tyrosine	Included
UDP-glucose	Not included

Uridine	Not included
Valine	Included

[1] Plasma metabolites analysed at day 63 ± 8.6 (T2) from 24 pigs (IUGR = 12, NORM = 12).

[2] Included = metabolites with plasma concentration in the quantitation range for each sample, included in the statistical analyses; not included = metabolites with plasma concentration not detectable in any (2-hydroxybutyrate, 3-hydroxybutyrate, 3-methyl-2-oxovalerate, anserine, carnosine, hypoxanthine, isopropanol, methanol, pyroglutamate, theophylline, UDP-glucose, and uridine) or most (2,3 butanediol, 3-methylhistidine, alpha-ketoisovalerate, dimethylamine, ethanol, histidine, levulinate, methylmalonate, and pyruvate) of the samples after centrifugation, not included in the statistical analysis.

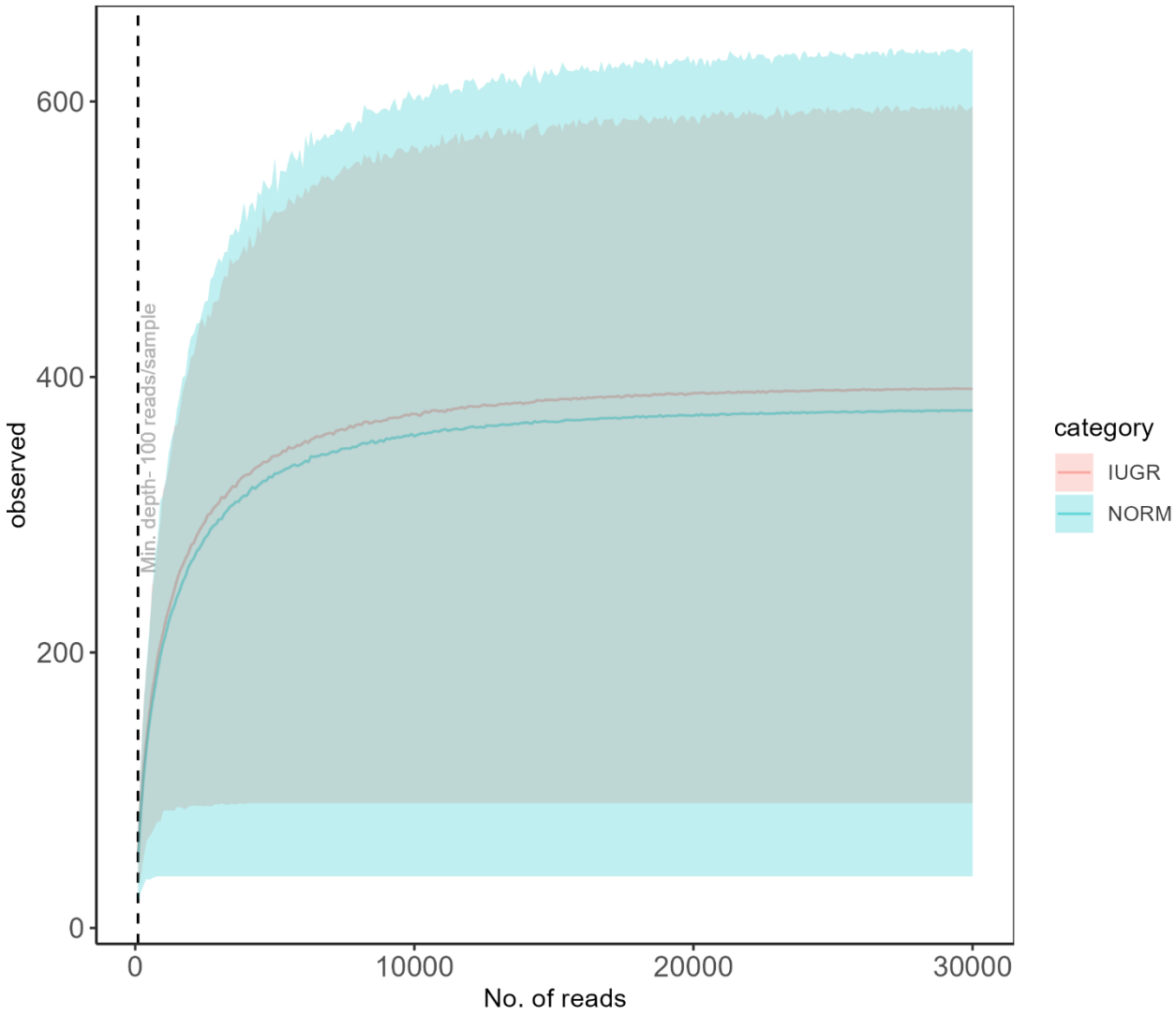

Supplementary Fig. S1. Rarefaction curve of faecal samples of piglets generated through sequencing the V3–V4 region of the 16s rRNA gene with the MiSeq platform (Illumina Inc., San Diego, CA, USA).

6. General discussion

The lack of an accurate and non-invasive method to diagnose IUGR still makes this condition a major challenge in both human and animal health (Felicioni et al., 2019), as the development of management interventions is limited by poor diagnosis. In newborn piglets, the identification of IUGR commonly relies on their head shape and/or BtW due to the practical applicability of these methods on farms and in research settings. Growth restriction in the uterus often results in SGA piglets (Radlowski et al., 2014) characterized by a distinctive head shape (Hansen et al., 2018). As a consequence, IUGR is typically defined as a piglet weighing 1.5 SD units lower than the average BtW of the litter (D'inca, 2010), weighing below 1.1 kg at birth (Ji et al., 2017), or exhibiting features such as a dolphin-like head shape, wrinkles perpendicular to the mouth, bulging eyes, and hair with no directional growth (Amdi et al., 2020; Hales et al., 2013; Chevaux et al., 2010). However, a more appropriate metric for assessing the degree of IUGR should consider the ratio between the weight of the brain and the weight of other organs (Felicioni et al., 2019), as it directly reflects the brain-sparing effect.

For the experiment described in **manuscript I**, we used CT scan to assess the weight of the brain and liver in newborn piglets and to compare the diagnoses based on BrW/LW, BtW, and head shape. Our results demonstrated that a BtW below 1.1 kg or the presence of a characteristic "IUGR" head shape did not consistently correspond to an elevated BrW/LW. These findings support our first hypothesis, suggesting that the identification of IUGR piglets only based on the head morphology or BtW might not always provide an accurate diagnosis of IUGR and can lead to a misclassification of this condition. A LBtW does not necessarily imply IUGR (Gupta, 2008), and the subjective nature of head shape classification introduces observer-dependent variations. Additionally, the head morphology of the piglets may be influenced by natural changes, unrelated to pathology, resulting in distinct characteristics

among them, similar to the diversity observed in humans. For these reasons, to accurately assess growth restriction in piglets, measurements such as BtW and head shape should be complemented by evaluating the relative brain-to-body weight ratio or BrW/LW (Chand et al., 2022; Felicioni et al., 2019).

In the experiment described in **manuscript II**, the BtW was recorded, and the weight of the brain and liver of newborn piglets were measured through either scale measurement after natural death or euthanasia or by extrapolation from CT scan images. In addition, pictures of the same piglets were taken to capture specific body measurements which were used to predict the weight of the brain, the liver, and the BrW/LW through linear regression models. These findings confirmed our second hypothesis, indicating that specific morphometric traits can function as reliable indicators for both brain and liver weights, enabling non-invasive and accurate diagnosis of IUGR.

By incorporating the distance between the ears alongside BtW, the proposed model can predict the weight of the brain with a 6% margin of error. Significantly, studies by Amdi et al. (2013) and Hansen et al. (2018) indicated that if the relative weight of the brain of a newborn piglet is below 3% of its BtW, the piglet can be diagnosed as normal. As a consequence, the weight of the brain estimated with our model can be simply compared with the piglet's BtW, enabling accurate identification of normal piglets with a minimal margin of error. This comparison also provides insights into piglets with a relative BrW above 3% of their BtW, suggesting potential growth restriction in the uterus.

Using the area of the body delimited by a square along with the BtW allows for the estimation of the LW with a 17% error rate. As the LW increases, the predictive accuracy of the model worsens, implying that beyond a specific LW, the body's structure may no longer be associated with the organ's weight, unlike what was observed for the brain. Likewise, a combination of

BtW, distance between the ears, and area of the body delimited by a square enables the estimation of BrW/LW with a 17% margin of error.

Future research should focus on the identification of innovative traits or different models to estimate the weight of the liver, with the goal of increasing prediction accuracy. Efforts should also be directed towards the development of techniques for automating the extraction of morphometric traits from images. Furthermore, these models need to be validated in larger populations and with different breeds, and their applicability tested under real-world field conditions. The developed models provide a promising tool for the early identification of IUGR piglets, and accurate diagnostic approaches will facilitate interventions to minimize the negative effects of IUGR. This might involve manipulating gut microbiota via prebiotics and probiotics, adjusting diets, administering metabolic intermediates to optimize impaired metabolic pathways, and ensuring optimal environmental conditions for the affected piglets.

Indeed, the third hypothesis of this Ph.D. thesis was that the IUGR condition has a long-lasting and negative influence on a wide range of physiological functions in pigs, ultimately resulting in impaired growth, altered gut microbiota, and blood metabolome profile.

Piglets experiencing IUGR typically exhibit slower growth rates and delayed development compared to their normal littermates (Wu et al., 2006). In the study reported in **manuscript I**, we employed the BrW/LW to evaluate the physiological traits of pigs exposed to IUGR during foetal development. Our findings revealed an inverse relationship between the BrW/LW and the ADG from birth to slaughter, with a decreasing effect of the ratio over time. Several studies reported a reduced ADG in IUGR pigs, from birth to weaning (Hansen et al., 2018), from birth to the growing phase (Lynegaard et al., 2020; Alvarenga et al., 2012), or from birth to slaughter (Santos et al., 2022; Xiong et al., 2020). Similar to our investigation, Alvarenga et al. (2012) observed that IUGR pigs, identified by LBtW, initially exhibited lower ADG from birth to the grower phase. However, by day 150, their ADG became comparable to that of normal pigs.

Indeed, it has been demonstrated that the impact of BtW on ADG diminishes over time, and BtW correlates with ADG until approximately 70 days of age (Dwyer et al., 1993; Gondret et al., 2005). This phenomenon can be partially explained by the increased fat deposition with age in both IUGR and normal pigs. The conversion of dietary fat to triglycerides in the body is less efficient (weight gain/feed intake) compared to the conversion of dietary protein into protein in muscle (Ji et al., 2017).

Nevertheless, despite the diminishing influence of BtW on ADG over time, our findings, detailed in **manuscript I**, showed an inverse relationship between the BrW/LW and the gain-to-feed ratio during the grower–finisher period. Since the overall feed intake remained unaffected by the ratio in this phase, the reduced gain-to-feed ratio could be solely attributed to the lower ADG in IUGR compared to normal pigs. Additionally, in line with other studies (Gondret et al., 2005), IUGR was consistently associated with an extended time to reach the market slaughter weight, resulting in increased management costs (Díaz et al., 2017).

These findings validate part of our third hypothesis, showing that piglets exposed to IUGR exhibit reduced growth rates, as well as decreased efficiency in nutrient utilization compared to their normal littermates throughout their postnatal life.

The existing literature regarding IUGR suggests that the diminished growth rate observed in the affected pigs is programmed during foetal development in the uterus (Foxcroft and Town, 2004). For instance, studies demonstrated that insults experienced at different stages of prenatal life can compromise the development of the GIT, resulting in lower nutrient digestion and absorption and, consequently, impaired growth during postnatal life (Santos et al., 2022; Zhang et al., 2019). IUGR-affected pigs exhibit alterations in intestinal structure, including reduced intestinal length and weight, decreased villus height, increased crypt depth, and changes in GIT transcriptomic and proteomic profiles from the lactation period (He et al., 2011; D'inca et al., 2010; Wang et al., 2008; Wang et al., 2005) up to 70 days of age (Santos et al., 2022).

Furthermore, growth restriction in the uterus influences the microbial colonization of the GIT. The findings reported in **manuscript III** demonstrated that IUGR has a significant impact on the faecal microbiota composition in pigs across different developmental stages. Our investigation revealed a strong influence of IUGR on the Beta diversity of the faecal microbiota during the lactation, starter, and grower periods. This aligns with the findings of Xiong et al. (2020), who reported significant alterations in the microbial community of the small intestine in pigs at 25, 50, and 100 kg BW due to IUGR.

In the experiment described in **manuscript III**, IUGR piglets showed lower abundances of bacteria belonging to the *Lachnospiraceae*, *Lactobacillaceae*, and *Prevotellaceae* families compared to normal pigs in the lactation, starter, and grower periods, respectively. Bacteria from the *Lachnospiraceae* and *Prevotellaceae* families are involved in fermenting dietary fiber and producing short-chain fatty acids, which contribute to intestinal health by enhancing barrier function and mitigating inflammation (Lan et al., 2023; Xiong et al., 2020). The *Lactobacillaceae* family, positively linked to nitrogen and energy digestibility in grower-finisher pigs (Le Sciellour et al., 2018), is known to enhance small intestine health through modulation of gut microbiota, stimulation of beneficial fermentation, and antagonistic activity against pathogens (Dowarah et al., 2017). The changes in abundances observed between IUGR and normal pigs partly validate our third hypothesis, showing that growth restriction in the uterus has a significant impact on the faecal microbiota composition, affecting bacteria involved in nutrient digestion and absorption, inflammatory responses, and disease susceptibility.

Another example of foetal programming in the context of IUGR regards skeletal muscle and adipose tissue development and growth. Studies demonstrated that intrauterine overcrowding compromises muscle hyperplasia in piglets, particularly in the formation of secondary myofibers (Bérard et al., 2010; Foxcroft et al., 2006). Furthermore, it has been proposed that

compromised embryonic myogenesis may prioritize adipose tissue development over skeletal muscle (Kablar et al., 2003; Ji et al., 2017). Newborn piglets experiencing growth restriction during gestation typically exhibit fewer muscle fibers when compared to their normal littermates (Bérard et al., 2010; Alvarenga et al., 2013; Felicioni et al., 2020). As a consequence, some researchers suggested that the lower number of muscle fibers at birth may not be fully compensated for by postnatal growth, resulting in diminished overall growth and increased adiposity in the affected pigs (Liu et al., 2015; Krueger et al., 2014; Gondret et al., 2006).

However, in the experiment reported in manuscript I, the BrW/LW did not affect the fat and muscle mass of the pigs at any of the growing stages, nor in the carcasses, despite a negative correlation of the ratio with the protein deposition rate and protein efficiency in the grower–finisher period. Accordingly, in the study described in manuscript III, the plasma metabolome profile was not affected by IUGR in the lactation period and the only significantly lower metabolite at the end of the starter period in IUGR compared to normal pigs was asparagine. This amino acid is not involved in lipid metabolism and is only partially involved in energy metabolism, as a precursor of aspartate, glutamine, and glutamate, which are the major contributors to the generation of ATP in mammalian enterocytes.

Our findings regarding the body composition comply with the study of Lynegaard et al. (2020), in which no differences in fat or muscle percentage were found in relation to BW at 24 days of age between the IUGR and normal pigs, as well as with studies by Gondret et al. (2005) and Nissen and Oksbjerg (2011), which observed no effect of BtW on lean and fat tissue deposition in finisher pigs. On the contrary, several studies reported higher fat deposition and a lower proportion of muscle in IUGR compared to normal pigs at different developmental stages. Increased adipocyte proliferation was previously observed in IUGR foetuses, likely to improve

the long-term ability to store fatty acids, which can undergo oxidation and provide additional energy to the slow-developing foetus. (Sarr et al., 2012; Attig et al., 2008).

This tendency towards increased fat deposition is supported by studies investigating the blood metabolome profile in piglets, which revealed increased adipogenesis and lipid oxidation and impaired energy and protein metabolism in IUGR-affected piglets compared to their normal littermates (Lin et al., 2012; He et al., 2011). Additionally, proteomic analysis by Wang et al. (2008) found lower levels of enzymes involved in protein synthesis and increased concentrations of proteasome, involved in protein breakdown, in the skeletal muscle of IUGR piglets at birth compared to their normal littermates.

Numerous studies have also reported higher fat deposition and a lower proportion of muscle in IUGR compared to normal pigs at the end of the production cycle (Liu et al., 2015; Krueger et al., 2014; Gondret et al., 2006). In the study of Gondret et al. (2006), the low weight at birth unequivocally led to higher carcass fatness. Krueger et al. (2014) demonstrated that female IUGR pigs, defined by their BtW, have a reduced capacity for muscle development and metabolize less fat than normal pigs, contributing to their higher body fat levels and accelerated fat deposition at an earlier age.

Since no significant differences in the blood metabolome profile were observed between IUGR and normal pigs during the lactation period, and the lean and fat deposition was not affected by the BrW/LW at any of the growing stages, part of our third hypothesis had to be rejected. Indeed, we expected IUGR-affected pigs to have a lower percentage of lean tissue and an increased susceptibility to fat deposition compared to their normal littermates, as well as alterations in metabolite concentrations related to lipid oxidation, energy, and amino acid metabolism, as suggested by previous research.

However, it is important to consider that in the existing literature, IUGR pigs are frequently identified based on their BtW, and there is variability in the threshold of BtW used across

different studies to distinguish between IUGR and normal pigs. Furthermore, variations in the timing of euthanizing animals for body composition analysis, either at a targeted age or a targeted BW, can influence results. Differences in muscle growth between IUGR and normal pigs may emerge depending on the choice between age-based or BW-based slaughter. If slaughtered at a specific age, IUGR pigs might not have had sufficient time to reach their full muscle growth potential, resulting in less muscle deposition compared to their normal counterparts. Conversely, if slaughtered at the same BW, IUGR pigs might have had adequate time for their muscles to develop according to their growth potential, leading to comparable body composition between IUGR and normal pigs.

Another explanation for the observed similarity in body composition between IUGR and normal pigs is that normal pigs, especially the fastest-growing ones, may not be expressing their full growth potential. Indeed, Alvarenga et al. (2013) suggested that typical commercial diets might not be formulated to meet the nutritional needs of the fastest-growing pigs preventing them from growing as much as they could. In this scenario, IUGR pigs, although less protein-efficient than their normal counterparts, may exhibit similar muscle and fat percentages as normal pigs when slaughtered at the same BW.

Finally, despite having a lower number of fibers at birth, IUGR and LBtW tend to exhibit myofiber diameters equal to or even larger than those of their heavier littermates at a constant slaughter weight (Dwyer et al., 1993; Gondret et al., 2006; Alvarenga et al., 2013; Felicioni et al., 2020). A higher rate of hypertrophy associated with fewer muscle fibers could compensate for the limited fiber count without affecting total lean and fat deposition. This may explain why no differences in muscle and fat percentages were observed in our as well as in other studies between IUGR and normal pigs (Gondret et al., 2005; Lynegaard et al., 2020; Beaulieu et al., 2010).

The presence of enlarged myofibers in skeletal muscle (Gondret et al., 2006), alongside increased oxidative stress and decreased antioxidant capacity in pigs affected by IUGR compared to their normal counterparts (Chen et al., 2023; He et al., 2023; Cheng et al., 2020), might explain why growth restriction in the uterus can also impact *postmortem* biochemical changes, leading to variations in meat quality traits.

The results reported in **manuscript I** showed that the BrW/LW was negatively correlated with the lightness of the LT muscle, in agreement with other studies (Matyba et al., 2021; Liu and He, 2014). The decreased lightness due to IUGR could potentially impact consumer perception, although it is unclear whether this altered colour is noticeable to consumers. Moreover, the BrW/LW tended to have a negative correlation with cooking loss, which, on the contrary, is often considered a favourable trait for consumers. Likewise, Liu and He (2014) reported a lower cooking loss in the meat of IUGR compared to normal pigs. However, results on the impact of IUGR on meat quality are often inconsistent. For instance, depending on the study, the pH in the LT of IUGR pigs was reported to be equal to, higher, or lower than their normal littermates (Chen et al., 2023; Matyba et al., 2021; Zhang et al., 2018 Li et al., 2015; Liu and He, 2014). In addition, in contrast with our findings, Chen et al. (2023) and Li et al. (2015) reported a lighter colour of the LT in IUGR compared to normal pigs. Variances among studies may be attributed to differences in the ages at which the animals are slaughtered. Latorre et al. (2003) and Virgili et al. (2003), demonstrated that older pigs produced redder and darker skeletal muscle compared to their younger counterparts. Indeed, in our experiment, IUGR pigs were older than their normal littermates at a constant slaughter weight and this may explain the darker colour of their meat. Considering these findings, we also had to partially reject the hypothesis that IUGR influences *postmortem* biochemical changes of the muscle, thereby deteriorating meat quality traits.

To the best of our knowledge, this research is the first to identify IUGR pigs using the BrW/LW as a diagnostic metric. Consequently, comparing our findings with studies that diagnose IUGR based on head shape or BtW is challenging, not only for meat quality but also for all the other parameters analysed. Grouping based on head shape or BtW may include a mix of IUGR and normal pigs within these categories, potentially contributing to the occasional inconsistencies observed between our results and those of other studies. These findings highlight the need for an accurate and standardized diagnostic approach to further investigate the physiological traits of IUGR-affected pigs, and to enable consistent comparisons between studies.

Using predictive models based on image analysis represents a promising approach for the early identification of IUGR piglets. In the last few years, machine learning, particularly convolutional neural networks (CNNs), has proven to be a powerful tool to detect diseases from images. These networks can quickly learn complex representations from data, enabling accurate differentiation between normal and abnormal features (Anwar et al., 2018). Nevertheless, to train these networks a large and diverse dataset is needed, and this represents a big challenge when the data available is limited, as in our study. For this reason, in this Ph.D. thesis, despite working initially with CNNs, we decided to rely on simpler predictive models based on multiple linear regressions and to report only the outcomes of these models (**manuscript II**). Linear regression models are easier to develop and require less data compared to machine-learning approaches. The models utilizing BtW and morphometric traits (developed and detailed in **manuscript II**) appear to offer the most effective means of evaluating IUGR both in farm and research contexts. The approach is non-invasive, cost-effective, and relatively easy to apply, even within farm settings. While the methodology still needs to be improved in terms of error rates, especially regarding liver weight prediction, integrating this approach with the identification of IUGR based on head morphology and BtW could substantially enhance prediction accuracy and provide a reliable diagnosis of IUGR.

However, considering the rapid evolution of artificial intelligence it might be also possible in the coming years to apply CNNs even in situations where the data is limited. In the context of IUGR, this could further increase diagnostic accuracy. In addition, further research on the microbiota composition of IUGR-affected pigs may reveal specific taxa, consistent across various studies, that could serve as biomarkers for diagnosing this condition.

Regardless of the methodology employed, an increased diagnostic accuracy can foster the development of effective interventions. The economic and environmental impact of treatments for IUGR pigs cannot be underestimated. Indeed, a rising global population is increasing the demand for meat products (FAOSTAT, 2023). This growing demand is coupled with the commitment to reduce livestock production's environmental footprint and with rising concerns about the welfare of livestock animals. In light of these considerations, a shift towards more sustainable and ethical production is essential, even if it is often difficult to find a balance between these objectives.

In this context, one might question the trend towards increased prolificacy. The increase in litter size, driven by genetic selection for prolificacy, led to an increase in the percentage of piglets weighing below 1 kg at birth, which have less than a 75% chance of surviving to weaning (Quesnel et al., 2008), and an increase in the number of piglets exposed to IUGR. IUGR-affected piglets are more susceptible to diseases and have a higher mortality rate. In addition, in this Ph.D. thesis, we demonstrated that IUGR pigs have stunted growth, lower efficiency in utilizing feed and, particularly, protein, and require more time to reach the desired slaughter weight. Being less efficient, IUGR pigs may require more feed to achieve the same growth as their normal counterparts, contributing to higher resource usage, including land, water, and energy. Moreover, inefficient protein utilization by IUGR pigs may result in higher nitrogen content in their manure, which can lead to environmental issues, including water pollution and emissions of ammonia and nitrous oxide (Meade et al., 2011). Therefore,

considering the absence of an effective treatment to mitigate IUGR's negative effects, revaluating the strategy of increasing litter size becomes essential to ensure sustainable pig production systems.

7. Conclusion

The current challenge of accurately diagnosing IUGR limits the development of effective treatments. While traditional methods like BtW and head shape have been employed in several studies for IUGR identification in newborn piglets, our research used a more accurate metric, the BrW/LW, to characterize physiological traits in pigs affected by this condition.

Our findings demonstrated that relying solely on head shape or BtW for IUGR diagnosis might lead to misclassification, as these features are not consistently associated with an increased BrW/LW. Instead, our study showed the potential of alternative morphometric traits, such as the distance between the ears and the area of the body delimited by a square, in predicting the BrW/LW and diagnosing IUGR.

From a physiological perspective, our research confirmed the negative and lasting consequences of IUGR on a wide spectrum of postnatal traits, including diminished growth rates, reduced protein efficiency, and impacts on faecal microbiota composition.

The development of predictive models based on morphometric traits and the physiological characterisation of the affected pigs may enable the development of effective treatments. Moreover, an accurate diagnosis could facilitate the genetic selection of the sows which produce fewer IUGR piglets.

Successfully treating IUGR-affected pigs holds the potential to increase the overall efficiency and sustainability of pig production systems. In the absence of effective treatments for IUGR, the strategy of increasing litter size to enhance productivity should be revaluated. Balanced approaches that consider both economic demands and sustainability are needed.

References

Adebami, O. J., & Owa, J. A. (2008). “Comparison between CANSCORE and other anthropometric indicators in fetal malnutrition.” The Indian Journal of Pediatrics, 75, 439-442.

Alexandre-Gouabau, M.-C. F., E. Bailly, T. L. Moyon, I. C. Grit, B. Coupé, G. Le Drean, H. J. Rogniaux and P. Parnet (2012). "Postnatal growth velocity modulates alterations of proteins involved in metabolism and neuronal plasticity in neonatal hypothalamus in rats born with intrauterine growth restriction." The Journal of Nutritional Biochemistry 23(2): 140-152.

Alvarenga, A. L. N., Chiarini-Garcia, H., Cardeal, P. C., Moreira, L. P., Foxcroft, G. R., Fontes, D. O., and Almeida, F. R. C. L. (2013). “Intra-uterine growth retardation affects birthweight and postnatal development in pigs, impairing muscle accretion, duodenal mucosa morphology and carcass traits.” Reproduction, Fertility and Development. 25(2), 387-395.

Amat, S., H. Lantz, P. M. Munyaka and B. P. Willing (2020). "Prevotella in pigs: the positive and negative associations with production and health." Microorganisms 8(10): 1584.

Amdi, C. (2012). The effect of varying feeding levels for thin and fat sows during gestation on muscle and adipose tissue of progeny. PhD thesis, Royal Veterinary College, University of London, London, UK.

Amdi, C., J. C. Lynegaard, T. Thymann and A. R. Williams (2020). "Intrauterine growth restriction in piglets alters blood cell counts and impairs cytokine responses in peripheral mononuclear cells 24 days post-partum." Scientific Reports 10(1): 4683.

Amdi, C., U. Krogh, C. Flummer, N. Oksbjerg, C. Hansen and P. Theil (2013). "Intrauterine growth restricted piglets defined by their head shape ingest insufficient amounts of colostrum." Journal of Animal Science 91(12): 5605-5613.

Anwar, S. M., M. Majid, A. Qayyum, M. Awais, M. Alnowami and M. K. Khan (2018). "Medical image analysis using convolutional neural networks: a review." Journal of Medical Systems 42: 1-13.

Ashworth, C. J., M. O. Nwagwu and H. J. McArdle (2013). "Genotype and fetal size affect maternal–fetal amino acid status and fetal endocrinology in Large White× Landrace and Meishan pigs." Reproduction, Fertility and Development 25(2): 439-445.

Attig, L., J. Djiane, A. Gertler, O. Rampin, T. Larcher, S. Boukthir, P. Anton, J.-Y. Madec, I. Gourdou and L. Abdennebi-Najar (2008). "Study of hypothalamic leptin receptor expression in low-birth-weight piglets and effects of leptin supplementation on neonatal growth and development." American Journal of Physiology-Endocrinology and Metabolism 295(5): E1117-E1125.

Austin, P. C. and E. W. Steyerberg (2015). "The number of subjects per variable required in linear regression analyses." Journal of Clinical Epidemiology 68(6): 627-636.

Bahado-Singh, R. O., A. Yilmaz, H. Bisgin, O. Turkoglu, P. Kumar, E. Sherman, A. Mrazik, A. Odibo and S. F. Graham (2019). "Artificial intelligence and the analysis of multi-platform metabolomics data for the detection of intrauterine growth restriction." PLoS One 14(4): e0214121.

Bamberg, C., & Kalache, K. D. (2004). Prenatal diagnosis of fetal growth restriction. In Seminars in Fetal and Neonatal Medicine (Vol. 9, No. 5, pp. 387-394). WB Saunders.

Bauer, R., B. Walter, A. Hoppe, E. Gaser, V. Lampe, E. Kauf and U. Zwiener (1998). "Body weight distribution and organ size in newborn swine (sus scrofa domestica) — A study describing an animal model for asymmetrical intrauterine growth retardation." Experimental and Toxicologic Pathology 50(1): 59-65.

Bauer, R., B. Walter, P. Brust, F. Füchtner and U. Zwiener (2003). "Impact of asymmetric intrauterine growth restriction on organ function in newborn piglets." European Journal of Obstetrics & Gynecology and Reproductive Biology 110: S40-S49.

Baxter, E., S. Jarvis, R. D'eath, D. Ross, S. Robson, M. Farish, I. Nevison, A. Lawrence and S. Edwards (2008). "Investigating the behavioural and physiological indicators of neonatal survival in pigs." Theriogenology 69(6): 773-783.

Bérard, J., Pardo, C. E., Béthaz, S., Kreuzer, M., & Bee, G. (2010). "Intrauterine crowding decreases average birth weight and affects muscle fiber hyperplasia in piglets." Journal of Animal Science, 88(10), 3242-3250.

Bernstein, P. S., & Divon, M. Y. (1997). "Etiologies of fetal growth restriction." Clinical Obstetrics and Gynecology, 40(4), 723-729.

Brugaletta, G., A. De Cesare, L. Laghi, G. Manfreda, M. Zampiga, C. Oliveri, E. Pérez-Calvo, G. Litta, S. Lolli and F. Sirri (2022). "A multi-omics approach to elucidate the mechanisms of action of a dietary muramidase administered to broiler chickens." Scientific Reports 12(1): 5559.

Calderón Díaz, J. A., A. Diana, L. A. Boyle, F. C. Leonard, M. McElroy, S. McGettrick, J. Moriarty and E. García Manzanilla (2017). "Delaying pigs from the normal production flow is associated with health problems and poorer performance." Porcine Health Management 3: 1-6.

Callahan, B. J., P. J. McMurdie, M. J. Rosen, A. W. Han, A. J. A. Johnson and S. P. Holmes (2016). "DADA2: High-resolution sample inference from Illumina amplicon data." Nature Methods 13(7): 581-583.

Campbell, S., & Thoms, A. (1977). "Ultrasound measurement of the fetal head to abdomen circumference ratio in the assessment of growth retardation." BJOG: An International Journal of Obstetrics & Gynaecology, 84(3), 165-174.

Campos, P. H. R. F., B. A. N. Silva, J. L. Donzele, R. F. M. Oliveira and E. F. Knol (2012). "Effects of sow nutrition during gestation on within-litter birth weight variation: a review." Animal 6(5): 797-806.

Cao, Y., Q. Dong, D. Wang, P. Zhang, Y. Liu and C. Niu (2022). "microbiomeMarker: an R/Bioconductor package for microbiome marker identification and visualization." Bioinformatics 38(16): 4027-4029.

Cetin, I., & Alvino, G. (2009). “Intrauterine growth restriction: implications for placental metabolism and transport.” A review. Placenta, 30, 77-82.

Chakraborty, S., K. Karthik and S. Banik (2021). "Graph Synthesis for Pig Breed Classification From Muzzle Images." IEEE Access 9: 127240-127258.

Chand, K. K., K. Pannek, P. B. Colditz and J. A. Wixey (2022). "Brain outcomes in runted piglets: a translational model of fetal growth restriction." Developmental Neuroscience 44(4-5): 194-204.

Chao de la Barca, J. M., F. Chabrun, T. Lefebvre, O. Roche, N. Huetz, O. Blanchet, G. Legendre, G. Simard, P. Reynier and G. Gascoin (2022). "A Metabolomic Profiling of Intra-Uterine Growth Restriction in Placenta and Cord Blood Points to an Impairment of Lipid and Energetic Metabolism." Biomedicines 10(6): 1411.

Chen, S., Y. Liu, X. Wang, H. Wang, S. Li, H. Shi, H. Zhu, J. Zhang, D. Pi and C.-A. A. Hu (2016). "Asparagine improves intestinal integrity, inhibits TLR4 and NOD signaling, and differently regulates p38 and ERK1/2 signaling in weanling piglets after LPS challenge." Innate Immunity 22(8): 577-587.

Chen, S., Zhou, B., Zhang, J., Liu, H., Ma, L., Wang, T., & Wang, C. (2023). “Effects of Dietary Nano-Zinc Oxide Supplementation on Meat Quality, Antioxidant Capacity and Cecal Microbiota of Intrauterine Growth Retardation Finishing Pigs.” Foods, 12(9), 1885.

Cheng, K., C. Yu, Z. Li, S. Li, E. Yan, Z. Song, H. Zhang, L. Zhang and T. Wang (2020). "Resveratrol improves meat quality, muscular antioxidant capacity, lipid metabolism and fiber type composition of intrauterine growth retarded pigs." Meat Science 170: 108237.

Chevaux, E., Sacy, A., Le Treut, Y., and Martineau, G. (2010). "Intrauterine growth retardation (IUGR): Morphological and behavioural description." Proceedings of the 21st IPVS Congress, 18-21 July 2010, Vancouver, Canada, 18-21.

Cisneros, F., Ellis, M., Baker, D. H., Easter, R. A., & McKeith, F. K. (1996). The influence of short-term feeding of amino acid-deficient diets and high dietary leucine levels on the intramuscular fat content of pig muscle. Animal Science, 63(3), 517-522.

Cohen, E., Baerts, W., and van Bel, F. (2015). “Brain-sparing in intrauterine growth restriction: Considerations for the neonatologist.” Neonatology. 108(4), 269-276

Cortes-Araya, Y., C. Stenhouse, M. Salavati, S. O. Dan-Jumbo, W. Ho, C. J. Ashworth, E. Clark, C. L. Esteves and F. X. Donadeu (2022). "KLB dysregulation mediates disrupted muscle development in intrauterine growth restriction." The Journal of Physiology 600(7): 1771-1790.

De Bie, H. M. A., Oostrom, K. J., & Delemarre-Van De Waal, H. A. (2010). “Brain development, intelligence and cognitive outcome in children born small for gestational age.” Hormone Research in Paediatrics, 73(1), 6-14.

De Onis, M. (2020). “Intrauterine growth retardation. Health and Nutrition Emerging and Reemerging Issues in Devel-oping Countries.” Vision Focus 5.

De Onis, M., Blössner, M., & Villar, J. O. S. É. (1998). “Levels and patterns of intrauterine growth retardation in developing countries.” European Journal of Clinical Nutrition, 52, S5-15.

De Vos, M., Che, L., Huygelen, V., Willemen, S., Michiels, J., Van Cruchten, S., & Van Ginneken, C. (2014). “Nutritional interventions to prevent and rear low-birthweight piglets.” Journal of Animal Physiology and Animal Nutrition, 98(4), 609-619.

Den Besten, G., K. Van Eunen, A. K. Groen, K. Venema, D.-J. Reijngoud and B. M. Bakker (2013). "The role of short-chain fatty acids in the interplay between diet, gut microbiota, and host energy metabolism." Journal of Lipid Research 54(9): 2325-2340.

Dickerson, J., A. Merat and E. Widdowson (1971). "Intra-uterine growth retardation in the pig. 3. The chemical structure of the brain." Biology of the Neonate 19(4/6): 354-362.

Dieterle, F., A. Ross, G. Schlotterbeck and H. Senn (2006). "Probabilistic quotient normalization as robust method to account for dilution of complex biological mixtures. Application in 1H NMR metabonomics." Analytical Chemistry 78(13): 4281-4290.

D'Inca, R., Che, L., Thymann, T., Sangild, P. T., & Le Huërou-Luron, I. (2010). “Intrauterine growth restriction reduces intestinal structure and modifies the response to colostrum in preterm and term piglets.” Livestock Science, 133(1-3), 20-22.

Dixon, P. (2003). "VEGAN, a package of R functions for community ecology." Journal of Vegetation Science 14(6): 927-930.

Douglas, S. L., Edwards, S. A., & Kyriazakis, I. (2016). “Are all piglets born lightweight alike? Morphological measurements as predictors of postnatal performance.” Journal of Animal Science, 94(8), 3510-3518.

Dowarah, R., A. Verma and N. Agarwal (2017). "The use of Lactobacillus as an alternative of antibiotic growth promoters in pigs: A review." Animal Nutrition 3(1): 1-6.

Dullemen, M. v. (2011). "Doppler ultrasonography in the middle cerebral artery and the umbilical artery of piglets: an exploratory study."

Dwyer, C. M., Fletcher, J. M., & Stickland, N. C. (1993). “Muscle cellularity and postnatal growth in the pig.” Journal of Animal Science, 71(12), 3339-3343.

Edwards, S. and E. Baxter (2015). Piglet mortality: causes and prevention. The gestating and lactating sow, Wageningen Academic Publishers: 649-653.

Escobar, J., Frank, J. W., Suryawan, A., Nguyen, H. V., Kimball, S. R., Jefferson, L. S., & Davis, T. A. (2005). “Physiological rise in plasma leucine stimulates muscle protein synthesis in neonatal pigs by enhancing translation initiation factor activation.” American Journal of Physiology-Endocrinology and Metabolism, 288(5), E914-E921.

FAOSTAT, 2023. Food and agriculture data. http://www.fao.org/faostat/en/

Farmer, C. and S. Edwards (2022). "Improving the performance of neonatal piglets." Animal 16: 100350.

Favretto, D., E. Cosmi, E. Ragazzi, S. Visentin, M. Tucci, P. Fais, G. Cecchetto, V. Zanardo, G. Viel and S. D. Ferrara (2012). "Cord blood metabolomic profiling in intrauterine growth restriction." Analytical and Bioanalytical Chemistry 402: 1109-1121.

Feldpausch, J. A., J. Jourquin, J. R. Bergstrom, J. L. Bargen, C. D. Bokenkroger, D. L. Davis, J. M. Gonzalez, J. L. Nelssen, C. L. Puls and W. E. Trout (2019). "Birth weight threshold for identifying piglets at risk for preweaning mortality." Translational Animal Science 3(2): 633-640.

Felicioni, F., A. D. Pereira, A. L. Caldeira-Brant, T. G. Santos, T. M. Paula, D. Magnabosco, F. P. Bortolozzo, S. Tsoi, M. K. Dyck and W. Dixon (2020). "Postnatal development of skeletal muscle in pigs with intrauterine growth restriction: morphofunctional phenotype and molecular mechanisms." Journal of Anatomy 236(5): 840-853.

Felicioni, F., T. G. Santos, T. d. M. D. e Paula, H. Chiarini-Garcia and F. R. C. L. de Almeida (2019). "Intrauterine growth restriction: screening and diagnosis using animal models." Animal Reproduction 16(1): 66.

Fernstrom, J. D. (2013). "Large neutral amino acids: dietary effects on brain neurochemistry and function." Amino Acids 45: 419-430.

Foxcroft, G. R. and S. C. Town (2004). "Prenatal programming of postnatal performance-the unseen cause of variance." Advances in Pork Production 15: 269-279.

Foxcroft, G., W. Dixon, S. Novak, C. Putman, S. Town and M. Vinsky (2006). "The biological basis for prenatal programming of postnatal performance in pigs." Journal of Animal Science 84(suppl_13): E105-E112.

Gatford, K. L., Simmons, R. A., De Blasio, M. J., Robinson, J. S., and Owens, J. A. (2010). “Placental programming of postnatal diabetes and impaired insulin action after IUGR.” Placenta. 31, S60-S65.

Gaukroger, C. H., C. J. Stewart, S. A. Edwards, J. Walshaw, I. P. Adams and I. Kyriazakis (2020). "Changes in faecal microbiota profiles associated with performance and birthweight of piglets." Frontiers in Microbiology 11: 917.

Gilchrist, C., Cumberland, A., Walker, D., & Tolcos, M. (2018). “Intrauterine growth restriction and development of the hippocampus: implications for learning and memory in children and adolescents.” The Lancet Child & Adolescent Health, 2(10), 755-764.

Gondret, F., L. Lefaucheur, H. Juin, I. Louveau and B. Lebret (2006). "Low birth weight is associated with enlarged muscle fiber area and impaired meat tenderness of the longissimus muscle in pigs." Journal of Animal Science 84(1): 93-103.

Gondret, F., L. Lefaucheur, I. Louveau, B. Lebret, X. Pichodo and Y. Le Cozler (2005). "Influence of piglet birth weight on postnatal growth performance, tissue lipogenic capacity and muscle histological traits at market weight." Livestock Production Science 93(2): 137-146.

Gondret, F., M.-H. Perruchot, S. Tacher, J. Bérard and G. Bee (2011). "Differential gene expressions in subcutaneous adipose tissue pointed to a delayed adipocytic differentiation in small pig fetuses compared to their heavier siblings." Differentiation 81(4): 253-260.

Gupta, M. (2008). “Intrauterine growth restriction. In Primary care of the premature infant” (ed. Brodsky, D., Ouellette, M. A.). W.B. Saunders, Philadelphia, US, pp. 77–83.

Gutaj, P., & Wender-Ozegowska, E. (2016). “Diagnosis and management of IUGR in pregnancy complicated by type 1 diabetes mellitus.” Current Diabetes Reports, 16, 1-9.

Hales, J., V. Moustsen, M. Nielsen and C. Hansen (2013). "Individual physical characteristics of neonatal piglets affect preweaning survival of piglets born in a noncrated system." Journal of Animal Science 91(10): 4991-5003.

Handel, S. E., & Stickland, N. C. (1987). “Muscle cellularity and birth weight.” Animal Science, 44(2), 311-317.

Hansen, C. F., Hales, J., Amdi, C., & Moustsen, V. A. (2018). “Intrauterine growth-restricted piglets defined by their head shape have impaired survival and growth during the suckling period.” Animal Production Science, 59(6), 1056-1062.

Hawe, S. J., Scollan, N., Gordon, A., & Magowan, E. (2020). “What is the current significance of low birthweight pigs on commercial farms in Northern Ireland in terms of impaired growth and mortality?.” Translational Animal Science, 4(3), txaa147.

Hawkins, D. M. (2004). "The problem of overfitting." Journal of Chemical Information & Computer Sciences 44(1): 1-12.

He, Q., P. Ren, X. Kong, W. Xu, H. Tang, Y. Yin and Y. Wang (2011). "Intrauterine growth restriction alters the metabonome of the serum and jejunum in piglets." Molecular BioSystems 7(7): 2147-2155.

He, Y., Liu, Y., Guan, P., He, L., & Zhou, X. (2023). “Serine administration improves selenium status, oxidative stress, and mitochondrial function in longissimus dorsi muscle of piglets with intrauterine growth retardation.” Biological Trace Element Research, 201(4), 1740-1747.

Hennington, B. S., and Alexander, B. T. (2013). “Linking intrauterine growth restriction and blood pressure: Insight into the human origins of cardiovascular disease.” Circulation. 128(20), 2179-2180.

Herpin, P., Damon, M., & Le Dividich, J. (2002). “Development of thermoregulation and neonatal survival in pigs.” Livestock Production Science, 78(1), 25-45.

Huang, S., N. Li, C. Liu, T. Li, W. Wang, L. Jiang, Z. Li, D. Han, S. Tao and J. Wang (2019). "Characteristics of the gut microbiota colonization, inflammatory profile, and plasma metabolome in intrauterine growth restricted piglets during the first 12 hours after birth." Journal of Microbiology 57: 748-758.

Huting, A., P. Sakkas, I. Wellock, K. Almond and I. Kyriazakis (2018). "Once small always small? To what extent morphometric characteristics and postweaning starter regime affect pig lifetime growth performance." Porcine Health Management 4(1): 1-14.

Jahan-Mihan, A., Rodriguez, J., Christie, C., Sadeghi, M., and Zerbe, T. (2015). “The role of maternal dietary proteins in development of metabolic syndrome in offspring.” Nutrients. 7(11), 9185-9217.

Jenkins, D. G. and P. F. Quintana-Ascencio (2020). "A solution to minimum sample size for regressions." PloS One 15(2): e0229345.

Ji, X., Q. Shen, P. Wu, H. Chen, S. Wang, D. Chen, Y. Yu, Z. Guo, J. Wang and G. Tang (2022). "Pituitary-Gland-Based Genes Participates in Intrauterine Growth Restriction in Piglets." Genes 13(11): 2141.

Ji, Y., Z. Wu, Z. Dai, X. Wang, J. Li, B. Wang and G. Wu (2017). "Fetal and neonatal programming of postnatal growth and feed efficiency in swine." Journal of Animal Science and Biotechnology 8(1): 1-15.

Kablar, B., K. Krastel, S. Tajbakhsh and M. A. Rudnicki (2003). "Myf5 and MyoD activation define independent myogenic compartments during embryonic development." Developmental Biology 258(2): 307-318.

Kaneko, J. J., Harvey, J. W., & Bruss, M. L. (Eds.). (2008). “Clinical biochemistry of domestic animals.” Academic Press.

Kasper, C., P. Schlegel, I. Ruiz-Ascacibar, P. Stoll and G. Bee (2021). "Accuracy of predicting chemical body composition of growing pigs using dual-energy X-ray absorptiometry." Animal 15(8): 100307.

Kemp, B., Da Silva, C. L., & Soede, N. M. (2018). “Recent advances in pig reproduction: Focus on impact of genetic selection for female fertility.” Reproduction in Domestic Animals, 53(S2), 28-36.

Kielland, C., Wisløff, H., Valheim, M., Fauske, A. K., Reksen, O., & Framstad, T. (2018). “Preweaning mortality in piglets in loose-housed herds: etiology and prevalence.” Animal, 12(9), 1950-1957.

Kim, H. B., Borewicz, K., White, B. A., Singer, R. S., Sreevatsan, S., Tu, Z. J., & Isaacson, R. E. (2011). “Longitudinal investigation of the age-related bacterial diversity in the feces of commercial pigs.” Veterinary Microbiology, 153(1-2), 124-133.

Kneen, M. and H. Annegarn (1996). “Algorithm for fitting XRF, SEM and PIXE X-ray spectra backgrounds." Nuclear Instruments and Methods in Physics Research Section B: Beam Interactions with Materials and Atoms 109: 209-213.

Krueger, R., M. Derno, S. Goers, B. U. Metzler-Zebeli, G. Nuernberg, K. Martens, R. Pfuhl, C. Nebendahl, A. Zeyner and H. M. Hammon (2014). "Higher body fatness in intrauterine growth retarded juvenile pigs is associated with lower fat and higher carbohydrate oxidation during ad libitum and restricted feeding." European Journal of Nutrition 53: 583-597.

Lan, Q., Y. Lian, P. Peng, L. Yang, H. Zhao, P. Huang, H. Ma, H. Wei, Y. Yin and M. Liu (2023). "Association of gut microbiota and SCFAs with finishing weight of Diannan small ear pigs." Frontiers in Microbiology 14: 1117965.

Latorre, M., P. Medel, A. Fuentetaja, R. Lázaro and G. Mateos (2003). "Effect of gender, terminal sire line and age at slaughter on performance, carcass characteristics and meat quality of heavy pigs." Animal Science 77(1): 33-45.

Le Sciellour, M., E. Labussière, O. Zemb and D. Renaudeau (2018). "Effect of dietary fiber content on nutrient digestibility and fecal microbiota composition in growing-finishing pigs." PLoS One 13(10): e0206159.

Lemke, A. J., Brinkmann, M. J., Schott, T., Niehues, S. M., Settmacher, U., Neuhaus, P., & Felix, R. (2006). Living donor right liver lobes: preoperative CT volumetric measurement for calculation of intraoperative weight and volume. Radiology, 240(3), 736-742.

Li, B., W. Li, H. Ahmad, L. Zhang, C. Wang and T. Wang (2015). "Effects of choline on meat quality and intramuscular fat in intrauterine growth retardation pigs." PLoS One 10(6): e0129109.

Li, N., S. Huang, L. Jiang, W. Wang, T. Li, B. Zuo, Z. Li and J. Wang (2018). "Differences in the gut microbiota establishment and metabolome characteristics between low-and normal-birth-weight piglets during early-life." Frontiers in Microbiology 9: 1798.

Li, T., Huang, S., Lei, L., Tao, S., Xiong, Y., Wu, G., Hu, J., Yuan, X., Zhao, S., Zuo, B., Yang, H., Xiao, Y., Lin G., and Wang J. (2021). “Intrauterine growth restriction alters nutrient metabolism in the intestine of porcine offspring.” Journal of Animal Science and Biotechnology 12, 1-12.

Liland, K. H., T. Almøy and B.-H. Mevik (2010). "Optimal choice of baseline correction for multivariate calibration of spectra." Applied Spectroscopy 64(9): 1007-1016.

Lin, G., Liu, C., Feng, C., Fan, Z., Dai, Z., Lai, C., Li, Z., Wu, G. and Wang, J. (2012). “Metabolomic analysis reveals differences in umbilical vein plasma metabolites between normal and growth-restricted fetal pigs during late gestation.” The Journal of Nutrition, 142(6), 990-998.

Liu, J. B., & He, J. (2014). "Effects of birth weight and postnatal high-fat diet on growth performance, carcass and meat quality in pigs." JAPS: Journal of Animal & Plant Sciences, 24(6).

Liu, J. B., Yang, Y. K., & He, J. (2015). "Intrauterine growth retardation increases lipid deposition in adipose tissue of pigs in response to high-fat/high energy diets." Livestock Science, 177, 95-102.

Liu, J., X.-X. Chen, X.-W. Li, W. Fu and W.-Q. Zhang (2016). "Metabolomic research on newborn infants with intrauterine growth restriction." Medicine 95(17).

Lodygensky, G. A., Seghier, M. L., Warfield, S. K., Tolsa, C. B., Sizonenko, S., Lazeyras, F., & Hüppi, P. S. (2008). "Intrauterine growth restriction affects the preterm infant's hippocampus." Pediatric Research, 63(4), 438-443.

Louveau, I., M. Dauncey and J. Le Dividich (2000). "Regulation of development by nutrition and by the somatotrophic and thyroid axes in the neonatal pig." Livestock Production Science 66(2): 121-131.

Lynegaard, J. C., Hales, J., Nielsen, M. N., Hansen, C. F., and Amdi, C. (2020a). "The stomach capacity is reduced in intrauterine growth restricted piglets compared to normal piglets." Animals. 10(8), 1291.

Lynegaard, J. C., Hansen, C. F., Kristensen, A. R., and Amdi, C. (2020b). "Body composition and organ development of intra-uterine growth restricted pigs at weaning." Animal. 14(2), 322-329.

Mallard, E. C., Rehn, A., Rees, S., Tolcos, M., & Copolov, D. (1999). "Ventriculomegaly and reduced hippocampal volume following intrauterine growth-restriction: implications for the aetiology of schizophrenia." Schizophrenia Research, 40(1), 11-21.

Martin, R. J., Hausman, G. J., & Hausman, D. B. (1998). "Regulation of adipose cell development in utero." Proceedings of the Society for Experimental Biology and Medicine, 219(3), 200-210.

Matheson, S. M., Walling, G. A., and Edwards, S. A. (2018). "Genetic selection against intrauterine growth retardation in piglets: A problem at the piglet level with a solution at the sow level." Genetics Selection Evolution. 50(1), 1-11.

Matyba, P., T. Florowski, K. Dasiewicz, K. Ferenc, J. Olszewski, M. Trela, G. Galemba, M. Słowiński, M. Sady and D. Domańska (2021). "Performance and meat quality of intrauterine growth restricted pigs." Animals 11(2): 254.

Maynard, C. L., Elson, C. O., Hatton, R. D., & Weaver, C. T. (2012). "Reciprocal interactions of the intestinal microbiota and immune system." Nature, 489(7415), 231-241.

McMurdie, P. J. and S. Holmes (2013). "phyloseq: an R package for reproducible interactive analysis and graphics of microbiome census data." PLoS One 8(4): e61217.

Meade, G., K. Pierce, J. O'Doherty, C. Mueller, G. Lanigan and T. Mc Cabe (2011). "Ammonia and nitrous oxide emissions following land application of high and low nitrogen pig manures to winter wheat at three growth stages." Agriculture, Ecosystems & Environment 140(1-2): 208-217.

Miller, S. L., P. S. Huppi and C. Mallard (2016). "The consequences of fetal growth restriction on brain structure and neurodevelopmental outcome." The Journal of Physiology 594(4): 807-823.

Moeser, A. J., Pohl, C. S., & Rajput, M. (2017). "Weaning stress and gastrointestinal barrier development: Implications for lifelong gut health in pigs." Animal Nutrition, 3(4), 313-321.

Muns, R., M. Nuntapaitoon and P. Tummaruk (2016). "Non-infectious causes of preweaning mortality in piglets." Livestock Science 184: 46-57.

Münzberg, H., Gettys, T.W. (2013). Evolving Concepts of Leptin. Encyclopedia of Biological Chemistry (Second Edition), Academic Press, 256-261.

Nissen, P. and N. Oksbjerg (2011). "Birth weight and postnatal dietary protein level affect performance, muscle metabolism and meat quality in pigs." Animal 5(9): 1382-1389.

Nowland, T., R. Kirkwood and J. Pluske (2022). "Can early-life establishment of the piglet intestinal microbiota influence production outcomes?" Animal 16: 100368.

Obermier, D., Eickhoff, M., Mote, B. E., Uitermarkt, A., Frobose, H., & Borg, B. (2021). 57 The Impact of Functional Teat Number on Piglet Survival and Sow Efficiency. Journal of Animal Science, 99(Suppl 1), 149.

Oliviero, C. (2022). Offspring of hyper prolific sows: Immunity, birthweight, and heterogeneous litters. Molecular Reproduction and Development.

Oliviero, C., Junnikkala, S., & Peltoniemi, O. (2019). “The challenge of large litters on the immune system of the sow and the piglets.” Reproduction in Domestic Animals, 54, 12-21.

Osuchukwu, O. O., & Reed, D. J. (2020). Small for gestational age.

Pedersen, L. J., Berg, P., Jørgensen, G., & Andersen, I. L. (2011). Neonatal piglet traits of importance for survival in crates and indoor pens. Journal of Animal Science, 89(4), 1207-1218.

Pedroso, A. P., A. P. Souza, A. P. Dornellas, L. M. Oyama, C. M. Nascimento, G. M. Santos, J. C. Rosa, R. P. Bertolla, J. Klawitter and U. Christians (2017). "Intrauterine growth restriction programs the hypothalamus of adult male rats: integrated analysis of proteomic and metabolomic data." Journal of Proteome Research 16(4): 1515-1525.

Père, M. C., & Etienne, M. (2000). Uterine blood flow in sows: effects of pregnancy stage and litter size. Reproduction Nutrition Development, 40(4), 369-382.

Pereira-da-Silva, L., Virella, D., & Fusch, C. (2019). Nutritional assessment in preterm infants: a practical approach in the NICU. Nutrients, 11(9), 1999.

Pieper, R., C. V. Tudela, M. Taciak, J. Bindelle, J. F. Pérez and J. Zentek (2016). "Health relevance of intestinal protein fermentation in young pigs." Animal Health Research Reviews 17(2): 137-147.

Pluske, J. R., Turpin, D. L., & Kim, J. C. (2018). “Gastrointestinal tract (gut) health in the young pig.” Animal Nutrition, 4(2), 187-196.

Priante, E., Verlato, G., Giordano, G., Stocchero, M., Visentin, S., Mardegan, V., & Baraldi, E. (2019). Intrauterine growth restriction: new insight from the metabolomic approach. Metabolites, 9(11), 267.

Quast, C., E. Pruesse, P. Yilmaz, J. Gerken, T. Schweer, P. Yarza, J. Peplies and F. O. Glöckner (2012). "The SILVA ribosomal RNA gene database project: improved data processing and web-based tools." Nucleic Acids Research 41(D1): D590-D596.

Quesnel, H., Farmer, C., & Devillers, N. (2012). Colostrum intake: Influence on piglet performance and factors of variation. Livestock Science, 146(2-3), 105-114.

Quesnel, H., L. Brossard, A. Valancogne and N. Quiniou (2008). "Influence of some sow characteristics on within-litter variation of piglet birth weight." Animal 2(12): 1842-1849.

Quiniou, N., J. Dagorn and D. Gaudré (2002). "Variation of piglets’ birth weight and consequences on subsequent performance." Livestock Production Science 78(1): 63-70.

R Core Team. R (2020). “A language and environment for statistical computing.”.

Radlowski, E. C., M. S. Conrad, S. Lezmi, R. N. Dilger, B. Sutton, R. Larsen and R. W. Johnson (2014). "A neonatal piglet model for investigating brain and cognitive development in small for gestational age human infants." PLoS One 9(3): e91951.

Redmer, D. A., Wallace, J. M., & Reynolds, L. P. (2004). Effect of nutrient intake during pregnancy on fetal and placental growth and vascular development. Domestic Animal Endocrinology, 27(3), 199-217.

Resnik, R. (2002). Intrauterine growth restriction. Obstetrics & Gynecology, 99(3), 490-496.

Rideau Batista Novais, A., H. Pham, Y. Van de Looij, M. Bernal, J. Mairesse, E. Zana-Taieb, M. Colella, P. H. Jarreau, J. Pansiot and F. Dumont (2016). "Transcriptomic regulations in oligodendroglial and microglial cells related to brain damage following fetal growth restriction." Glia 64(12): 2306-2320.

Rosenberg, A. (2008, June). The IUGR newborn. In Seminars in Perinatology (Vol. 32, No. 3, pp. 219-224). WB Saunders.

Ruggeri, R., G. Bee, P. Trevisi and C. Ollagnier (2024). "Intrauterine growth restriction defined by increased brain-to-liver weight ratio affects postnatal growth and protein efficiency in pigs." Animal 18(1): 101044.

Santos, T. G., S. D. Fernandes, S. B. de Oliveira Araújo, F. Felicioni, T. de Mérici Domingues e Paula, A. L. Caldeira-Brant, S. V. Ferreira, L. de Paula Naves, S. P. de Souza and P. H. R. F. Campos (2022). "Intrauterine growth restriction and its impact on intestinal morphophysiology throughout postnatal development in pigs." Scientific Reports 12(1): 11810.

Sarr, O., Yang, K., & Regnault, T. R. (2012). In utero programming of later adiposity: the role of fetal growth restriction. Journal of Pregnancy, 2012.

Schild, S.-L. A., L. Foldager, L. Rangstrup-Christensen and L. J. Pedersen (2020). "Characteristics of piglets born by two highly prolific sow hybrids." Frontiers in Veterinary Science 7: 355.

Sharma, D., Shastri, S., Farahbakhsh, N., & Sharma, P. (2016). “Intrauterine growth restriction–part 1.” The Journal of Maternal-Fetal & Neonatal Medicine, 29(24), 3977-3987.

Shen, L., M. Gan, S. Zhang, J. Ma, G. Tang, Y. Jiang, M. Li, J. Wang, X. Li and L. Che (2018). "Transcriptome analyses reveal adult metabolic syndrome with intrauterine growth restriction in pig models." Frontiers in Genetics 9: 291.

Shi, Q., Y. Zhu, J. Wang, H. Yang and W. Zhu (2019). "Protein restriction and succedent realimentation affecting ileal morphology, ileal microbial composition and metabolites in weaned piglets." Animal 13(11): 2463-2472.

Sizonenko, S. V., Borradori-Tolsa, C., Vauthay, D. M., Lodygensky, G., Lazeyras, F., & Hüppi, P. S. (2006). Impact of intrauterine growth restriction and glucocorticoids on brain development: insights using advanced magnetic resonance imaging. Molecular and Cellular Endocrinology, 254, 163-171.

Sjaastad, O. V., Sand, O., & Hove, K. (2010). Physiology of Domestic Animals. Scan. Vet. Press.

Spinillo, A., B. Gardella, S. Bariselli, A. Alfei, E. M. Silini and B. D. Bello (2014). "Cerebroplacental Doppler ratio and placental histopathological features in pregnancies complicated by fetal growth restriction." Journal of Perinatal Medicine 42(3): 321-328.

Staarvik, T., Framstad, T., Heggelund, M., Brynjulvsrud Fremgaarden, S., & Kielland, C. (2019). Blood-glucose levels in newborn piglets and the associations between blood-glucose levels, intrauterine growth restriction and preweaning mortality. Porcine Health Management, 5, 1-10.

Stephens, A. S., Bentley, J. P., Taylor, L. K., and Arbuckle, S. M. (2015). Diagnosis of fetal growth restriction in perinatal deaths using brain to liver weight ratios. Pathology. 47(1), 51-57.

Suryawan, A., Jeyapalan, A. S., Orellana, R. A., Wilson, F. A., Nguyen, H. V., & Davis, T. A. (2008). “Leucine stimulates protein synthesis in skeletal muscle of neonatal pigs by enhancing mTORC1 activation.” American Journal of Physiology-Endocrinology and Metabolism, 295(4), E868-E875.

Takahashi, S., J. Tomita, K. Nishioka, T. Hisada and M. Nishijima (2014). "Development of a prokaryotic universal primer for simultaneous analysis of Bacteria and Archaea using next-generation sequencing." PLoS One 9(8): e105592.

Theil, P. K., Cordero, G., Henckel, P., Puggaard, L., Oksbjerg, N., & Sørensen, M. T. (2011). Effects of gestation and transition diets, piglet birth weight, and fasting time on depletion of glycogen pools in liver and 3 muscles of newborn piglets. Journal of Animal Science, 89(6), 1805-1816.

Town, S. C., Putman, C. T., Turchinsky, N. J., Dixon, W. T., & Foxcroft, G. R. (2004). Number of conceptuses in utero affects porcine fetal muscle development. Reproduction, 128(4), 443-454.

Trayhurn, P., Temple, N. J., & Aerde, J. V. (1989). Evidence from immunoblotting studies on uncoupling protein that brown adipose tissue is not present in the domestic pig. Canadian Journal of Physiology and Pharmacology, 67(12), 1480-1485.

Upadhaya, S. D., & Kim, I. H. (2022). Maintenance of gut microbiome stability for optimum intestinal health in pigs–a review. Journal of Animal Science and Biotechnology, 13(1), 1-11.

Van Ginneken, C., M. Ayuso, L. Van Bockstal and S. Van Cruchten (2023). "Preweaning performance in intrauterine growth-restricted piglets: Characteristics and interventions." Molecular Reproduction and Development 90(7): 697-707.

Vernunft, A., A. Eggert and K.-P. Brüssow (2022). "Ultrasonographic monitoring of fetal growth and fetal weight calculation in sows during gestation." Agriculture 13(1): 16.

Virgili, R., M. Degni, C. Schivazappa, V. Faeti, E. Poletti, G. Marchetto, M. Pacchioli and A. Mordenti (2003). "Effect of age at slaughter on carcass traits and meat quality of Italian heavy pigs." Journal of Animal Science 81(10): 2448-2456.

Wang, H., R. Xu, H. Zhang, Y. Su and W. Zhu (2020). "Swine gut microbiota and its interaction with host nutrient metabolism." Animal Nutrition 6(4): 410-420.

Wang, J., L. Chen, D. Li, Y. Yin, X. Wang, P. Li, L. J. Dangott, W. Hu and G. Wu (2008). "Intrauterine growth restriction affects the proteomes of the small intestine, liver, and skeletal muscle in newborn pigs." The Journal of Nutrition 138(1): 60-66.

Wang, T., C. Liu, C. Feng, X. Wang, G. Lin, Y. Zhu, J. Yin, D. Li and J. Wang (2013). "IUGR alters muscle fiber development and proteome in fetal pigs." Front Biosci (Landmark Ed) 18(2): 598-607.

Wang, T., Y. J. Huo, F. Shi, R. J. Xu and R. J. Hutz (2005). "Effects of intrauterine growth retardation on development of the gastrointestinal tract in neonatal pigs." Neonatology 88(1): 66-72.

Wang, W., J. Degroote, C. Van Ginneken, M. Van Poucke, H. Vergauwen, T. M. T. Dam, D. Vanrompay, L. J. Peelman, S. De Smet and J. Michiels (2016). "Intrauterine growth restriction

in neonatal piglets affects small intestinal mucosal permeability and mRNA expression of redox-sensitive genes." The FASEB Journal 30(2): 863-873.

Wang, X., Y. Liu, S. Li, D. Pi, H. Zhu, Y. Hou, H. Shi and W. Leng (2015). "Asparagine attenuates intestinal injury, improves energy status and inhibits AMP-activated protein kinase signalling pathways in weaned piglets challenged with Escherichia coli lipopolysaccharide." British Journal of Nutrition 114(4): 553-565.

Whang, K. and R. Easter (2000). "Blood urea nitrogen as an index of feed efficiency and lean growth potential in growing-finishing swine." Asian-Australasian Journal of Animal Sciences 13(6): 811-816.

Wilkinson, S., Lu, Z. H., Megens, H. J., Archibald, A. L., Haley, C., Jackson, I. J., Groenen, M. A. M., Crooijmans, R. P. M. A., Ogden, R., Wiener, P., Wiener, P. (2013). "Signatures of diversifying selection in European pig breeds". PLoS Genetics, 9, e1003453.

Wishart, D. S., D. Tzur, C. Knox, R. Eisner, A. C. Guo, N. Young, D. Cheng, K. Jewell, D. Arndt and S. Sawhney (2007). "HMDB: the human metabolome database." Nucleic Acids Research 35(suppl_1): D521-D526.

Wixey, J. A., Lee, K. M., Miller, S. M., Goasdoue, K., Colditz, P. B., Tracey Bjorkman, S., & Chand, K. K. (2019). "Neuropathology in intrauterine growth restricted newborn piglets is associated with glial activation and proinflammatory status in the brain. " Journal of Neuroinflammation, 16, 1-13.

Wootton, R., Flecknell, P. A., Royston, J. P., & John, M. (1983). "Intrauterine growth retardation detected in several species by non-normal birthweight distributions." Reproduction, 69(2), 659-663.

Wu, G. (2013). “Functional amino acids in nutrition and health.” Amino Acids, 45, 407-411.

Wu, G., Bazer, F. W., Cudd, T. A., Meininger, C. J., & Spencer, T. E. (2004). Maternal nutrition and fetal development. The Journal of Nutrition, 134(9), 2169-2172.

Wu, G., Bazer, F. W., Wallace, J. M., & Spencer, T. E. (2006). “Board-invited review: intrauterine growth retardation: implications for the animal sciences.” Journal of Animal Science, 84(9), 2316-2337.

Wu, H., Liu, Y., Pi, D., Leng, W., Zhu, H., Hou, Y., Li, S., Shi, H., Wang, X. (2015). “Asparagine attenuates hepatic injury caused by lipopolysaccharide in weaned piglets associated with modulation of Toll-like receptor 4 and nucleotide-binding oligomerisation domain protein signalling and their negative regulators.” British Journal of Nutrition, 114(2), 189-201.

Xiong, L., You, J., Zhang, W., Zhu, Q., Blachier, F., Yin, Y., & Kong, X. (2020). “Intrauterine growth restriction alters growth performance, plasma hormones, and small intestinal microbial communities in growing-finishing pigs.” Journal of Animal Science and Biotechnology, 11(1), 1-18.

Yan, H., P. Zheng, B. Yu, J. Yu, X. Mao, J. He, Z. Huang and D. Chen (2017). "Postnatal high-fat diet enhances ectopic fat deposition in pigs with intrauterine growth retardation." European Journal of Nutrition 56: 483-490.

Yan, X., Zhu, M. J., Dodson, M. V., & Du, M. (2013). Developmental programming of fetal skeletal muscle and adipose tissue development. Journal of Genomics, 1, 29.

Yang, Q., X. Huang, S. Zhao, W. Sun, Z. Yan, P. Wang, S. Li, W. Huang, S. Zhang and L. Liu (2017). "Structure and function of the fecal microbiota in diarrheic neonatal piglets." Frontiers in Microbiology 8: 249405.

Yang, Y., Y. Liu, J. Liu, H. Wang, Y. Guo, M. Du, C. Cai, Y. Zhao, C. Lu and X. Guo (2021). "Composition of the fecal microbiota of piglets at various growth stages." Frontiers in Veterinary Science 8: 661671.

Yin, Y., K. Yao, Z. Liu, M. Gong, Z. Ruan, D. Deng, B. Tan, Z. Liu and G. Wu (2010). "Supplementing L-leucine to a low-protein diet increases tissue protein synthesis in weanling pigs." Amino Acids 39: 1477-1486.

Yu, Q. P., D. Y. Feng, J. Xiao, F. Wu, X. J. He, M. H. Xia, T. Dong, Y. H. Liu, H. Z. Tan and S. G. Zou (2017). "Studies on meat color, myoglobin content, enzyme activities, and genes associated with oxidative potential of pigs slaughtered at different growth stages." Asian-Australasian Journal of Animal Sciences 30(12): 1739.

Zhang, J., E. Yan, L. Zhang, T. Wang and C. Wang (2022). "Curcumin reduces oxidative stress and fat deposition in longissimus dorsi muscle of intrauterine growth-retarded finishing pigs." Animal Science Journal 93(1): e13741.

Zhang, L., W. Wu, Y.-K. Lee, J. Xie and H. Zhang (2018). "Spatial heterogeneity and co-occurrence of mucosal and luminal microbiome across swine intestinal tract." Frontiers in Microbiology 9: 48

Zhang, L., Y. Wang, Y. Kong, H. Ahmad, R. Yan, L. Dong, J. Zhang and T. Wang (2018). "Effects of intrauterine growth retardation on growth, meat quality and muscle fiber composition of pigs." Pakistan Journal of Zoology 50(3): 1137-1146.

Zhang, W., Ma, C., Xie, P., Zhu, Q., Wang, X., Yin, Y., & Kong, X. (2019). Gut microbiota of newborn piglets with intrauterine growth restriction have lower diversity and different taxonomic abundances. Journal of Applied Microbiology, 127(2), 354-369.